EXPLORING THE MECHANISMS RESPONSIBLE FOR ENERGETIC DYSFUNCTION WITHIN THE TYPE 2 DIABETIC HEART

Matthew Kerr

Pembroke College

A thesis submitted for the degree of *Doctor of Philosophy*

Trinity 2019

ACKNOWLEDGMENTS

This body of work was completed over the course of four years and would not have been possible without a great deal of support and assistance. I would like to firstly thank Professors Lisa Heather and Damian Tyler for their supervision. You provided an atmosphere which allowed personal development whilst providing exceptional guidance and support whenever wanted or needed.

It has been a true privilege to work in the cardiac metabolism research group (CMRG) and I cannot imagine a setting more conducive to developing a genuine excitement for scientific research. In particular; Drs. Maria da Luz Sousa Fialho, Colleen Lopez and Dragana Savic made coming into, and leaving, the laboratory an experience to look forward to every day. Discussions about philosophy with Dr. Cher-rin Chong and everyday physiology with Javier Gilbert Jaramillo and Ujang Purnama provided the ideal conclusion in my fourth year.

I thoroughly enjoyed everyday chats with Dr. Carolyn Carr and Vicky Ball over the course of my master's project and the promise of this continuing was instrumental in my desire to carry on in the CMRG for my PhD. I would like to thank Sophie Stiewe and Sara Rohling for putting up with my supervision and for all your assistance, as well as Claudia Aparicio de Montes for her guidance on music, and help in the laboratory. Dr. Jack Miller provided not only invaluable expertise on magnet related work and statistical analysis, but also exemplified sincere scientific enthusiasm.

I will finish by thanking the people whose support and love has enabled me to reach this point; Margaret, my grandmother, who has supported me with academics since school, Megan, my partner, who created all the diagrams in this work, lent a sympathetic ear and made every day more enjoyable than it otherwise would have been, and lastly, my parents, John and Janet, whose continual academic and personal support has made me who I am today.

ABSTRACT

Cardiovascular disease accounts for 70% of mortality within type 2 diabetic (T2D) patients. Energetic dysfunction is apparent within the T2D heart, presenting as a decreased phosphocreatine/adenosine triphosphate (PCr/ATP) ratio. This pathophysiology is an independent predictor for mortality risk within the setting of heart failure. While most clinical measurements of cardiac PCr/ATP ratios within T2D patients display a reduced PCr/ATP ratio some disagree, showing no defect. Emerging work indicates that this may be due to simultaneous reductions in PCr and ATP masking a decrease in their ratio. Energetic dysfunction can be primarily attributed to impaired mitochondrial respiration but there is no comprehensive explanation for why T2D cardiac mitochondria produce less ATP despite the excess of fatty acid substrates within the T2D heart.

This work began through the characterisation of energetics within the T2D rodent heart via ^{31}P-MRS in perfused hearts. The addition of a phosphorous standard allowed calculation of absolute ATP and PCr concentrations showing that T2D hearts had an 18% reduction in PCr and a 12% reduction in ATP, with no overall decrease in the PCr/ATP ratio. Reduced ATP turnover was displayed through a 61% reduction in the rate of ATP degradation in T2D hearts, which was associated with a 12-24% reduction in respiratory rates in T2D cardiac mitochondrial populations. Two avenues were investigated to explain this reduction in mitochondrial respiratory rates; acute inhibition of the ATP/ADP carrier (AAC) by long chain acyl-CoAs (LCAC), and post-translational modifications (PTMs) of mitochondrial proteins. Targeted mass spectrometry and *ex vivo* inhibition assays demonstrated, for the first time, that LCAC-mediated inhibition of the AAC, although present, was not of a sufficient magnitude to explain the inhibition of mitochondrial respiration observed under physiological conditions.

There are many PTMs which are dysregulated in T2D, but perhaps the most relevant to mitochondrial function is that of protein acetylation, which was increased by 50% in T2D mitochondria. The effect of this PTM was elucidated through *in vitro* acetylation of control mitochondria, which demonstrated that protein acetylation depressed respiratory rates. Honokiol, an activator of the mitochondrial deacetylase Sirt3, was employed *in vivo* to correct mitochondrial hyperacetylation and displayed complete removal

of hyperacetylation following a ten-day dosing regimen. This normalisation of the hyperacetylation within T2D restored respiratory function to that of control mitochondria through a 17-28% increase in respiration. This increased the concentration of ATP and PCr in the T2D heart back to control levels, through a 31% and 29% increase, respectively. In addition, honokiol increased the rate of ATP turnover by 88% in T2D hearts, reverting it to the level of control hearts.

This work demonstrated energetic dysfunction in the absence of a decrease in the PCr/ATP ratio within T2D hearts, providing an explanation for a disparity in the field of cardiac energetics. It also provides the most comprehensive analysis of LCAC inhibition of the AAC within T2D to date, presenting strong evidence that this is not physiologically relevant. Instead, mitochondrial protein hyperacetylation was proposed as the prominent cause of energetic dysfunction within the T2D heart and a safe, bioavailable therapeutic agent was characterised which corrected this hyperacetylation. The pathogenicity of hyperacetylation was demonstrated through its amelioration, which completely corrected; mitochondrial respiration, absolute ATP and PCr concentrations, and ATP turnover within the T2D heart. Overall, evidence is presented which demonstrates that mitochondrial hyperacetylation is a novel, but substantial, aspect of T2D cardiac dysfunction therefore suggesting that honokiol may be a powerful therapeutic agent in preventing cardiovascular mortality.

CONTENTS

ABBREVIATIONS

α-KGDH	α-ketoglutarate dehydrogenase
AAC	ATP/ADP carrier
ADP	Adenosine diphosphate
AMPK	AMP-activated protein kinase
ATP	Adenosine triphosphate
ATPIF1	ATP synthase inhibitory factor 1
BKA	Bongkrekic acid
BSA	Bovine serum albumin
CATR	Carboxyatractyloside
CPT-I	Carnitine palmitoyltransferase – 1
CS	Citrate synthase
CVD	Cardiovascular death
DCM	Dilated cardiomyopathy
DMSO	Dimethyl sulfoxide
DNP	2,4-dinitrophenol
ECL	Enhanced chemiluminescence
EDP	End-diastolic pressure
FA	Fatty acid
$FABP_{PM}$	Fatty acid binding protein (plasma membrane)
$FAD(H_2)$	Flavin adenine dinucleotide (reduced)

FAT	Fatty acid translocase
FATP	Fatty acid transport protein
FCCP	carbonyl cyanide-*p*-trifluoromethoxyphenol hydrazine
GCN5L1	General control of amino-acid synthesis 5-like-1
GDH	Glutamate dehydrogenase
GLUT	Glucose transporter
GPM	Glutamate, pyruvate and malate
GPMPCar	Glutamate, pyruvate, malate and palmitoyl-carnitine
IFM	Inter-fibrillar mitochondria
IMM	Inner mitochondrial membrane
IMS	Intermembrane space
KEGG	Kyoto encyclopaedia of genes and genomes
KH	Krebs-Henseleit
LCAC	Long chain acyl-CoA
LCAD	Long chain acyl-CoA dehydrogenase
LPL	Lipoprotein lipase
M-CoA	Malonyl-CoA
MDH	Malate dehydrogenase
MIS	Mitochondrial isolation solution
mPTP	Mitochondrial permeability transition pore
MRS	Magnetic resonance spectroscopy

NAD(H)	Nicotinamide adenine dinucleotide (reduced)
NAM	Nicotinamide
NEFA	Non-esterified fatty acid
NMR	Nuclear magnetic resonance
O-CoA	Oleoyl-CoA
P-CoA	Palmitoyl-CoA
PDH	Pyruvate dehydrogenase
PDK4	Pyruvate dehydrogenase kinase 4
Pi	Inorganic phosphate
PiC	Phosphate carrier
PPAR	Peroxisome proliferator-activated receptor
PTM	Post-translational modification
ROS	Reactive oxygen species
SDS-PAGE	Sodium dodecyl sulphate-polyacrylamide gel electrophoresis
Sirt3	Sirtuin 3
SPE	2-(2-pyridyl) ethyl functionalised silica gel
SSM	Sub-sarcolemmal mitochondria
STZ	Streptozotocin
T2D	Type 2 diabetes
TAG	Triacylglycerol
VDAC	Voltage dependent anion channel

1 INTRODUCTION

The average human heart beats over 2.5 billion times in a lifetime, with each beat requiring the contraction of ventricular and atrial cardiomyocytes. These contractions rely on adenosine triphosphate (ATP) breakdown to power both myofibrillar shortening and ion fluxes. It is testament to cardiac metabolism that it facilitates not only this extraordinarily high ATP throughput (around 15-20 times the weight of the heart every day)[1,2], but it can also adapt to fluctuations in energetic demand within a matter of seconds.

A reduction in the capacity of the heart to maintain this high energetic flux occurs within a wide range of cardiovascular diseases[1,3–10], with the severity of energetic dysfunction correlating with associated mortality rates[11]. This is particularly apparent in type 2 diabetes (T2D), where patients display dysfunctional cardiac energetics[3,5] and over 70% of mortality arises from cardiovascular causes[12]. T2D cardiac energetic dysfunction associates with altered metabolism, and in particular with hyperlipidemia[5,13], but the exact source is still unknown. The work described in this thesis will focus on delineating the causes of the energetic dysfunction observed in the type 2 diabetic heart and determining its potential for therapeutic targeting.

1.1 CARDIAC METABOLISM IN THE HEALTHY HEART

ATP plays a central role in energetic processes in all cells, acting as an immense store of free energy due to its phosphodiester bonds, which have a large decrease in free energy associated with their hydrolysis. ATP hydrolysis can be coupled to a wide variety of reactions to drive them in a 'biologically favourable' direction. It is therefore imperative that the heart can continuously regenerate ATP for the many energetically intense processes it must sustain.

The heart uses 0.5 μmol/gww of ATP every second[2] to support its massive energetic demand amounting to around 10% of the total cardiac ATP pool[1] and therefore necessitating rapid regeneration of ATP from adenosine diphosphate (ADP). ATP generation in the heart can be divided into three primary stages; transport of metabolic fuels into the myocardial cell, mitochondrial metabolism, and high energy

phosphoryl transfer from the mitochondria to the site of ATP utilization. A deficiency in any of these stages rapidly leads to decreased myocardial function.

The heart is a metabolically versatile organ, capable of swapping between different carbon substrates to meet its energetic needs ensuring a high ATP synthesis rate under every physiological setting. Over 95% of cardiac ATP is generated through oxygen-dependent oxidative phosphorylation[14,15], with the remainder coming from substrate-level phosphorylation by oxygen-independent reactions in both the cytosol and mitochondrial matrix. Fatty acids (FAs) are the main substrate for ATP generation, with the heart producing around 60-70% of its ATP from FA oxidation, with the remaining 30-40% coming from the oxidation of glucose, lactate, amino acids or ketone bodies[16], as illustrated in figure 1.1. This high dependence on FAs to support cardiac function explains why chronic changes in FA metabolism can have profound effects on cardiac output.

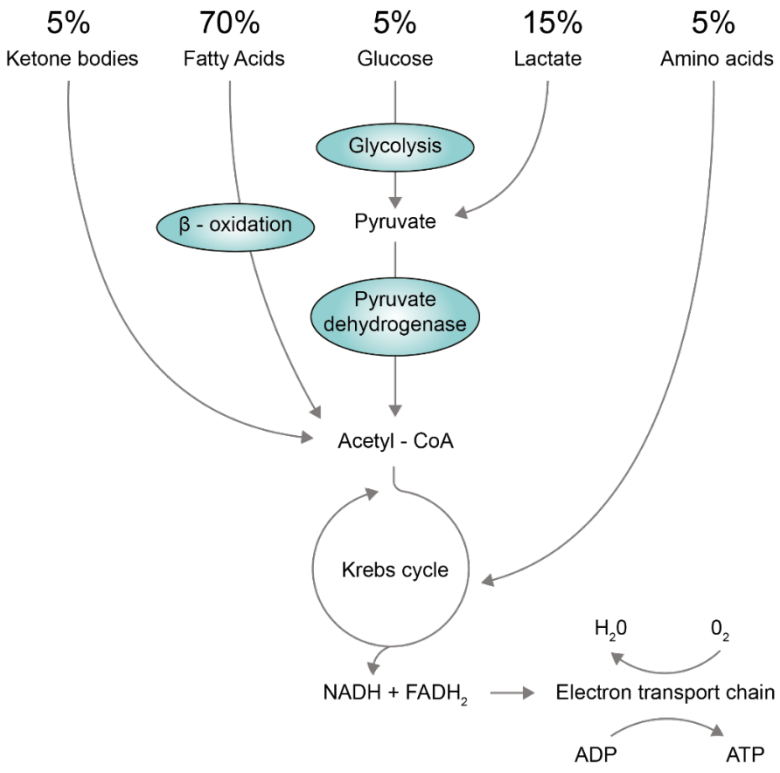

Figure 1.1 – Displaying the substrate usage of the heart, with key crossroads in substrate processing illustrated[16,322,23,24].

1.1.1 Cardiac metabolism of non-fatty acid substrates

Whilst FAs are the main fuel used by the heart, glucose, lactate, ketone bodies and amino acids also play a key role in supporting metabolism. A brief discussion of the metabolism of these other carbon sources is necessary to offer a more integrated picture at the level of the mitochondrion. Intra-myocardial glucose can be sourced either from the hydrolysis of intracellular glycogen, or from the uptake of plasma glucose. Despite the energetic needs of the heart, intracellular glycogen stores are relatively low (at around 115 μmol/gdw)[17], only reaching approximately 20% of the level of skeletal muscle. The heart compensates for this by achieving a very rapid turnover of glycogen, allowing around 40% of glucose-mediated ATP production to arise from glycogen breakdown[17].

Due to the low intra-myocardial pool of glucose sources, the rate limiting step for glucose metabolism in the myocardium is its movement across the sarcolemma[18]. There are two primary transporters, belonging to the larger glucose transporter (GLUT) family, which facilitate the transport of glucose into the myocardium. Transport is predominantly mediated via the insulin-responsive GLUT4, with some uptake also occurring via the obligate transporter GLUT1[19,20]. Once internalised, free glucose is rapidly phosphorylated to glucose-6-phosphate, metabolically locking it within the cell. Glycolysis then serves as the primary pathway for intracellular glucose generating a small amount of ATP through oxygen-independent substrate level phosphorylation. The final product of glycolysis is pyruvate, which is either transported into the mitochondria for oxidation, or reduced to lactate in the cytosol.

The heart is a well perfused, and oxygenated organ, and so is generally considered a lactate acceptor. Findings that cardiac mitochondria possess the ability for complete lactate oxidation, through mitochondrial monocarboxylate transport proteins[21] for import and lactate dehydrogenase[22] to generate pyruvate, support this notion. Indeed, cardiac lactate oxidation may outweigh glucose oxidation under physiological settings[23,24], accounting for up to 17% of ATP production when present at 0.5 mM[25]. Amino acids primarily serve as an anaplerotic substrate for the Krebs cycle, which will be discussed in more detail later.

1.1.2 Fatty acid uptake into the heart

Fatty acid metabolism is the primary means of cardiac ATP generation, and can be broadly divided into four processes: FA uptake into the heart, cytosolic lipid storage, mitochondrial FA uptake and β-oxidation.

Triacylglycerols (TAGs) are a major source of FAs for the heart[26,27] and their transport around the body occurs in lipoproteins; macromolecules which consist of a core of TAGs and cholesteryl esters surrounded by an outer surface monolayer of phospholipid, free cholesterol and apolipoproteins. In this lipoprotein-bound form, the cell must first hydrolyse the TAG molecules, a process mediated by the endothelial enzyme lipoprotein lipase (LPL), releasing non-esterified fatty acids (NEFAs) for cellular uptake. Free NEFAs represent the other major FA source for the heart, and are predominantly derived via lipolysis from adipose tissue[27] and transported to the heart bound to albumin in the plasma.

Once liberated from either albumin or lipoproteins, NEFAs are transported across the sarcolemma via two distinct processes; spontaneous membrane transversal and protein-mediated uptake. Spontaneous membrane transversal, through a flip-flop mode of translocation, serves as the slower, basal mechanism for FA entry to the cell, as the process is limited by desorption from the membrane into the cytosol[28]. Protein-mediated uptake of FAs occurs via three main FA transport proteins; fatty acid translocase (FAT/CD36)[29], plasma membrane fatty acid binding protein ($FABP_{PM}$)[30], and fatty acid transport protein (FATP)[31,32], with FAT/CD36 responsible for the majority of cellular FA uptake[33].

FAT/CD36 can translocate between intracellular vesicles and the plasma membrane, where it actively participates in FA uptake. This translocation of FAT/CD36 can occur rapidly giving up to twofold upregulation of FA transport, with movement towards the membrane induced by insulin and contraction[34,35], and movement away from the membrane induced by ischaemia[36]. Upon entry, long chain FAs are activated through acylation, forming long chain acyl-CoA (LCAC). The FATP contains intrinsic acyl-CoA synthetase ability, coupling uptake to activation within the same protein-mediated reaction[37].

1.1.3 Cytosolic fatty acid storage

Cardiac tissue undergoes very rapid changes in FA fluxes, both in terms of entry to the cell, and the rate of oxidation. Therefore, in addition to immediate oxidation for ATP generation in the mitochondria cardiac FAs can also be stored for future use as TAG droplets in the cytosol. The ability to store lipids gives the cell a buffering capacity, allowing the heart to rapidly increase substrate availability in settings of increased cellular energy demand whilst preventing the cytosolic accumulation of toxic FA intermediates.

The primary destination of exogenous FAs following uptake is the myocardial TAG pool, with FAs imported from the circulation first esterified into TAGs, then hydrolysed from this intermediary lipid pool for oxidation in the mitochondria when required[38]. Studies which demonstrate that rates of TAG turnover are four times higher than the rates of β-oxidation in the heart indicate that the major source of FAs for β-oxidation in the cell are the intracellular TAG stores, supporting this notion[39]. In a similar fashion to both ATP and glycogen, high levels of flux are maintained in cardiac TAG stores despite a relatively small overall store, reaching just 15% of hepatic levels[40].

1.2 MITOCHONDRIAL FUNCTION AND CARDIAC ENERGETICS

Mitochondria, which generate over 95% of cardiac ATP, make up 30% of the cardiomyocyte volume[41], a reflection of the intense energetic demand of the heart. Cardiac mitochondria are divided into (at least) two populations, which are spatially separated[42–45]. Sub-sarcolemmal mitochondria (SSM) are located directly beneath the sarcolemmal membrane whereas inter-fibrillar mitochondria (IFM) reside in between the myofibrils of the heart, as shown in figure 1.2. These separate cardiac mitochondrial populations were first described by Hoppel *et al.* in 1977[46], who demonstrated that each population required different isolation protocols, and that the IFM population achieved higher rates of substrate oxidation. In addition to the altered respiratory kinetics, the pathophysiology of these mitochondrial populations is also different; the SSM population have a greater inner membrane permeability (especially to NADH)[47] and are more susceptible to ischaemic damage[48], whereas the IFM population are more susceptible to diabetes-related damage[49].

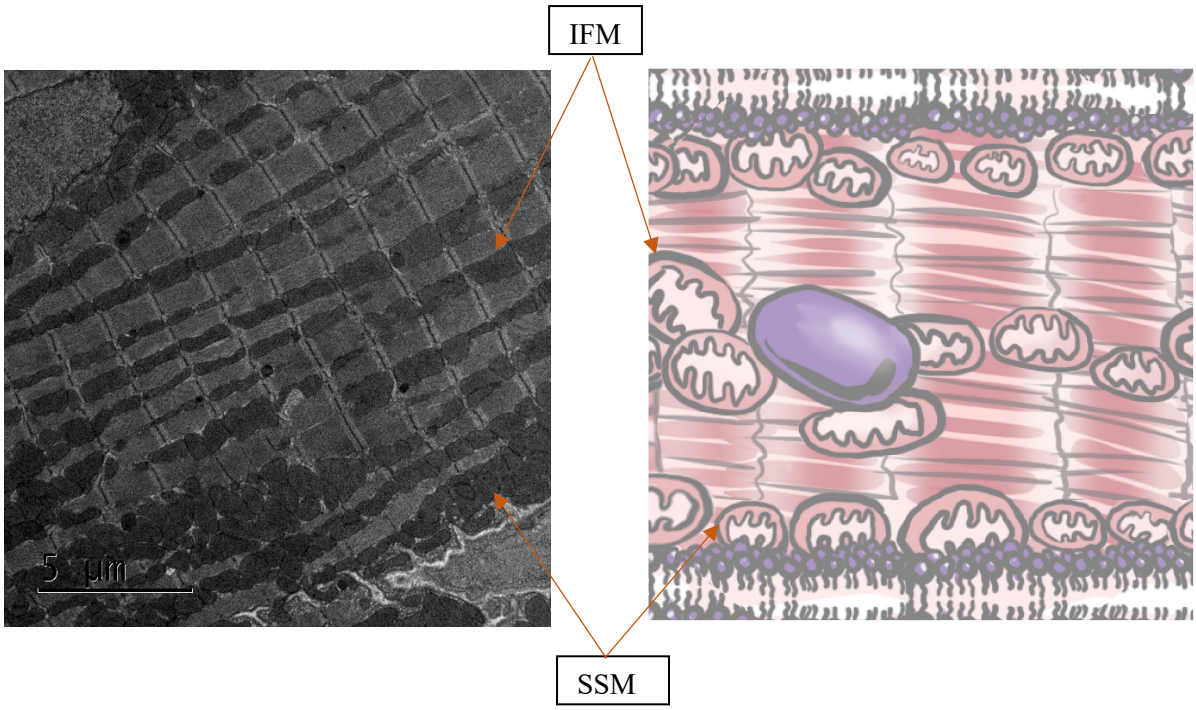

Figure 1.2 – Illustrating the spatial separation between the SSM and IFM, as shown through electron microscopy of cardiac tissue (left – obtained with the assistance of Dr. Helen Christian) and illustrated (right). The relative disorganisation of the SSM can be noted with regards to the linear organisation of the IFM.

1.2.1 Mitochondrial FA uptake and β-oxidation

To allow the development of a trans-membrane proton gradient the inner mitochondrial membrane is impermeable to most charged or large substrates, including the primary mitochondrial substrate; LCAC. Instead, LCACs undergo a covalent modification which facilitates their protein-mediated transport into the mitochondrion. This transport system is the primary control point in mitochondrial FA oxidation. Activated LCACs are converted into fatty acyl carnitine moieties via carnitine palmitoyltransferase-I (CPT-I). The outer mitochondrial membrane is permeable to fatty acyl carnitines, allowing free passage into the intermembrane space, whereupon transport through the inner-mitochondrial membrane is mediated by the carnitine-acylcarnitine translocase. This protein is responsible for both the internalisation of fatty acyl carnitines and the externalisation of mitochondrial carnitine. Once transported into the mitochondrial matrix LCACs are regenerated by CPT-II.

CPT-I is well established in its physiological regulation of FA metabolism through malonyl-CoA (M-CoA) based inhibition. In the heart, a reverse relationship has been shown between FA oxidation rates and tissue M-CoA concentrations[50,51], thus oxidation decreases when M-CoA concentrations are

elevated. In lipogenic tissues the negative relationship between M-CoA (the first committed step of FA synthesis) and FA oxidation is a convenient mechanism to prevent the concomitant degradation and synthesis of FAs. In non-lipogenic tissues, such as the heart, it serves as a method to relate FA oxidation to energy availability, as both enzymes involved in the regulation of M-CoA levels (acetyl-CoA carboxylase which synthesises M-CoA, and M-CoA decarboxylase which degrades it) are regulated by AMP-activated protein kinase (AMPK)[52–55].

Once LCACs reach the mitochondrial matrix, they undergo β-oxidation, each cycle of which is comprised of four reactions and generates one acetyl-CoA moiety. The four steps involve; a dehydrogenation reaction catalysed by acyl-CoA dehydrogenase (ACAD), a hydration reaction catalysed by enoyl-CoA hydratase, a second dehydrogenation reaction catalysed by 3-hydroxyacyl-CoA dehydrogenase and a final thiolytic cleavage catalysed by beta-ketoacyl-CoA thiolase. Although the primary control point for FA oxidation occurs at CPT-I there is evidence that the first step of intra-mitochondrial FA oxidation; ACAD, can be the rate limiting step for β-oxidation[56–58].

1.2.2 The Krebs cycle

The Krebs cycle, first described in 1937[59], accepts and sequentially oxidises acetyl-CoA generated from glucose, fatty acids or amino acids. This sequential oxidation provides the reducing power to produce three NADH molecules (with a redox potential of -320mV), and one $FADH_2$ molecule (with a redox potential of -219mV). Decarboxylation of pyruvate into acetyl-CoA via the pyruvate dehydrogenase (PDH) complex is one of two major entry points for glycolysis into the Krebs cycle, with the other major entry point involving the carboxylation of pyruvate into oxaloacetate by pyruvate carboxylase[60]. PDH is sensitive to both energy level regulation (in the form of an ATP/ADP ratio and NADH/NAD^+ ratio), the concentrations of pyruvate and acetyl-CoA[61], and reversible phosphorylation of the PDH complex by PDH kinases and phosphatases[62]. Fatty acids enter the Krebs cycle directly through acetyl-CoA, which is sequentially liberated from LCACs through β-oxidation. FAs with an even-carbon chain length result in the end-production of multiple acetyl-CoA molecules, whereas FAs with an odd-carbon chain length result in acetyl-CoA and propionyl-CoA as products. If the Krebs cycle was a closed system it would maintain a constant level of carbon, however there are multiple exit points for

biosynthesis or feedback regulation, necessitating several positions where the cycle can be restocked through anaplerosis. To facilitate this, glucose can feed in though pyruvate carboxylation into oxaloacetate, amino acids can feed in as aspartate into oxaloacetate and glutamate into α-ketoglutarate, and branched chain amino acids (as well as odd chain length FAs) can feed in through succinyl-CoA, as illustrated in figure 1.3.

1.2.3 The electron transport chain

The highly reducing electrons, in the form of NADH and $FADH_2$, generated through the Krebs cycle feed into the electron transport chain to generate ATP. The mammalian mitochondrial electron transport chain consists of four primary complexes, denoted as complex I through IV and two mobile cofactors; ubiquinone and cytochrome C. Complexes I-IV contain redox centres, which are sequentially oxidised by the electrons provided by NADH and $FADH_2$ through a redox potential span of 1.1V (from the NAD^+/NADH couple at -320mV to the O_2/H_2O couple at 810mV). The sequential oxidation and reduction of these complexes provides the energy to translocate protons through the inner mitochondrial membrane (with four protons pumped at complex I and III, and effectively two protons pumped at complex IV). In this way, the electron transport chain links the oxidation of carbon substrates to the generation of a proton-motive force across the inner mitochondrial membrane. The redox span of $FADH_2$ is lower than NADH (-219mV vs -320mV) meaning that $FADH_2$ must feed straight into the ubiquinone pool through complex II, therefore missing out complex I and the associated proton translocation. As the fate of the electrons provided by $FADH_2$ is still the terminal electron acceptor O_2, $FADH_2$ has a lower associated P/O (Phosphate/Oxygen) ratio when compared with NADH.

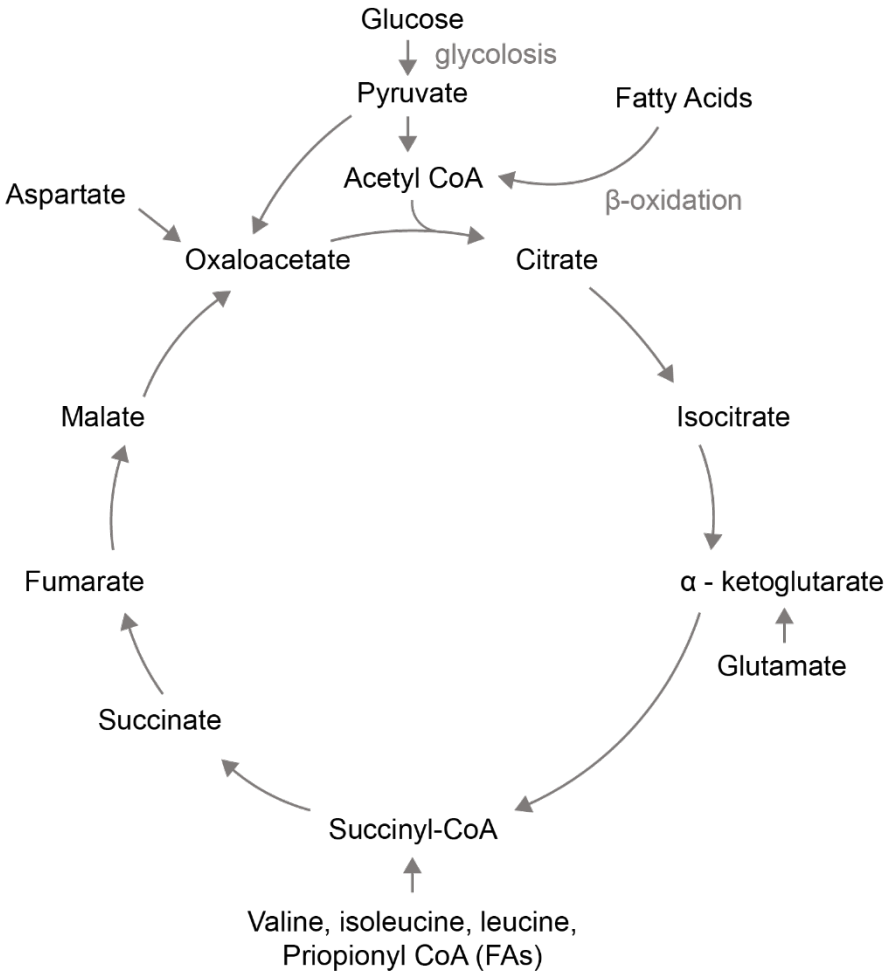

Figure 1.3 – Showing the key points of anaplerotic entry into the Krebs cycle.

1.2.4 The phosphorylation apparatus

The phosphorylation apparatus consists of the ATP synthase, the phosphate carrier (PiC) and the ATP/ADP carrier (AAC). ATP synthase functions as two rotary subunits (F0 and F1) connected through a stator, which ensures that both subunits turn in the same direction. The F0 subunit rotates in response to the flow of protons across the inner mitochondrial membrane (dissipating the proton-motive force) which drives ATP synthesis within the F1 subunit.

The outer mitochondrial membrane is relatively permeable to molecules up to 1000 Daltons due to the presence of a large porin; the voltage dependent anion channel (VDAC). In contrast, the impermeable inner mitochondrial membrane requires the AAC and PiC, obligate transporters belonging to the mitochondrial carrier family, to move ADP and phosphate into the mitochondrial matrix. Although both

these transport processes are necessary for sustained ATP generation, the PiC has little control over the rate of respiration, with a 60% PiC depletion having no effect on the rate of mitochondrial respiration[63]. In stark contrast the AAC, which is the most abundant protein in the inner mitochondrial membrane, is the rate-limiting step for respiration in isolated mitochondria[64,65]. Four AAC isoforms exist within humans, with AAC1 primarily expressed in tissues with restricted mitotic regeneration (such as the heart)[66], AAC2 found in growth regulated tissue (such as the kidney)[67], and AAC4 existing as a testes specific isoform[68]. AAC3 is expressed to a low level in all tissue types[69], but is not found in rodents, which only present with three isoforms, analogous to AAC1, 2 and 4[66,70]. Although the primary function of all the AAC isoforms is identical, there is evidence that they have different kinetics for ADP and ATP transport, with AAC1 presenting as the slowest isoform and AAC2 as a moderate speed isoform[71].

The importance of the AAC in the heart is shown by its essential nature in normal myocardial development, with AAC1 knockouts developing cardiac hypertrophy[72]. Dysfunction around the AAC is also implicated in a myriad of cardiovascular conditions[73–75] such as dilated cardiomyopathy (DCM) where AAC autoantibodies have been shown to decrease AAC transport capacity[76]. In addition, within DCM there is an increase in the AAC1 isoform and a decrease in the AAC2 isoform which correlates with a decrease in respiratory rate[77,78] strongly implicating AAC dysfunction in the pathology.

As the phosphorylation apparatus is the primary control point for mitochondrial respiration *in vitro*, it can sometimes mask dysfunction in other areas of mitochondrial metabolism. The use of uncoupling agents, compounds that allow the free movement of protons through the inner mitochondrial membrane through charge delocalisation over a large aromatic ring, bypasses the phosphorylation apparatus providing a useful tool for the *in vitro* study of mitochondrial metabolism. Carbonyl cyanide-*p*-trifluoromethoxyphenyl hydrazine (FCCP) and 2,4-dinitrophenol (DNP) are the most commonly employed protonophores *in vitro*. The effect of protonophores is illustrated in figure 1.4.

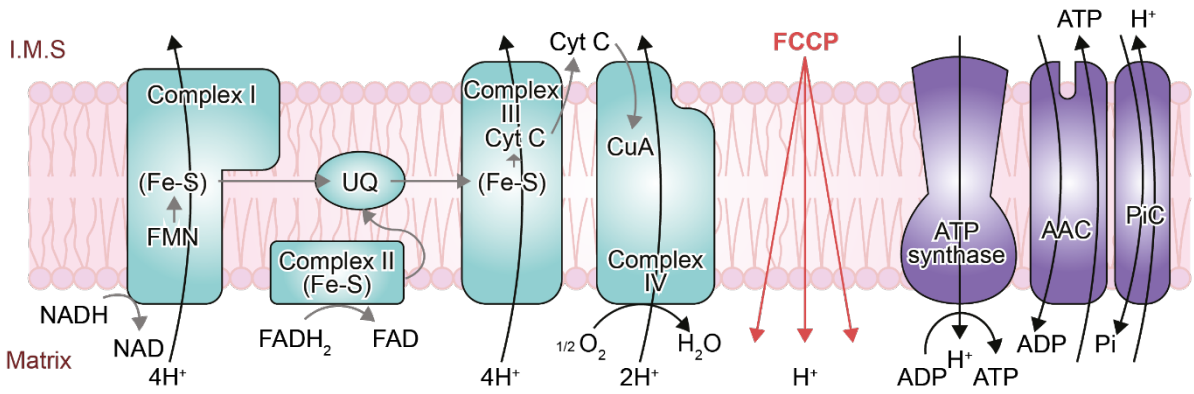

Figure 1.4 – The electron transport chain uses the reductive power of NADH and $FADH_2$ to power proton translocation through the inner mitochondrial membrane, which generates a gradient that can be used by ATP synthase to synthesise ATP. This can be short-circuited through the addition of the protonophore; FCCP.

1.2.5 Cardiac energetics

ATP generated within mitochondria is rapidly consumed elsewhere by ion pumps or the myofibrils. The creatine kinase system, which catalyses the reversible trans-phosphorylation of creatine to phosphocreatine (PCr) and ADP to ATP, forms the major pathway for cellular energetic transfer in vertebrates. PCr, being smaller and less polar than ATP, can diffuse across the cell much faster and so serves as the cellular high energy phosphate transport molecule. The PCr/ATP ratio is maintained above one at baseline such that in times of intense energetic stress PCr can also serve as an internal buffer for high energy phosphates, regenerating dwindling stocks of ATP (maintaining a high free energy associated with its hydrolysis).

The heart strives to maintain constant energy levels, but this can be disrupted in some pathologies such as DCM which displays a reduced PCr/ATP ratio indicating dysfunctional energetics. Isolated heart work in animal models of both DCM and heart failure have shown that clinical observations of a decreased PCr/ATP ratio can be attributed to decreases in both PCr and ATP concentrations, with a greater decrease in PCr driving the observed shift in the ratio[79,80]. This reduced PCr/ATP ratio has been identified as a significant multivariate predictor of cardiovascular mortality in DCM patients, with greater predictive power than left ventricular ejection fraction[11]. This indicates that dysfunctional

cardiac energetics may play a causative role within the pathologies of some cardiovascular conditions. Supporting this notion, two of the most commonly used treatments in cardiovascular disease; β-blockers and ACE inhibitors, have been shown to improve PCr/ATP ratios, as well as improving patient outcomes[81–85].

1.3 MITOCHONDRIAL PROTEIN ACETYLATION

Mitochondrial ATP synthesis is vital in maintaining cardiac energetics, a necessary facet of which is the mitochondrial ability to respond rapidly to changes in cardiac energy demands. Mitochondria have three distinct approaches to deal with variations in respiratory demand each with a different time-course; short-term control occurs through allosteric enzyme activation/inhibition, medium-term through post-translational modifications (PTMs) and long-term changes through altered protein transcription. Separate regulatory pathways enable mitochondria to respond rapidly whilst also adapting to long term changes. Each modification facilitates a mitochondrial 'memory' of the cell's nutritional and energetic status, with small molecule inhibition lasting seconds, PTMs lasting minutes to hours, and transcriptional changes lasting days to weeks.

Acetylation is a PTM where an acetyl group is added to the ε-amino group of lysine residues. Modifying lysine in this way neutralises its otherwise positive charge, therefore potentially altering interactions with; nearby amino acids (adjusting the tertiary structure of the protein), other proteins, and substrates. Lysine acetylation was originally discovered on histone proteins, where it reduces the affinity for the negative charge of DNA. Since then, lysine acetylation has been shown to occur on proteins found outside the nucleus as well and in particular within the mitochondria where around 35% of proteins can be acetylated on 1 or more sites[86].

1.3.1 Regulation of mitochondrial protein acetylation

PTMs such as protein acetylation are rapidly added and removed, with the interplay between these two processes defining the level of protein acetylation at a given time. In the nucleus there are defined regulators of histone acetylation, with enzymes identified for both the acetylation and deacetylation of histones. However, the regulation of mitochondrial protein acetylation is a subject of on-going research.

Work defining the regulation of mitochondrial protein acetylation began with the assumption that it would be regulated in a similar fashion to nuclear histone acetylation, with protein acetyltransferases and deacetylases. One protein has been implicated as a protein acetyltransferase; general control of amino-acid synthesis 5-like 1 (GCN5L1), which is named after the nuclear acetyltransferase GCN5. GCN5L1's exact role is disputed; knockout models of the GCN5L1 protein show reduced levels of mitochondrial protein acetylation indicating that it plays a role in the regulation of protein acetlyation[87], however GCN5L1 lacks most of the canonical GCN5 acetyltransferase-like domain. This has raised the possibility that GCN5L1 functions by increasing the local concentration of acetyl-CoA around proteins in the mitochondrial matrix facilitating spontaneous protein acetylation[88].

Spontaneous acetylation is thought to be the primary source of mitochondrial protein acetylation and is unique to mitochondria as it is dependent on the environment within the mitochondrial matrix. The mitochondrial matrix has a high concentration of acetyl-CoA (the primary acetyl group donor for protein acetylation) and is comparatively alkaline (due to the extrusion of protons across the inner mitochondrial membrane), with a pH around 0.8 pH units higher than the nucleus (7.9-8.0 vs 7.2)[89]. Both these factors have been shown to facilitate spontaneous lysine acetylation in the absence of protein factors[90].

Although the processes regulating acetylation are still under debate, deacetylation is known to be primarily facilitated by a protein class called sirtuins, of which three members localise to the mitochondrial matrix; Sirt3, 4 and 5[91]. Of these sirtuins, only Sirt3 has been shown to have potent deacetylase activity[92], with Sirt5 exhibiting some deacylase activity[93], and Sirt4 not well characterised.

Sirt3's activity is dependent on both protein expression levels and the availability of the substrate for its reaction, nicotinamide adenine dinucleotide (NAD). Physiologically therefore, the primary modulator for acetylation status is nutrient availability. During the normal fed/fasted cycle, the fed state will tend to favour mitochondrial protein acetylation (with a low ratio of NAD/NADH, and a relative excess of acetyl-CoA), whereas the fasted state will tend to favour mitochondrial protein deacetylation (with high ratios of NAD/NADH, and a relative scarcity of acetyl-CoA), as illustrated in figure 1.5.

The mitochondrial acetylome is altered in the long-term by chronic nutrient availability, being increased by both protracted caloric restriction[94,95], as well as by sustained high fat feeding[96]. At first glance, the fact that acetylation can be induced by either chronic over or under-feeding seems paradoxical. However, both these states increase the availability of acetyl-CoA in the mitochondrial matrix through elevating FA oxidation. This therefore points towards the primary factor in determining the acetylation status of mitochondrial proteins being the level of acetyl-CoA available and by extension the degree of fatty acid oxidation occurring in that tissue. This is supported by the fact that ethanol supplementation (which increases acetyl-CoA availability) increases mitochondrial protein acetylation in the liver[97].

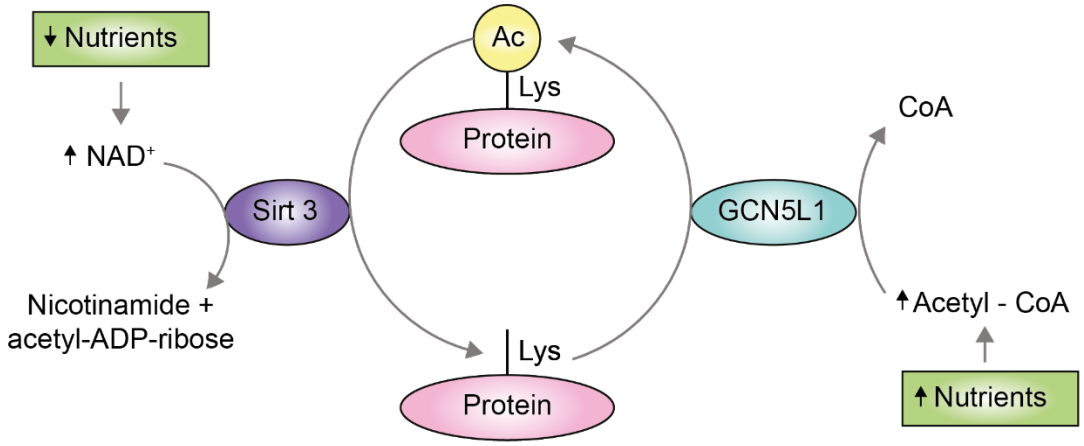

Figure 1.5 – The mitochondrial protein acetylome is governed by the deacetylase Sirt3 and the acetyltransferase GCN5L1, the activities of which are dependent on the nutritional status of the cell.

1.3.2 The effect of protein acetylation on enzymatic function

Much of the work on defining the effect of protein acetylation on enzymatic function comes from studies where either hypo or hyperacetylation of mitochondrial proteins altered cellular energy status. In general, increasing mitochondrial protein acetylation seems to decrease both mitochondrial respiratory rates and organ ATP levels, whereas decreasing mitochondrial protein acetylation seems to have the opposite effect (as shown in table 1.1).

Table 1.1 – A summary of known modulators of mitochondrial protein acetylation

Modulation	Acetylation levels	Sirt3	Respiratory rates	ATP levels
High fat diet feeding[98,99]	Increased (liver)	Decreased activity	Decreased	Decreased cardiac PCr/ATP
Calorie restriction[94]	Increased (liver), decreased (BAT) no change (heart, kidney)	Increased (liver)	Unknown	Unknown
Fasting[95,100]	Increased	Decreased expression	Decreased	Unknown
Type 1 diabetes[101,102]	Increased	Unknown	Decreased	Decreased cardiac PCr/ATP
Mitochondrial acetic anhydride incubation [101]	Increased	N.A.	Decreased	N.A.
Doxorubicin treatment[103,104]	Increased	Decreased both activity and expression	Decreased	Decreased both [ATP] and [PCr] by 20%
Sirt3 knockout (cell)[105]	Increased	Knocked out	Decreased	30% reduction in [ATP]
Sirt3 knockout (mouse)[105–107]	Increased	Knocked out	Decreased	50% reduction in [ATP] in the heart
Knockdown of GCN5L1[108]	Decreased	Unknown	Increased	Increased
Honokiol[109,110]	Decreased	Increased activity	Increased	Unknown

Since systemic alterations in mitochondrial protein acetylation are well correlated with decreased metabolic rates, one might expect that acetylation uniformly decreases the catabolic activity of enzymes. This seems to be the case for enzymes involved in the processing of glucose or amino acid metabolism, but it is less clear for enzymes involved in fatty acid oxidation in the heart (table 1.2).

Table 1.2 – A summary of the effect of acetylation on mitochondrial proteins

Enzyme	Model	Effect of acetylation on activity	Evidence	
			Tissue	Technique
Pyruvate carrier	Mutant protein[111]	Decreased	HCT15 cells	Oxidation measurements
Acetyl-CoA synthetase	*In vitro* acetylation[112]	Decreased	Recombinant protein	Isolated assay
Aconitase	In vitro, and diet modification[113]	Increased	Heart	Isolated assay
Glutamate dehydrogenase	Sirt3 KO mice[92]	(Showed increased acetylation)	Liver	Immunoblotting
	Isolated protein[114]	Decreased	Bovine sample	Isolated assay
	Sirt3 KO mice[106]	Decreased	Heart	Isolated assay
Isocitrate dehydrogenase	Isolated enzyme[114]	Decreased	Bovine sample	Isolated assay
Long chain acyl CoA dehydrogenase	Sirt3 KO mice[107]	Decreased	Liver	Isolated assay
	High fat diet[115]	Decreased	Liver	Isolated assay
	Sirt3 KO mice[106]	Decreased	Heart	Isolated assay
	Diet modification[116]	Increased	Heart	Isolated assay
	Sirt3 KO mice[116]	Increased	Heart	Isolated assay
	In vitro acetylation[117]	Decreased	Recombinant protein	Isolated assay
Succinate dehydrogenase	Sirt3 KO mice[118]	Decreased	Liver	Isolated assay
	Sirt3 KO mice[105]	No change	Liver	Mitochondria
	Sirt3 KO MEFs and mice[119]	Decreased in MEFs and BAT, no change in liver	MEFs, liver and BAT mitochondria	Isolated assay
ATP synthetase subunit β	siRNA for Sirt3 in HEK cells + mutants[120]	Decreased	HEK cells transfected with human protein	Isolated assay
ATP-ADP carrier 1	Molecular modelling[121]	Decreased	N.A.	*In silico*
Malate dehydrogenase	Sirt3 KO MEFs[122]	Decreased	MEF	Isolated enzyme
NDUFA9 (complex I)	Sirt3 KO mice[105]	Decreased	Liver	Mitochondria
	In vitro deacetylation[105]	Decreased	HeLa cell mitochondria	Isolated enzyme

Of interest is the disparity in the effect of acetylation on the activity of long chain acyl-CoA dehydrogenase (LCAD), which has been shown to both be activated and inhibited by acetylation[106,116]. Generally, findings have shown that in the liver, acetylation of LCAD is inhibitory, whereas in the heart it may be an activator. The liver and heart have very different roles to play during long-term fasting, with the liver primarily involved in maintaining whole body metabolic homeostasis and the heart focused on maintaining function for as long as possible. This disparity in the effect of acetylation may therefore be something selected for evolutionarily with tissue specific effects of acetylation on protein activity potentially working through differential site acetylation. LCAD has at least 8 potential acetylation sites[107] and thus the different effects of acetylation may arise from different sites of acetylation, requiring further work to truly delineate organ-specific effects.

With cardiovascular mortality tightly correlated with cardiac energetic function, and mitochondrial protein acetylation intrinsically linked to normal cardiac energy generation, it is reasonable that dysregulated mitochondrial protein acetylation is implicated across cardiovascular diseases. The role of mitochondrial protein acetylation in the heart is most evident in the Sirt3 KO mouse, which shows impaired recovery post-myocardial infarction[123], a finding of interest given that Sirt3 levels are decreased following ischaemia-reperfusion[124]. Reduced Sirt3 activity has also been implicated in the pathology of cardiac hypertrophy and heart failure[125,126] and overexpression of Sirt3 can ameliorate doxorubicin induced cardiotoxicity[103,127]. Finally, Sirt3 can prevent some damage associated with diabetic cardiomyopathy[128]. Overall these studies indicate that hyperacetylation is associated with increased cardiovascular risk, whereas hypoacetylation is associated with decreased risk.

1.4 TYPE 2 DIABETES

Type 2 diabetes (T2D) is a chronic metabolic disease characterised by insulin insensitivity as a result of; peripheral insulin resistance, declining insulin production, and eventual pancreatic β-cell failure[129,130]. In addition to the widely recognised changes in blood glucose and insulin concentrations large changes in lipid concentrations also occur in T2D, with elevated circulating levels of triglycerides, cholesterol and NEFAs. Cardiovascular disease is the leading cause of mortality in diabetes and in

addition to the acceleration of traditional risk factors, such as hypertension and vascular disease, abnormalities in cardiac metabolism have also been implicated in diabetic cardiomyopathy (see[131] for review).

1.4.1 Metabolic changes in the diabetic heart

Increased cardiac FA uptake and oxidation have been reported in most patient and animal studies in both type 1 and T2D[132–135]. This increased rate of FA uptake and oxidation has been shown to correlate positively with the degree of insulin resistance[132,136] with McGill *et al.* demonstrating a step wise increase in FA utilisation associated with the transition from obesity to T2D[132]. Thus, the more severe the diabetes, the greater the rate of cardiac FA oxidation. Multiple rodent models of T2D display this increase in cardiac FA oxidation[137–143] and it has been calculated that FA oxidation accounts for over 90% of ATP generation in the *db/db* mouse heart[139]. Interestingly, in some models, the increased FA oxidation precedes hyperglycaemia with cardiac FA metabolism tracking with the circulating hyperlipidaemia[138] suggesting that increased FA supply in T2D drives changes in cardiac fuel selection.

Not only is FA oxidation increased in the diabetic heart but the storage of lipids, in the form of TAG droplets within the myocardium is also upregulated[144,145]. The increased oxidation and storage of FA is driven by both increased circulating levels of plasma FAs and an increased capacity for FA uptake across the sarcolemma. FA uptake capacity is elevated due to an increase in the protein content of FA transporters and a permanent subcellular relocation such that a greater number of transporters are resident at the membrane to facilitate FA uptake[34]. This, in combination with the increased circulating lipid level drives prolific cardiac FA uptake, eventually overloading the diabetic heart with FAs[146] and driving systemic activation of the peroxisome proliferator-activated receptor alpha (PPARα) transcription factor. PPARα activation induces the transcription of target genes involved in; FA uptake, mitochondrial FA import, β-oxidation and TAG storage[147]. This accumulation of FAs also generates intermediates in FA metabolism such as ceramide, diacylglycerol and LCACs which are considered lipotoxic for the heart (see[148,149] for reviews on this subject).

1.4.2 The relationship between metabolism and function in the diabetic heart

The relationship between cardiac metabolism and function within T2D is most evident in relation to diastolic function and the ability to respond to cardiac stress. Myocardial TAG content correlates negatively with diastolic function in patients[144] and palmitate oxidation rates correlate negatively with post-ischaemic recovery of function in mice[150].

Research from the groups of Aasum and Larson showed that elevated levels of FA metabolism associated with the diabetic heart increased the oxygen requirement of both basal metabolism and excitation-contraction coupling[151] which could be improved by decreasing FA oxidation[150]. Some mechanisms have been proposed for the elevated oxygen usage in the diabetic heart including; increased mitochondrial oxygen wasting through uncoupling proteins, increased futile cycling of lipids and abnormal calcium handling[151–153]. These may explain in part why diabetic hearts have impaired myocardial energetics, with decreased PCr/ATP ratios preceding vascular disease and contractile dysfunction[5]. The scale of the decrease in the PCr/ATP ratio[3,5] in diabetic patients is in excess of what one might expect simply by futile cycling alone. Therefore, questions remain around the increased FA oxidation and decreased energetics in the diabetic heart.

1.4.3 Mitochondrial dysfunction in the diabetic heart

Evidence for mitochondrial dysfunction in the diabetic heart can be deduced from the fact that the diabetic heart displays altered PCr/ATP ratios which, through *in silico* modelling[154], can be traced to dysfunctional mitochondria. Mitochondrial dysfunction was identified in isolated diabetic mitochondria as early as the 1980s where Kuo *et al.* showed impairments in state 3 respiration in mitochondria isolated from T2D *db/db* mouse hearts[155,156]. More recent studies have confirmed this in permeabilised cardiac fibres in T2D *ob/ob* mice[157]. Despite early identification, the mechanisms behind the reduced oxidative capacity within T2D mitochondria are still a matter of research.

The current paradigm hypothesises that mitochondrial dysfunction can be attributed to; excessive reactive oxygen species damage of the electron transport chain, altered proteome expression and altered post-translational protein modifications. Within the field of T2D cardiac mitochondrial dysfunction,

ROS damage has received the most attention to date[158]. The study of ROS induced damage began with the discovery of markers of oxidative stress within the blood of both T2D animals and patients[159,160]. The work of Shen *et al.* revealed, through inhibition studies, that mitochondria were the main source of ROS (at least in T2D cardiac cells from mouse models)[161]. Based on work carried out on human atrial tissues taken from T2D patients, which showed elevated H_2O_2, reduced glutathione levels and enhanced lipid peroxides[162,163] it was hypothesised that antioxidants would confer cardioprotective effects within T2D. However, the use of general antioxidants in clinical trials has been disappointing, with no observed protection against CVD[164–166].

Altered protein expression[167–170] and post-translational modifications[101,171,172], have been widely studied in the type 1 diabetic heart, but are relatively uncharacterised in the T2D heart. The AAC, which is the primary control point of mitochondrial respiraiton[64,65] has reduced expression in the T2D heart[173,174]. The potential pathophysiological role of reduced AAC expression can be inferred from overexpression studies which were cardio-protective in both type 1 diabetes[175] and in hypertension-induced heart disease[176]. This therefore indicates that AAC may play a role in energetic dysfunction within T2D cardiac mitochondria.

The mitochondrial landscape of protein post-translational modifications is complex and relatively uncharted. Despite this, mitochondrial protein acetylation has been suggested to be of significance within T2D and cardiovascular dysfunction[177]. This is due to a polymorphism in Sirt3 (the primary mitochondrial deacetylase), which is associated with the development of metabolic syndrome[115]. Furthermore, decreased Sirt3 expression has been identified in the skeletal muscle of high-fat diet induced obese mice, and contributes to the pathogenesis of T2D[178]. Both the mechanisms involved and the physiological significance in T2D remain to be studied.

1.5 THESIS AIMS

The work described in this thesis intends to characterise cardiac energetic dysfunction in a rodent model of T2D. It will furthermore examine the cause of energetic dysfunction at the level of the mitochondria, with the aim of correcting the dysfunctional energetics through pharmacological manipulation. This will be achieved through four chapters, focusing on;

1. Measuring the concentrations of ATP and PCr in actively contracting hearts, and the respiratory capacity of mitochondria isolated from the type 2 diabetic heart.
2. Investigating the physiological relevance of long chain acyl-CoA inhibition of the ATP/ADP carrier in both the T2D and healthy heart under both normal and ischaemic states.
3. Determining the degree and effect of non-specific mitochondrial protein acetylation in the diabetic heart.
4. Interrogating whether pharmacological manipulation of the acetylation status of mitochondrial proteins in the diabetic heart can ameliorate its associated energetic dysfunction.

2 METHODS

2.1 ANIMAL WORK

Male Wistar rats were purchased from Envigo (UK). All investigations conformed to UK Home Office guidelines under The Animal (Scientific Procedures) Act, 1986.

2.1.1 Generation of the high fat/streptozotocin type 2 diabetes model

Upon arrival, animals were weight matched into two groups. The diabetic cohort was fed a high fat diet (60% kcal from fat, 35% kcal from protein and 5% kcal from carbohydrate, with an Atwater fuel energy of 5.3 kcal/g, from Special Diet Services) whereas the control group was chow fed (with an Atwater fuel energy of 3 kcal/g, from Harlan laboratories). Both groups were fed *ad libitum*. At 2 weeks both groups were fasted overnight and the diabetic group given a low-dose streptozotocin (STZ) (Sigma, UK) intraperitoneal injection (25 mg/kg) dissolved in 300 μL of citrate buffer (30 mM citric acid and 20 mM sodium citrate, pH 4) whilst the control group received citrate buffer alone. Animals were maintained on their respective diets for a further 5 weeks. This protocol has been shown to result in a type 2 diabetes model, as previously defined in this laboratory[179].

2.1.2 Measurement of blood plasma metabolites

Fasted blood samples were obtained from the saphenous vein during 1.5% isoflurane anaesthesia. Terminal blood was taken from tail pricks during terminal anaesthesia. The Accu-chek compact plus (Accu-chek, Roche, UK) was used to determine blood glucose concentrations from blood drops. Plasma was separated via centrifugation at 16,000 g for 10 minutes at 4°C and stored at -80°C for subsequent analyses. Plasma was analysed on an ABX Pentra 400 system (Horiba ABX diagnostics) for; glucose, triglycerides and non-esterified fatty acids.

2.2 LANGENDORFF HEART PERFUSION

2.2.1 Krebs-Henseleit buffer preparation

Krebs-Henseleit (KH) buffer (see section 2.9) was prepared and filtered at 0.45 μm. For the modified KH buffer (see section 2.9) fatty acid-free bovine serum albumin (BSA) (Lampire, USA) was bound to 0.4 mM palmitate before being dialysed overnight against the BSA and palmitate-free KH buffer. Immediately prior to use free calcium, sodium and potassium concentrations were measured using a Radiometer blood gas analyser and adjusted to 1.75 mM, 118 mM and 4.7 mM respectively.

2.2.2 Retrograde Langendorff perfusion

Rodents were anaesthetised with an intraperitoneal injection of sodium pentobarbital (700 μL) and hearts rapidly excised, weighed and arrested in ice-cold modified KH buffer. For each heart, the aorta was then dissected free and the heart rapidly cannulated via the aorta. Modified KH buffer (37^{o}C, oxygenated with 95% O_2, 5% CO_2) was used to perfuse the heart in a recirculating, retrograde Langendorff mode at a constant hydrostatic pressure of 100 mmHg.

2.2.3 Haemodynamic measurements

A phenylphosphonic acid (100 mM) filled Clingfilm balloon was inserted into the left ventricle through an incision made into the left atrium, via the mitral valve. The Clingfilm balloon was filled to achieve an end-diastolic pressure (EDP) of between 3-5 mmHg. This balloon was connected to a pressure transducer via polyethylene tubing and signal acquired via a bridge amplifier connected to a PowerLab data acquisition system (ADinstruments, Oxfordshire, UK). The heart was allowed to equilibrate for 10 minutes, at the end of which the EDP was re-adjusted if needed to between 3-5 mmHg. All haemodynamic measurements were analysed using LabChart 8 reader (ADInstruments) with data collated and measurements averaged for every minute of the perfusion.

2.2.4 ^{31}P-NMR measurements

The beating, perfused heart was placed into a glass NMR sample tube (bore of 20 mm) and lowered, into the isocentre of an 11.7 T vertical bore MR scanner (Magnex scientific), maintaining a constant

hydrostatic pressure of 100 mmHg at all times. A temperature-controlled dual tune $^{1}H/^{31}P$ volume coil was used for ^{31}P-MRS measurements tuned to 202.46 MHz for phosphorous. The hearts were contained entirely within the NMR-sensitive volume of the coil and so NMR spectra obtained were of the whole heart. After the acquisition of appropriate localiser gradient echo scans to verify that the heart was correctly located in the coil, simple pulse/acquire ^{31}P was performed for approximately five minutes (10 second TR, 32 averages, 90° flip angle, 10 kHz, 2048 complex points). Owing to time considerations the flip angle was not calibrated for each heart, but rather on one separate acquisition. As conductive Krebs-Henseleit buffer dominates coil loading effects this was assumed to be applicable for all subsequent experiments.

Following simple pulse/acquire spectroscopy, a saturation transfer protocol was implemented to estimate the reverse rate constant for ATP synthesis as outlined previously[180]. This protocol consists of the saturation of PCr and Pi, nulling magnetisation in exchanging metabolites, with the saturation duration iterated over. The saturation pulse consisted of a dual-band saturation pulse designed by an optimal control algorithm originally repurposed for the technically similar problem of accelerated simultaneous multi-slice imaging[181] (5 second TR, 16 averages per time point, 10 kHz acquisition bandwidth, 2048 complex points).

The dual-frequency specific saturation pulse was 50 ms long and [0, 6, 11, 23, 90] iterations of the pulse were played, corresponding to total saturation duration of [0, 0.3, 0.55, 1.15, 4.5] seconds. The pulse was numerically optimised to avoid partially saturating other resonances and had a particularly "clean" stop-band outside of its designed window of saturation. Additional power-calibration experiments, carried out by Dr. Jack J. Miller, verified that the correct frequency-domain saturation behaviour, and time-domain kinetics, were observed for these novel pulses. All magnet protocol development and pulse sequence generation were carried out by Drs. Jack J. Miller and Angus Z. Lau.

Upon completion of the saturation transfer perfusion protocol, three pulse/acquire ^{31}P measurements (10 second TR, 16 averages, 90° flip angle, 10 kHz, 2048 complex points) were carried out to generate a standard curve, relating signal to the absolute concentration of phosphorous, through the internal PPA standard. In between each pulse/acquire, the internal balloon was inflated with 10 μmole PPA.

All ^{31}P-NMR data were peak-fitted using the AMARES algorithm[182] within the jMRUI software package[183,184]. Spectra were curve-fitted using Lorentzian line shapes and PCr was assigned as 0 ppm. In accordance with previous literature[180] the results of each transient saturation transfer protocol, composed of the full sequence of saturation times, were fitted to the equation below using the user-defined equation function within the nonlinear regression set of GraphPad Prism:

$$Y = Mo - \left(k \times \tau \left(1 - e^{\frac{-x}{\tau}}\right)\right)$$

Y the saturation time

X the metabolite concentration (at t=Y)

Mo the initial metabolite concentration (at t=0)

k the rate constant

τ related to the T_1 by $1/\tau = 1/T1 + k$

2.2.5 Langendorff perfusion rig

The measurement of high energy phosphates in this fashion required the creation of a Langendorff perfusion rig which was magnet compatible and could maintain constant hydrostatic perfusion pressure when lowered 150 cm into the bore of an 11.7 T vertical magnet. This was achieved through modification of a rig designed by Dr. M. Cole where both buffer reservoirs and the lung were mounted onto a wooden frame which could be lowered along with the heart, maintaining a constant distance, and so pressure, between the lung and heart (figure 2.1).

The lung/reservoirs and umbilical were maintained at 37°C using two separate water baths, which were oxygenated with 95% O_2, 5% CO_2 to prevent any buffer deoxygenation. In addition, the bore of the magnet was warmed to 37°C with a temperature controlled hot air blower placed beneath the bore.

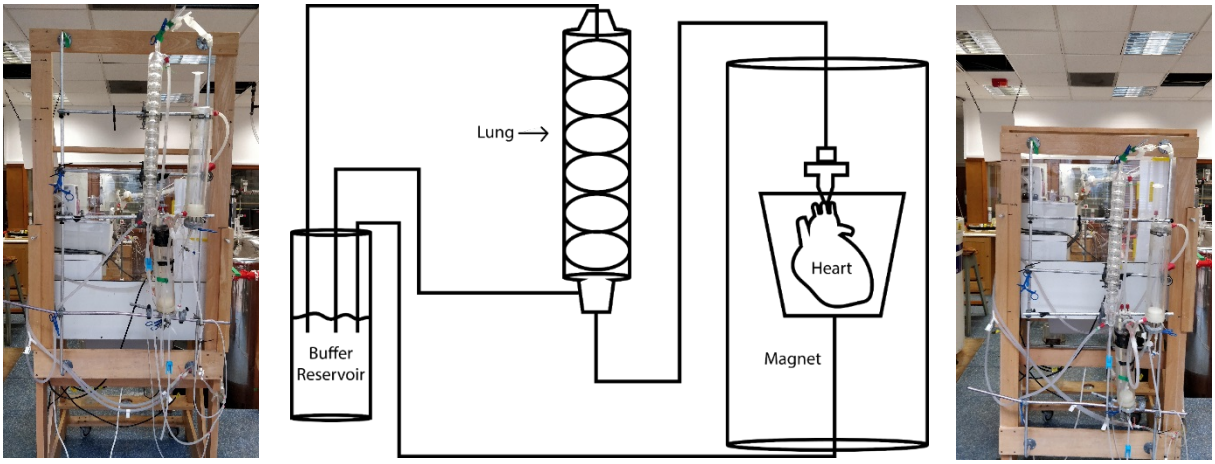

Figure 2.1 – The Langendorff perfusion rig employed to measure high energy phosphates in actively contracting hearts. The heart was cannulated on the end of a 200 cm umbilical, which was maintained at a constant temperature of 37°C and which could be lowered within the bore of the 11.7 T magnet experiments were carried out on. The lung and buffer reservoirs were mounted on a wooden frame, which could be lowered at the same time, and to the same extent, as the heart thus maintaining a constant hydrostatic pressure upon the heart.

2.3 MITOCHONDRIAL ISOLATION AND RESPIRATION

2.3.1 Mitochondrial isolation

Hearts were excised under terminal isoflurane anaesthesia. Buffers (see section 2.9) were maintained at 4°C throughout. Sub-sarcolemmal (SSM) and interfibrillar mitochondria (IFM) were isolated from the heart using a method modified from Palmer *et al.*[46]. The hearts were taken and stored in MIS1 before being homogenised in MIS2. SSM were extracted from this homogenate through polytron and Potter-Elvejhem homogenisation and IFM extracted through trypsin digestion (5 mg/gww) and further homogenisation. Mitochondria were then purified through differential centrifugation (at 3020 g) before being re-suspended in 0.4 mL MIS3.

2.3.2 Mitochondrial respiration

Mitochondrial respiration was measured using a Clark-type oxygen electrode (Strathkelvin, UK) at 30°C, as previously described[185]. Mitochondria were incubated in respiration media (see section 2.9) and respiration measured using a range of substrates; Palmitoyl-CoA (10 µM) and carnitine (5 mM), palmitoyl-carnitine (10 µM), glutamate (20 mM), pyruvate (10 mM) and malate (5 mM). State 3

respiration was induced with 200 µM ADP, and maximal (uncoupled respiration) induced with 5 µM FCCP. Traces were analysed with the Strathkelvin 782 oxygen system v3.0.

2.3.3 Mitochondrial membrane potential measurements

Respiration media (see section 2.9) was supplemented with 5 µM Safranine O and 1.875 mg/mL mitochondria and all experiments carried out in a 96-well black plate (Grenier Bio-one 655076). After establishment of a baseline, substrates were added (as described in detail in section 4.5.3 and section 5.4.3) and fluorescence measured at an excitation wavelength of 495 nm and emission wavelength of 586 nm using a FLUOstar Omega (BMG Labtech).

For the measurement of absolute membrane potentials a potassium clamp was set up as first described by Akerman and Wikstrom[186]. Valinomycin (40 ng/mL) was added before potassium was titrated in (0.375 mM KCl for the first three measurements, then 0.5 mM for the second 3 measurements, and finally 0.75 mM for the last 3 measurements). Between KCl additions, a steady state of the fluorescence was established. The membrane potential was calculated using the Nernst equation, defined below:

$$\Delta\Psi = 60 \times \log \frac{K_{in}^{+}}{K_{out}^{+}}$$

$\Delta\Psi$ denotes the mitochondrial membrane potential

K_{in}^{+} was taken to be 120 mM[187]

K_{out}^{+} represents the potassium concentration added

2.4 WESTERN BLOTTING

2.4.1 Protein lysis

Lysis buffer (see section 2.9) was added at 10 µL/mg to powdered, frozen cardiac tissue. The sample underwent Polytron homogenisation and was boiled for 5 minutes. Protein content was measured (see section 2.6.1) and β-mercaptoethanol added to 5% of the total volume, prior to heating at 70°C for 5 minutes.

2.4.2 Electrophoresis

Protein (30 µg) was loaded onto an SDS-PAGE gel (NuPAGE™ 4-12% Bis-Tris Midi Protein Gels, 20-well) and separated with an applied voltage of 200 V for 55 minutes using electrophoresis buffer (NuPAGE™ MOPS SDS running buffer – Thermofisher). The gel was then transferred onto nitrocellulose membranes (Biotrace NT – Pall Corporation) at 180 mA for 1 hour in transfer buffer (see section 2.9). Even loading across lanes was ensured by Ponceau S staining of bands and membranes were blocked with 5% milk (dissolved in TBS-Tween) for 1 hour at room temperature. Membranes were incubated overnight at 4°C with primary antibody (see section 2.4.4 for dilutions). Membranes were then washed with TBS-Tween and incubated with an appropriate secondary antibody (see section 2.4.4) for one hour. The blot was washed for a further 30 minutes with TBS-Tween and developed with the Licor C-Digit, using enhanced chemiluminescence (Amersham ECL Prime western Blotting Detection Reagent).

2.4.3 Antibody generation

There are no commercially available antibodies that can satisfactorily differentiate between AAC isoforms 1 and 2, therefore custom-made antibodies were generated. A sequence alignment of AAC1 and 2 revealed that residues 144-157 displayed significant divergence. Eurogentec used these peptide sequences (DV GKG SSQ REF NGL G for AAC1, DV GKA GAE REF KGL G for AAC2) to raise antibodies, which showed good activity and high specificity, for their peptides. To ensure expected specificity tissue expression profiles were carried out on the final product according to published data[73]. These expression patterns followed expected values and showed the high expression in isolated mitochondrial samples (figure 2.2).

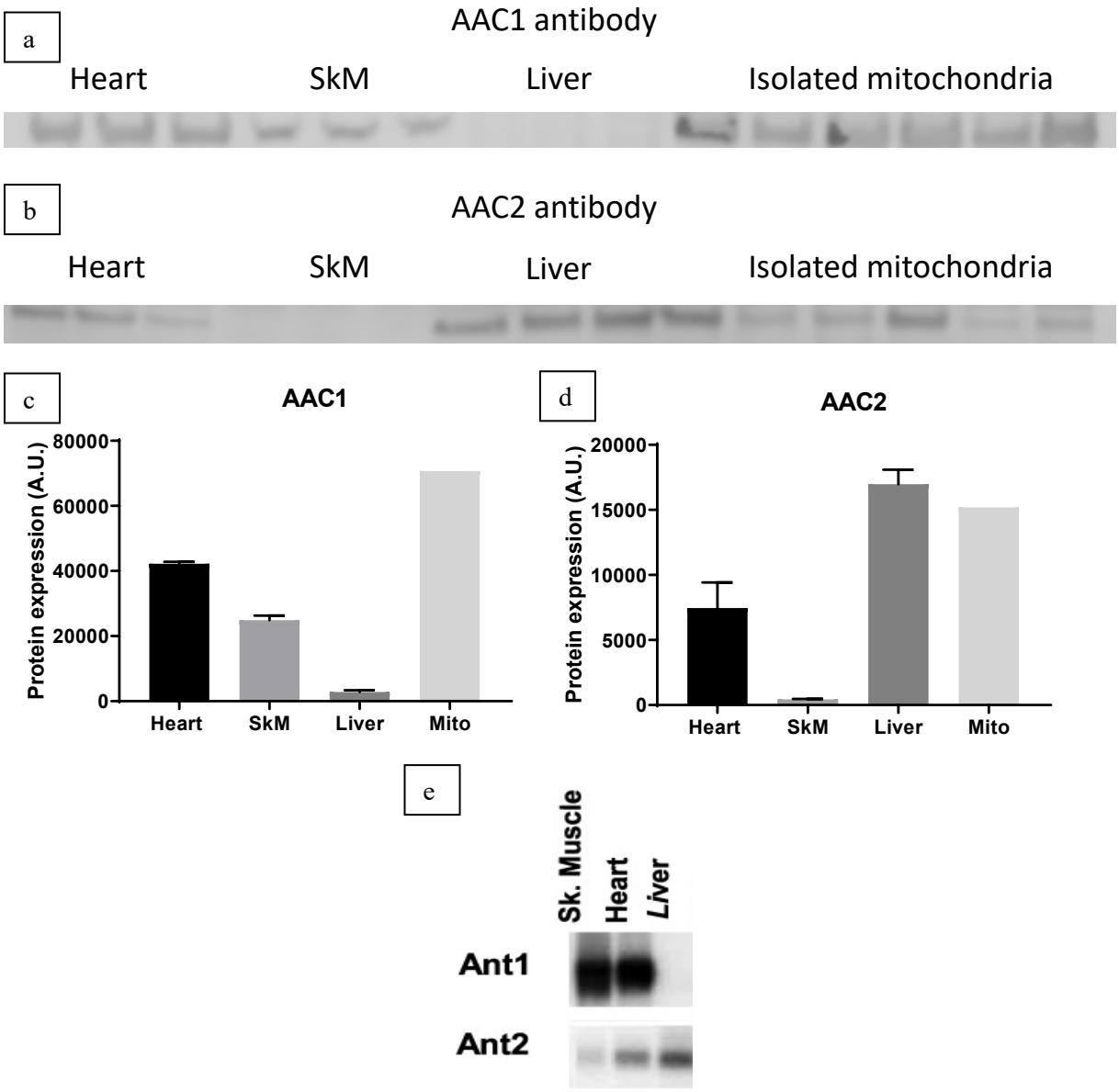

Figure 2.2 – Representative western blots of protein lysates from; heart tissue, skeletal muscle (SkM) tissue, liver tissue, or mitochondria isolated from the heart, blotted with either the generated AAC1 (a) or AAC2 (b) antibody as denoted. Analysis of the western blots (c,d) agree well with expected data (e), adapted from Kokoszka *et al*[73]. showing AAC1 and AAC2 protein expression in different tissues.

2.4.4 Antibodies used

Table 2.3 – Antibodies used over the course of this work, with appropriate dilutions.

Protein target	Antibody	Primary dilution (5% milk)	Secondary dilution (5% milk)
Cyclophilin b	**Ab178397**	**1:1000**	**1:2000**
GDH1	**Ab166618**	**1:1000**	**1:2000**
Sirt3	**Ab86671**	**1:1600**	**1:2000**
Acetyl-lysine (rabbit)	**9441S**	**1:2000**	**1:2000**
Acetyl-lysine (mouse)	**9681S**	**1:2000**	**1:2000**
PPARγ	**Ab209350**	**1:1500**	**1:1000**
AAC1	**Custom generated**	**1:2000**	**1:2000**
AAC2	**Custom generated**	**1:1000**	**1:2000**
Anti-rabbit (2°)	**Ab6721**		
Anti-mouse (2°)	**Ab97023**		

GDH: Glutamate dehydrogenase, Sirt3: Sirtuin 3, PPARγ: Peroxisomal proliferation activated receptor 1, AAC1: ATP/ADP carrier 1, AAC2: ATP/ADP carrier 2

2.5 MOLECULAR BIOLOGY ANALYSIS

2.5.1 Genomic DNA extraction

DNA was extracted from frozen cardiac tissue using the Qiagen DNeasy blood and tissue kit, following the manufacturer's instructions. DNA concentrations were measured using the NanoDrop^{TM}UV spectrometer and samples stored at -80°C until further use.

2.5.2 RNA extraction and cDNA conversion

RNA was extracted from frozen cardiac tissue using the Qiagen RNeasy Mini Kit, following the manufacturer's instructions. RNA concentrations were measured using the NanoDrop^{TM}UV spectrometer. RNA (1 μg) was converted into cDNA using the high capacity cDNA reverse transcriptase kit (Applied Biosystems) according to the manufacturer's protocol.

2.5.3 Quantitative Polymerase Chain Reaction

qPCR was performed using the SYBR detection method (Applied Biosystems). Samples were loaded as a 20 μL reaction volume containing 12.5 ng cDNA, with 10 μL of SYBR reagent master mix and 1 μM primers. Samples were loaded onto 96-well qPCR plates (MicroAmp fast, applied Biosystems) and a standard SYBR cycle was applied, using a StepOnePlus Real-Time PCR system (Applied Biosystems). Analysis was carried out by the ΔΔCt methodology. Primers were produced by Sigma Aldrich UK and designed using Primer Blast 2, as follows:

1. Cytochrome B (mtDNA)
    a. Sense GGGTATGTACTCCCATGAGGAC
    b. Antisense CCTCCTCAGATTCATTCGAC
2. GAPDH (nuclear DNA)
    a. Sense AGTATGTCGTGGAGTCTACTGGTG
    b. Antisense TGAGTTGTCATATTTCTCGTGGTT
3. AAC 1 (AAC 1 expression)
    a. Sense AGCAGTTCTGGCGCTACTTC
    b. Antisense CCATTGAACTCACGCTGGGA
4. AAC 2 (AAC 2 expression)
    a. Sense CAAAGGGAATGCTCCCGGAT
    b. Antisense ATCTTCCGCCAGCAGTCAAG
5. HPRT (Housekeeper)
    a. Sense CTCATGGACTGATTATGGACAGGAC
    b. Antisense GCAGGTCAGCAAAGAACTTATAGCC
6. SDHA (Housekeeper)
    a. Sense TCCTTCCCACTGTGCATTACAA
    b. Antisense CGTACAGACCAGGCACAATCTG

2.6 BIOCHEMICAL ASSAYS

2.6.1 Protein assay

Protein concentrations were determined by the Pierce bicinchoninic acid method, following kit instructions (Pierce BCA protein assay kit – ThermoFisher Scientific). Mitochondrial proteins were first solubilised with 5% triton.

2.6.2 Citrate synthase assay

The established protocol of Darley-Usmar *et al.*[188] was modified as follows: powdered frozen cardiac tissue was added to citrate synthase homogenisation buffer (section 2.9) at 15 mgs/mL and underwent Polytron homogenisation. Triton (10 μL/mL) was added and the sample incubated for 1 hour at 4°C prior to centrifugation at 1,000rpm at 4°C. This supernatant was added to citrate synthase assay buffer (see section 2.9) at a 1:3:5 ratio (supernatant: buffer: ddH_2O) and incubated at 30°C for 4 minutes.

Following this, oxaloacetate (500 µM) was added and reaction kinetics followed at 412 nm for 4 minutes (at 30°C).

2.6.3 Electron transport chain complex activity assays

The established protocols of Darley-Usmar *et al.*[188] were modified as follows:

Complex I: Freeze-thawed mitochondria (20 µg protein) were added to 1 mL of complex 1 assay buffer (see section 2.9) and reaction kinetics followed at 340 nm for 1 minute at 30°C. Rotenone (5.1 µM) was added to measure background activity.

Complex II: Freeze-thawed mitochondria (20 µg protein) were added to 985 µL of complex 2 assay buffer (see section 2.9) and the sample incubated for 10 minutes at 30 °C. Complex 2 inhibitory buffer (10 µL) (see section 2.9) was added and reaction kinetics followed for 1 minute at 600 nm at 30°C. 5 µL of coenzyme Q (13 mM) was added, and reaction kinetics followed at 600 nm for a further 2 minutes.

Complex III: Freeze-thawed mitochondria (20 µg protein) were added to 1 mL of complex 3 assay buffer (see section 2.9) at 30°C. Decycloubiquinol (16 µM) was added, and reaction kinetics followed at 550 nm for 1 minute at 30°C.

Complex IV: Freeze-thawed mitochondria (10 µg protein) were added to 1 mL of complex 4 assay buffer (see section 2.9) at 30°C. Reaction kinetics were followed for 3 minutes at 550 nm, against a blank of 1 mM potassium ferricyanide at 30°C.

2.6.4 Pyruvate dehydrogenase assay

Freeze-thawed mitochondria (10 µg protein) were assayed for PDH activity according to the manufacturer's protocol. (MAK183-1KT).

2.6.5 Malate dehydrogenase assay

Freeze-thawed mitochondria (10 µg protein) were assayed for MDH activity according to the manufacturer's protocol. (MAK196-1KT).

2.6.6 Glutamate dehydrogenase assay

Freeze-thawed mitochondria (10 μg protein) were assayed for GDH activity according to the manufacturer's protocol. (MAK099-1KT).

In addition, GDH activity was also assayed using a protocol adapted from Passoneau et al.[189] Freeze-thawed mitochondria (40 μg protein) were added to 960 μL of glutamate dehydrogenase assay buffer (section 2.9). Substrates (2 mM α-ketoglutarate and 25 mM ammonium acetate) were added alongside 100 μM ADP, 200 μM NADH and 2.5 μg rotenone and reaction kinetics followed at 340 nm for 2 minutes.

2.6.7 α-ketoglutarate dehydrogenase assay

Freeze-thawed mitochondria (10 μg protein) were assayed for α-KGDH activity according to the manufacturer's protocol. (MAK189-1KT).

2.6.8 ATP synthase assay

Freeze-thawed mitochondria (8 μg protein) were assayed for ATP synthase activity according to the manufacturer's protocol (ab109714-96).

2.7 LIPIDOMICS

2.7.1 Extraction

The protocol of Hoppel *et al.*[190] for isolation of long-chain acyl-coenzyme esters was modified as follows: powdered, frozen cardiac tissue was suspended in a 3:1 mix of acetonitrile and isopropanol at 1 μL/mg. KH_2PO_4 (0.5 mL of 0.1 M at pH 6.7) was added and the mixture vortexed. Samples were centrifuged at 16,000 g for 5 minutes. The supernatant was removed and acidified by the addition of 0.25 mL of glacial acetic acid.

An SPE column (2-(2-pyridyl) ethyl functionalised silica gel – Supelco 54127-U) was conditioned with 1 mL of acetonitrile: isopropanol: water: acetic acid (9:3:4:4) (conditioning solution). The sample was then applied to this column and the column washed with the conditioning solution. Acyl-CoA esters

were eluted with 10 mL of methanol and ammonium formate (4:1). The elutant was immediately placed on dry ice, before analysis was carried out via mass spectrometry.

2.7.2 Mass spectrometry analysis

The HPLC-MS procedure was carried out by Dr. George Berridge at the Nuffield Department of Medicine as follows: dried lipids were reconstituted in 60% acetonitrile and 2 µL of sample injected for LC separation. Samples were injected onto a Waters C18 column (BEH, 2.1 mm x 150 mm, 1.7 µM) and eluted at a flow of 0.2 mL/min using the following gradient:

0-5 min: 95% A, 05% B
5-7 min: 50% A, 50% B
7-30 min: 5% A, 95% B
30-35 min: 95% A, 5% B

Solvent A: 60% acetonitrile, 10 mM ammonium formate
Solvent B: 90% isopropanol, 10% acetonitrile, 10 mM ammonium formate

MS was carried out using an Agilent 6560 IM-QToF, and data collected in QToF only mode. Integrated areas of the target analytes were extracted using MassHunter Qualitative software version B.07.

Targeted lipidomics were carried out for palmitoyl-CoA (P-CoA) and oleoyl-CoA (O-CoA). Standard curves were generated, as shown in figure 2.3, allowing for the calculation of absolute concentrations of fatty acyl-CoA moieties in cardiac samples.

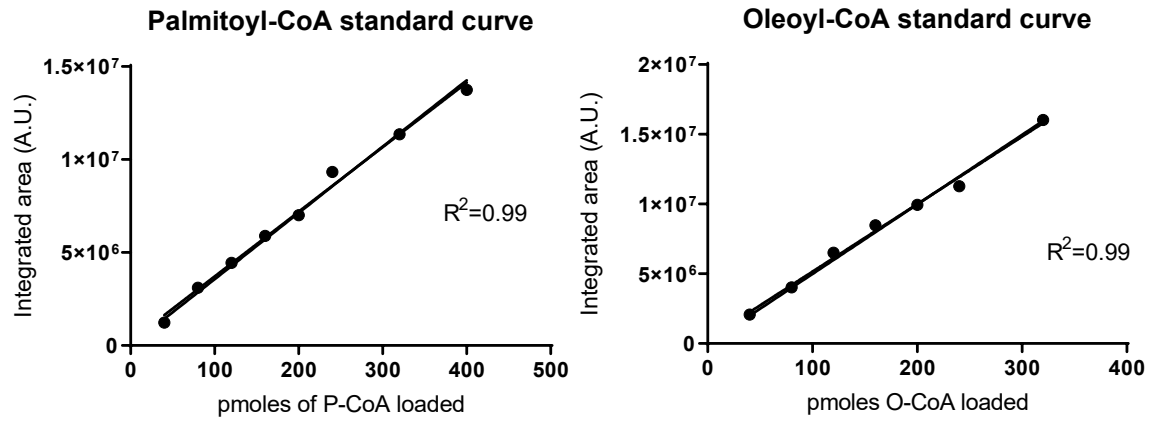

Figure 2.3 – Standard curves generated by loading multiple dilutions of both P-CoA and O-CoA onto the mass spectrometer show good linearity.

2.8 ACETYL-LYSINE IMMUNOPRECIPITATION

2.8.1 Sample preparation

Anti-acetyl-lysine antibody (5 µg) was incubated with 30 µL of Smart digest protein A (ThermoFisher) for 4 hours and the resin washed 3 times with PBS. Lysed mitochondrial protein (200 µg) diluted in 500 µL of PBS-T was added to 30 µL of the bead-antibody conjugate and incubated overnight at 4°C with rotation. The bead-antibody-antigen conjugate was pelleted and the supernatant aspirated. 400 µL of wash buffer was added and the conjugate pelleted again. This wash was repeated 4 times, after which the bead-antibody conjugate was suspended in 200 µL of Smart digest 1A buffer. Samples were heated at 70°C for 4 hours to ensure trypsin digestion.

2.8.2 Proteomic analysis

The mass spectrometry procedure was carried out by Dr. George Berridge at the Nuffield Department of Medicine. Samples were prepared following the Sep-Pak C18 purification method using the Sola cartridges for low amounts of peptides. Samples were resuspended into 10 µL proteomic spectroscopy buffer (see section 2.9) and 1 µL was loaded onto a C18 column and eluted with an acetonitrile gradient from 2-45% containing 0.1% trifluoroacetic acid and 1% DMSO into the Fusion Lumos Mass spectrometer. The data was aligned using Progeneis software and searched against a Rat database with PEAKS 8.5.

Statistics were performed using Perseus with assistance from Dr. Roman Fischer at the Nuffield Department of Medicine. Proteins with no unique peptides were deleted and the remaining values transformed by $\log_2$ and medians subtracted for normalisation. Missing values were imputed based on the normal distribution and multi-scatter plots were used as a quality control. Data were analysed and interpreted using principle component analysis, hierarchical clustering and volcano plots.

2.9 BUFFERS

Buffer	Components
Krebs-Henseleit (KH) buffer	118 mM NaCl, 4.7 mM KCl, 1.2 mM $MgSO_4 \cdot 7H_2O$, 1.75 mM $CaCl_2 \cdot 2H_2O$, 0.5 mM Na_2EDTA, 11 mM glucose, 25 mM $NaHCO_3$, 1.2 mM KH_2PO_4
Modified KH buffer	As above, with 1.5% bovine serum albumin (BSA), 0.4 mM palmitate
Mitochondrial isolation solution 1 (MIS1)	100 mM KCl, 50 mM MOPS, 5 mM $MgSO_4$, 1 mM EGTA, 1 mM ATP, pH 7.4
Mitochondrial isolation solution 2 (MIS2)	100 mM KCl, 50 mM MOPS, 5 mM $MgSO_4$, 1 mM EGTA, 1 mM ATP, pH 7.4, 2 mg/mL BSA, 10 mM nicotinamide, 500 nM Trichostatin A
Mitochondrial isolation solution 3 (MIS3)	100 mM KCl, 50 mM MOPS, 0.5 mM EGTA, 10 mM nicotinamide, 500 nM Trichostatin A
Respiration media	100 mM KCl, 50 mM MOPS, 1 mM EGTA. 5 mM KH_2PO_4, 1 mg/mL BSA
mPTP assay buffer	0.2 M sucrose, 10 mM Tris, 10 mM MOPS, 5 mM sodium succinate dibasic hexahydrate, 10 μM EGTA, 0.5 mM sodium dihydrogen phosphate, 2 μM rotenone, pH 7.4
Lysis buffer	75 mM Tris-HCl, 3.8% SDS, 4 M urea, 20% glycerol, 10 mM nicotinamide, 500 nM Trichostatin A
Western blot transfer buffer	25 mM Tris-Base, 192 mM Glycine, 20% methanol
TBS-Tween	150 mM NaCl, 20 mM Tris, 0.1% Tween 20, pH 7.4
Citrate synthase assay homogenisation buffer	100 mM imidazole, 1 mM EGTA, 5 mM $MgCl_2$, pH 7.2

Citrate synthase assay buffer	1 M Tris-HCl, 1 mM dithionitrobenzoic acid, 140 µM acetyl-coenzyme A, pH 8.1
Complex 1 assay buffer	18 mM K_2HPO_4, 7 mM KH_2PO_4, 5 mM $MgCl_2$, 130 µM NADH, 65 µM Coenzyme Q1, 2.5 mg/mL BSA, 3.6 µM Antimycin A, pH 7.2
Complex 2 assay buffer	18 mM K_2HPO_4, 7 mM KH_2PO_4, 5 mM $MgCl_2$, 2 mM sodium succinate dibasic hexahydrate, pH 7.2
Complex 2 inhibitory buffer	2 mg/L antimycin A, 1 mg/L rotenone, 50 µM dichlorophenolindophenol
Complex 3 assay buffer	36 mM K_2HPO_4, 14 mM KH_2PO_4, 3 mM sodium azide, 1.5 µM rotenone, 616 mg/L cytochrome C, pH 7.2
Complex 4 assay buffer	6.2 mM K_2HPO_4, 3.9 mM KH_2PO_4, 50 µM reduced cytochrome C, pH 7.0
Glutamate dehydrogenase assay buffer	50mM imidazole, 0.05% BSA
PBS	10 mM Na_2HPO_4, 137 mM NaCl, 1.8 mM KH_2PO_4, 2.7 mM KCl, pH 7.4
PBS-Tween	As above, with 0.05% Tween 20, pH 7.4
Proteomic spectrometry buffer	98% MilliQ-H_20, 2% CH_3CN, 0.1% trifluoroacetic acid

3 ENERGETIC IMPAIRMENT IN THE TYPE 2 DIABETIC HEART

3.1 ABSTRACT

Reduced ratios of phosphocreatine (PCr) / adenosine triphosphate (ATP), a common indicator of energetic health, have been reported in type 2 diabetic (T2D) patients. However, this indicator is insensitive to decreases in both PCr and ATP, therefore may not report the full profile of cardiac dysfunction. Over 95% of ATP generation within the heart occurs within mitochondria, making them the logical source of energetic failure, yet no study has measured rates of whole heart ATP synthesis and associated these with rates of respiration in isolated mitochondria. In this work cardiac energetics have been elucidated in a rodent model of T2D through the measurement of absolute concentrations of ATP and PCr, as well as through assessment of rates of ATP synthesis. These whole heart rates of ATP synthesis were subsequently related to the source of dysfunction - isolated cardiac mitochondria.

To investigate whole heart energetics, T2D and control hearts were perfused in Langendorff mode, and high energy phosphates measured with ^{31}P-NMR. Absolute concentrations of PCr and ATP were decreased in T2D hearts by 18% and 12%, respectively. As these decreases were of similar magnitudes there was no net change in the PCr/ATP ratio. This energetic dysfunction was manifest even in the absence of functional impairment within these hearts in this early stage model of T2D. Analysis of the rate of ATP degradation, through saturation transfer experiments, revealed that T2D hearts had a 61% reduction in ATP turnover indicating severely reduced rates of ATP synthesis. Mitochondrial respiration was measured using a Clark-type oxygen electrode in mitochondrial sub-populations isolated from control and T2D rodent hearts. ADP-stimulated respiratory rates were 12% and 24% lower in T2D mitochondrial sub-populations when respired in the absence of fatty acids.

T2D hearts therefore display energetic dysfunction, even before functional impairment, which can present without a significant decrease in the PCr/ATP ratio. This energetic dysfunction is revealed as reduced ATP turnover, which can be linked to reduced rates of mitochondrial respiration within the T2D heart.

3.1 INTRODUCTION

Cardiovascular disease is the primary source of mortality within T2D and the energetic status of the heart has emerged as a strong predictor of this cardiovascular mortality risk. The PCr/ATP ratio has been adopted as a clinical marker of available high energy phosphates in the heart[3–5,13,191–193] with patients who present with more energetically dysfunctional hearts (as measured by decreased PCr/ATP ratios) significantly more likely to suffer cardiovascular related death[11]. In agreement with their elevated risk, T2D patients present with significantly decreased cardiac PCr/ATP ratios[3,5,13].

The use of a ratio is clinically necessary because ^{31}P-MRS is a relatively low sensitivity technique such that absolute concentrations of the individual phosphorous containing metabolites cannot easily be determined. However, measurement of the PCr/ATP ratio cannot distinguish simultaneous reductions in the concentrations of both ATP and PCr. Due to this, the necessity for the measurement of absolute concentrations of high energy phosphates in the heart is becoming recognised clinically[1]. This is supported by some studies which show similar decreases in PCr and ATP, providing a potential explanation for the seemingly contradictory findings of groups looking at energetic dysfunction in the T2D heart showing decreased[3,5,13,192] or unaltered[193] cardiac PCr/ATP ratios. The placement of a phosphorous standard within the heart would enable calculation of absolute concentrations of ATP and PCr but is only possible within the perfused heart.

Although the availability of high energy phosphates is a good clinical marker for mortality, cardiac concentrations of ATP remain above those required for ATP-consuming reactions, such as the myosin-ATPase, even in end-stage heart failure[194]. This indicates that a substantial decrease in the concentration of ATP would be required before there was a detrimental effect on processes involved in contractility. A more comprehensive measure of energetic dysfunction is the rate of ATP turnover, in terms of synthesis and degradation, within the heart. This can be measured through the use of saturation transfer techniques developed by Forsen and Hoffman in the 1960s[195,196] and extended to a double saturation technique by Spencer *et al.*[180]

Energetic dysfunction, like that observed within the T2D heart[140,197] can be traced to mitochondrial dysfunction through *in silico* modelling[154]. To date however, no study has been carried out which investigates both high energy phosphates and mitochondrial function within the diabetic heart. This would give insight into both the effect, and cause, of cardiac energetic dysfunction within T2D.

3.2 AIMS

Energetic dysfunction within the heart is thought to play a key role in cardiovascular mortality within T2D but there is disagreement between studies reporting the PCr/ATP ratio. This chapter therefore aimed to investigate both the PCr/ATP ratio and absolute concentrations of PCr and ATP in the T2D heart, as well as generating a more comprehensive overview of cardiac energetics through measurement of ATP turnover. The proposed source of cardiac energetic dysfunction is mitochondrial dysfunction and so mitochondrial dysfunction was also investigated in these hearts.

This was achieved through three objectives:

1. The ratios and absolute concentrations of high energy phosphates were measured in the actively contracting control and type 2 diabetic heart.
2. Rates of ATP degradation in the T2D heart were determined.
3. Mitochondrial respiration was investigated, and dysfunction assayed through the measurement of enzyme activities involved in respiration.

3.3 METHODS

3.3.1 Langendorff perfusion with absolute measurements of PCr and ATP

Langendorff perfusions were carried out following the protocol set out in section 2.2.

3.3.2 Mitochondrial respiration

Mitochondrial respiration measurements were carried out following the protocol set out in section 2.3.

3.3.3 Mitochondrial enzyme assays

All mitochondrial enzyme assays were carried out following the protocols set out in section 2.6.

3.3.4 TMPD respiration

A 25 mM stock of [N,N,N',N'-tetramethyl-p-phenylenediamine] was made up with 250 mM L-ascorbic acid in ddH_2O at pH 7. This solution was added at a final TMPD concentration of 1 mM to 0.15 mg of mitochondria in 500 µL of respiration media (see section 2.9). State 3 measurements were then acquired by measuring oxygen consumption upon the addition of 200 µM ADP.

3.3.5 Statistical tests

Datasets containing two groups (control and diabetic) were analysed using the two-tailed parametric unpaired t test function within GraphPad Prism 8.0.0. A reported P value less than 0.05 was taken as significantly different.

3.4 RESULTS

3.4.1 The type 2 diabetic model

The combination of high fat diet feeding and low dose streptozotocin injection resulted in a T2D phenotype as evidenced by hyperglycaemia in the diabetic cohort, with a 22% increase in fed glucose concentrations (figure 3.1a) and a 31% increase in fasted glucose concentrations (figure 3.1b). In addition, the induced diabetes caused hyperlipidaemia as measured by a 243% increase in fed blood non-esterified fatty acid concentrations (figure 3.1c).

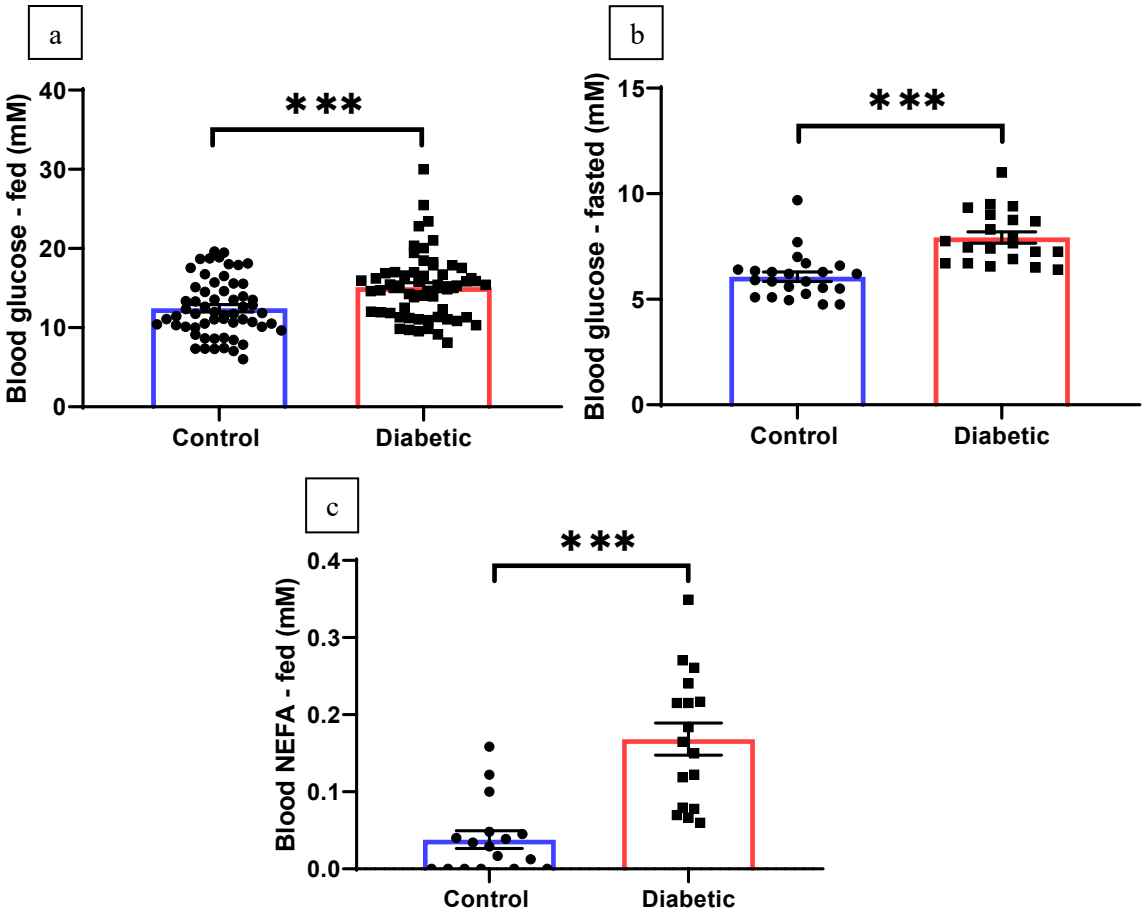

Figure 3.1 – Diabetic rodents presented with hyperglycaemia in the fed (a) and fasted (b) state, as well as fed hyperlipidaemia (c). NEFA – Non-esterified fatty acid. *** indicates P<0.001 between control and diabetic.

This model of T2D was distinct from type 1 diabetes as it induced a 6% increase in body weight (figure 3.2a) and a 55% increase in adiposity (figure 3.2b). There was no change in the heart weight/body weight ratio (figure 3.2c), indicating that there was no evidence of cardiac hypertrophy.

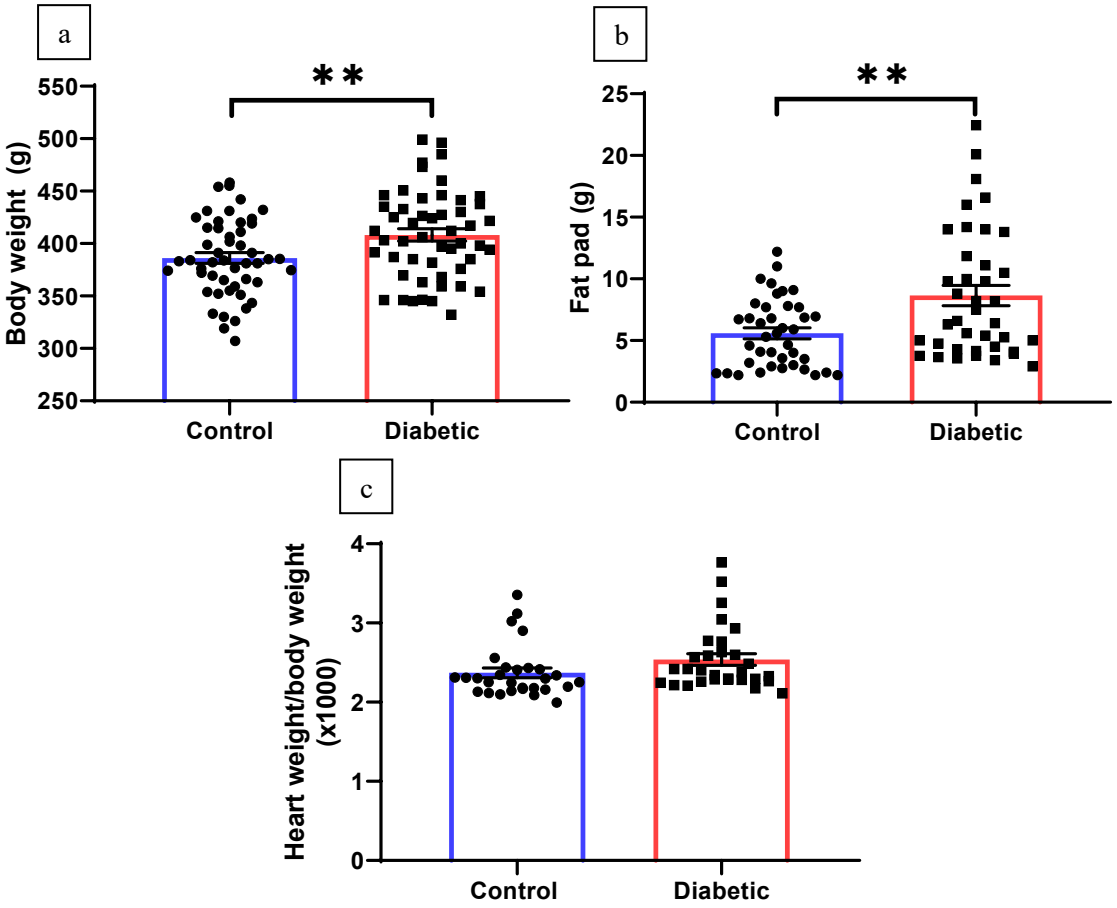

Figure 3.2 – Diabetic rodents presented with elevated body weights (a) and increased adiposity (b), without increases in the heart weight to body weight ratio (c). ** indicates $p<0.005$ between control and diabetic.

3.4.2 Type 2 diabetic hearts have dysfunctional energetics

Hearts were isolated from control and T2D rodents and perfused in a retrograde Langendorff fashion. Cardiac haemodynamic measurements were obtained through a Clingfilm balloon inserted into the left ventricle. These haemodynamic measurements showed no functional impairment associated with T2D with no difference in either developed pressure (figure 3.3a), heart rate (figure 3.3b) or end-diastolic pressure (figure 3.3c) between control and diabetic hearts.

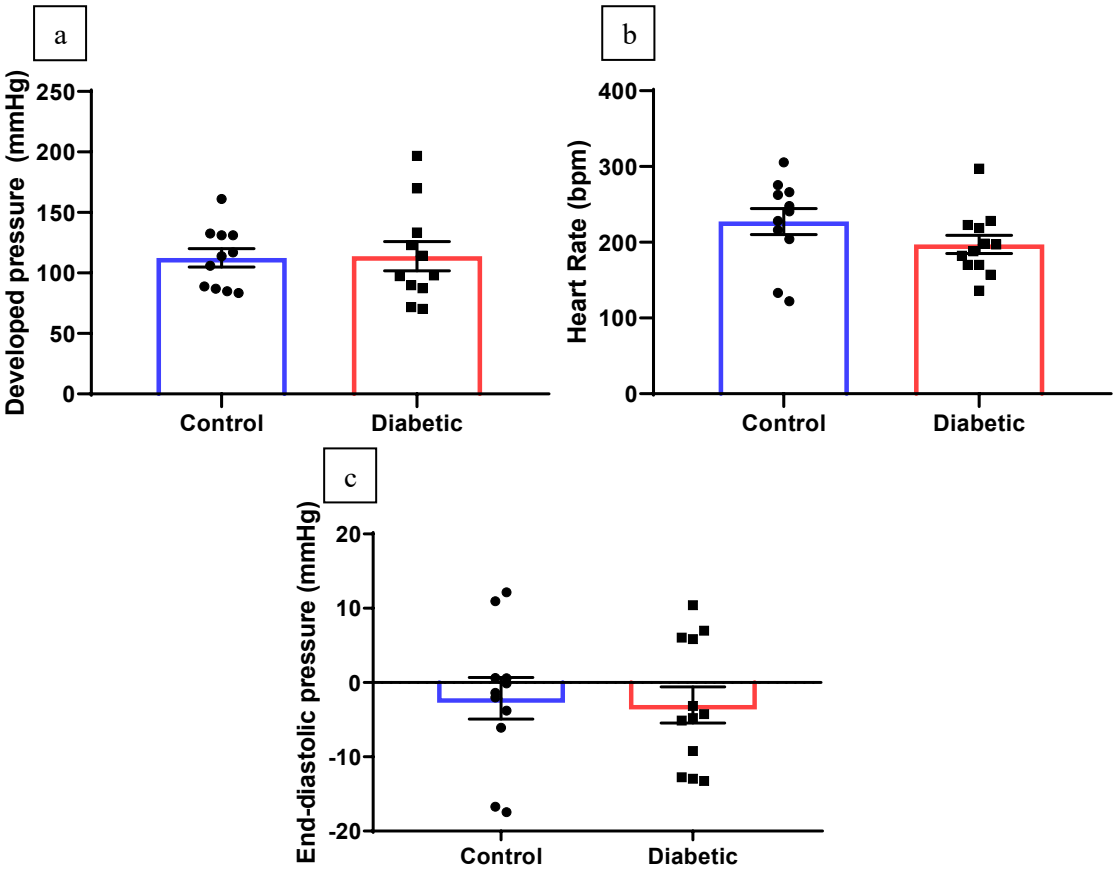

Figure 3.3 – Diabetic rodents presented with no functional impairments, as evidenced by unaltered developed pressure (a), heart rate (b) and end-diastolic pressure (c) in the retrograde Langendorff perfused heart.

For the measurement of high energy phosphates these beating perfused hearts were lowered within the bore of an 11.7 T magnet and fully relaxed ^{31}P-MRS spectra acquired (as shown in figure 3.4).

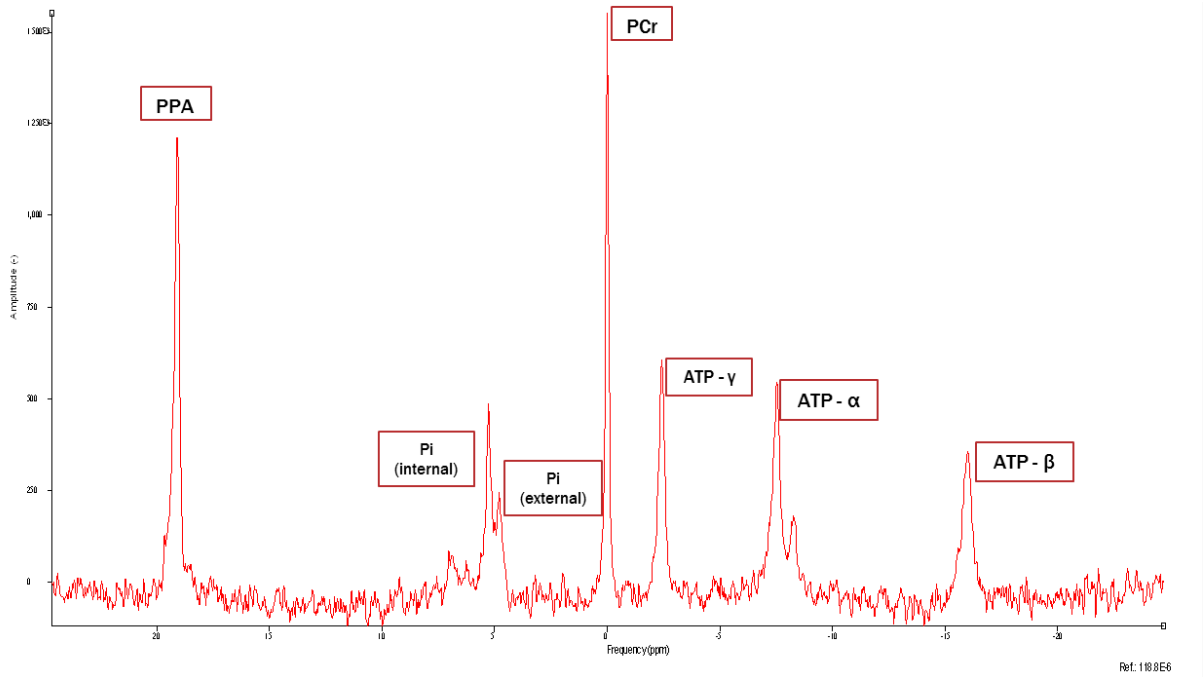

Figure 3.4 – A representative fully relaxed ^{31}P spectra, with phosphate peaks of interest labelled.

These spectra were quantified using an internal standard of phenylphosphonic acid (PPA) so that absolute quantification of ATP and PCr could be undertaken, following equation 3.1. These could then be related to absolute cardiac concentrations following equation 3.2.

Equation 3.1 – Calculating the moles of PCr in the heart

$$PCr\ (mmol) = \frac{PCr\ (a.u.)}{Calibration\ coefficient\ (\frac{a.u.}{mmol})}$$

Equation 3.2 – Calculating the concentration of PCr in the heart

$$[PCr]\ (mM) = \frac{PCr\ (mmol)}{\frac{Heart\ weight\ (g)}{Specific\ gravity\left(\frac{g}{mL}\right)}} \times Intracellular\ volume\ fraction$$

PCr (a.u.)	(the value obtained from peak integration)	Measured
Calibration coefficient	(calculated from the PPA standard curve)	Measured
Specific gravity of cardiac tissue	(converting gww to volume)	= 1.05g/mL[198]
Intracellular volume fraction	(to calculate a concentration)	= 48%[199,200]

T2D hearts were energetically dysfunctional, with a 12% reduction in the concentration of ATP (figure 3.5a) and an 18% reduction in the concentration of PCr (figure 3.5b). There was a small decrease in the cardiac PCr/ATP ratio in the T2D population but, due to the similar decrease in PCr and ATP in T2D hearts this study was underpowered to resolve significant changes in this ratio (figure 3.5c).

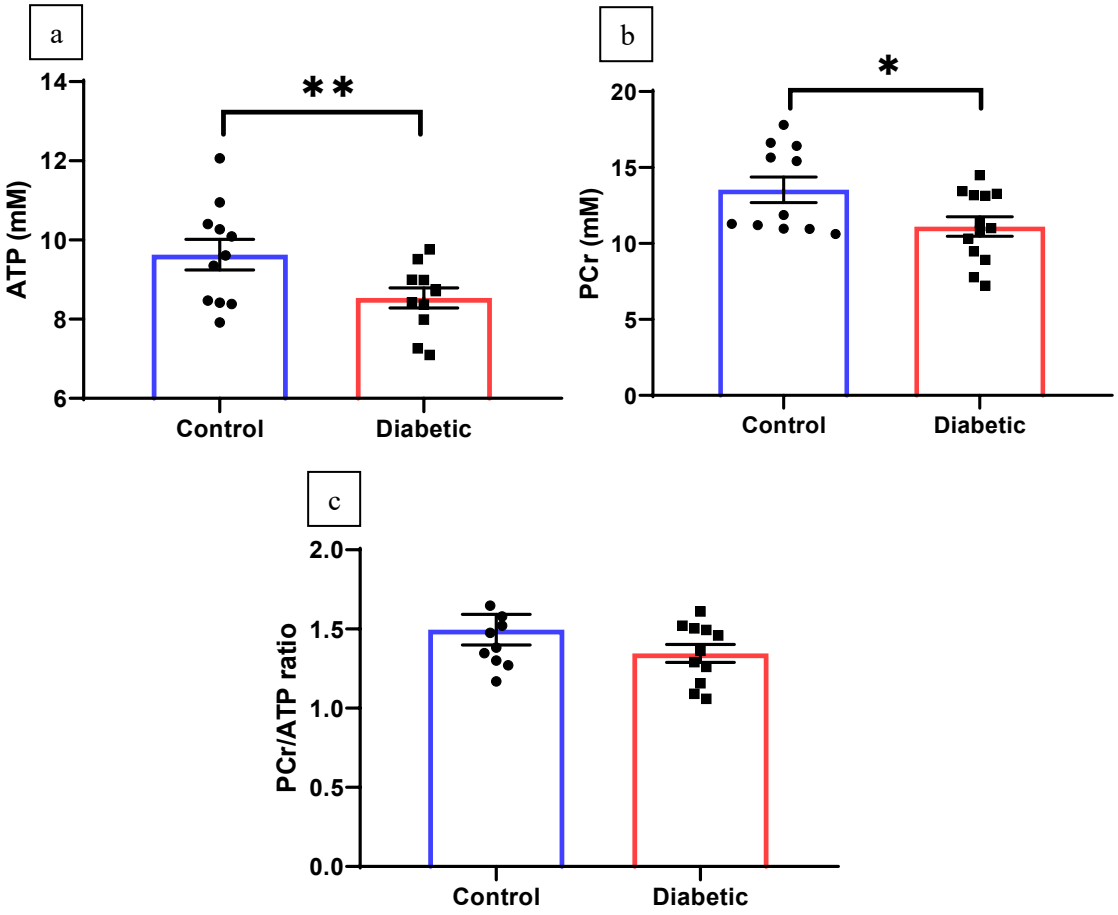

Figure 3.5 – Diabetic rodents presented with cardiac energetic dysfunction, displaying reduced concentrations of global ATP (a) and PCr (b) in the Langendorff perfused heart. The magnitude of the decrease in ATP and PCr were similar resulting in no significant change to the PCr/ATP ratio (c). * denotes P<0.05, ** denotes P<0.005 between control and diabetic.

The absolute concentrations of high energy phosphates in the heart is a good surrogate measure for energetic dysfunction yet, even in the most severe heart failure, it is rare for ATP concentrations to drop to a level below the Km of muscle contraction. Therefore, a more comprehensive read out of energetic functionality in the heart is the rate of ATP synthesis and degradation. Double resonance saturation transfer experiments, saturating both the PCr and Pi peaks (as illustrated in figure 3.6), were carried out to measure the rate of ATP degradation.

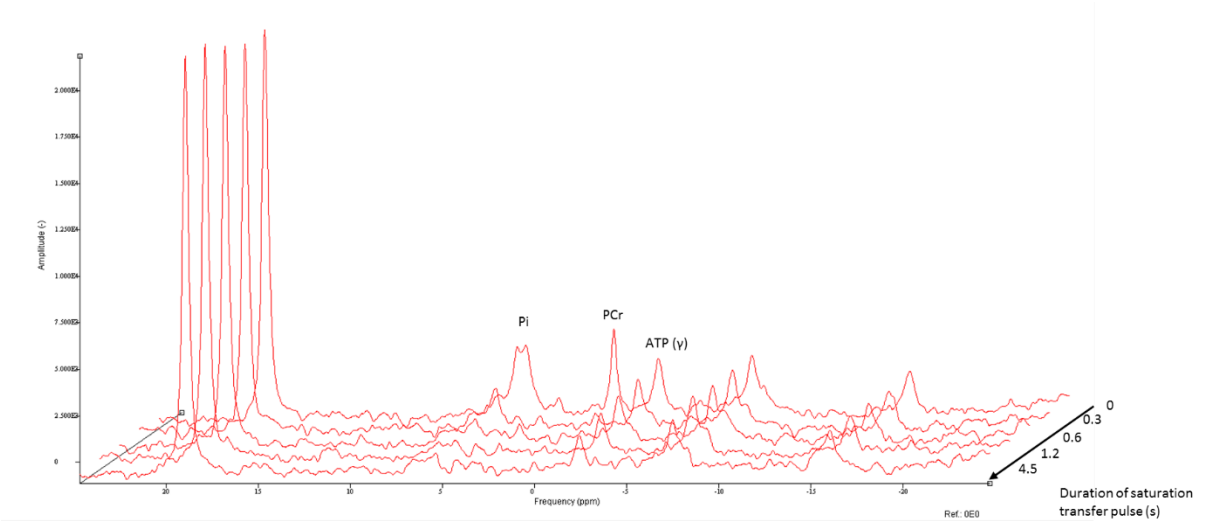

Figure 3.6 – The spectra obtained from a representative saturation transfer experiment. Any duration of saturation transfer pulse leads to complete loss of both Pi and PCr peaks and ATPγ can be seen to decrease with increased duration of saturation transfer pulse, with an exponential decay function.

The decay constant obtained from these saturation transfer experiments represents the rate constant for the movement of ATP both into PCr as well as inorganic phosphate. T2D hearts displayed further energetic impairment, with a 53% reduction in the rate of ATP degradation (figure 3.7a). This was the primary driver for the 61% reduction in turnover, the product of the rate constant and ATP concentration, of ATP in the diabetic heart (figure 3.7b).

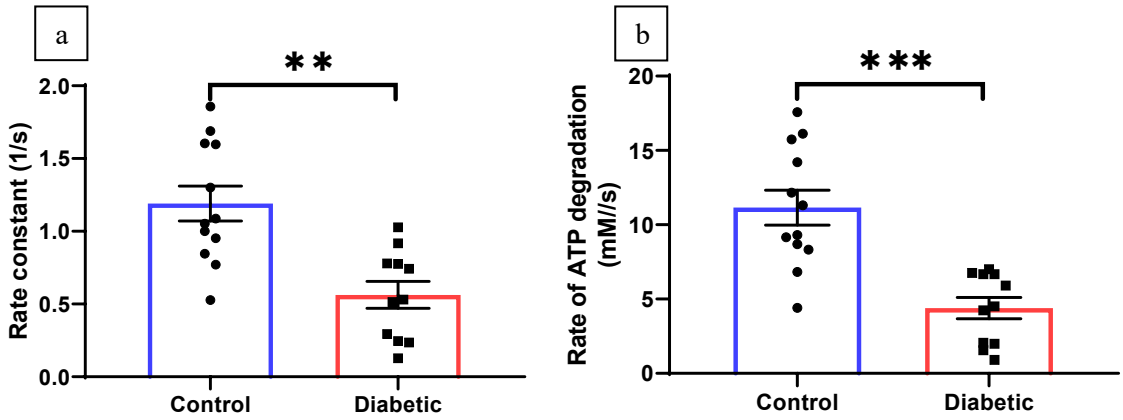

Figure 3.7 – Diabetic rodents presented with lower rates of cardiac ATP degradation (a) measured through saturation transfer. This reduced ATP degradation was the primary driver for a reduction in ATP turnover (b). ** denotes P<0.005, *** denotes P<0.001 between control and diabetic.

The concentration of ATP was stable in both control and T2D hearts over the time course of the perfusion indicating that the rates of ATP synthesis and degradation were well matched in both cohorts (figure 3.8). The reduction in the rate of ATP degradation therefore indicates that T2D hearts also have significantly reduced rates of ATP synthesis compared to control hearts.

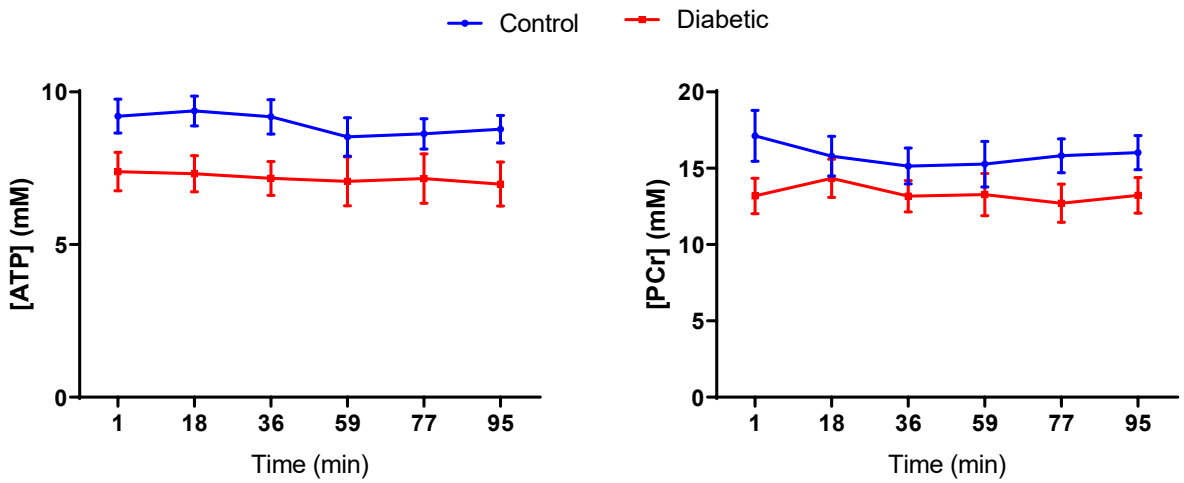

Figure 3.8 - ATP and PCr concentrations remained stable over the course of the perfusion (n=7).

3.4.3 Type 2 diabetic cardiac mitochondria have reduced respiratory rates

T2D hearts are energetically dysfunctional as evidenced by a reduction in the absolute concentration, and the turnover, of ATP. Mitochondria generate over 95% of ATP in the heart and so are the logical candidate for energetic dysfunction. To determine if cardiac mitochondrial density was altered by T2D the mitochondrial content of both control and T2D hearts was measured through both citrate synthase activity (a marker for matrix volume) and mtDNA copy number (a marker for mitochondrial number). Mitochondria isolated from T2D hearts showed a 29% increase in citrate synthase activity (figure 3.9a), but no change in mtDNA copy number (figure 3.9b). These data therefore indicated an increase in mitochondrial size in the T2D heart with no change to mitochondrial number.

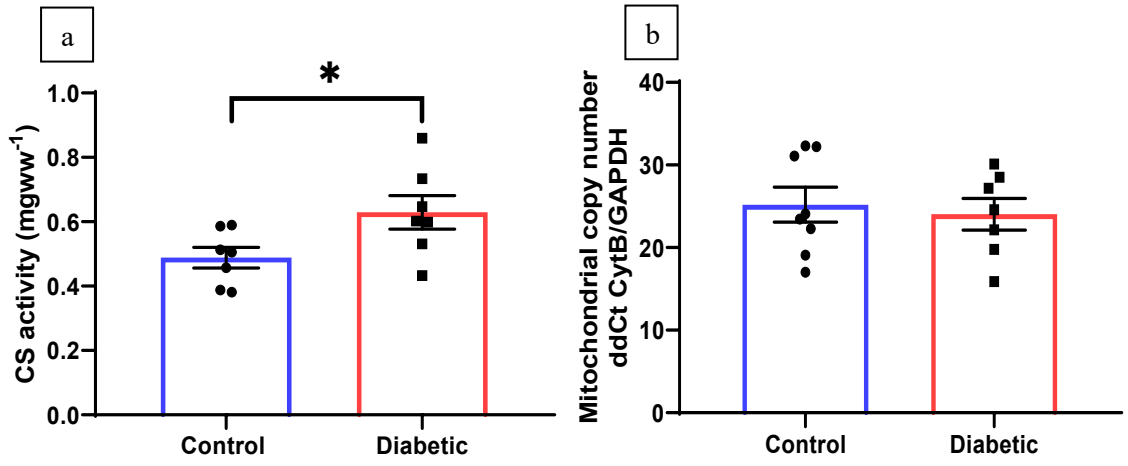

Figure 3.9 – Diabetic rodents presented with larger cardiac mitochondria as shown by a higher citrate synthase activity, indicating a higher matrix volume (a), with no overall increase in mitochondrial number (b). * denotes P<0.05 for control vs diabetic.

The decreased rate of ATP turnover in the T2D heart cannot therefore be attributed to a reduction in mitochondrial density and so may be due to reduced mitochondrial function. In order to investigate mitochondrial respiratory rates mitochondria were isolated from control and T2D hearts and their rates of respiration measured using a Clark-type oxygen electrode. Mitochondria were respired under glutamate, pyruvate and malate (GPM) representing a non-fatty acid substrate mix as well as GPM with palmitoyl-carnitine (GPMPCar) representing a fatty acid substrate mix. Both SSM (figure 3.10a) and IFM (figure 3.10b) populations from T2D hearts displayed reduced state 3 respiratory rates under GPM, by 12% and 24%, respectively. These state 3 respiratory rates were normalised when mitochondria were respired in the presence of fatty acids due to an increase in respiration in T2D mitochondria by 22% in the SSM and 35% in the IFM population, with no respiratory change in control mitochondria.

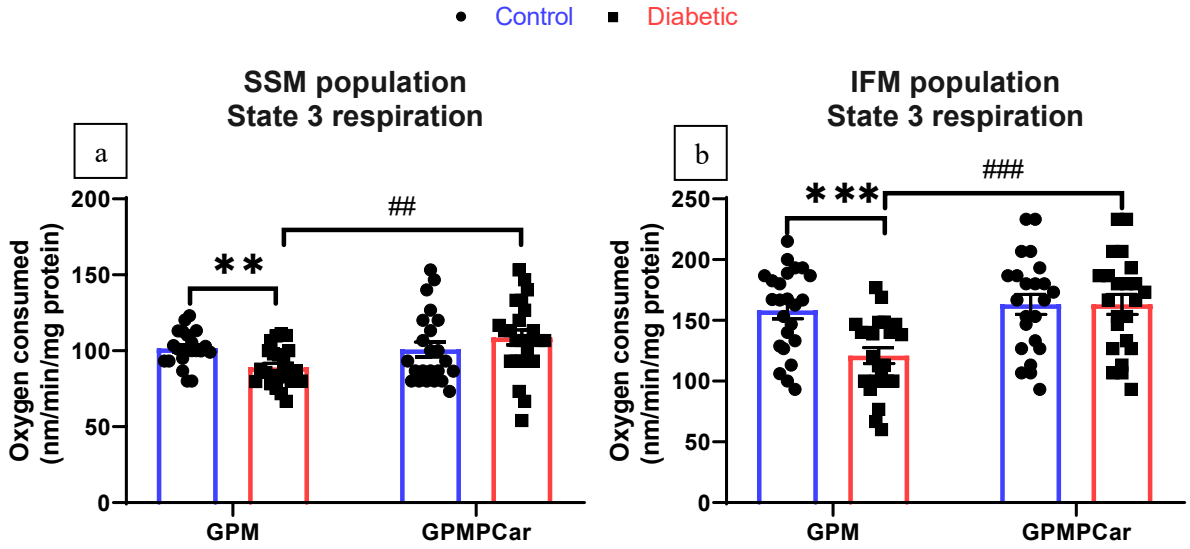

Figure 3.10 – Diabetic rodents presented with dysfunctional mitochondria. Cardiac T2D mitochondrial respiration was lower compared to control hearts when respired in the absence of fatty acids (GPM), both in the SSM (a) and IFM (b) population. The addition of fatty acids (GPMPCar) significantly increases respiration in the diabetic cohort, but not the control cohort, resulting in no overall significant difference between diabetics and controls. ** denotes P<0.005 and *** denotes P<0.001 for control vs diabetic, ## denotes P<0.005 for GPM vs GPMPcar, ### denotes P<0.001 for GPM vs GPMPCar

A common source of reduced mitochondrial respiratory rates is reduced flux through the electron transport chain and ATP synthase. The activities of complexes in the electron transport chain were therefore assayed *in vitro.* Complex activity was the same between control and diabetic mitochondria in the SSM population (figure 3.11a) and only complex 4 showed depressed activity, by 32%, in the IFM population (figure 3.11b).

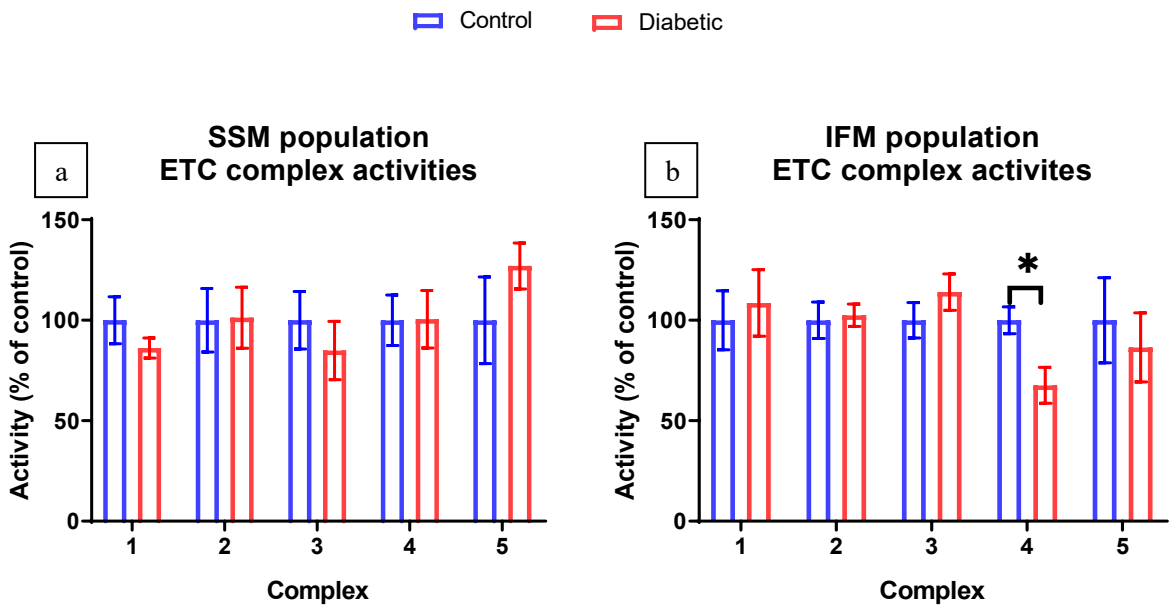

Figure 3.11 – Diabetic rodents presented with normal electron transport chain complex activities in the SSM (a) and IFM (b) population. Complex 4 activity in the T2D IFM population showed a significant reduction in enzymatic activity. n = 8 for each group, * denotes P<0.05 for control vs diabetic.

To investigate whether reduced complex IV activity would affect physiological levels of mitochondrial respiration oxygen consumption was measure in the presence of TMPD, a substrate which feeds in directly at complex 4. The normal respiratory rate when respired on TMPD indicated that any defect in the activity of the isolated complex IV could not explain the reduced rate of respiration in T2D mitochondria (figure 3.12).

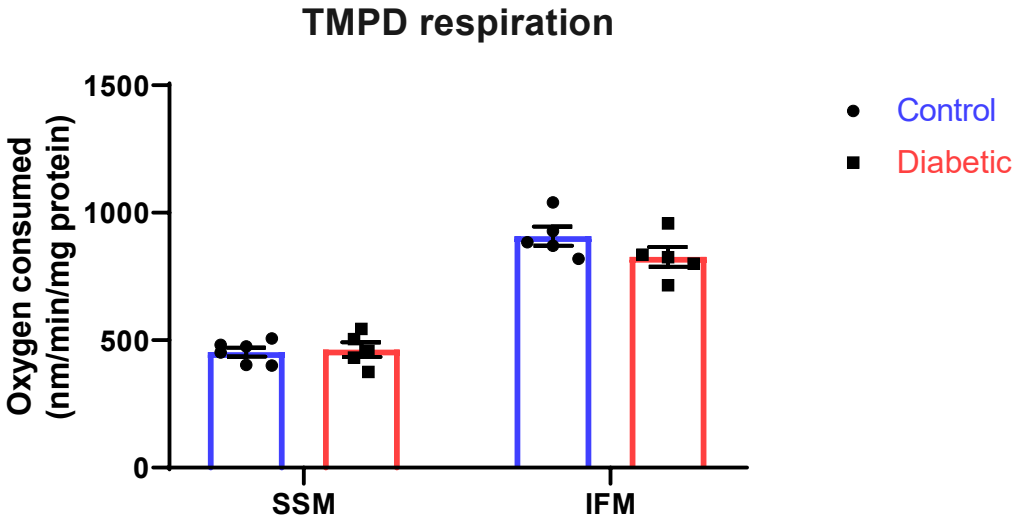

Figure 3.12 – TMPD respiration, representing respiration through complex 4, revealed no significant difference in complex 4 activity in the diabetic IFM population.

3.5 DISCUSSION

3.5.1 The type 2 diabetic heart has reduced concentrations of high energy phosphates and decreased rates of ATP synthesis

T2D hearts perfused in a retrograde Langendorff mode present with normal function with unchanged developed pressures and heart rates. This closely matches clinical measurements of early stage T2D patients and echocardiography measurements of cardiac function within this T2D rodent model. Modest diastolic dysfunction has previously been observed in this T2D rodent model[201], but it is possible that the Langendorff setup which requires setting the end-diastolic pressure through inflation of the balloon masks this modest dysfunction in relaxation.

These data indicate that the T2D heart is energetically dysfunctional, with a significant reduction in the cardiac concentrations of PCr and ATP. Of interest, this reduction was observed in the absence of a statistically significant decrease in the PCr/ATP ratio, the most commonly used clinical marker for cardiac energetic dysfunction. The importance of absolute measurements of the concentrations of ATP and PCr in addition to the PCr/ATP ratio has been clinically observed: Beer *et al*[1]. demonstrated across three separate cardiac conditions (hypertensive heart disease, aortic stenosis and dilated cardiomyopathy) that absolute concentrations of PCr and ATP showed a stronger negative correlation with cardiac function (as measured by ejection fraction and end-diastolic volume) than the PCr/ATP ratio. Furthermore, they noted that decreases in both PCr and ATP concentrations can result in non-significant changes to the PCr/ATP ratio[1], as observed in this current study.

This masking of energetic dysfunction due to similar decreases in both ATP and PCr concentrations (as observed in these data) may explain some contradictory findings in the field: The power of the PCr/ATP ratio was first observed in diabetes in 2003 by Scheuermann-Freestone *et al*.[5] who identified a reduced PCr/ATP ratio in T2D patients. This finding was corroborated in obese patients in 2012 by Rider *et al*.[4] who demonstrated that this decrease was furthered by stress, a phenomenon which also occurred in T2D patients[3]. Furthermore, a decreased PCr/ATP ratio was shown to correlate with diastolic dysfunction[13] and to respond to weight loss in obese patients[191]. However, this ratio was not seen to improve with

either pioglitazone treatment[193] or exercise training[192], despite improvements in cardiac function in both cases. Considering the findings presented in this study, we suggest that the disparity between PCr/ATP ratios and cardiac function observed in these cases may be due to increases in both metabolites masking changes to the PCr/ATP ratio.

It is noted that the rate constant calculated from these data for ATP degradation in the control heart (1.19±0.15 from Figure 3.7a) fits remarkably well with the value obtained by Spencer *et al.* 30 years ago (1.15±0.19)[180], truly indicating the pioneering nature of their work. The rate constant for ATP degradation was significantly reduced in T2D hearts, which drove a significant reduction in the ATP turnover in these hearts. The value obtained is the sum of flux from ATP into both PCr (*Kr*) and through ATPases into ADP and Pi (*K'r*) as shown in reactions 3.1 and 3.2.

Reaction 3.1 – The reversible reaction between creatine and ATP, with rate constants (Kf and Kr) labelled

$$PCr + ADP + H^+ \underset{Kr}{\overset{Kf}{\leftrightarrow}} Cr + ATP$$

Reaction 3.2 – The reversible reaction between ADP and ATP, with rate constants (K'f and K'r) labelled

$$ADP + Pi \underset{K\prime r}{\overset{K\prime f}{\leftrightarrow}} ATP$$

The observed reduction in the sum of *Kr* and *K'r* could therefore be driven by a reduction in flux through creatine kinase, or through ATPases. Recent literature has shown that creatine kinase flux is not decreased in the heart in models of T2D[10], therefore the reduction in ATP degradation is likely to be caused by a reduction in the *K'r* term. As there is no change in the concentration of ATP or PCr over the time course of the perfusion, it is reasonable to state that in both control and T2D hearts the ratios of *Kf/Kr* and *K'f/K'r* are close to one. Therefore, the reduction in *K'r* indicates a reduction in mitochondrial ATP synthesis (*K'f*), which fits well with the 12-24% reduction in state 3 respiration measured in T2D mitochondria (figure 3.10).

The magnitude of the reduction observed in ATP turnover in the T2D heart is notable, especially given the apparent lack of functional defect in these hearts (figure 3.3). It is of interest that the decrease in the

rate constant for ATP degradation observed in this dataset (53% from figure 3.7a) fits well with the 64% decrease in the rate constant for ATP synthesis observed by Luptak *et al.* in a model of metabolic heart disease[8].

3.5.2 Mitochondria isolated from T2D hearts are larger and exhibit metabolic inflexibility

It is inherently difficult to definitively state that mitochondrial dysfunction causes the energetic, and later functional, defects observed in the T2D heart as T2D is associated with many other comorbidities. Evidence supporting mitochondrial dysfunction leading to functional defects comes from studies showing that the induction of insulin resistance in cardiac cells is associated with cardiac dysfunction[202] and that the extent of mitochondrial dysfunction is correlated with reduced contractile function (as measured through twitch force) in diabetic, but not obese patients[203].

This chapter provides the first study to date that investigates cardiac energetic dysfunction and sub-population mitochondrial dysfunction within the same model. The observed cardiac energetic dysfunction cannot be attributed to a reduced mitochondrial volume within the T2D hearts, as these hearts presented with the same number of mitochondria, which were larger than those in controls hearts (figure 3.9). A finding which fits well with evidence showing that chronic PPARα activation in diabetes can drive a mitochondrial biogenic response[174,204,205].

T2D mitochondria have significantly reduced rates of respiration in the SSM and IFM population when respired on GPM but not when respired in the presence of fatty acids (on GPMPCar). This agrees well with the view of the T2D heart as a metabolically inflexible organ[17,206], less able to oxidise non-fatty acid substrates in an animal[207] and patient setting[162]. Of note, diabetic heart samples which have been stressed by perfusion without fatty acids[197] and more severe diabetes phenotypes[155,156,174] display reduced oxidation both with and without fatty acids. The normal oxidative rates with fatty acids within our model of T2D further indicates that this model represents that of an early stage patient. Taken together, these data show that mitochondrial, and hence cardiac, energetic dysfunction prelude the

development of functional impairment in the diabetic heart indicating that mitochondria may play a causative role in diabetic cardiomyopathies.

3.6 CONCLUSION

T2D rodent hearts display energetic dysfunction at the level of the whole heart and the level of isolated mitochondria even in the absence of functional impairment. This energetic dysfunction can be fully realised through quantitative ^{31}P-NMR, which displayed reduced absolute concentrations of PCr and ATP and a reduction in ATP turnover within the heart. The observed divergence between the absolute concentrations of PCr and ATP and the clinically measured PCr/ATP ratio may explain some discrepancy between cardiac energetics and function within T2D patients within the literature. This is the first study which investigates dysfunctional energetics at the whole heart level and subsequently at the level of isolated mitochondria, therefore representing a powerful confirmation of the role of mitochondrial energetic dysfunction within diabetic heart disease.

4 THE ADP-ATP CARRIER LOSES SENSITIVITY TO LONG CHAIN ACYL-COAS IN THE DIABETIC HEART

4.1 ABSTRACT

Lipotoxicity and energetic dysfunction are common features of the type 2 diabetic (T2D) heart. Although these two phenomena centre upon mitochondrial dysfunction, the link between them has not been well-defined. The ATP/ADP carrier (AAC) is the rate limiting step for mitochondrial respiration but can be inhibited by long chain acyl-CoA (LCAC), an intermediate in the fatty acid processing pathway, and so represents a good candidate for this link. This chapter will firstly evaluate the contribution of LCAC mediated inhibition of the AAC to energetic dysfunction within T2D cardiac mitochondria and then will investigate physiological roles of this inhibition.

LCAC concentrations in native heart samples were measured through mass spectrometry, showing that T2D hearts have a 74% increase in LCACs. The effect of these LCACs was investigated on isolated mitochondria through the measurement of state 3 respiratory rates and the generation of both Michaelis-Menten like kinetics, and inhibition curves for the AAC (with regards to ADP and P-CoA respectively). These demonstrated that although control and T2D mitochondria can be inhibited by LCACs, T2D mitochondria have a reduced sensitivity to this inhibition making LCACs an unlikely candidate to explain the observed mitochondrial dysfunction within the T2D heart. Two novel physiological roles of LCAC mediated AAC inhibition were uncovered through the development of a model of ischaemic/anoxic mitochondria, showing that AAC inhibition by LCACs in ischaemia can both prevent excessive ATP hydrolysis and alter mPTP opening.

This work therefore answered a long-held debate around whether LCAC mediated inhibition of the AAC is responsible for energetic dysfunction within T2D and uncovered novel mechanisms by which AAC inhibition during ischaemia/anoxia may be cardioprotective.

4.2 INTRODUCTION

4.2.1 The ATP/ADP carrier

It is a fundamental necessity of the mitochondrial inner membrane that it must be highly impermeable to allow the generation of a transmembrane proton-motive force. Mitochondria therefore require a family of transporters, termed the solute carrier family 25, to facilitate the transport of essential ions across this membrane. The most abundant member of this family is the ATP/ADP carrier (AAC).

The AAC's primary structure shows three homologous sequence repeats[208], each of which contain the mitochondrial carrier family motif (PX[DE]XX[KR]). Although a subject of recent debate, the AAC is thought to function as a monomer with three-fold symmetry consistent with the three sequence repeats[209]. Structurally, the AAC has six transmembrane α helices, which are highly tilted to form an α-helical barrel around the central water filled cavity, which serves as the pore for ADP and ATP transport[210]. Central to this cavity is the substrate binding site where ADP and ATP bind. Arginine residues attract the phosphate moieties (R79, 235 and 279) and a lysine, serine and alanine residue bind the adenine moiety (K22, S21 and A284)[211,212]. Functionally, the AAC acts in a similar fashion to a canal lock existing in three major forms; open to the matrix, open to the inter-membrane space or closed to both faces. The AAC cycles between these forms through 2 sets of 3 salt bridges localised on either face of the protein[213,214] formed of the canonical mitochondrial carrier motif on the cytoplasmic side.

Exogenous inhibitors (bongkrekic acid - BKA[215] and carboxyatractyloside - CATR[216]) were integral in facilitating crystal generation and subsequent structural analysis of the AAC. Although endogenous inhibitors (LCAC[217,218]) and activators (Bcl2[219]) for this protein have been found, their physiological function has been a source of debate for some time. BKA and CATR have directionality associated with their inhibition, with BKA binding and locking the AAC open to the matrix side and CATR the intermembrane space[220,221]. LCACs however are bidirectional, able to both compete with CATR in inhibition of the AAC (indicating inhibition from the intermembrane space) and to inhibit transport in sub-mitochondrial particles (indicating inhibition from the matrix side)[222,223].

LCAC inhibition of the AAC is likely due to the CoA group, which displays a very similar chemical and physical structure to the channel's preferred substrates; ATP and ADP. LCAC chain length has been shown to influence the kinetics of the inhibition, with generally shorter (C:16) and more saturated LCACs inhibiting the protein to a greater extent than longer, unsaturated LCACs[224]. LCACs are predominantly (92-95%) localised within the mitochondrial matrix of the cell[225,226] which increases their local concentration within the mitochondria facilitating inhibition of the AAC. In spite of this, there is widespread debate in the literature as to whether physiological LCAC levels would reach the point of AAC inhibition in the heart[227,228].

The AAC is more sensitive to LCAC mediated inhibition than any other mitochondrial protein, as evidenced by its low Ki value for P-CoA inhibition; 0.1 μM for the AAC compared with 3.2-4.5 μM for the tricarboxylic acid carrier, 7.1-9.5 μM for the dicarboxylate carrier and 25 μM for the phosphate carrier[224]. It is therefore reasonable to assume that decreases in state 3 respiration when mitochondria are exposed to low levels of P-CoA are due primarily to decreased flux through the AAC. Although the physiological relevance of AAC inhibition has been questioned, its role within pathological conditions is of particular interest. Type 2 diabetes (T2D) is associated with cardiac lipid accumulation and LCACs are implicated in aspects of the pathophysiology[149]. The question of whether LCACs are able to inhibit mitochondrial respiration in the diabetic heart via the AAC is one that has been posed[13,229], but not satisfactorily answered to date.

4.2.2 Reverse ATP synthesis in ischaemia

Both the AAC[230,231] and ATP synthase are bidirectional, with adenine nucleotides equilibrating across the mitochondrial membrane due to their concentration gradient and ATP generation occurring at the F1 stalk due to the proton gradient across the inner mitochondrial membrane (IMM). This gradient requires the constant movement of protons through the IMM, facilitated by the electron transport chain, which in turn requires a constant flux of electrons down the chain into the terminal electron acceptor, oxygen. In cardiac ischaemia vessel occlusion prevents the delivery of oxygen to large areas of tissue, leading to the rapid inhibition of complex IV in the electron transport chain, reducing proton pumping and preventing regeneration of the proton gradient.

This electron transport chain blockade quickly prevents the oxidation of all substrates, but in particular fatty acid oxidation which requires more oxygen for oxidation than other fuels. Ischaemia, therefore, rapidly leads to the accumulation of fatty acid intermediates, with a demonstrated 300% increase in LCAC abundance[232]. In addition, the dissipation of the proton motive force removes the drive for ATP synthase to function in a forward fashion allowing the complex to reverse and hydrolyse, rather than synthesise, ATP[233]. As a consequence of this ATP synthase re-generates, rather than uses, the proton gradient (as illustrated in figure 4.1). This hydrolysis around ATP synthase reduces the concentration of ATP in the mitochondrial matrix, generating a concentration gradient between the mitochondrial matrix and cytoplasm. The concentration gradient reverses the directionality of the AAC importing ATP into the mitochondrial matrix and exporting the hydrolysed ADP. It is estimated that around 30% of ATP hydrolysis in cardiac ischaemia is due to this futile mitochondrial ATP degradation[234].

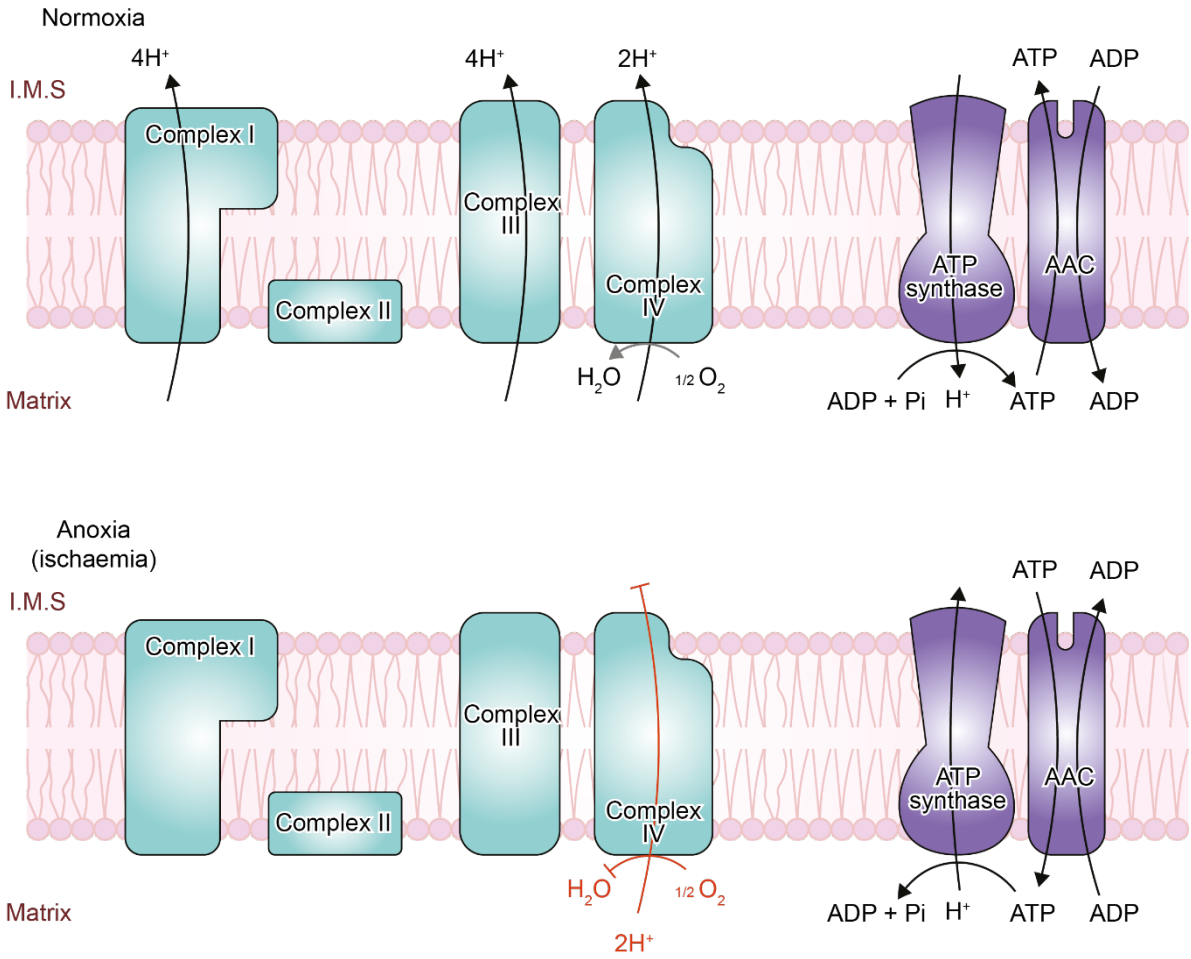

Figure 4.1 – An illustration of normal ATP generation within normoxic conditions and ATP degradation around the ATP synthase during anoxia with reversal of the AAC and inhibition of complex IV. IMS – Intermembrane space, AAC – ADP/ATP carrier.

ATP hydrolysis in ischaemia would be detrimental to the heart. In recognition of this there is an endogenous protein, inhibitory factor 1 (IF1), which binds to and inactivates ATP synthase in the reverse direction[235]. This protein has been pharmacologically mimicked by Bristol-Myers Squibs with the compound BMS199264 which acts in a similar fashion to IF1 preventing the reverse, but not the forward direction, of ATP synthase[234,236].

Given that there is a system in place to prevent the reverse functionality of ATP synthase, it is not unreasonable that there should be an endogenous system that prevents the reverse function of the AAC in this setting. This chapter hypothesises that the acute elevation in LCAC concentrations during ischaemia inhibits the AAC, reducing futile mitochondrial ATP hydrolysis in ischaemia.

4.2.3 The mPTP

The mitochondrial permeability transition pore (mPTP) is a protein complex formed in the inner mitochondrial membrane in times of energetic stress. Opening of the mPTP increases the permeability of the inner mitochondrial membrane, allowing molecules weighing up to 1500 Daltons through. This leads to mitochondrial swelling, and cell death, and has been heavily implicated in reperfusion injury during cardiac ischaemia (Halestrap *et al*.[237] provides a comprehensive review on the mPTP).

The AAC is thought to play a crucial role in mPTP formation[238] and, even though the exact role has been recently brought into question[239], the dramatic effects of molecules that interact with the AAC (BKA, CATR and Bcl2) on mPTP opening point demonstrate its impact[240]. Indeed, the directionality of the AAC (whether it is matrix open, or intermembrane space open) affects the likelihood of mPTP opening. The mPTP can only open when the AAC is open to the intermembrane space therefore incubation with BKA, locking the AAC in the matrix facing orientation, prevents mPTP opening whereas incubation with CATR, locking it in an inter-membrane space orientation, facilitates mPTP opening[241]. It is worth noting that LCACs, which can inhibit the AAC from both directions, can have either stimulatory or inhibitory effects on mPTP opening dependent on which side of the AAC the LCACs are present.

4.3 AIMS

Energetic dysfunction is widely observed in the T2D heart and is associated with the increased oxidation, and prevalence, of fatty acids within these hearts. This chapter proposed that LCAC inhibition of the AAC could mediate this reduction in ATP synthesis observed within the T2D heart. LCAC levels are acutely elevated during ischaemia and anoxia, settings where excessive mitochondrial activity can cause myocardial damage. It is therefore proposed that LCAC-mediated AAC inhibition could serve as a beneficial mechanism to reduce mitochondrial activity within these pathophysiological settings. These hypotheses were investigated through the interrogation of four key objectives:

1. The concentration of LCACs within the type 2 diabetic (T2D) heart was measured.
2. The effect of LCAC-mediated AAC inhibition was determined in mitochondria isolated from T2D and control hearts.
3. The physiological effect of LCAC inhibition of the AAC in cardiac ischaemia, with regards to preventing excessive ATP hydrolysis in the mitochondrial matrix, was investigated.
4. The physiological effect of LCAC inhibition of the AAC in cardiac ischaemia, with regards to mPTP opening, was measured.

4.4 METHODS

4.4.1 Mitochondrial isolation

Mitochondria were isolated as per section 2.3.1.

4.4.2 Mitochondrial respiration in the presence of palmitoyl-CoA

Freshly isolated mitochondria (0.15 mg protein) were incubated in 500 µL of mitochondrial respiration media (section 2.9) with 20 mM glutamate, 10 mM pyruvate and 5 mM malate (GPM) as substrates. State 3 (pre) respiration was induced with 200 µM ADP and oxygen consumption was measured using a Clark-type electrode. Upon returning to state 4 mitochondria were incubated with 10 µM palmitoyl-CoA (P-CoA) for 3 minutes. Following this incubation state 3 (post) respiration was measured again, through the addition of 200 µM ADP.

4.4.3 Generating Michaelis-Menten like kinetics around the AAC

Mitochondrial respiration in the presence of P-CoA was measured following the protocol as defined in section 4.4.2, with the exception that the state 3 (post) respiration was induced with a range of ADP concentrations (40 – 1000 µM). These data were plotted and Michaelis-Menten kinetics generated (state 3 (post) respiration vs [ADP]) using the Michaelis-Menten equation in the nonlinear regression analysis section of GraphPad Prism 8.0.0.

4.4.4 Calculating the IC50 of the AAC with regards to palmitoyl-CoA

Mitochondrial respiration in the presence of P-CoA was measured following the protocol defined in section 4.4.2, with the exception that a range of P-CoA concentrations were added (0 – 52 µM). These data were plotted, and fitted, using the equation; [Inhibitor] vs. response – Variable slope in the nonlinear regression analysis section of GraphPad Prism 8.0.0.

4.4.5 Mitochondrial permeability transition pore opening assay

Opening of the mPTP results in mitochondrial swelling that can be measured spectrophotometrically at 540 nm[242,243]. mPTP opening was induced as described previously[243]: 0.25 mg of freshly isolated mitochondria was added to 1 mL of mPTP assay buffer (see section 2.9) and incubated for 60 seconds.

$CaCl_2$ (5 µM) was added and the solution incubated for a further 104 seconds. The mPTP inducer (either 200 nM FCCP, 4 µM palmitoyl-CoA or 10 µM palmitoyl-CoA) was added and reaction kinetics followed at 540 nm for 180 seconds. All incubations and measurements were carried out at 30°C. Data were expressed as the plateau point (minima) and decay constant (K) calculated from decay curves as shown in figure 4.2.

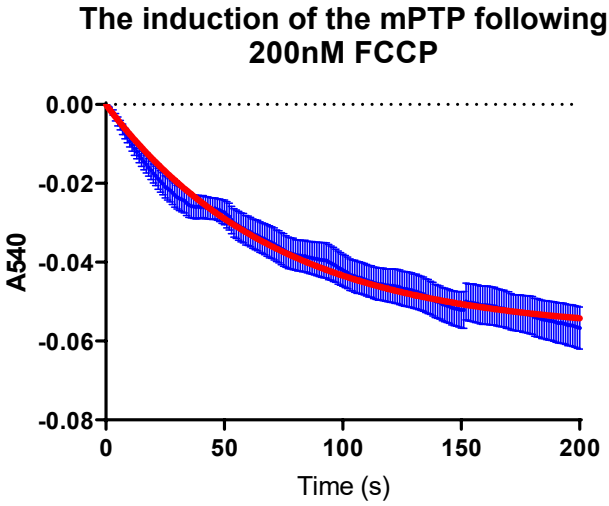

Figure 4.2 – The addition of 200 nM FCCP (at t=0) induces mPTP opening in a mitochondrial population. mPTP opening within 200 seconds displays a decay curve, which can be fitted (as shown by solid red line), giving a plateau point and decay constant.

4.4.6 Statistical analysis

Datasets containing two groups (control and diabetic) were analysed using the two-tailed parametric unpaired t-test function within GraphPad Prism 8.0.0. A reported P value less than 0.05 was taken as significantly different.

Datasets containing multiple groups, but one variable, were analysed using an ordinary one-way ANOVA. Significance was followed up with post-hoc Dunnett multiple comparison tests, comparing the mean of each column with the mean of the control column.

Datasets containing multiple groups, and multiple variables were analysed using ordinary two-way ANOVA. Significance was followed up with Turkey's multiple comparison tests, with individual variances computed for each comparison.

Michaelis-Menten kinetics were fitted using the Michaelis-Menten analytical derivative found under ‘enzyme kinetics – velocity as a function of substrate’ within GraphPad Prism 8.0.0. IC50 graphs were fitted using the ‘[Inhibitor] vs response (three parameters)’ within GraphPad Prism 8.0.0.

4.5 RESULTS

4.5.1 The concentrations of long chain acyl-CoAs are elevated in the type 2 diabetic heart

The T2D heart is known to be lipid overloaded and this chapter will focus on determining the effect of LCACs on mitochondrial function. This requires the measurement of intra-myocardial levels of LCAC. Thus, the concentrations of the most abundant LCACs; P-CoA and oleoyl-CoA (O-CoA) in native cardiac tissue from both control and diabetic hearts were measured, using targeted lipidomics. This demonstrated that diabetic hearts have elevated concentrations of LCACs, by 74% (figure 4.3a), compared to control hearts. The elevation in total LCAC was due to a 250% increase in O-CoA concentrations, (figure 4.3b), with no change to P-CoA concentrations (figure 4.3c).

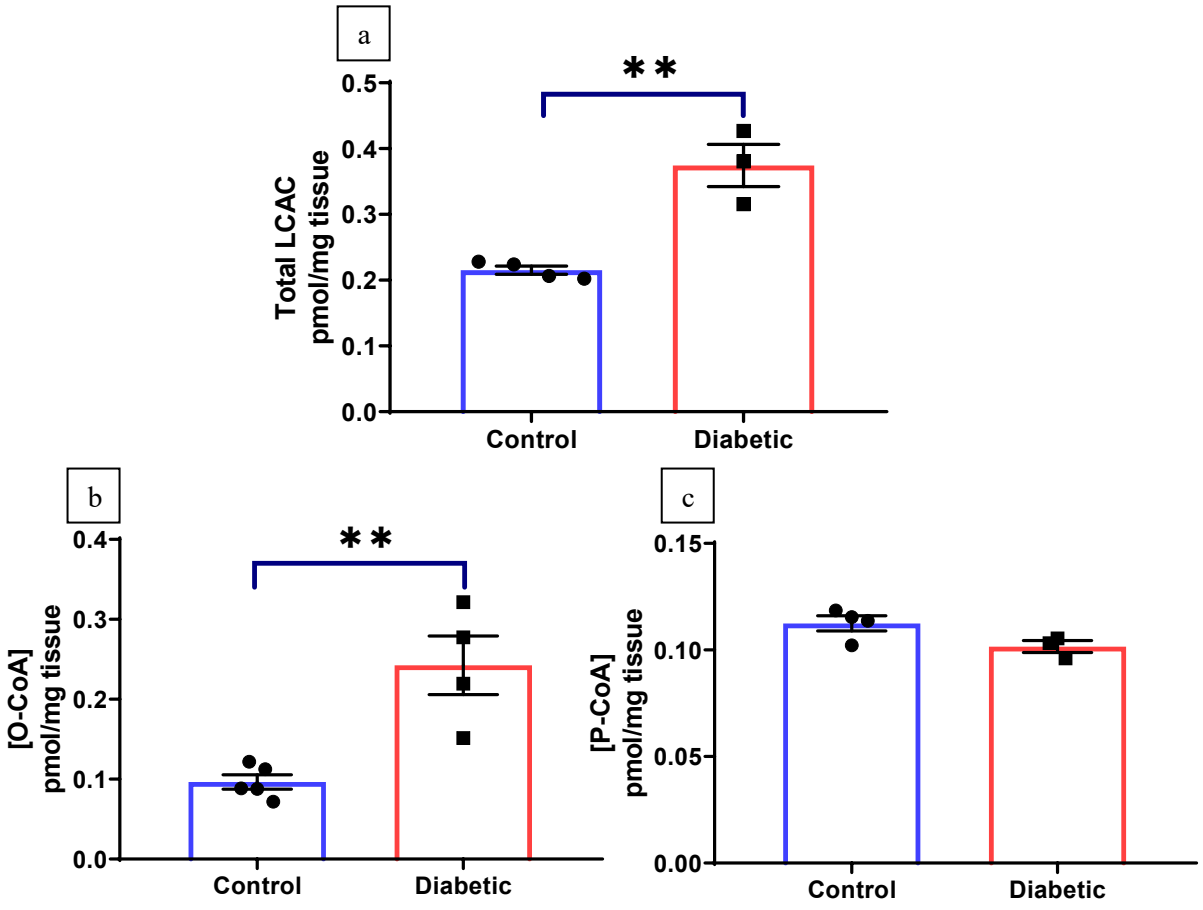

Figure 4.3 – There is a significantly greater abundance of LCAC in the diabetic heart (a). This arises from a significant elevation in the concentration of O-CoA (b) in spite of no change in the P-CoA concentration (c). ** denotes $p<0.005$ for control vs diabetic.

In order to work out the physiologically relevant concentration of these LCACs with regards to AAC inhibition one must calculate the [LCAC] within the mitochondrial matrix, following the equation set out below:

$$[Matrix\ LCAC] = \frac{Specific\ gracivty\ of\ cardiac\ tissue\ \times nmol/gww}{Mitochondrial\ cell\ fraction\ \times LCAC\ localised\ to\ the\ matrix}$$

Specific gravity of cardiac tissue	(converting gww to volume)	= 1.05g/mL[198]
nmol/gww	(from figure 4.3)	= 0.22 (Control) 0.37 (T2D)
Mitochondrial cell fraction	(% of the cell that is mitochondria)	= 30% (0.3)[41]
LCAC localised to the matrix	(% of LCACs found in the matrix)	= 95% (0.95)[225]

Using the data in figure 4.3 it is possible to calculate that the [LCAC] is 0.81 μM in the matrix of control mitochondria and 1.36 μM in the matrix of T2D mitochondria.

4.5.2 Diabetic mitochondria are less sensitive to long chain acyl-CoA inhibition

T2D hearts have significantly elevated levels of LCAC, which this chapter proposes may contribute to the reduction in the rate of ATP synthesis observed in the T2D heart through inhibition of the AAC. Therefore, to determine whether LCACs could acutely reduce mitochondrial respiratory rates, isolated mitochondria were incubated with P-CoA.

Incubation of control mitochondria with P-CoA decreased S3 respiration by 41% in the SSM population and 50% in the IFM population (figure 4.4a,b). This inhibition did not occur if either palmitoyl carnitine, or P-CoA and carnitine (which is converted to palmitoyl-carnitine by the mitochondria), was used instead of P-CoA (figure 4.4a,b) therefore indicating that it is the CoA moiety responsible for mediating inhibition. The addition of an uncoupling agent (FCCP) bypassed the phosphorylation apparatus and removed the inhibitory effect of P-CoA incubation (figure 4.4c,d) therefore indicating that inhibition was centred on the phosphorylation apparatus, of which the AAC is the primary component.

The AAC can be inhibited by LCAC in control mitochondria and these data demonstrated that 10 μM P-CoA represents around 50% inhibition in control mitochondria. Inhibitory kinetics were therefore next investigated in diabetic mitochondria. Mitochondria isolated from T2D hearts showed a similar overall profile to control mitochondria with 40% inhibition from LCAC incubation in the SSM population and 34% inhibition in the IFM population (figure 4.5a,b). This inhibition was again only mediated by the acyl-CoA moiety and was removed when mitochondrial respiration was uncoupled (figure 4.5c,d).These data show that mitochondria from control and T2D hearts can be inhibited by LCACs and that this inhibition is centred upon the AAC.

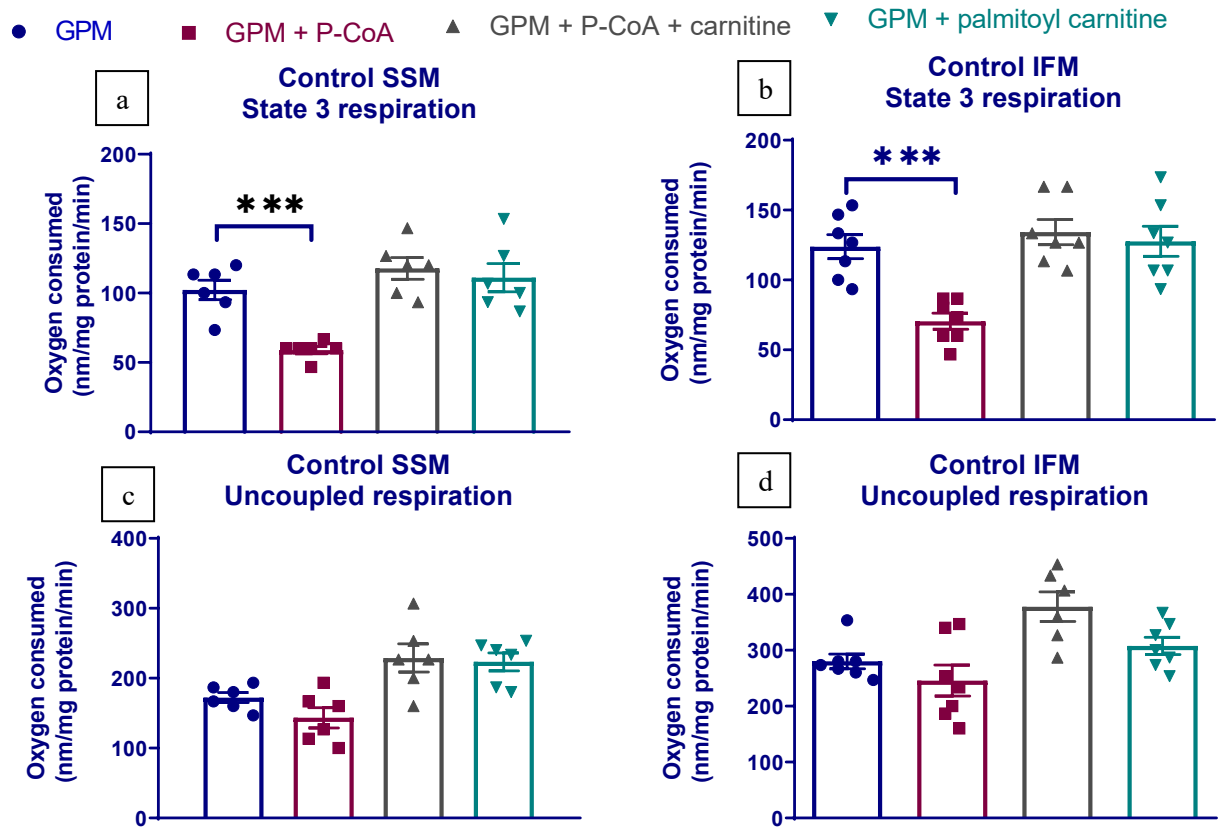

Figure 4.4 - State 3 (a,b) and uncoupled (c,d) respiratory rates were measured in control mitochondrial populations. Mitochondria were respired under either glutamate, pyruvate and malate alone (GPM) or, in addition to palmitoyl-CoA (P-CoA), palmitoyl-CoA and carnitine, or palmitoyl carnitine. *** denotes P<0.001 compared with GPM alone.

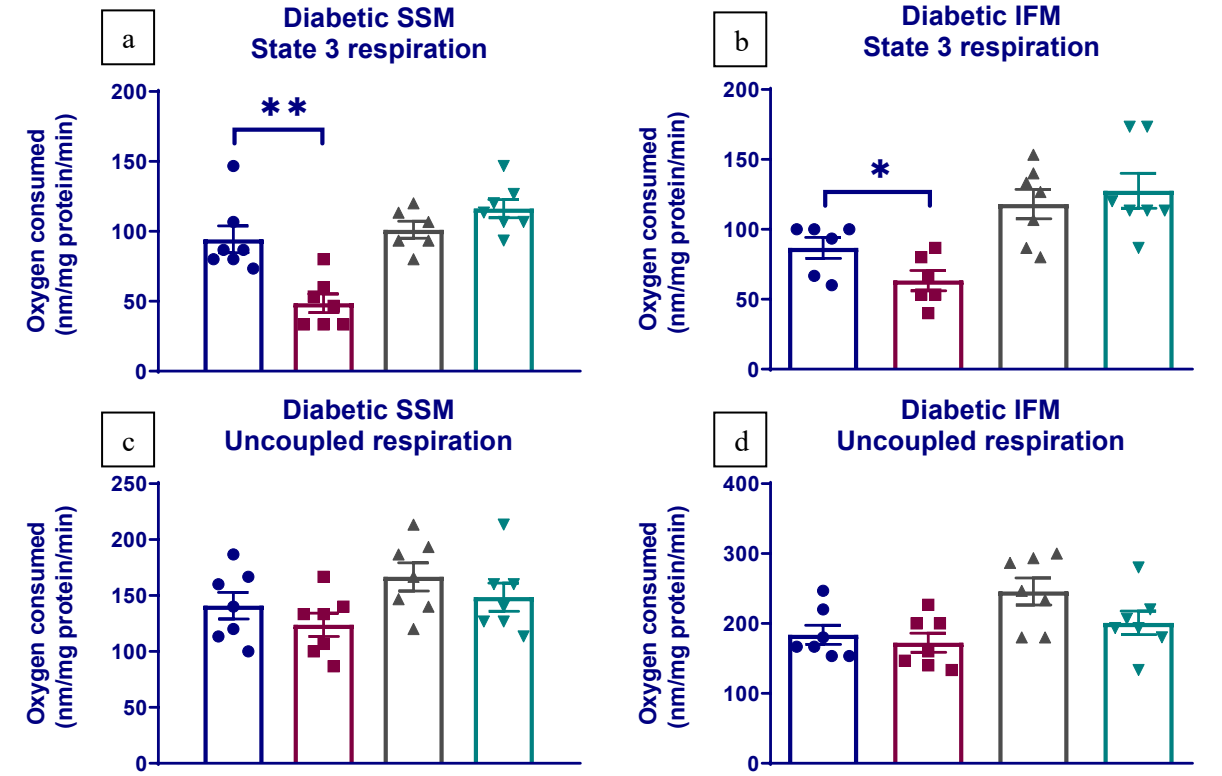

Figure 4.5 – State 3 (a,b) and uncoupled (c,d) respiratory rates were measured in diabetic mitochondrial populations. Mitochondria were respired under either glutamate, pyruvate and malate alone (GPM) or in addition to palmitoyl-CoA (P-CoA), palmitoyl-CoA and carnitine, or palmitoyl carnitine. * denotes P<0.05, ** denotes P<0.005 compared with GPM alone.

Determination of inhibition at one set concentration of inhibitor (LCAC) and substrate (ADP) provides only a snapshot of inhibitory kinetics. Therefore, the kinetics of LCAC inhibition were probed through the generation of Michaelis-Menten like kinetic curves of the concentration of ADP against state 3 respiration.

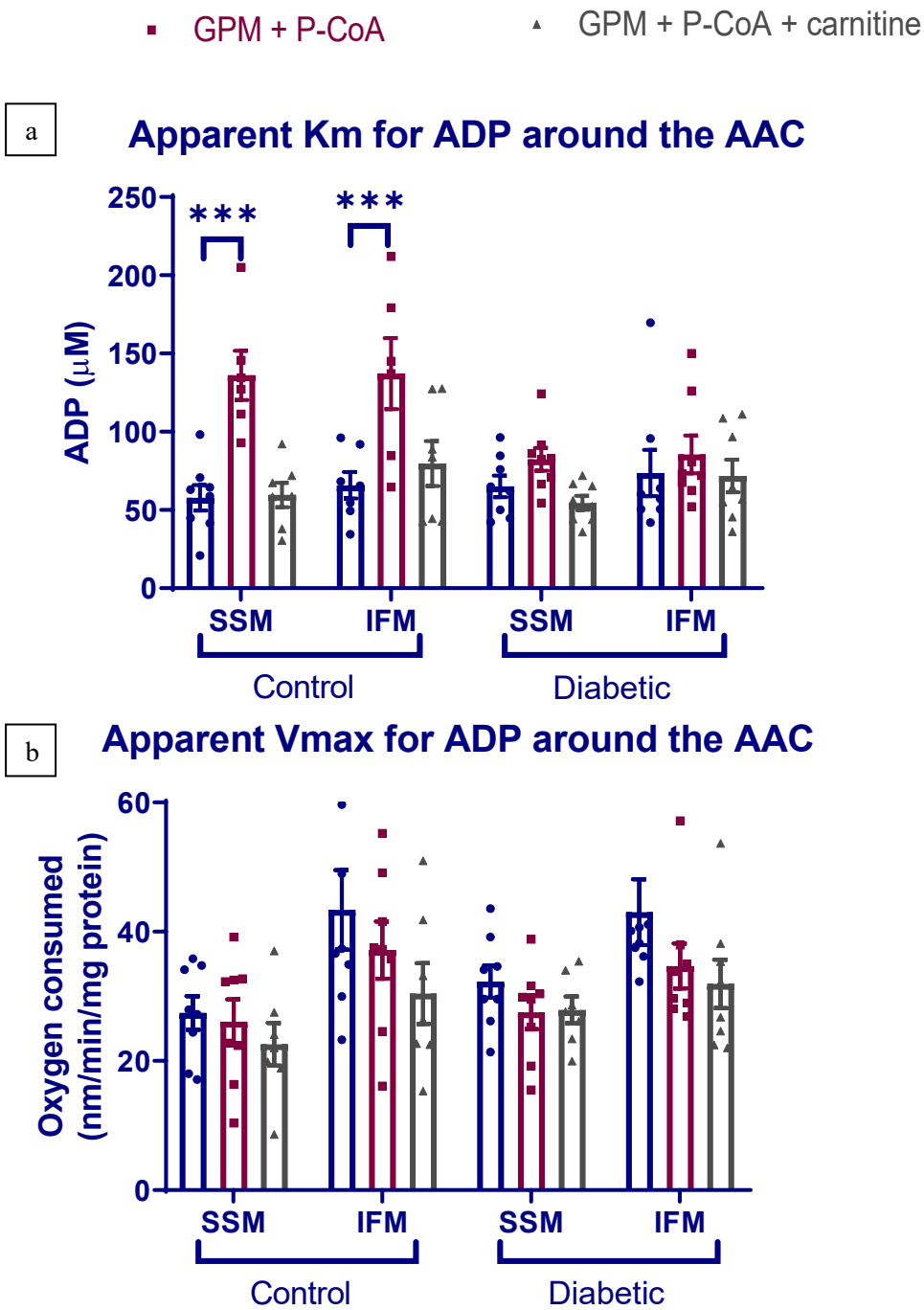

Figure 4.6 – The Km for the AAC with regards to ADP is significantly increased by the addition of P-CoA in control mitochondria (both SSM and IFM), but not in diabetic mitochondria. The addition of carnitine removes any inhibition arising from P-CoA, indicating that it is the CoA moiety that is responsible for inhibition (a). Vmax is not significantly altered by either substrate mix, or disease state (b). *** denotes P<0.001 vs GPM.

Michaelis-Menten like kinetic curves allowed the generation of Km and Vmax values in the presence, and absence, of P-CoA inhibition. These data showed that in control mitochondria the addition of P-CoA significantly increases the AAC Km, by 235% in the SSM population and 208% in the IFM population (figure 4.6a). The elevation in the Km occurred without a significant change in Vmax (figure 4.6b), indicating that LCAC inhibition is competitive. The addition of carnitine removed any increase in Km (and therefore inhibition), further confirming that the acyl-CoA is the inhibitory moiety in control mitochondria. In contrast, incubation with 10 μM P-CoA had no effect on either Km or Vmax in either diabetic mitochondrial population.

These data indicate that LCAC inhibition of the AAC significantly differs between control and diabetic mitochondria. In order to investigate this difference in LCAC inhibition kinetics mitochondria were incubated with a range of P-CoA concentrations and state 3 respiratory rates measured to generate IC50 values for LCAC inhibition. IC50 values demonstrated that whilst control and diabetic mitochondria can be inhibited by LCACs, (figure 4.7), diabetic SSM require 44% more P-CoA than control SSM. Furthermore, the SSM population required 48% more P-CoA to be inhibited by 50% compared to the IFM population.

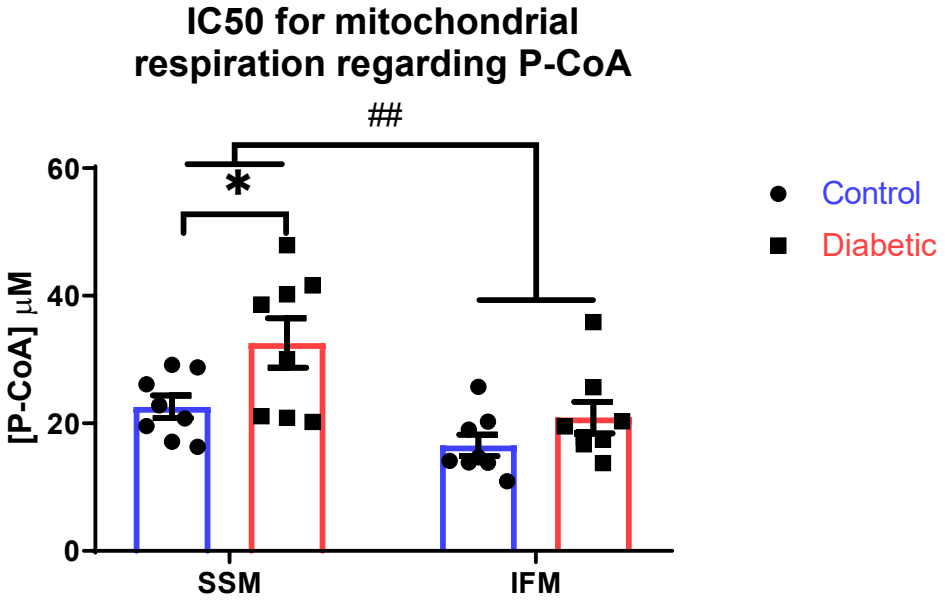

Figure 4.7 – P-CoA incubation significantly inhibits state 3 respiratory rates in both control and diabetic SSM and IFM populations. Diabetic mitochondria are less sensitive to P-CoA inhibition, especially in the SSM population. Overall, IFM populations are less sensitive to P-CoA inhibition than SSM populations. * denotes P<0.05 for control vs diabetic, ## denotes P<0.005 for SSM vs IFM

This combination of high-fidelity mass spectrometry and IC50 measurements allowed physiological levels of AAC inhibition to be calculated. The depression in state 3 respiratory rates can be intrapolated from the data used to generate IC50 values, (figures 4.8a,b), with levels of LCAC in the heart, from figure 4.3, displayed on enhanced graphs (figure 4.8c,d). As shown in figure 4.8e LCAC inhibits the IFM population by 39% more than the SSM population. However, at physiological concentrations of P-CoA, there is no significant difference in percentage inhibition between control and diabetic mitochondria, despite a trend for increased inhibition in diabetic mitochondria.

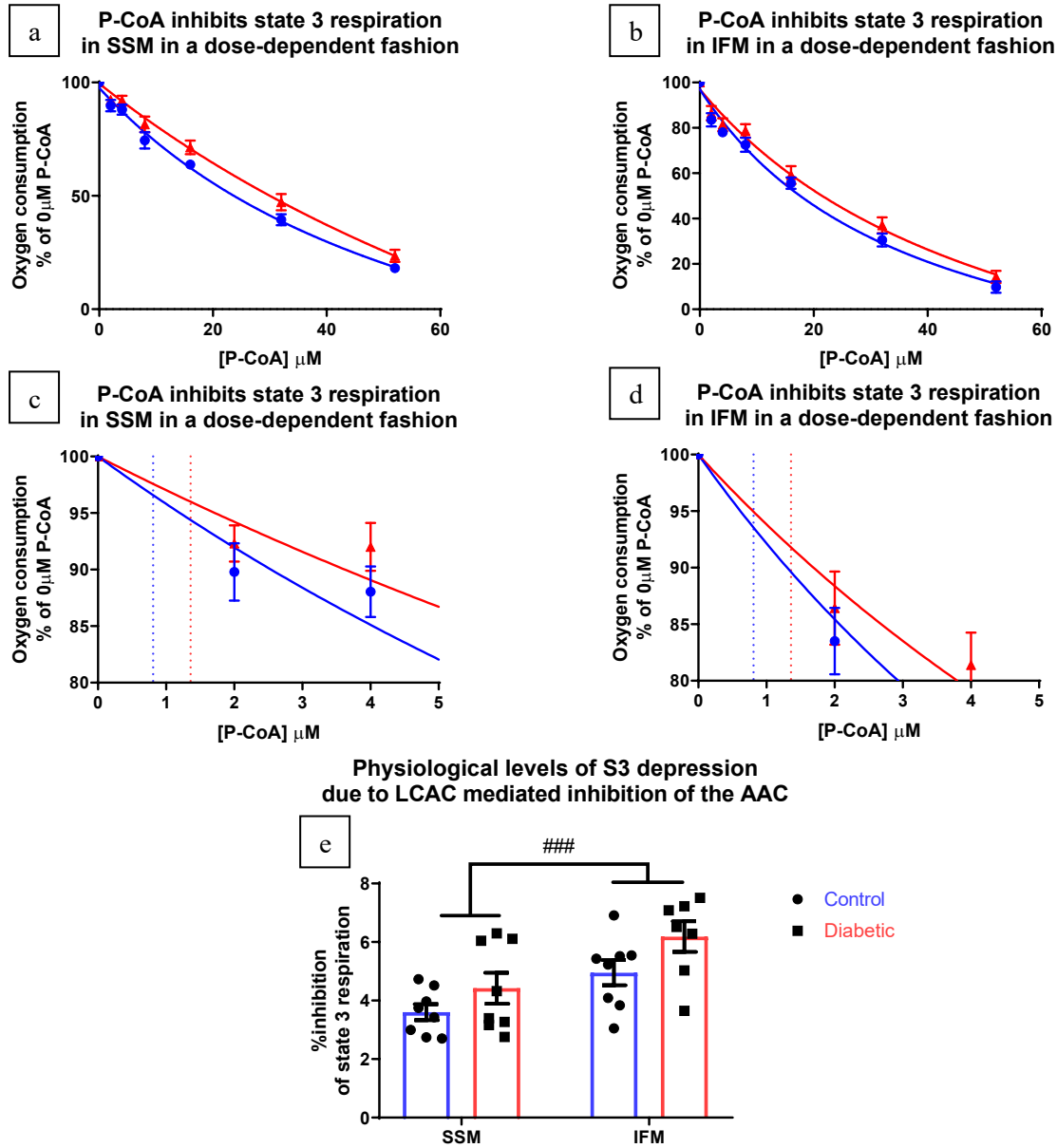

Figure 4.8 – (a,b) Mitochondrial state 3 respiration was measured across concentrations of palmitoyl-CoA, and the percentage of baseline respiratory rates plotted against the concentration of P-CoA. Data were fitted with the model; [inhibitor] vs normalised response, part of the non-linear regression curve fitting package in Prism. (c,d) show enhanced versions of the same graph, with cardiac concentrations of LCAC displayed as dotted lines (blue: control, red: diabetic). (e) shows calculated physiological levels of inhibition expected from the calculated LCAC concentrations. ### denotes P<0.001 for SSM vs IFM.

There are two primary cardiac isoforms of the AAC (AAC1 and 2), which have different kinetics for ADP transport and therefore may have different kinetics for LCAC inhibition. Primers were therefore created to measure AAC1 and AAC2 mRNA expression through qPCR.

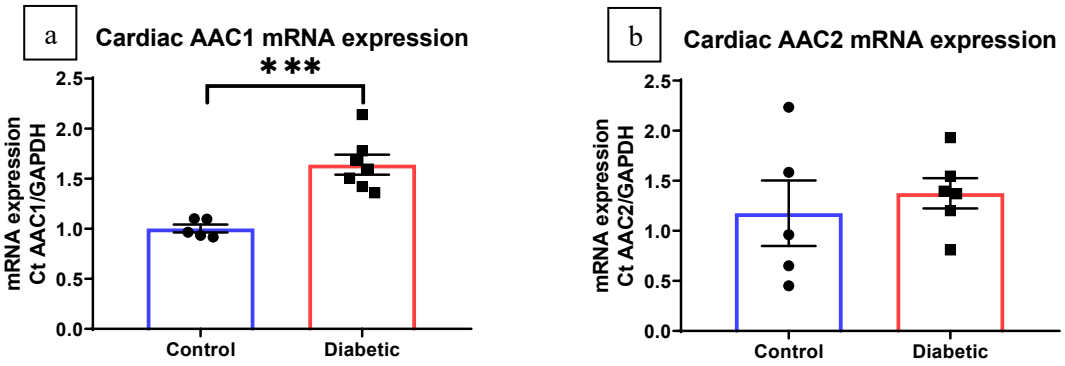

Figure 4.9 – mRNA expression of AAC1 (a) and AAC2 (b) was measured in diabetic and control hearts, with diabetic expression of AAC1 elevated compared to controls (*** denotes P<0.0001 for control vs diabetic). Data are expressed relative to the housekeeper (GAPDH).

These data showed that there was a 64% elevation in AAC1 (figure 4.9a), but not AAC2 (figure 4.9b), mRNA expression in diabetic hearts compared to control hearts. This indicated that the AAC isoforms may be under different transcriptional regulation, leading to a shift in the isoform ratio in the diabetic heart. Total ANT expression was therefore measured through western blotting of cardiac lysates, which displayed a 50% increase in AAC expression within the diabetic heart (figure 4.10a). In order to determine the relative increase in AAC1 and AAC2 specific antibodies were generated, as per section 2.4.3, and cardiac lysates were western blotted. These data showed that there was a 50% increase in both AAC1 (figure 4.10b) and AAC2 (figure 4.10c) protein expression.

Previous work indicated that mitochondrial density may be elevated in the diabetic heart (figure 3.9). Therefore, western blotting was performed on isolated mitochondria for AAC1 and AAC2. Figure 4.11 showed that the elevated AAC1 and AAC2 expression observed in the whole cardiac lysate could be traced to elevated mitochondrial mass and that AAC1 and AAC2 expression was not changed at the mitochondrial level. These data therefore show that the differential sensitivity to LCAC observed in T2D mitochondria cannot be explained by altered AAC isoform expression.

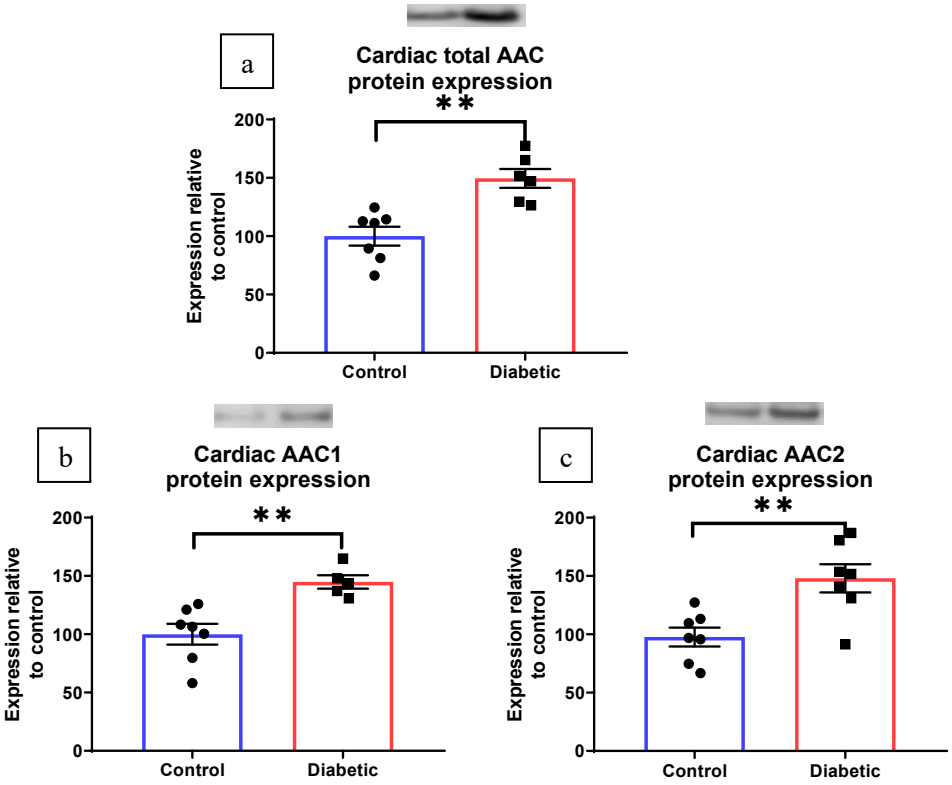

Figure 4.10 – Western blotting was performed on whole cardiac lysates using a total AAC antibody (a), followed by specific antibodies for AAC1 (b) and AAC2 (c). ** denotes P<0.001 for control vs diabetic. Data are expressed with control expression set to 100%.

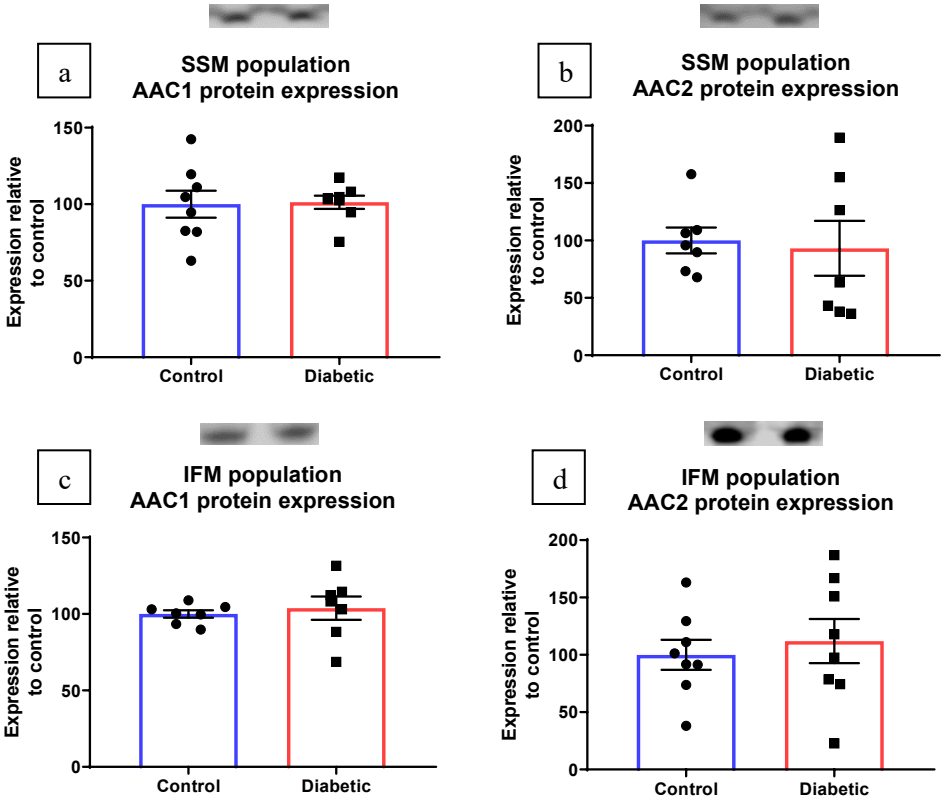

Figure 4.11 – Western blotting was performed on isolated cardiac mitochondria, using specific antibodies for AAC1 (a,c) and AAC2 (b,d). Data are expressed with control expression set to 100%.

4.5.3 ADP/ATP carrier inhibition in the ischaemic heart reduces reverse ATP synthesis

The AAC has differential kinetics with regards to LCAC inhibition between SSM and IFM populations, and between control and diabetic mitochondria. Although LCAC concentrations were elevated in the native diabetic heart, this wasn't sufficient to account for differences in baseline respiration. However, anoxia/ischaemia is accompanied by acute elevations in LCAC concentrations, and therefore represent pathological situations where LCAC inhibition may be of relevance, particularly considering the accelerated vascular disease in diabetes.

The first proposed pathological setting of AAC inhibition by LCACs is mitochondrial ATP hydrolysis in the ischaemic heart. Investigation of this required a reliable model of ischaemia in isolated mitochondria, which should feature the prevention of mitochondrial substrate oxidation, through blockade of the electron transport chain. Myxothiazol, an inhibitor of complex III has been used previously as an anoxia mimetic[233] and was therefore selected for this preparation.

Mitochondria (1.875 mg/mL) were incubated with safranine O (5 μM), resulting in a membrane polarisation around -150 mV (figure 4.12). The addition of substrates (5 μM glutamate, 5 μM pyruvate and 5 μM malate) hyperpolarised the membrane further, reaching -167 mV in control SSM vs -174 mV in diabetic SSM, and -173 mV in control IFM vs -172 mV in diabetic IFM. These values agreed well with values in the literature between -170 mV and -180 mV[244].

Myxothiazol depolarised the membrane potential in a dose-dependent fashion (figure 4.12). The addition of 100 μM ADP then lowered the membrane potential further, with no regeneration, indicating that the electron transport chain had been fully inhibited. ATP added post mitochondrial ischaemia showed significant regeneration of the mitochondrial membrane potential, which can be attributed to ATP degradation. This recovery was independent of the level of anoxia in the mitochondrial sample, determined by the concentration of myxothiazol. For further experiments 8 μM myxothiazol was taken forward, as this caused no membrane potential reduction by itself, but led to a reduction when ADP was added, indicating electron transport chain blockade, with no membrane damage.

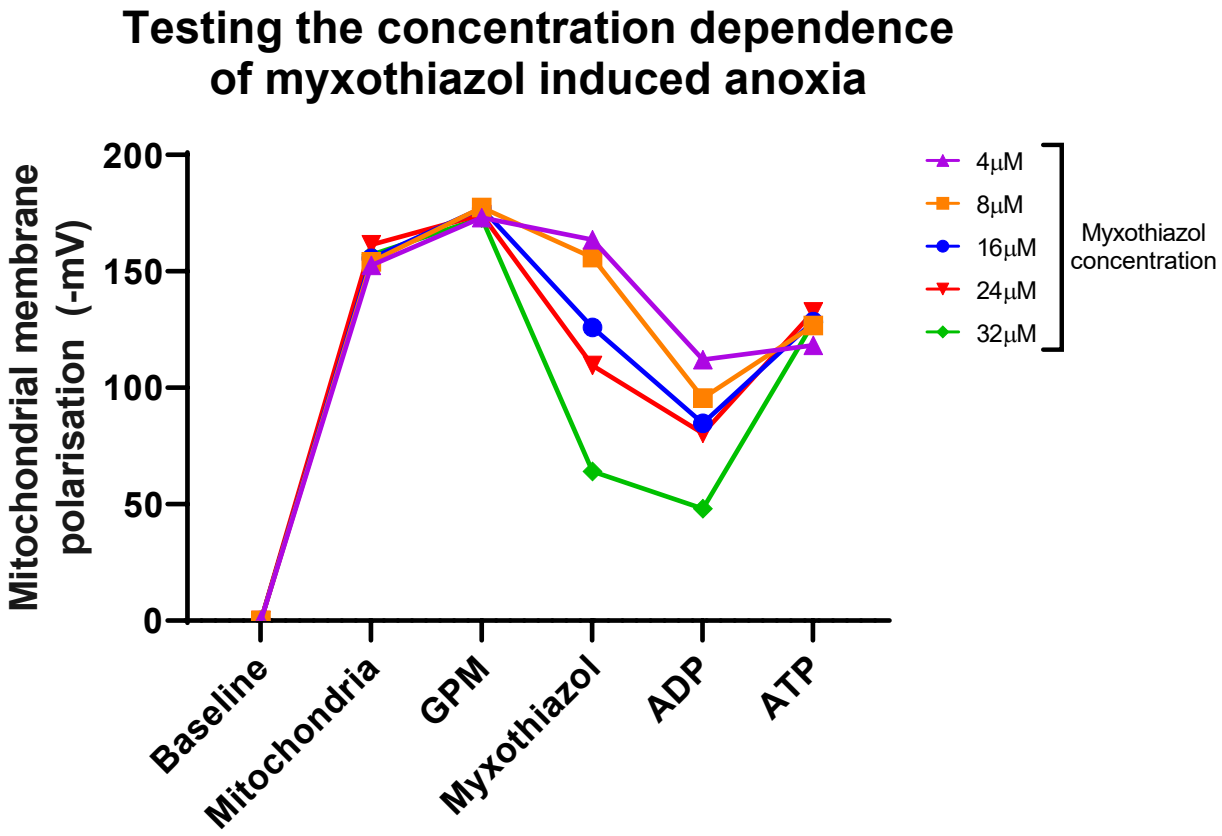

Figure 4.12 – Mitochondrial membrane potentials were measured by incubating mitochondria in the presence of Safranine O, resulting in a membrane potential around -150mV. The addition of substrates; glutamate, pyruvate and malate (GPM) hyperpolarised the membrane, to between -170mV and -180mV. Myxothiazol reduced the membrane potential in a dose dependent fashion, and ADP depolarised it further, with no recovery (indicating blockade of the electron transport chain). ATP was able to recover the membrane potential, indicating ATP hydrolysis by ATP synthase and proton pumping by the Fo domain in reverse.

This therefore provides a reasonable analogue of the ischemic mitochondrion, which features recovery of the mitochondrial membrane potential upon incubation with ATP. This finding can be explained by ATP degradation by the ATP synthase driving the proton pumping mechanism in reverse, thus polarising the membrane. In order to test that this reverse ATP synthesis was the cause of the membrane polarisation, inhibitors of either ATP synthase or the AAC were added before the addition of ATP.

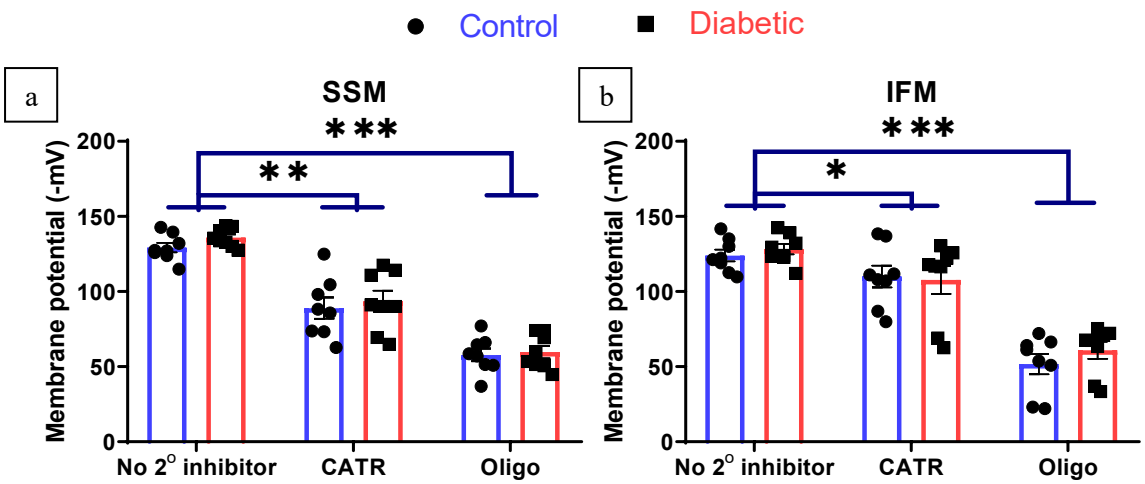

Figure 4.13 – The addition of ATP recovers membrane potential, as shown in the case of no secondary inhibitor. Inhibition of either ATP synthase (as by oligomycin) or the AAC (as be CATR) reduced this membrane polarisation as shown by a lower membrane potential. * denotes P<0.05, ** denotes P<0.005, *** denotes P<0.001 vs no secondary inhibitor.

These data show that while ATP can recover the membrane potential, this could be stopped either through blocking ATP import through the AAC with 2.5 mM CATR or preventing ATP degradation at the ATP synthase with 10 μM oligomycin (figure 4.13). Oligomycin was the stronger inhibitor, blocking membrane potential recovery by 56%, whilst CATR reduced membrane recovery by 31% in the SSM population and 12% in the IFMs. This strongly implicated that ATP hydrolysis at the ATP synthase was the driver for the observed recovery in membrane potential.

P-CoA can inhibit the mitochondrial AAC (figures 4.4 and 4.5), akin to CATR which potently prevents mitochondrial ATP degradation (figure 4.13). It was therefore hypothesised that the acute elevation in LCAC in the ischaemic heart could help to reduce mitochondrial ATP degradation. To test this, ischaemic mitochondria were incubated with P-CoA prior to ATP addition. These data (figure 4.14) showed that P-CoA can inhibit mitochondrial ATP degradation, in a dose-dependent fashion. Of note, this inhibition occurred at a lower concentration of P-CoA in control mitochondria compared to diabetic mitochondria, a finding which fits well with the previously observed reduced sensitivity of the AAC to LCAC in diabetic mitochondria (figures 4.6 and 4.7).

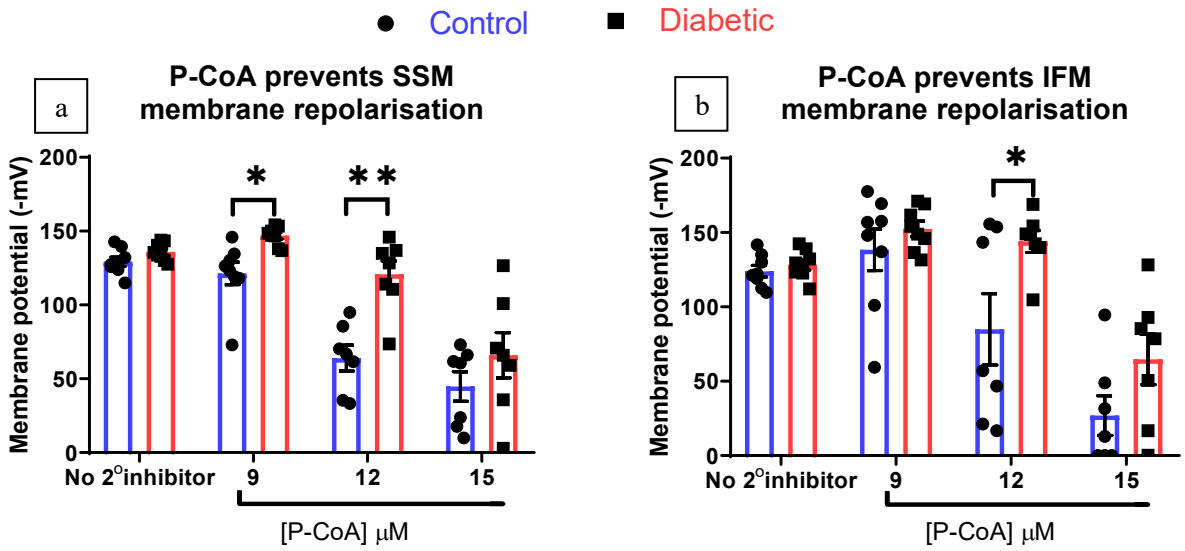

Figure 4.14 – Inhibition of the AAC, through P-CoA, dose dependently decreases the ATP-mediated membrane potential regeneration in both SSM and IFM populations. Diabetic mitochondria were less sensitive to this inhibition compared to control mitochondria. * denotes P<0.05, ** denotes P<0.005 for control vs diabetic.

Mitochondrial ATP degradation in the ischaemic heart can account for 30% of total myocardial energy depletion during a myocardial infarction[234]. Any mechanism to prevent this would therefore be cardioprotective, not only for the diabetic heart where we have shown that the lack of physiological AAC inhibition mediated by LCAC may cause excessive ATP hydrolysis (figure 4.14), but also in the case of the non-diabetic heart.

Oligomycin can potently inhibit ATP degradation (figure 4.13), however, this is not specific for the reverse mode of ATP synthase, and therefore would also prevent ATP synthesis under non-ischaemic conditions. BMS199264 - an IF1 mimetic - is specific for the reverse mode of ATP synthase[234–236]. This compound may therefore be able to reduce ATP hydrolysis rates in ischaemic mitochondria, whilst not affecting normal ATP synthesis. This inhibition of ATP hydrolysis was tested through incubation of ischaemic mitochondria with BMS199264 prior to ATP addition. BMS199264 reduced membrane repolarisation in control and diabetic ischemic mitochondria by 21% in the SSM (figure 4.15a) and 12% in IFM (figure 4.15a) populations. This prevention of membrane repolarisation indicated that BMS199264 can prevent mitochondrial hydrolysis of ATP within an ischemic setting.

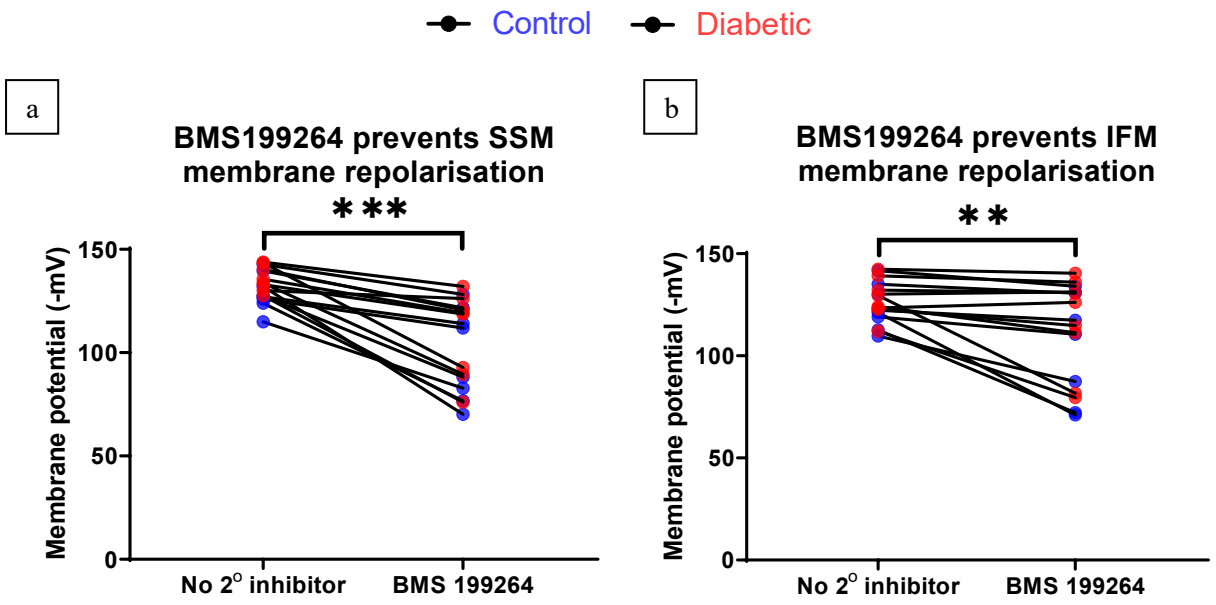

Figure 4.15 –ATP recovers membrane potential following ischemia (no secondary inhibitor). Inhibition of the reverse mode of ATP synthase, mediated by BMS199264, decreases this repolarisation. This effect was identical between control and diabetic mitochondria. ** denotes P<0.005, *** denotes P<0.001 for no secondary inhibitor vs BMS199264

4.5.4 Altered AAC LCAC sensitivity in T2D dysregulates mPTP opening

A major cause of cardiac ischaemia-reperfusion damage is opening of the mPTP. Work so far in this chapter has illustrated that LCAC, the concentration of which is acutely elevated during ischaemia, may have a physiological role in AAC regulation. LCACs are known to alter the conformation of the AAC, which can dramatically affect the severity, and speed of mPTP opening. The direct effect of LCAC on mPTP opening however, is unknown. The severity of mPTP opening in response to a high concentration of P-CoA was therefore compared to mitochondrial membrane depolarisation using FCCP, a known physiological inducer of the mPTP.

There was no difference in either the severity (figure 4.16a) or rate (figure 4.16b) of mPTP opening between controls and diabetics in response to FCCP in either mitochondrial population. Mitochondrial incubation with high concentrations of P-CoA induced rapid, and potent, mPTP opening with a 10-fold increase in the plateau point compared to FCCP incubation (figure 4.16c vs 4.16a). As previous data showed that the T2D AAC is less sensitive to inhibition (figures 4.6 and 4.7), the effect of a lower concentration of P-CoA on mPTP opening was examined.

Incubation of mitochondria with low concentrations of P-CoA still caused a rapid, and potent induction of mPTP opening, with plateau points 7-fold higher compared to membrane depolarisation alone (figure 4.17a vs 4.16a). The extent of this opening was 56% lower and the rate of opening unchanged in the diabetic SSM population compared to the control SSM population (figures 4.17a and b).

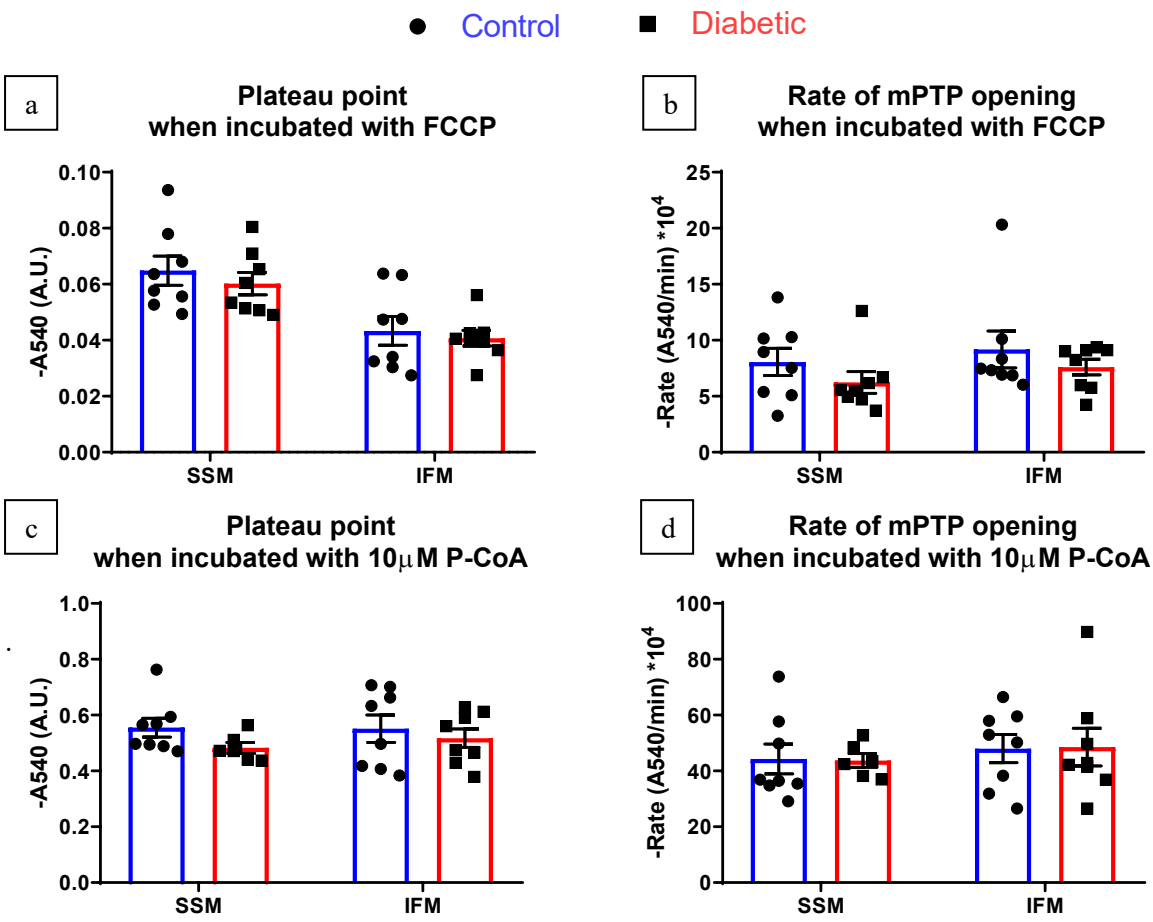

Figure 4.16 – a and b; depolarisation of the mitochondrial membrane potential with the uncoupling agent FCCP causes mPTP opening, as shown by a decrease in the A540. The kinetics of this opening were identical between control and diabetic mitochondria. Incubation of mitochondria with P-CoA caused rapid, and potent, induction of mPTP opening (c and d) displaying a 10-fold increase when compared to membrane depolarisation.

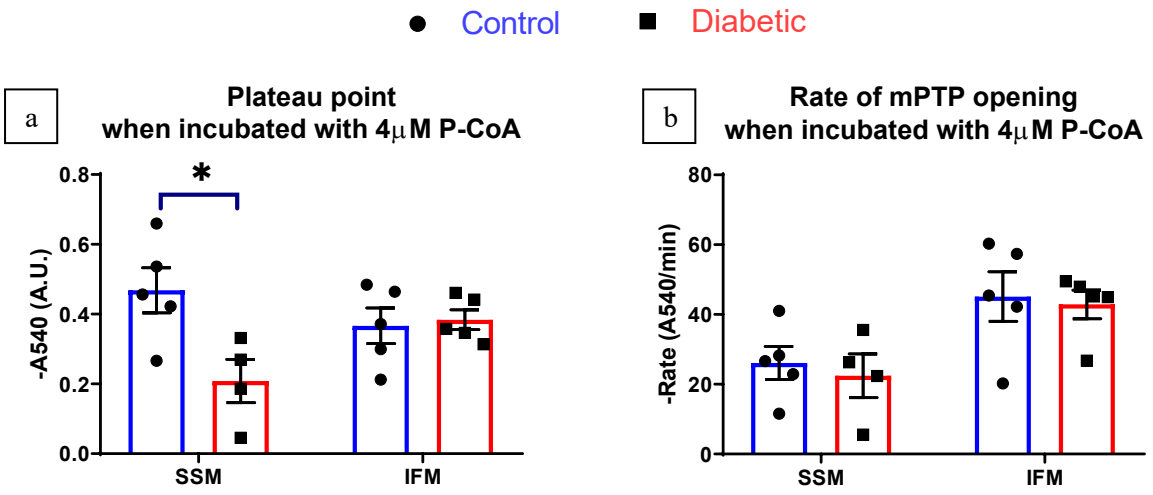

Figure 4.17 – Incubation of mitochondria with a low concentration of P-CoA caused modest mPTP opening. This opening was significantly reduced in the diabetic SSM population compared to controls. There was no difference in opening in the IFM population. * denotes $P<0.05$ for control vs diabetic.

Overall, these data indicate that LCAC inhibition of the AAC may be a key player in the regulation of mPTP opening in the ischaemic heart and that this is less relevant for diabetic mitochondria compared to control mitochondria. It is of interest to note that the effect of the AAC on mPTP opening is dependent on which state the AAC is locked in; locking the AAC in the matrix facing orientation (as facilitated by BKA) prevents mPTP opening whereas locking the AAC in the cytoplasmic facing orientation (as facilitated by CATR) induces mPTP opening. Therefore, whilst inhibition of the AAC by LCAC can occur from either side of the inner mitochondrial membrane, the effect of LCAC on mPTP opening would differ. In the work so far, LCACs have been present on the cytoplasmic face of the mitochondrial membrane, therefore locking the mPTP in the cytoplasmic facing orientation and inducing mPTP opening. *In vivo* however, 95% of LCACs exist within the mitochondrial matrix, and would therefore lock the AAC in a matrix facing orientation, preventing mPTP opening. The data displayed in figure 4.17a,b would be inverted in a physiological setting; with the increase in mitochondrial matrix levels of LCAC in ischaemia preventing mPTP opening. The reduced AAC sensitivity for LCAC in T2D mitochondria, would consequently lead to increased mPTP opening in T2D mitochondria.

In order to investigate the consequences of altered mPTP opening during ischaemia, citrate synthase (CS) activity (an indicator of mitochondrial volume) was assayed in cardiac samples pre, during, and post-ischaemia. These data showed that loss of CS activity occurred more rapidly in T2D hearts undergoing ischaemia than control hearts (figure 4.18) with only T2D hearts losing CS activity during the ischaemic insult. There was no change to mitochondrial DNA copy number, either during ischaemia or reperfusion, indicating that the loss of CS activity occurred independently of loss of mitochondrial number. During reperfusion, where fatty acid intermediates (such as LCAC) would be rapidly oxidised, both control and T2D mitochondria showed identical rates of CS activity loss. Taken together, this indicated that excessive loss of CS activity, indicating potential loss of mitochondrial volume, in the ischemic T2D heart may be due to reduced sensitivity of the AAC for LCACs in T2D mitochondria.

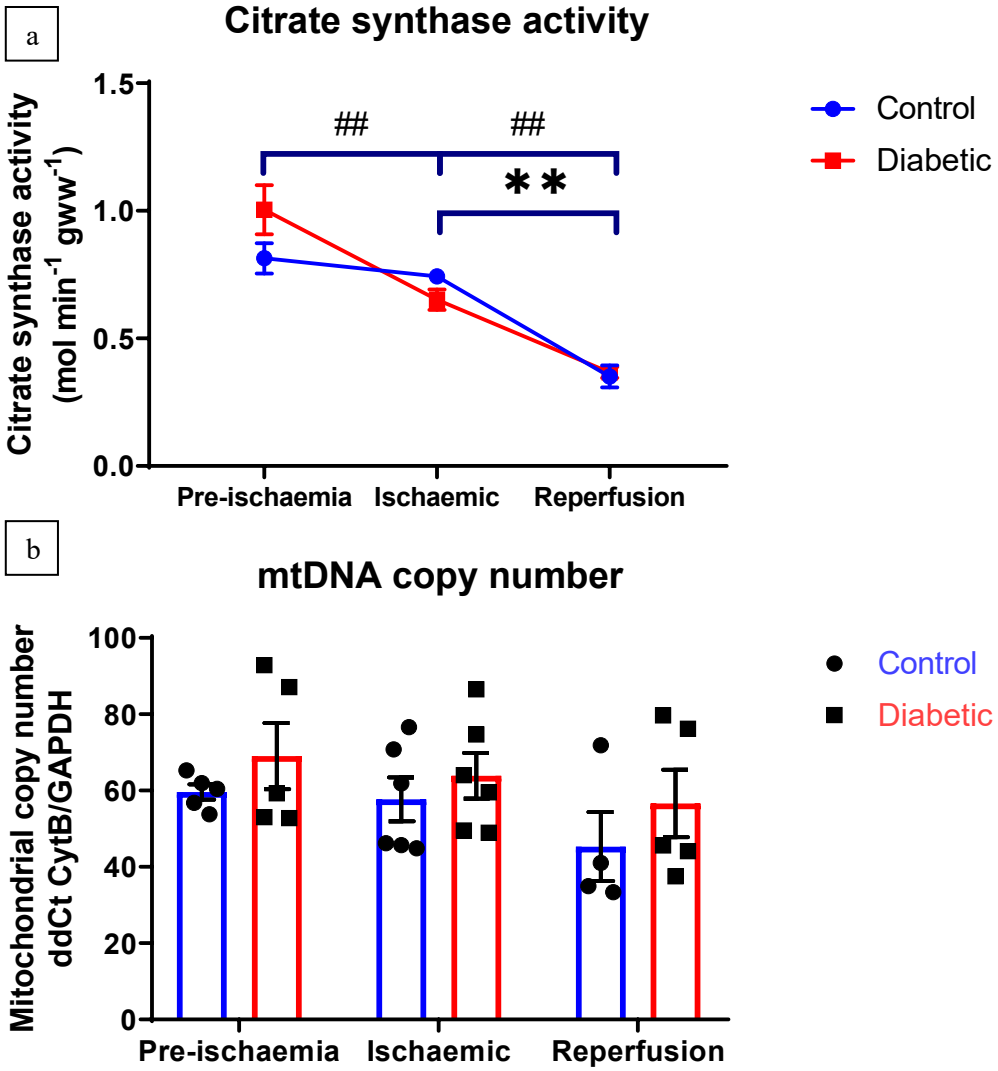

Figure 4.18 – Citrate synthase activity and mtDNA copy number was measured in control and T2D hearts, freeze-clamped either pre-ischaemia, after 30 minutes of ischaemia, or after 30 minutes of reperfusion. ** denotes P<0.005 between conditions for controls, ## denotes P<0.005 between conditions for diabetics.

4.6 DISCUSSION

4.6.1 Long chain acyl-CoA inhibition in the type 2 diabetic heart

The T2D heart is commonly associated with lipotoxicity. Supporting this, these data demonstrate that LCAC abundance is higher in the T2D heart, primarily due to elevated levels of O-CoA. This agrees well with the phenotype seen in intramuscular samples from T2D human patients[245].

These values (0.22 nmol/g(wet) in controls and 0.37 nmol/g(wet) in diabetics) obtained through mass spectrometry represent one of the most accurate measurements of LCAC concentrations in the T2D heart to date. Of interest, they are significantly lower than previous values obtained through hydrolysis of acyl-CoAs to acetyl-CoA, followed by fluorometric detection (93 nmoles/g(dry)[232], 20 nmol/g(wet)[226] and 1.3 nmol/mg mitochondrial protein[246]). Fluorometric techniques can introduce significant margin of error compared to mass spectrometry, and lead to a potential overestimation of acyl-CoA levels from other sources of acetyl-CoA.

This chapter has demonstrated that the AAC can be inhibited by LCACs (specifically P-CoA) in an isolated mitochondrial setting and has investigated the kinetics around the AAC regarding LCAC inhibition. This represents the first reported literature values for Km and Vmax with ADP titration, and IC50 values for LCAC in both control and T2D mitochondrial populations. Mitochondria isolated from T2D hearts are significantly less sensitive to this LCAC inhibition, with an elevated IC50, and no significant increase in the Km for ADP when palmitoyl-CoA is present. The IC50 values (22.6 μM in the SSM and 16.6 μM in the IFM population) are significantly higher than those reported elsewhere in the literature (between 0.2 μM[224] and 1 μM[247]). Current reported values deal primarily with isolated channels, whereas values reported in this chapter are obtained in intact mitochondria. In the isolated mitochondrial setting, LCACs can partition into the mitochondrial membrane, as would occur physiologically. This partitioning reduces the effective LCAC concentration thus requiring a higher total LCAC concentration compared to experiments with isolated channels.

The reduced sensitivity of the AAC to LCAC observed in this rodent model of T2D cannot be explained by changes in total AAC content or AAC isoform expression and may therefore be due to post-

translational modifications (PTMs). There are many forms of AAC PTM (phosphorylation[248], glutathionylation[249] and carbonylation[250]) but perhaps the most relevant in this setting is acetylation. This PTM involves the addition of an acetyl group onto a lysine residue of a protein. In the case of the AAC it has been implicated, through *in silico* modelling, in reducing the sensitivity of the protein to its primary substrates (ADP and ATP)[121]. This PTM is of particular interest in this setting as it alters the charge state of the central binding point (changing a positive lysine to neutral). Given that this alters the affinity of the binding sites for the negatively charged ATP and ADP, it is not unreasonable that it would also affect affinity for binding the negatively charged LCAC moiety. Despite multiple experiments, data could not be generated regarding the acetylation of the AAC in T2D, either in whole heart samples or in isolated mitochondrial sub-populations.

If therefore the AAC was hyper-acetylated in T2D one would expect a reduction in binding affinity for LCACs, as well as for ADP and ATP. The altered LCAC sensitivity has been displayed, and alterations to the Km for ADP in the absence of P-CoA have been observed in other models of T2D[251]. It is further noted that this reduced sensitivity also occurs in exercise training in humans[252], another model featuring chronically elevated LCAC levels, indicating that it may be a physiological adaptation to prevent the inhibition of mitochondrial respiration.

Through the combination of high fidelity mass spectrometry measurements of intra-myocardial LCAC concentrations, and measurements of the effect of LCAC on isolated mitochondria, this work concludes that LCAC inhibition of the AAC does not play a major role in the energetic dysfunction observed in the type 2 diabetic heart under normal physiological conditions, answering a question that has generated debate for over 40 years[253–255]. However, it may play a role when LCAC levels are acutely elevated, such as in anoxia or ischemia.

4.6.2 ATP/ADP carrier inhibition in the ischaemic heart reduces reverse ATP synthesis

To date, the only proposed physiological roles of LCAC inhibition of the AAC is in reducing energy generation in the livers of hibernating animals[218]. The role of this inhibition in the ischaemic heart is

generally assumed to be maladaptive[256,257], but here, two settings are presented where this inhibition would be cardioprotective.

The AAC can facilitate reverse ATP synthesis, and this work demonstrates this phenomenon in a novel model of isolated cardiac mitochondrial ischaemia. This chapter demonstrated that inhibition of the AAC, either by the exogenous inhibitor CATR or by endogenous LCACs, significantly reduced the rate of reverse ATP synthesis, thus preserving cytosolic ATP levels. In T2D mitochondria, which have reduced sensitivity of the AAC for LCACs, a greater concentration of LCAC is required to inhibit the AAC and prevent reverse ATP synthesis. Therefore, when oxygen is restricted, mitochondria in the diabetic myocardium would hydrolyse cytosolic ATP for longer, and at a faster rate upon entering ischaemia than healthy hearts.

It is possible that this phenomenon could explain some of the reduced rates of recovery observed in T2D hearts post ischaemia compared to control hearts. This phenomenon would be additive to other aspects of altered metabolism in the T2D heart, such as; impaired glycolysis, increased fatty acid uptake and increased mitochondrial uncoupling, which culminates in reduced recovery post-ischemia (see [258] for review). BMS199264, an IF1 mimetic, can reduce the rate of reverse ATP synthase, whilst not reducing normal function of the ATP synthase. It therefore provides an exciting therapeutic avenue, both for the diabetic and healthy heart.

4.6.3 Reduced ATP/ADP carrier long chain acyl-CoA sensitivity in type 2 diabetes affects mPTP opening

Nowhere is mPTP opening more acutely brought into focus than the setting of the ischaemic heart, where rapid mPTP opening dramatically reduces myocardial recovery post-ischaemia. Given the dramatic acute elevation in LCACs during cardiac ischaemia, and the potential for acute LCAC regulation on a key protein mediator in mPTP opening – the AAC (figures 4.5 and 4.6), it is important to define the role of LCAC mediated AAC regulation on mPTP opening

We have shown that mPTP opening occurs in response to acute extra-mitochondrial LCAC incubation in isolated mitochondria, and that this is a far more potent stimuli for mPTP opening that other

physiological stimuli such as membrane depolarisation (figure 4.16). This provides another mechanism to account for the lipotoxic effects of lipid intermediates during an ischaemic insult. Given the antagonistic roles of intra and extra-mitochondrial LCAC upon the AAC in the mPTP, one can infer that intra-mitochondrial LCAC incubation would provide a potent inhibitory stimulus to mPTP opening in a physiological setting. This leads to the conclusion that ischaemic LCAC elevation would be cardioprotective with regards to mPTP opening.

Work earlier in this chapter robustly demonstrated, through multiple derivations, that the AAC in T2D mitochondria has reduced sensitivity to LCAC incubation (figures 4.6 and 4.7). One would therefore expect that this may alter mPTP opening upon LCAC incubation in T2D mitochondria, and indeed this is the case. It is noted that differential mPTP opening was only observed between control and T2D mitochondria under low concentration of P-CoA in our SSM population, and not in the IFM population. This may be as our 'low' concentration of P-CoA still induces near maximal opening in both control and T2D mitochondria in the IFM population due to their lower IC50 than the SSM population (figure 4.7). It may be that at even lower concentrations of P-CoA one would see divergent effects between control and T2D mitochondria.

We therefore propose that T2D mitochondria would be significantly more likely to undergo mPTP opening during ischaemia than control mitochondria (as supported by figure 4.18), decreasing post-ischaemic recovery in these hearts.

4.7 CONCLUSION

In this chapter, the contribution of AAC inhibition by LCACs, towards the reduced respiratory function seen in T2D mitochondria was evaluated. The LCAC concentration was found to be elevated in the T2D heart, and the capacity of these LCACs to inhibit the AAC and so reduce mitochondrial respiration was demonstrated. However, it was found that the sensitivity of the AAC for LCACs is reduced in T2D mitochondria, and therefore shown that this mechanism is unlikely to be responsible for the reduction in mitochondrial respiratory rates observed in the T2D heart.

This work uncovered two novel potential physiological roles for LCAC inhibition of the AAC in cardiac ischaemia. Firstly, AAC inhibition during ischaemia may prevent excessive mitochondrial ATP hydrolysis, and reduce the rate of energy depletion in the ischaemic heart. Secondly the action of LCAC binding to the AAC and locking its orientation during ischaemia may prevent excessive mPTP opening. Both these effects of LCAC mediated AAC inhibition are significantly diminished in T2D mitochondria. This has severe potential implications for the T2D myocardium, which would futilely hydrolyse ATP at a greater rate, and undergo excessive mPTP opening, when compared to a healthy heart during ischaemia.

Overall, these data uncover a heretofore unseen mitochondrial adaptation to cope with the lipid overloading phenotype within the T2D heart. Furthermore, they illustrate how this process, although a possible adaptation to the lipotoxicity within the T2D heart, may blunt the response of the heart to ischaemic pathological insult. This work therefore provides additional therapeutic angles, and a candidate agent, in reducing myocardial ischaemic injury in the diabetic heart.

5 MITOCHONDRIAL PROTEIN HYPERACETYLATION DECREASES RESPIRATORY CAPACITY IN THE TYPE 2 DIABETIC HEART

5.1 ABSTRACT

Mitochondrial protein acetylation is a post-translation modification (PTM) associated with both reducing enzymatic activity and playing a role in the fine-tuning of metabolic rate during the fed-fasted cycle. Type 2 diabetes (T2D) is a classic example of dysfunction of the fed-fasted cycle, as insulin resistance prevents the normal insulin-induced transition in the fed state. This chapter will determine whether mitochondrial protein hyperacetylation is observed within the T2D heart and evaluate the hypothesis that this may contribute to the reduced respiratory rates observed in T2D cardiac mitochondria.

To interrogate this hypothesis western blotting was carried out on isolated mitochondria which demonstrated a 50% elevation in acetylation of mitochondrial proteins in T2D. This was further investigated through acetylomics showing that the hyperacetylation resulted from a global, rather than specific, upregulation of protein acetylation. To appraise the effect of global protein hyperacetylation a model of acute mitochondrial hyperacetylation was generated, which displayed reductions in respiratory rates on a similar order of magnitude to T2D mitochondria. To confirm that reduced respiratory rates could be traced to hyperacetylation within T2D mitochondria an acute model of mitochondrial deacetylation was generated, which showed improvements in maximal respiratory rates in T2D mitochondria.

In conclusion, this chapter demonstrates that T2D mitochondria are hyper-acetylated and, through the hyperacetylation of non-diabetic mitochondria and the deacetylation of T2D mitochondria, provides evidence that this hyperacetylation may be responsible for the reduction in respiratory rates observed in T2D mitochondria. Overall, this provides an exciting, and heretofore unexplored, route for the therapeutic amelioration of T2D cardiac energetic dysfunction.

5.2 INTRODUCTION

5.2.1 Mitochondrial protein acetylation

Acetylation is a post-translational protein modification (PTM) whereby an acetyl group is covalently bound to the ε-amino group of lysine residues. This modification neutralises the otherwise positive charge found on a lysine residue, therefore potentially altering interactions with; nearby amino acids (altering the tertiary structure of the protein), other proteins, and substrates. Acetylation is thought to primarily occur in a spontaneous fashion[90], although the putative acetyl-transferase GCN5L1 has been implicated in facilitating this process[88]. The only known enzyme with strong intra-mitochondrial deacetylase activity is the NAD^+-dependent Sirtuin family member Sirt3, which globally deacetylates mitochondrial proteins[92].

Acetylation has emerged as an important mechanism for controlling a broad array of proteins governing cellular adaptation to different metabolic fuels. The hyperacetylation of mitochondrial proteins is associated with a reduction in their enzymatic activity[98,99,118,120,103–107,113,115,117]. However cardiac mitochondrial hyperacetylation occurs only as a response to chronic alterations in metabolism, either due to disease states[101,103,104] or diet manipulation[95,98,99]. As mitochondrial hyperacetylation only occurs physiologically with altered metabolism, it is difficult to determine the effect of protein hyperacetylation on mitochondria without the measurement being confounded by the altered metabolic state of the cell. This chapter will therefore aim to investigate mitochondrial protein-hyperacetylation in an acute setting, without any change in cellular metabolism. It will endeavour to achieve this through the contrasting actions of acetic anhydride and honokiol.

5.2.2 *In vitro* acetylation - acetic anhydride

Acetic anhydride [$(CH_3CO)_2$] is a versatile agent, which is used widely for the introduction of acetyl groups to organic substrates. Its use as an *in vitro* protein acetylation agent was first demonstrated by Buechler *et al.* in 1990[259] and it has more recently been demonstrated that it can acetylate mitochondrial proteins, in a non-specific fashion, *in vitro*[101].

5.2.3 *In vitro* deacetylation - honokiol

The most promising target for specific mitochondrial deacetylation, both *in vitro* and *in vivo* on a wild type background is the therapeutic activation of Sirt3. Many approaches have been linked to Sirt3 activation, although few are thought to act primarily through Sirt3. These approaches can be broadly categorised into 4 groups; small molecule activators, upstream signalling pathways, microRNAs and traditional Chinese medicines.

The most well-known small molecule activator of overall Sirtuin activity is resveratrol, however, its effects on Sirt3 appear modest, with some studies indicating that it has no activity[260] and others indicating only a modest activity[261,262]. Sirt3 can also be targeted by melatonin and metformin, which can ameliorate cardiac dysfunction through a Sirt3 dependent mechanism[263,264] and normalise Sirt3 expression within type 2 diabetic (T2D) patients[265], respectively . However the activation of Sirt3 is not thought to be the primary mechanism of action for these drugs[266]. Sirt3 expression can be targeted through upstream pathways, but this is usually in addition to widespread activation of collateral mitochondrial pathways such as cAMP[267], AMPK[268], Sirt1[269] and PGC-1α[270]. As such, delineating the effect of the upstream signalling pathway from the effect of Sirt3 activation is difficult. MicroRNA manipulation of Sirt3 expression has been associated with a reduction, rather than increase, in Sirt3 levels and can be related to a shift towards a hypoxic phenotype through MIR-210[271] and with a circadian shift in neurons through MIR-92a[272].

The area of Sirt3 activation which has seen the most success is through activation with traditional Chinese medicines, and more specifically honokiol[109]. Honokiol [2-(4-hydroxy-3-prop-2-enyl-phenyl)-4-prop-2-enyl-phenol] is a small molecular weight polyphenol with high bioavailability derived from the bark of magnolia trees. Honokiol has been shown to increase Sirt3 expression and activity *in vivo* and to bind to and activate Sirt3 *in vitro*[109]. The relative specificity that honokiol shows for Sirt3 activation positions it as an exciting tool in the treatment of mitochondrial protein hyperacetylation.

5.3 AIMS

Section 3.4.3 demonstrated reduced rates of respiration in mitochondria isolated from T2D hearts, which is linked to cardiac energetic dysfunction and so to increased risk of cardiovascular mortality in diabetes. This chapter aims to address the hypothesis that protein hyperacetylation may cause the mitochondrial dysfunction observed in the T2D heart. This is based on two observations: firstly, mitochondrial protein hyperacetylation is linked to elevated levels of fatty acid oxidation, and secondly, that mitochondrial protein hyperacetylation is associated with reduced enzymatic activity (table 1.2, section 1.3.2). This was interrogated through three primary objectives;

1. Mitochondrial protein acetylation was measured within T2D hearts and acetylated proteins characterised through acetylomics.
2. The effect of *in vitro* acetylation of control mitochondria was investigated.
3. The effect of *in vitro* administration of honokiol on T2D mitochondria was investigated, with regards to mitochondrial protein acetylation and respiratory rates.

5.4 METHODS

5.4.1 Optimisation of *in vitro* mitochondrial acetylation

Acetic anhydride was dissolved in acetonitrile, an organic solvent which does not alter mitochondrial state 3 respiration at concentrations below 1% (v/v)[273]. Preliminary studies were carried out on control mitochondria to optimise the level of mitochondrial hyperacetylation upon 6 minutes incubation with acetic anhydride, as displayed in figure 5.1.

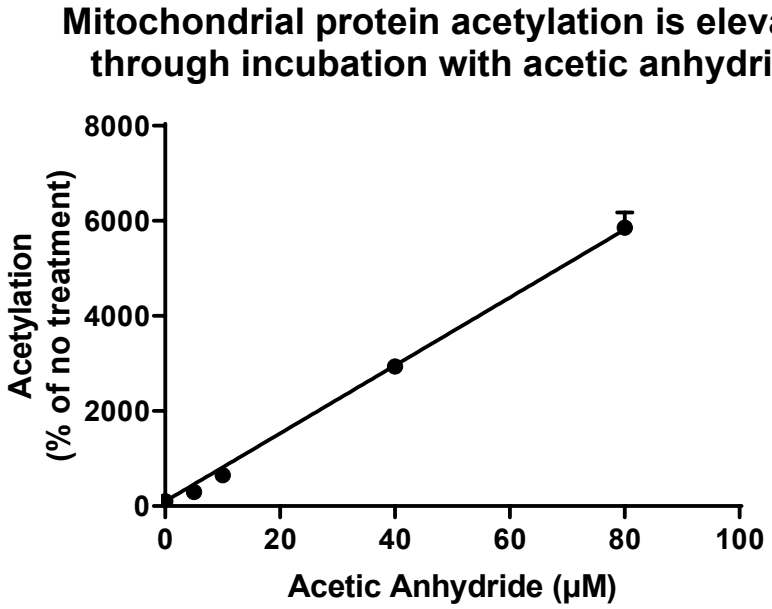

Figure 5.1 – Acute incubation with acetic anhydride resulted in a linear increase in mitochondrial protein acetylation, as measured through western blot analysis with a pan acetyl-lysine antibody (n=3).

These data displayed a linear correlation between the concentration of acetic anhydride used and the increase in acetylation. State 3 respiratory rates were measured through the addition of 200 µM ADP to these *in vitro* acetylated mitochondria, in the presence of 20 mM glutamate, 10 mM pyruvate and 5 mM malate, following the protocol defined in section 2.3.2. Plotting percentage inhibition of state 3 respiration against the concentration of acetic anhydride gave rise to a non-linear hyperbolic regression as shown in figure 5.2. Using these regression curves, it was calculated that incubation with 12 µM acetic anhydride would result in a 17% depression of respiration, equal to that observed in diabetic mitochondria (figure 3.10).

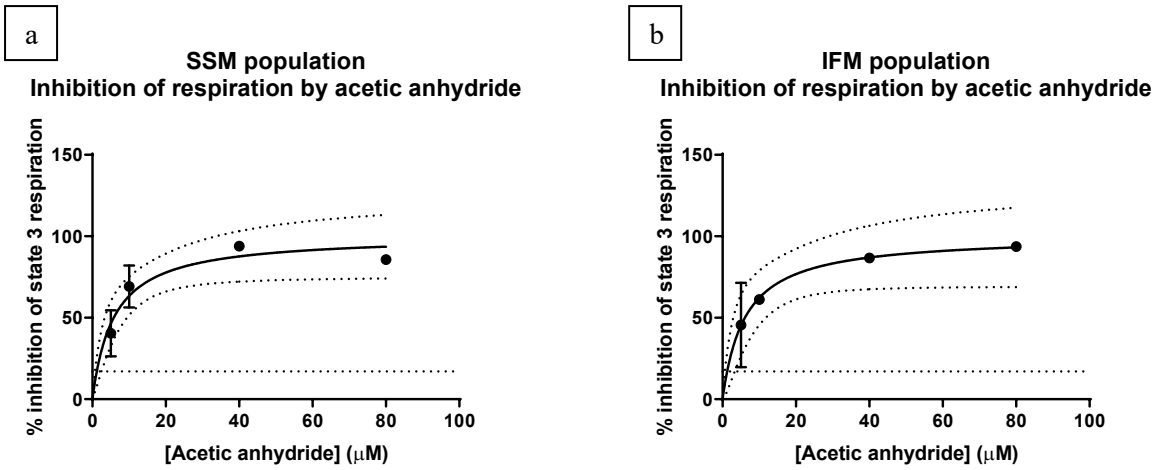

Figure 5.2 – *In vitro* protein-hyperacetylation reduced state 3 respiration in isolated mitochondria in a hyperbolic fashion in both the SSM (a) and IFM (b) populations.

Concentrations of 7 μM, 12 μM and 17 μM acetic anhydride were taken forward for *in vitro* mitochondrial acetylation experiments using the following protocol:

5.4.2 *In vitro* mitochondrial acetylation

Control mitochondria were isolated according to section 2.3.1 and stored at 4°C. A 2 mM stock solution of acetic anhydride was prepared on the day in 1 M acetonitrile. SSM and IFM (1.6 mg of mitochondrial protein) were added to 7 μM, 12 μM and 17 μM acetic anhydride. After manual inversion for 6 minutes, 9 mM lysine was added to fully quench the acetylation reaction. The sample was centrifuged at 3020g (4°C) for 5 minutes, before the pellet was re-suspended in the same volume of mitochondrial isolation solution 3 (section 2.9) used to obtain 1.6 mg mitochondria. Acetylated samples were then assayed for protein concentration and these values used to carry out mitochondrial respiratory measurements following the protocol defined in section 2.3.2.

5.4.3 Optimisation of *in vitro* honokiol incubation

The duration, and concentration, of *in vitro* honokiol incubation was optimised as follows. Durations of between 3 minutes and 12 hours were trialled and it was found that durations of over 10 minutes led to a reduction in state 3 respiration, potentially due to the depletion of NAD by the deacetylation reaction. Therefore, 3 minutes was taken forward as the incubation time. In order to investigate mitochondrial tolerance to honokiol, mitochondrial membrane potential was measured at various

honokiol concentrations both in the presence (figure 5.3a) and absence (figure 5.3b) of substrate (20 mM glutamate, 10 mM pyruvate and 5 mM malate).

a

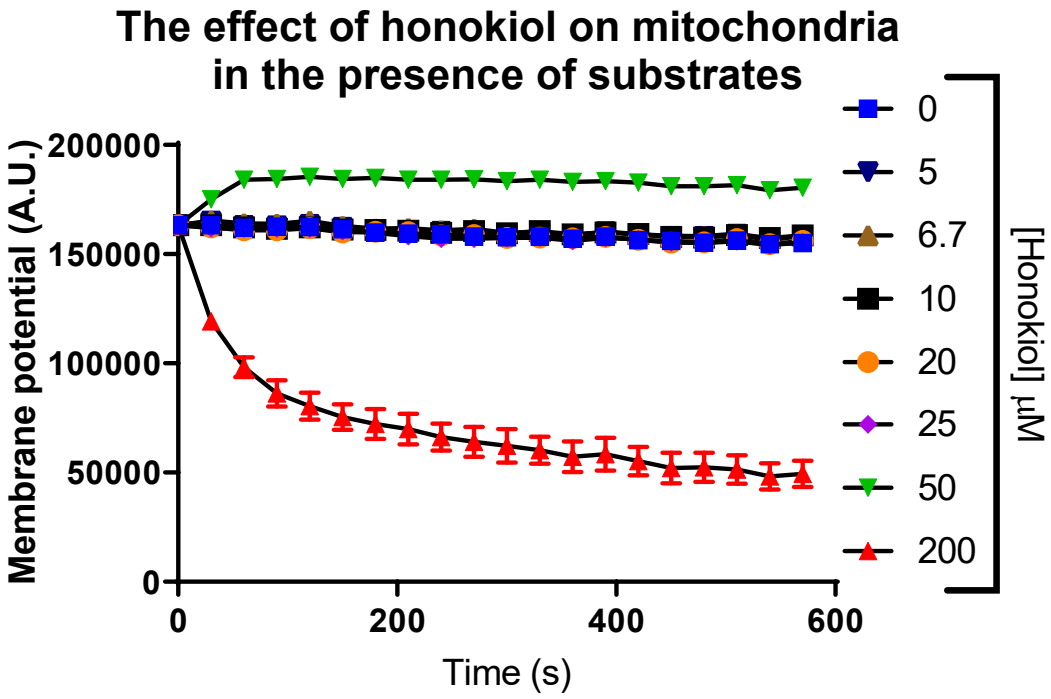

b

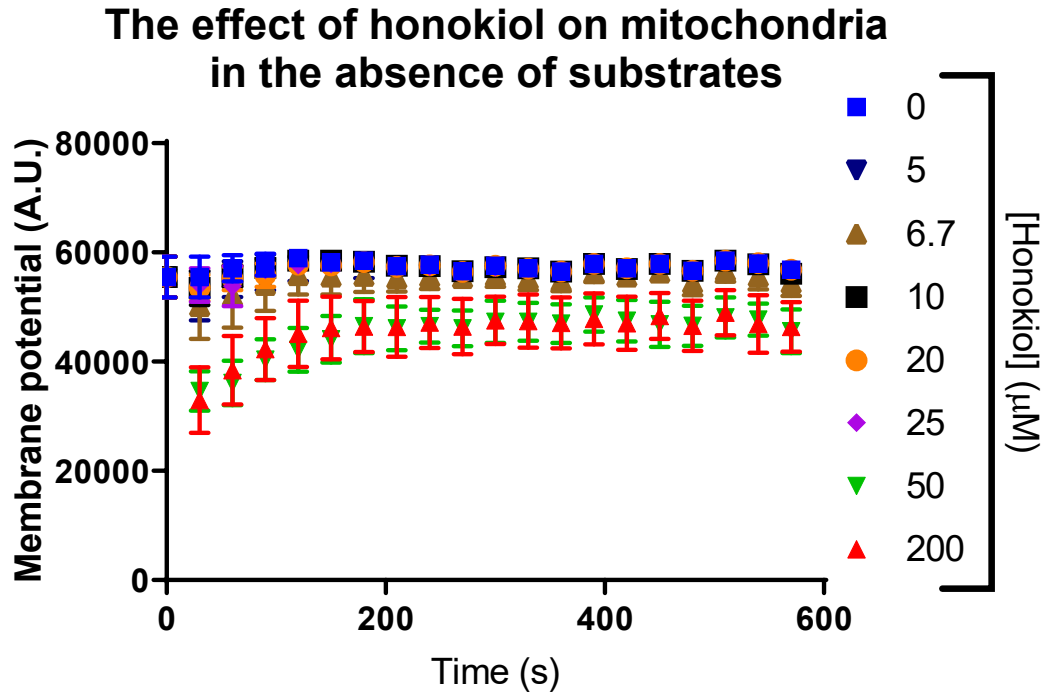

Figure 5.3 – High concentrations of honokiol (200 µM) caused mitochondrial membrane depolarisation in both the presence (a) and absence (b) of substrates (20 mM glutamate, 10 mM pyruvate and 5 mM malate), whilst moderate concentrations (< 25 µM) were well tolerated in both settings.

High concentrations of honokiol (200 μM) caused mitochondrial membrane depolarisation in both settings, whilst moderate concentrations (<25 μM) were well tolerated in both settings. Concentrations of honokiol around 10 μM were therefore selected as 10 μM honokiol showed no membrane depolarisation, indicating it was well-tolerated by mitochondria.

5.4.4 *In vitro* honokiol incubation

Honokiol was made up to a 20 mM solution in ethanol. Mitochondria were isolated according to section 2.3.1, and stored at 4°C. Mitochondria (0.15 mg of mitochondrial protein) were added to 500 μL of respiration media (see section 2.9) at 30°C. Honokiol was added to a final concentration of either 7 μM or 14 μM and the solution incubated for 3 minutes. Immediately following this, state 3 respiratory measurements were taken, following the protocol defined in section 2.3.2.

5.4.5 Statistical analysis

Datasets containing two groups were analysed using the two-tailed parametric unpaired t test function within GraphPad Prism 8.0.0. A reported P value less than 0.05 was taken as significantly different.

Proteomic data statistical analysis was carried out as multiple two tailed t-tests, with 250 randomisations, and a false discovery rate of 0.05 using the software Perseus.

Datasets which displayed linear correlations were fitted with a linear regression relationship (GraphPad Prism 8.0.0), with significance of a non-zero slope taken as $P<0.05$.

Datasets containing multiple groups, but one variable, were initially analysed using an ordinary one-way ANOVA, with no matching. Significance was followed up with post-hoc Dunnett multiple comparison tests, comparing the mean of each column with the mean of the control column.

5.5 RESULTS

5.5.1 Mitochondrial proteins exhibit hyperacetylation in the type 2 diabetic heart

In order to investigate mitochondrial protein acetylation in an unbiased fashion, lysates from control and T2D cardiac mitochondria underwent western blotting for pan acetyl-lysine. These data revealed hyperacetylation in T2D mitochondria, as evidenced by a 51% elevation in protein acetylation (figure 5.4a) in T2D SSM compared with controls and a 40% increase in acetylation in T2D IFM compared with controls (figure 5.4b).

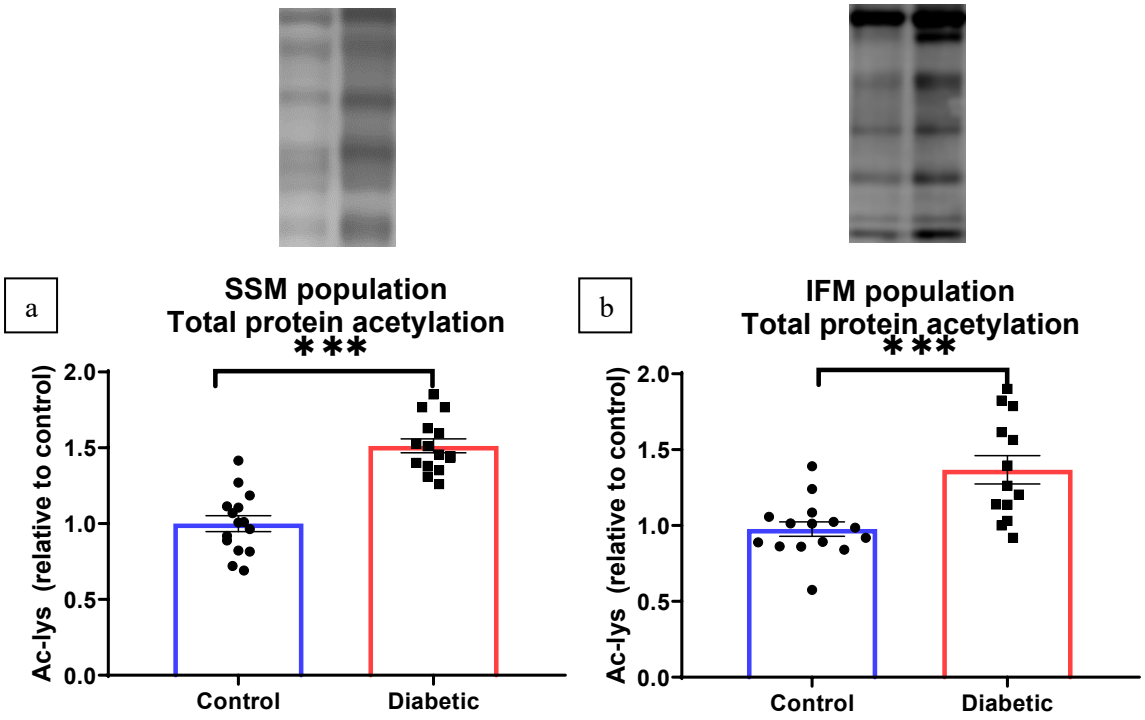

Figure 5.4 – Western blot analyses of mitochondrial protein acetylation show a significant increase in protein acetylation in mitochondria isolated from T2D hearts. *** denotes P<0.001 for control vs diabetic.

Acetylation status is dependent on the dynamic interplay between pro and anti-acetylation factors. The hyperacetylation exhibited in T2D mitochondria could therefore be due to either increased acetylation (from increased acetyl-CoA levels) or decreased deacetylation (from reduced NAD or Sirt3 levels). We have previously shown that NAD is decreased, and acetyl-CoA increased in the diabetic heart indicating a pro-acetylation environment[274]. Therefore, Sirt3 expression was assayed through western blot analysis, revealing that it is unaltered in the T2D heart (figure 5.5).

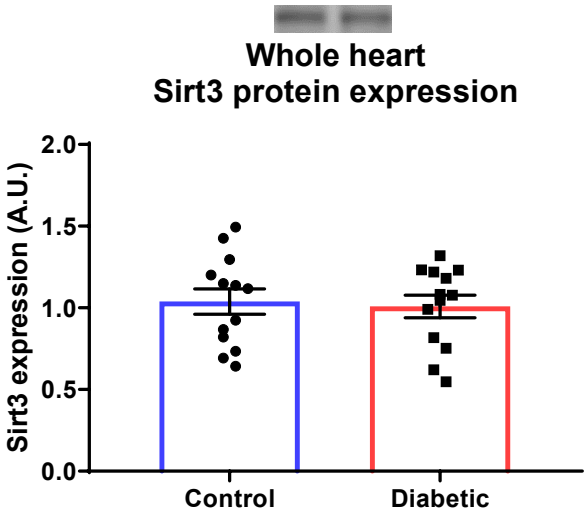

Figure 5.5 – Analysis of total Sirt3 expression in the whole heart via Western blotting showed similar levels of protein expression between control and diabetic hearts.

This increase in total protein acetylation in T2D mitochondria could be due either to a general increase in protein acetylation or due to acetylation of a specific sub-set of proteins. In order to answer this question, mitochondrial proteins were immunoprecipitated using an acetyl-lysine antibody, with this pulldown then subjected to proteomic analysis. Acetylomic analysis (figure 5.6b) supported data from western blots (figure 5.6a) that the distribution of protein acetylation differs dramatically between SSM and IFM populations from the same heart. KEGG pathway analysis revealed that the acetylation of proteins involved in both the Krebs cycle and fatty acid metabolism were significantly elevated in the IFM population compared to the SSM population, whereas acetylation of proteins in cardiac muscle contraction and oxidative phosphorylation were less acetylated (data points in red on figure 5.7).

Despite the 50% increase in protein acetylation associated with T2D mitochondria (figure 5.4), the distribution of acetylation was very similar between controls and diabetics (figure 5.8). Only the acetylation pattern of PDK4 differed between controls and diabetics in both the SSM (figure 5.8a) and IFM (figure 5.8b) populations, displaying a ten-fold elevation in acetylation in diabetic mitochondria compared to control mitochondria (figure 5.9). As this alone cannot account for all the hyperacetylation observed in T2D mitochondria, the protein hyperacetylation in T2D mitochondria must not associated with any one protein, but rather a global upregulation.

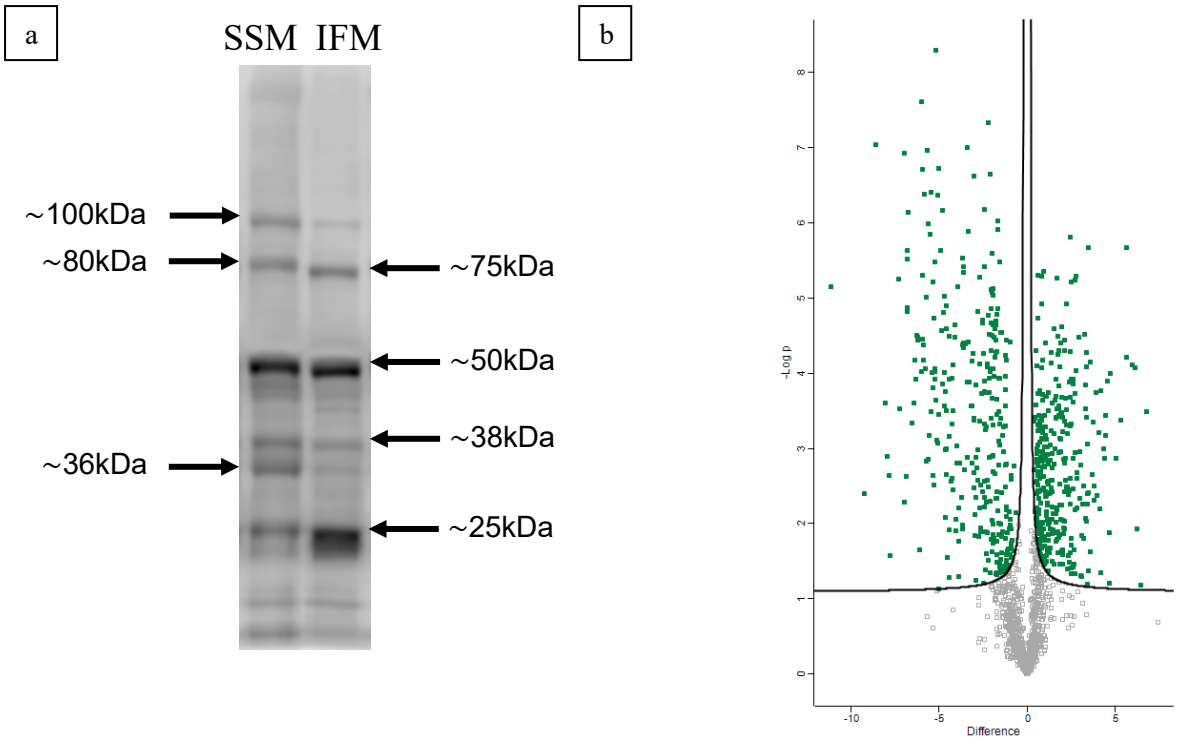

Figure 5.6 – The distribution of protein acetylation is distinctly different between SSM and IFM. This can be displayed through Western blotting with a pan acetyl-lysine antibody with key differences labelled for molecular weights (a) or proteomic analyses of acetylated proteins (b).

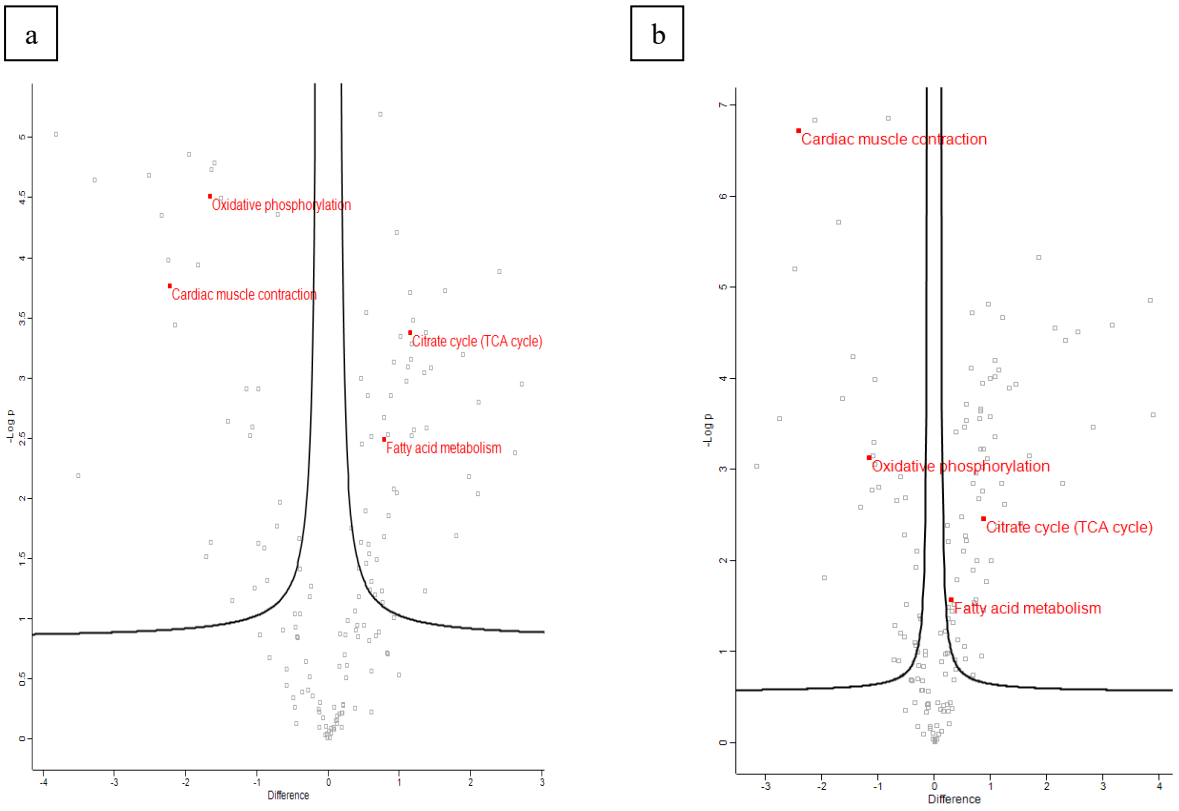

Figure 5.7 – KEGG pathway analysis shows vast differences in the level of acetylation in different pathways between SSM and IFM population in both control (a) and diabetic (b) mitochondria. Red points show results of interest (decreases in cardiac muscle contraction and oxidative phosphorylation, and increases in the Krebs cycle and fatty acid metabolism in the IFM population).

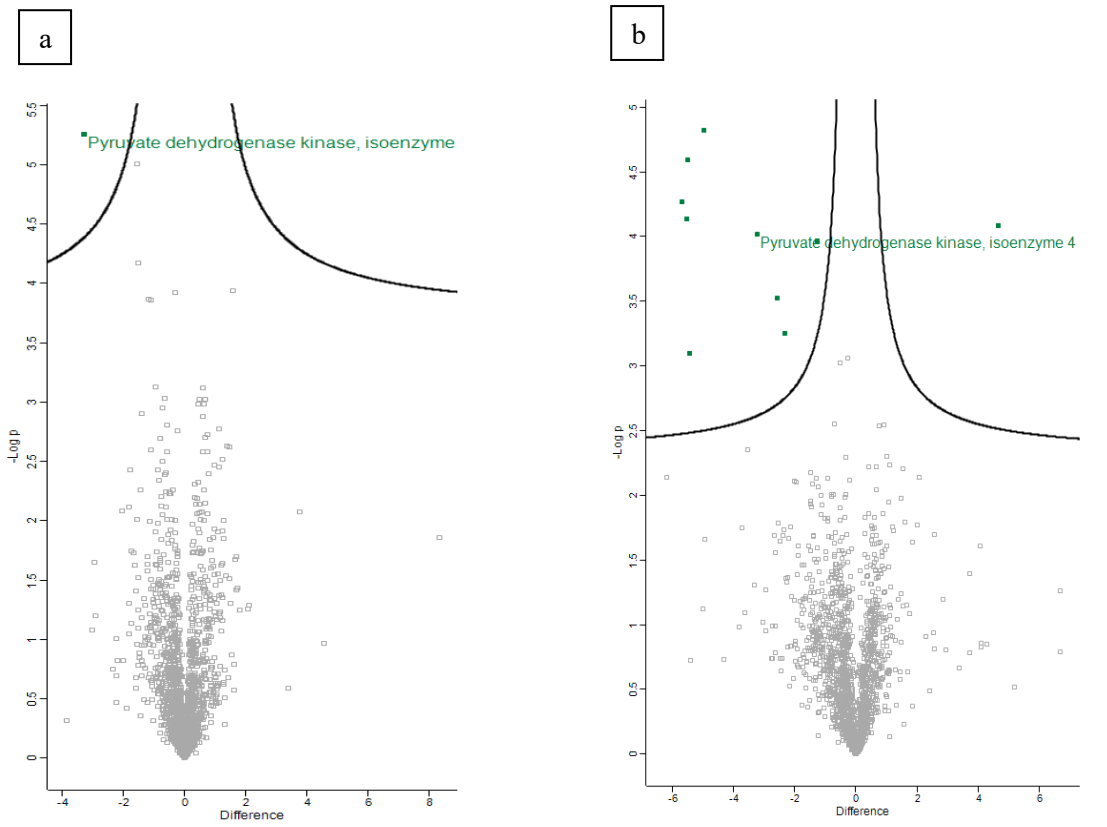

Figure 5.8 – Showing the log fold difference in protein expression observed between control and diabetic mitochondrial proteins pulled down with a pan-acetyl-lysine antibody. There is only 1 protein whose acetylation differs in the SSM (a) population (PDK4), which is also different in the IFM population (b).

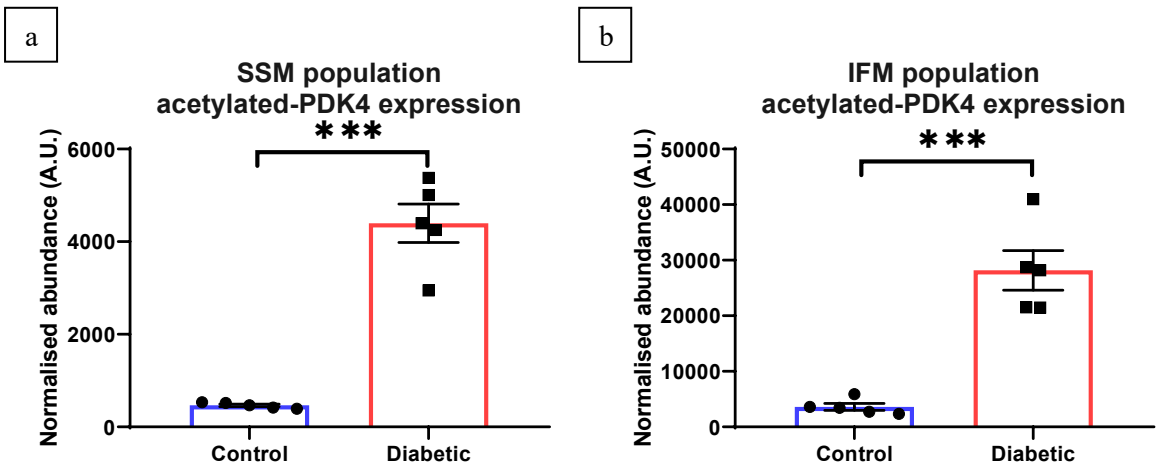

Figure 5.9 – Diabetic mitochondrial PDK4 is hyper-acetylated by around 10-fold in both the SSM (a) and IFM (b) population as assayed through proteomic analysis of acetyl-lysine pulldowns on isolated mitochondrial proteins. *** denotes P<0.001 for control vs diabetic.

5.5.2 *In vitro* mitochondrial acetylation decreased respiratory capacity

In order to determine the effect of global mitochondrial hyperacetylation, control mitochondria were *in vitro* acetylated following the protocol in section 5.4.2 resulting in hyperacetylation on a similar order of magnitude to the 50% increase observed in T2D mitochondria (figure 5.10).

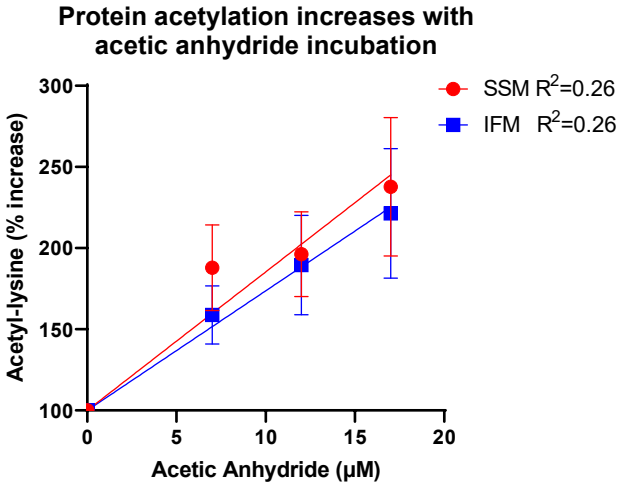

Figure 5.10 – Incubation of mitochondria with acetic anhydride induces a linear increase in mitochondrial protein acetylation.

This reliable, acute, *in vitro* chemical acetylation of wild-type mitochondria provided a powerful tool to determine the effect of global mitochondrial protein hyperacetylation. The respiratory rates of these *in vitro* acetylated mitochondria were therefore measured, respired on either 20 mM glutamate, 10 mM pyruvate and 5 mM malate (GPM) or GPM with 10 µM palmitoyl-carnitine (GPMPCar) as detailed in section 2.3.2. There was a strong correlation between the degree of protein hyperacetylation in these mitochondria and the reduction seen in state 3 respiration in both SSM (figure 5.11a,c) and IFM (figure 5.11b,d) populations, in both the presence (figure 5.11c,d) and absence (figure 5.11a,b) of fatty acids. Depression of S3 respiration was stronger in the SSM population than the IFM population (slope = -0.18 in SSM populations, and -0.11 in IFM populations).

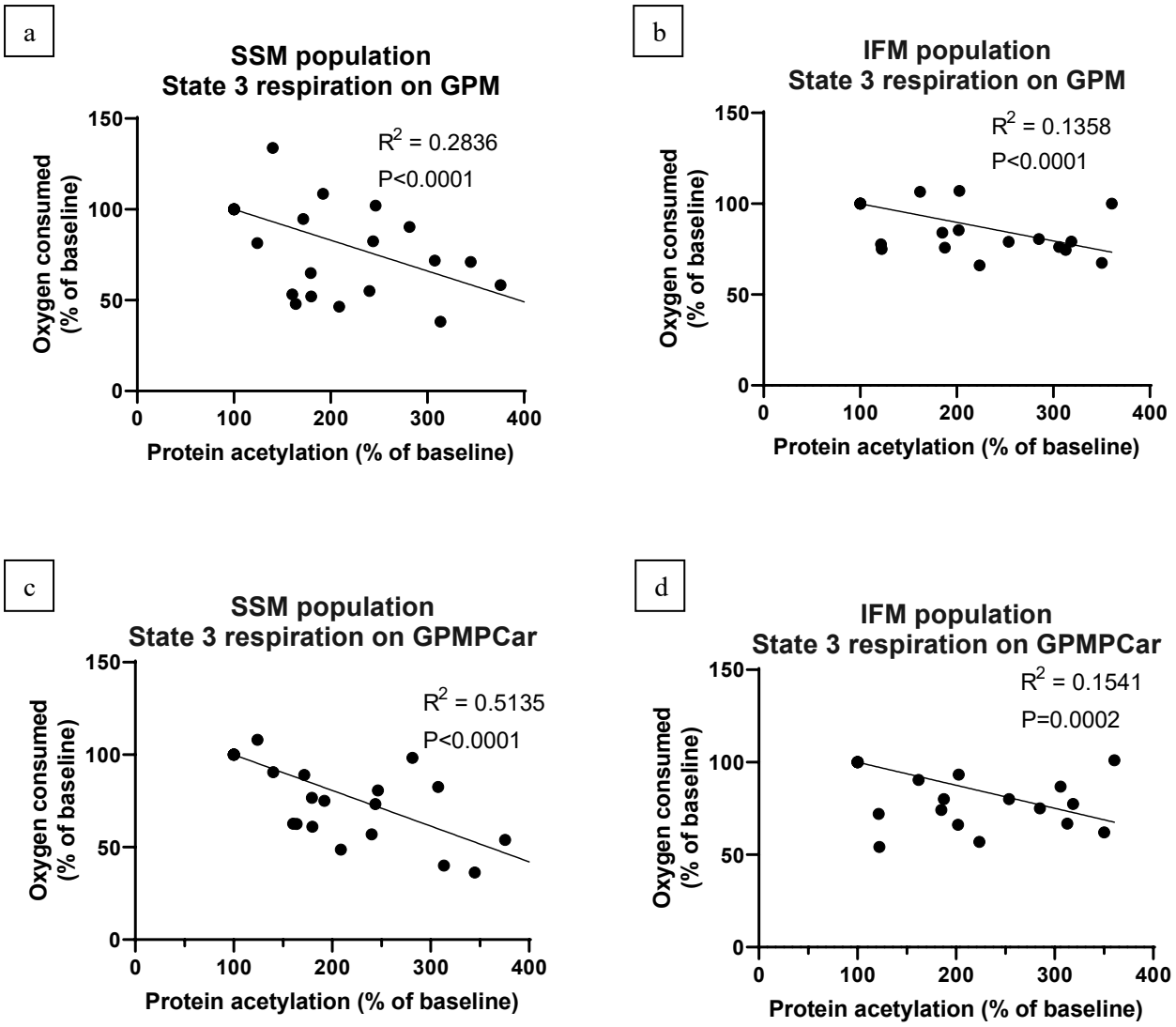

Figure 5.11 – State 3 respiration was reduced when mitochondria were *in vitro* acetylated via acetic anhydride incubation. Depression of state 3 respiration was observed in both SSM (a,c) and IFM (b,d) populations of mitochondria, and when the mitochondria were respired in the presence (GPMPCar – c,d) or absence (GPM – a,b) of fatty acids.

5.5.3 *In vitro* mitochondrial deacetylation increased maximal respiratory capacity

The data so far have demonstrated that mitochondrial protein acetylation significantly decreases total mitochondrial respiratory capacity, a finding which fits well with the respiratory depression and hyperacetylation seen in T2D mitochondria. Consequently, it was hypothesised that correcting the hyperacetylation associated with T2D mitochondria may rescue the reduction in state 3 respiration.

Mitochondria were isolated from T2D hearts and incubated *in vitro* with honokiol, following the protocol in section 5.4.4, to investigate the effects of acute protein deacetylation. This incubation with honokiol gave contrasting results between SSM and IFM populations, resulting in a dose dependent decrease in acetylation in SSM but a dose dependent increase in acetylation in the IFM population (figure 5.12).

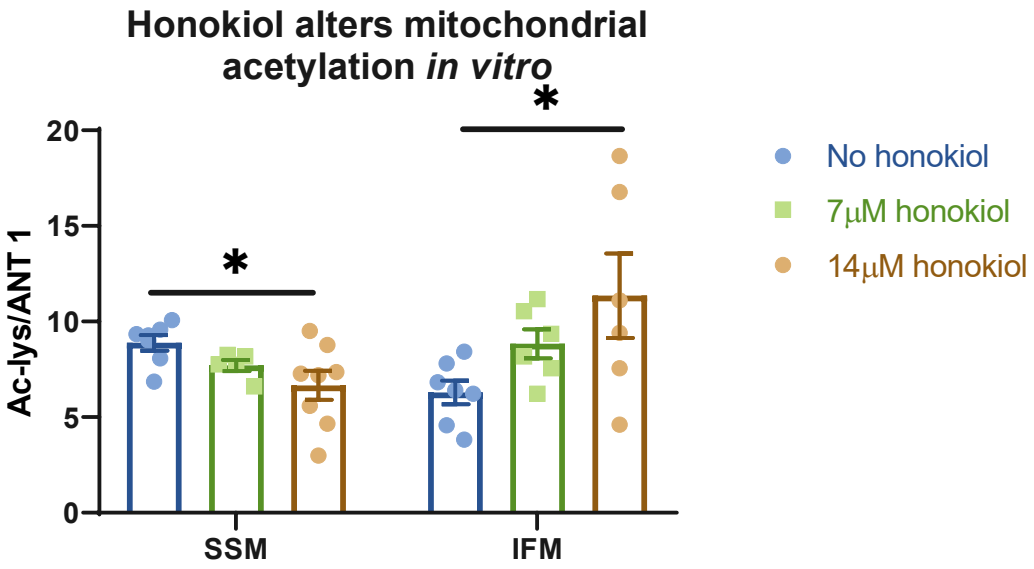

Figure 5.12 – 3 minute incubation of honokiol with type 2 diabetic mitochondria gave a dose dependent decrease in protein acetylation in the SSM population, but a dose dependent increase in acetylation in the IFM population (* indicates significance via one-way ANOVA) as measured by western blotting.

This unanticipated finding provided a unique setting in which to examine the effects of protein acetylation and deacetylation through the measurement of respiratory rates in these acetylated and deacetylated mitochondria.

In the SSM population, which was deacetylated by honokiol, there was a significant increase in uncoupled respiratory rates with honokiol treatment in both substrate conditions (figure 5.13a,b), with no effect on state 3 respiration when respired on GPM (figure 5.13c) and a modest decrease when respired on GPMPCar (figure 5.13d). In the IFM population, which was acetylated by honokiol, there was no increase in uncoupled respiratory rates (figure 5.14a,b), and a significant decrease in state 3 respiration on both GPM (figure 5.14c) and GPMPCar (figure 5.14d).

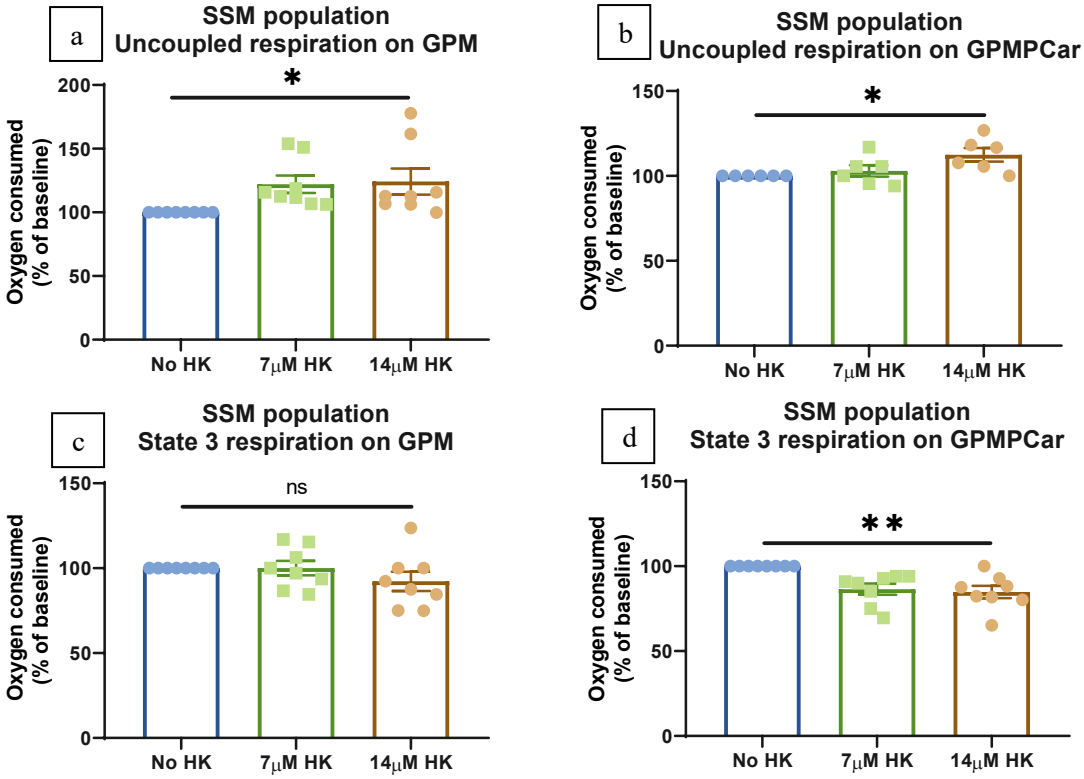

Figure 5.13 - Honokiol incubation acutely increases maximal respiratory capacity in SSM in a dose dependent fashion, both in the absence (a) and presence (b) of fatty acids. Honokiol has no effect on state 3 respiration without fatty acids (c), but shows a significant decrease with fatty acids (d). Data are normalised to no honokiol for each mitochondrial isolation (* indicates $p<0.05$, ** indicates $P<0.005$ via one-way ANOVA).

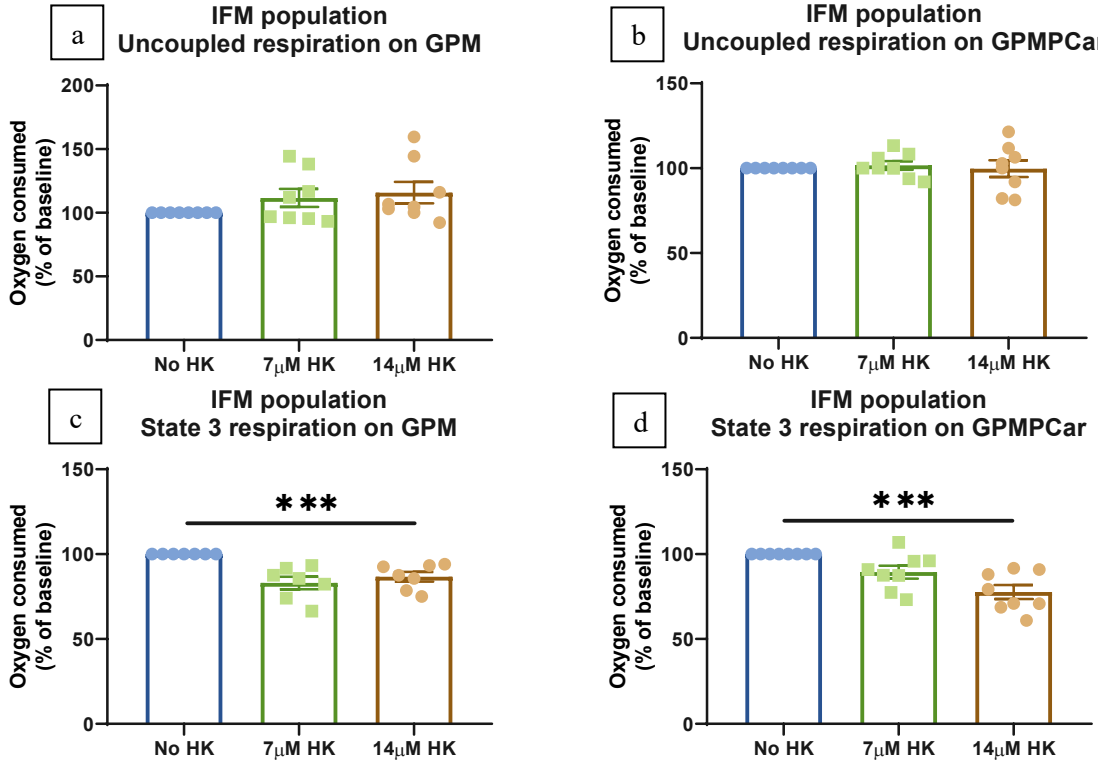

Figure 5.14 – Honokiol incubation has no effect on maximal respiratory capacity in the absence (a) or presence (b) of fatty acids, but decreases state 3 respiration both without (c) and with (d) fatty acids in IFM. Data are normalised to no honokiol for each mitochondrial isolation (*** indicates $p<0.001$ via one-way ANOVA).

5.6 DISCUSSION

5.6.1 Mitochondrial proteins are hyper-acetylated in the type 2 diabetic heart

Mitochondria isolated from T2D hearts displayed a dramatic increase in protein acetylation, with levels raised by 50% in the SSM population and 40% in the IFM population. This change in acetylation was independent of changes in Sirt3 protein expression, likely driven instead by elevations in the level of acetyl-CoA as well as a reduction in the availability of NAD in the diabetic heart. These factors would cause a decrease in the activity of Sirt3 independent of protein expression changes.

Of interest, whereas control and diabetic populations are very similar in terms of which proteins are acetylated there were large differences between SSM and IFM populations which is likely to be caused by differences in total protein expression, as seen in previous proteomic analyses of these groups[275]. The high level of similarity observed between the control and diabetic populations is indicative that the mechanism of acetylation in these groups is conserved, a finding which fits well with the concept that protein acetylation is spontaneous in its nature[90].

Acetylation was only differentially regulated in one protein between control and diabetic samples in both the SSM and IFM populations; PDK4. Although a small part of this elevation may be due to increased PDK4 expression in this T2D model, this can only account for around a two-fold increase[201], not the ten-fold increase observed here. PDK4 is integral in regulating PDH, the flux through which is decreased *in vivo* in this model of T2D[201]. The effect of acetylation upon PDK4 activity is not known, however, in the hyperacetylation state of the Sirt3 KO mouse PDH-E1α phosphorylation was shown to be increased on S300 and S232 but not S293 in skeletal muscle[95]. This pattern of phosphorylation is associated with the inhibitory action of PDK4, phosphorylating and reducing the enzymatic activity of the PDH complex, thus potentially linking PDK4 hyperacetylation with increased PDK4 activity and reduced PDH flux[95]. This differential regulation of acetylation on PDK4 indicates that there may be some specific regulation of acetylation beyond currently known factors.

5.6.2 SSM and IFM populations display differential acetylation

There were four groups of interest indicated in the KEGG pathway analysis as being differentially acetylated between SSM and IFM populations. Enzymes involved in both the TCA cycle and fatty acid metabolism exhibited higher levels of acetylation in the IFM population, whereas those for both cardiac muscle contraction and oxidative phosphorylation exhibited higher levels of acetylation in the SSM population. Given that protein acetylation reduces enzymatic activity (Figures 5.11, 5.14 and table 1.2), this would therefore indicate that the generation of highly reducing compounds (through the Krebs cycle and fatty acid metabolism) is higher in the SSM population, while contraction and the generation of ATP is higher in the IFM population. Of note, this is in support of a fascinating theory which has come to the forefront of myocardial mitochondrial energetics within recent years which features a cardiac mitochondrial network whereby the SSM population produces a proton-motive force, which is used by the IFM population to generate ATP for muscular contraction[276,277].

5.6.3 Acute mitochondrial protein acetylation decreases respiratory activity

There is a wealth of literature regarding the effect of mitochondrial protein acetylation (as summarised in section 1.3), showing a general trend that acetylation reduces enzymatic activity. These studies either investigate acetylation within a disease state, altered feeding pattern or on a single enzyme, making it difficult to draw conclusions around the effect of protein hyperacetylation on a whole mitochondrial level. The acute, global mitochondrial acetylation studied here provides a useful tool for delineating the effect of protein acetylation in isolation,

The data displayed in figures 5.11 and 5.14 support previous studies, with protein hyperacetylation displaying a reduction in respiratory rates on both fatty acid and non-fatty acid substrates. The lack of state 3 normalisation in the presence of fatty acids represents a difference between *in vitro* acetylated mitochondria and *in vivo* hyper-acetylated diabetic mitochondria. There are two potential mechanisms that can account for this; either the rapid, acute acetylation through acetic anhydride results in a different 'acetylome' compared to diabetic mitochondria, or the chronic adaptation to elevated fatty acids in the T2D mitochondria through altered protein expression balances out hyperacetylation associated decreases in enzyme rates.

It is noted that the effect of protein acetylation on the oxidation of fatty acids is a matter of dispute in the literature, with some studies showing that LCAD hyperacetylation is associated with elevated rates of FA oxidation[278] and others showing a decrease[106,107,115,117]. Our data support acetylation depressing LCAD activity, although it must be stated that hyperacetylation arising from acetic anhydride incubation may not accurately reflect some of the nuances of acetylation site selectivity in *in vivo* LCAD acetylation.

5.6.4 Acute mitochondrial protein deacetylation increases respiratory activity

Honokiol incubation dose dependently decreased acetylation in the SSM population, as expected from a Sirt3 activator, but dose dependently increased acetylation in the IFM population. This divergence is intriguing and may be caused by the mechanism of Sirt3 deacetylation, which is an NAD dependent process, generating NAM. *In vivo*, NAM can be regenerated into NAD, but this regeneration requires an extra-mitochondrial enzyme (nicotinamide mononucleotide adenylyl transferase). Therefore, in the isolated mitochondria the effect of Sirt3 activation through honokiol may be obscured by the effect of NAD depletion.

A previous study on the effect of honokiol on isolated liver mitochondria demonstrated that honokiol induced mitochondrial swelling (in accordance with increased mitochondrial permeability transition pore opening) as well as reducing maximal respiratory rates[279]. This negative finding may be explained by either the high concentrations of honokiol used (25 μM was the lowest concentration tested) or the organ differences between liver and heart. Indeed, mitochondrial membrane potential measurements confirmed that mitochondria tolerated the *in vitro* addition of 10 μM honokiol, but not higher concentrations of 50-200 μM (figure 5.3). The decrease in acetylation observed in the SSM population through honokiol incubation was seen to increase maximal rates of respiration (figure 5.13), a finding which fits well with the improved mitochondrial function upon honokiol administration *in vivo*[109,110].

5.7 CONCLUSION

The aim of this work was to define the effect of global protein acetylation on mitochondrial respiration, with a further focus on assessing whether this may be a contributing factor in the reduced state 3 respiration observed in mitochondria isolated from the T2D heart.

This work first demonstrated that diabetic mitochondria are hyper-acetylated compared to control mitochondria and that this is due to a non-specific increase in total protein acetylation. It then showed that *in vitro* mitochondrial hyperacetylation, as achieved both through incubating control mitochondria with acetic anhydride and through the action of honokiol on the T2D IFM population decreased mitochondrial state 3 respiratory rates. Adding to this, it was demonstrated that acutely decreasing mitochondrial protein acetylation, through the incubation of honokiol on T2D SSM increased mitochondrial capacity for maximal respiration, indicating an increased enzymatic capacity.

Overall, the work presented in this chapter demonstrates comprehensively that mitochondrial protein acetylation decreased enzymatic activity in an acute setting. This presents strong evidence that the mitochondrial protein hyperacetylation in the T2D heart could contribute to the reduction in respiratory rates observed in these mitochondria.

6 DEACETYLATION OF MITOCHONDRIA IN THE TYPE 2 DIABETIC HEART CORRECTS DYSFUNCTIONAL ENERGETICS

6.1 ABSTRACT

The type 2 diabetic (T2D) heart is energetically dysfunctional, a phenotype associated with its lipotoxicity and excessive oxidation of fatty acids. The paradoxical observation that increased substrate oxidation pairs with decreased energetics has been linked to; mitochondrial uncoupling, increased oxygen utilisation and futile cycling, yet none of these hypotheses fully explain why ATP turnover is decreased in a perfused T2D heart (as demonstrated in chapter three). Evidence was provided in chapter 5 which linked mitochondrial protein hyperacetylation in the T2D heart to reduced mitochondrial respiratory rates. Thus, this chapter employed the mitochondrial deacetylase activator honokiol to investigate whether correction of hyperacetylation normalised energetics within the T2D heart.

Administration of honokiol to T2D and control rodents for ten days was well tolerated and led to a 33% reduction in fed non-esterified fatty acid levels in T2D, with no significant effect on blood glucose levels or adiposity. Honokiol decreased T2D mitochondrial acetylation by 25%, normalising the hyperacetylation associated with the T2D heart. This correction increased T2D mitochondrial respiratory rates by 17% in sub-sarcolemmal mitochondria and by 28% in inter-fibrillar mitochondria, reverting respiratory rates back to the level found in control mitochondria. This restored the levels of high energy phosphates through a 31% elevation in the concentration of ATP and a 29% increase in the concentration of PCr in the T2D heart. Honokiol treatment increased the rate of ATP turnover by 88% in the T2D heart, completely returning this to the level found in control, healthy hearts.

This chapter provides demonstrating, for the first time, that some protein hyperacetylation is a source of dysfunction within T2D mitochondria. Furthermore, it shows that honokiol can completely correct this hyperacetylation, and the associated energetic dysfunction. Honokiol therefore provides a unique approach to rescue the dysfunctional energetics in the T2D heart which, given the link between cardiac energetics and mortality, presents a tempting therapeutic avenue for the treatment of cardiovascular-related death in T2D.

6.2 INTRODUCTION

The hypothesis that mitochondrial protein acetylation is associated with reduced mitochondrial activity and subsequent cellular energetic dysregulation is supported by a host of studies; *in silico*[280], isolated enzymes[111–114,122], *in vitro*[105,117,120], *in vivo*[98,99,103–107,113,115,118] and by work laid out in this thesis (chapter 5). It is therefore reasonable to propose that the mitochondrial protein hyperacetylation associated with the T2D heart may explain the reduced mitochondrial respiratory rates and further, that deacetylation may correct this dysfunction.

Honokiol provides a mechanism through which to specifically activate the mitochondrial deacetylase Sirt3 and was therefore employed for the *in vivo* deacetylation of T2D cardiac mitochondria. The reported *in vivo* dosing regimens amongst the literature for honokiol vary in terms of; the method of administration, the dose selected and the duration, as summarised in table 6.1. These variable study durations and doses make extracting a uniform effect of honokiol administration difficult, an issue that is further confounded by the fact that the method of administration alters its pharmacokinetics. Intravenous injection of honokiol in rats elicits a plasma half-life of between 40-60 minutes[281], while intraperitoneal injection in mice gives a half-life of 4-6 hours, with maximal effective doses achieved within 20-30 minutes[282]. Despite the variability, honokiol exerted cardioprotective effects in all studies; protecting against myocardial ischaemia-reperfusion injury both acutely[283] and chronically[284], as well as reversing cardiac hypertrophy[109] and doxorubicin-mediated cardiotoxicity[110].

The fact that honokiol mediates favourable effects, despite the variation in its dosing, indicates that honokiol provides both acute and chronic benefits. Deacetylation of mitochondrial proteins provides a likely explanation for its acute benefits, whereas chronic benefits may be mediated though PPARγ activation, which has been demonstrated *in silico*[285], *in vitro*[285] and *in vivo*[110,285], although requiring a concentration of honokiol above 30 μM[286]. As PPARγ activation is already known to be effective in the treatment of T2D[287] this chapter will focus on the effects of acute mitochondrial deacetylation, using intraperitoneal administration, and dosing for ten days to mitigate chronic effects.

Table 6.1 – A summary of the dosing regimens employed in *in vivo* honokiol studies

Dosing method	Study	Dose (mg/kg)	Duration (days)	Effect	Animal
Oral gavage	Sun *et al.*[288]	200	56	Improved blood, and physical parameters in T2D.	Mouse
	Atanasov *et al.*[285]	100	35	Improved blood and physical parameters in T2D.	Mouse
	Zhang *et al.*[284]	5	7	Improved recovery post ischaemic reperfusion.	Rat
Intra-peritoneal	Pillai *et al.*[109]	0.2	28	Reduced cardiac hypertrophy	Mouse
	Wang *et al.*[283]	5	1	Diminished ischaemia-reperfusion injury	Rat
	Huang *et al.*[110]	0.2	35	Reduced doxorubicin induced cardiotoxicity.	Mouse
Diet	Kim *et al.*[289]	Not measured, diet contained 0.02% honokiol by weight.	35	Improved blood parameters in T2D.	Mouse

6.3 AIMS

Previous chapters have demonstrated that the T2D heart has reduced concentrations and turnover of high energy phosphates and that this is associated with dysfunctional mitochondrial energetics, potentially due to mitochondrial protein hyperacetylation. This chapter will aim to assess whether honokiol mediates the same reduction in mitochondrial protein hyperacetylation *in vivo* in a T2D rodent model as shown *in vitro,* as well as investigating the effect of this reduced acetylation on mitochondrial respiratory rates. The effects on cardiac energetics will then be investigated *ex vivo*, using ^{31}P-magnetic resonance spectroscopy in a Langendorff perfused model. Three primary objectives were therefore investigated:

1. The effect of honokiol on blood parameters and cardiac mitochondrial protein acetylation was assayed within T2D and control rodents.
2. The effect of *in vivo* deacetylation on mitochondrial state 3 respiratory rates and enzymatic activities was measured.
3. The effect of *in vivo* mitochondrial protein deacetylation on global cardiac energetics was determined through the measurement of absolute concentrations of ATP and PCr, as well as the rate of ATP turnover.

6.4 METHODS

6.4.1 Honokiol administration

Honokiol was dissolved first into DMSO at 36 mg/mL. This solution was then suspended in corn oil to achieve a final concentration of 2 mg/mL. Rodent weights were taken daily and honokiol or vehicle (5.6% DMSO in corn oil) given at 0.4 mg/kg via intraperitoneal injection at 4pm for 10 days.

6.4.2 Mitochondrial isolation and respiration measurements

All mitochondrial isolation and respiration measurements were carried out as set out in section 2.3.

6.4.3 ^{31}P-Magnetic resonance spectroscopy

All ^{31}P-magnetic resonance spectroscopy (MRS) experiments and Langendorff perfusions were carried out as per section 2.2.

6.4.4 Hyperpolarised MRS

Hyperpolarized MRS involves the hyperpolarization of a compound, in this case ^{13}C-pyruvate, through dynamic nuclear polarization (DNP). This technique provides an increase in the signal-to-noise ratio of up to 20,000-fold over that normally obtained from pyruvate, thus allowing the real-time interrogation of carbon substrates through metabolic pathways *in vivo*. Pyruvate, which sits at the nexus of metabolic pathways, is the only hyperpolarized substrate to have made it into clinical trials and allows the assessment of pyruvate dehydrogenase flux through the measurement of the rate of appearance of the ^{13}C-bicarbonate peak using the following method:

Thus, rats were used for hyperpolarized [1-^{13}C] – pyruvate MRS, performed on a 7 T preclinical MRI system (Varian) as previously described[290]. For the hyperpolarized experiments, 1 mL of 80 mM [1-^{13}C]-pyruvate was injected into the tail vain over 10 s. ^{13}C MR spectra were acquired from the heart every second for 60 s using a 72 mm dual-tuned birdcage volume transmit ^{1}H/^{13}C coil and a ^{13}C two-channel surface receive coil (Rapid Biomedical; 15º hard pulse; 13.0 kHz bandwidth). All hyperpolarized experiments were carried out by Dr. Kerstin Timm. Multi-coil spectra were manually

added in phase, and the first 30 s of spectra from the first appearance of the pyruvate peak were summed and quantified with AMARES/jMRUI as described previously[182].

6.4.5 Statistical analysis

Datasets containing two groups were analysed using the two-tailed parametric unpaired t test function within GraphPad Prism 8.0.0. A reported P value less than 0.05 was taken as significantly different.

Datasets containing multiple groups (control and diabetic), and multiple variables (vehicle vs honokiol) were initially analysed using ordinary two-way ANOVAs. Significance was followed up with Turkey's multiple comparison tests, with individual variances computed for each comparison.

6.5 RESULTS

6.5.1 Honokiol corrects protein hyperacetylation in T2D cardiac mitochondria

To investigate the effect of mitochondrial protein deacetylation on cardiac energetics within an *in vivo* T2D model, honokiol, a potent Sirt3 activator, was administered through daily intraperitoneal injections for 10 days. Honokiol was well tolerated in all cases, with little effect on the T2D model, regarding terminal blood metabolites and physical parameters. The only physical effect of honokiol was a 33% reduction in fed non-esterified fatty acid (NEFA) levels in diabetic animals (figure 6.1a). There was no change in adiposity (measured by fat pad weights – figure 6.1b), blood glucose (fed – figure 6.1c or fasted – figure 6.1d), terminal body weights (figure 6.1e) or the heart weight/body weight ratio (figure 6.1f), a measure of cardiac hypertrophy.

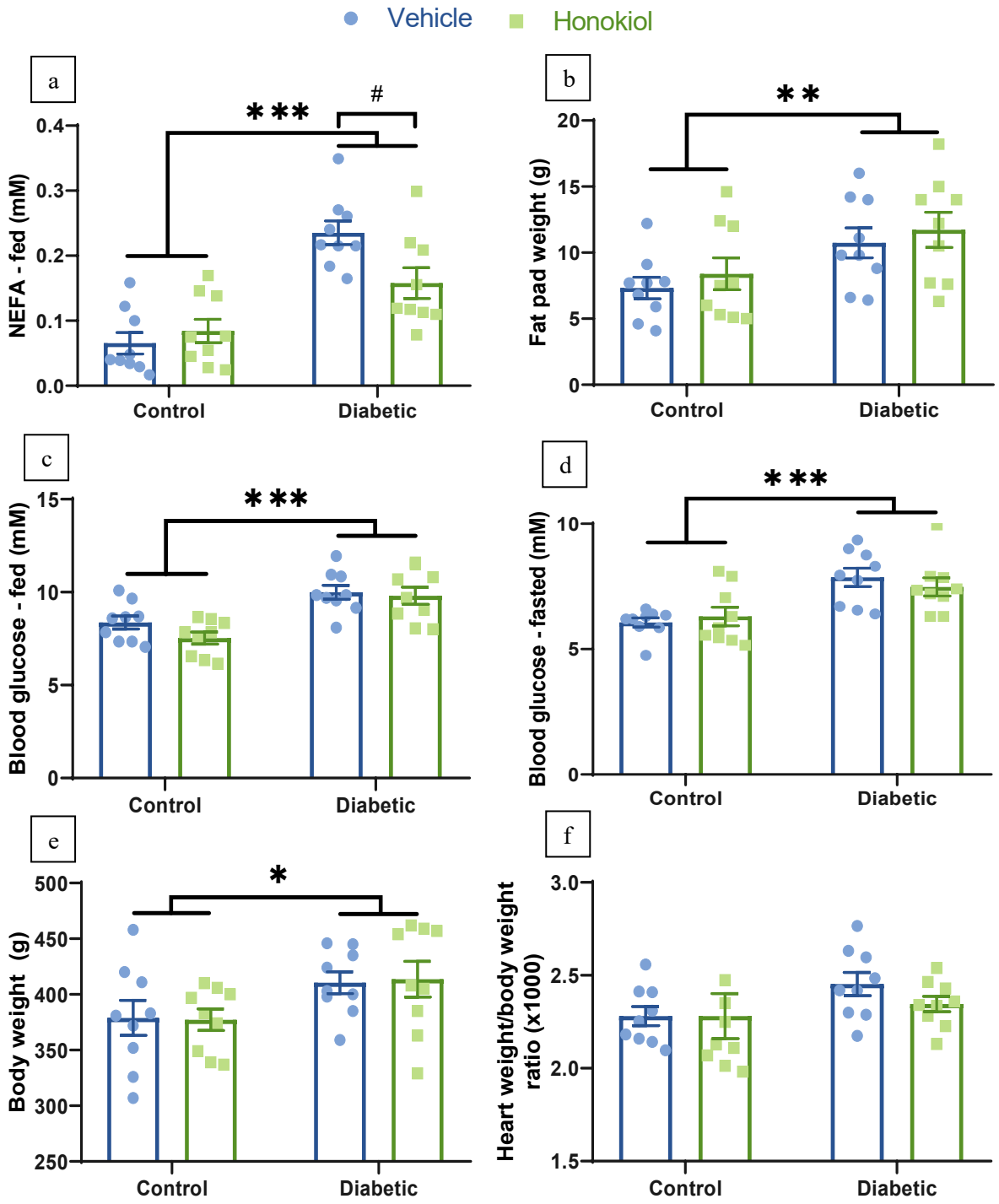

Figure 6.1 - Blood metabolite profiles, and physical parameters from control and diabetic animals, either treated with vehicle (corn oil + DMSO) or honokiol. Diabetic rodents present with hyperlipidaemia (a), increased adiposity (b), hyperglycaemia (c,d) and increased body weight (e) with no change in the heart weight/body weight ratio (f). Treatment with honokiol reduced hyperlipidaemia in the T2D state (a), but had no other effects in either control or T2D rodents. * denotes P<0.05, ** denotes P<0.005, *** denotes P<0.001 for control vs diabetic, # denotes P<0.05 for vehicle vs honokiol.

The primary target of honokiol is Sirt3, which honokiol has been shown to activate *in vitro* and enhance the expression of *in vivo,* leading to a reduction in mitochondrial protein acetylation. Protein acetylation was therefore measured in cardiac mitochondria, isolated from control and T2D rodents given either honokiol or vehicle. Honokiol decreased acetylation in T2D mitochondria by 33% in the SSM population and by 34% in the IFM population (figure 6.2). In control rodents, honokiol decreased acetylation by 21% in the IFM population but had no effect on the SSM population. Overall, honokiol corrected mitochondrial protein hyperacetylation in T2D, returning it to the level of control hearts

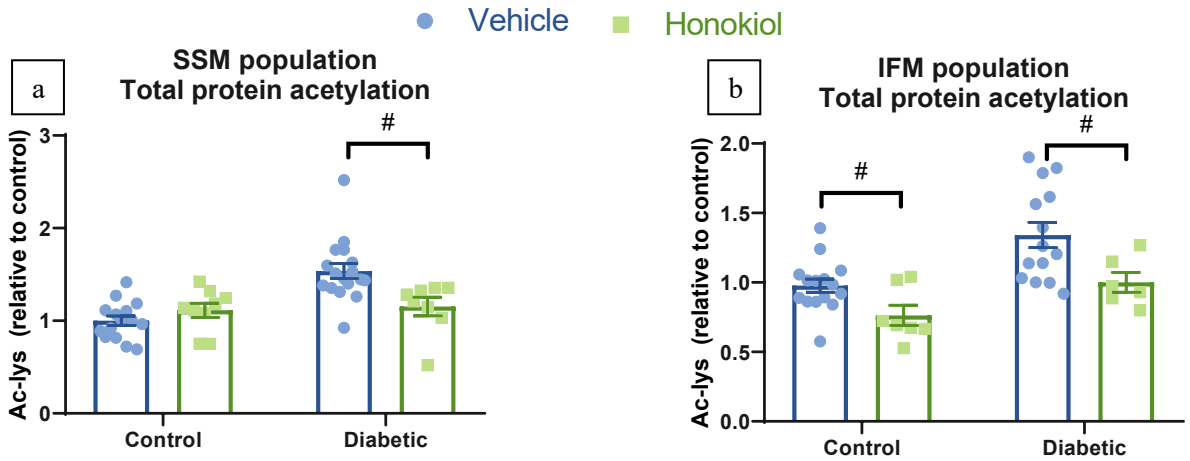

Figure 6.2 – Global protein acetylation was measured via western blotting of isolated cardiac mitochondria. Honokiol reduced acetylation in both SSM and IFM populations isolated from T2D hearts, and in the IFM population isolated from control hearts. # denotes P<0.05 for honokiol vs vehicle.

Honokiol can activate, and enhance the expression of, Sirt3. To examine which factor caused mitochondrial deacetylation, Sirt3 expression was measured through whole heart western blotting. This demonstrated that Sirt3 expression was unaltered by acute honokiol administration (figure 6.3), therefore indicating that elevated Sirt3 activity was the most likely mode of action for honokiol.

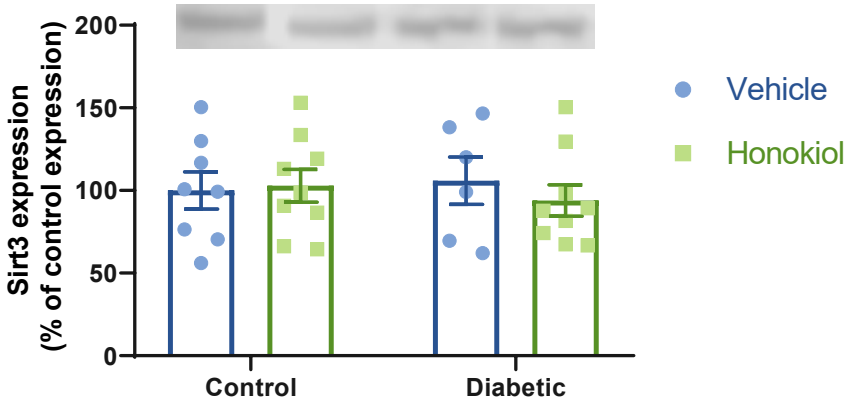

Figure 6.3 - Honokiol administration for 10 days did not alter global cardiac Sirt3 expression, in either the control or diabetic cohort, as assayed through western blotting.

6.5.2 Honokiol corrects mitochondrial respiration in the T2D heart

Previous data demonstrated a correlation between mitochondrial protein hyperacetylation and reduced mitochondrial rates of respiration (figure 5.11), two factors that are apparent in the diabetic heart. It was therefore hypothesised that correction of mitochondrial protein hyperacetylation *in vivo* may correct mitochondrial respiratory dysfunction. Honokiol increased state 3 respiratory rates by 17% in the SSM population (figure 6.4a) and by 28% in the IFM population (figure 6.4b) in T2D cardiac mitochondria when respired on GPM but had no effect when respired on GPMPCar (figure 6.4c,d). This increase on GPM restored state 3 respiratory rates to control levels in both the SSM and IFM population. Honokiol had no effect on control mitochondria whether respired on GPM or GPMPCar.

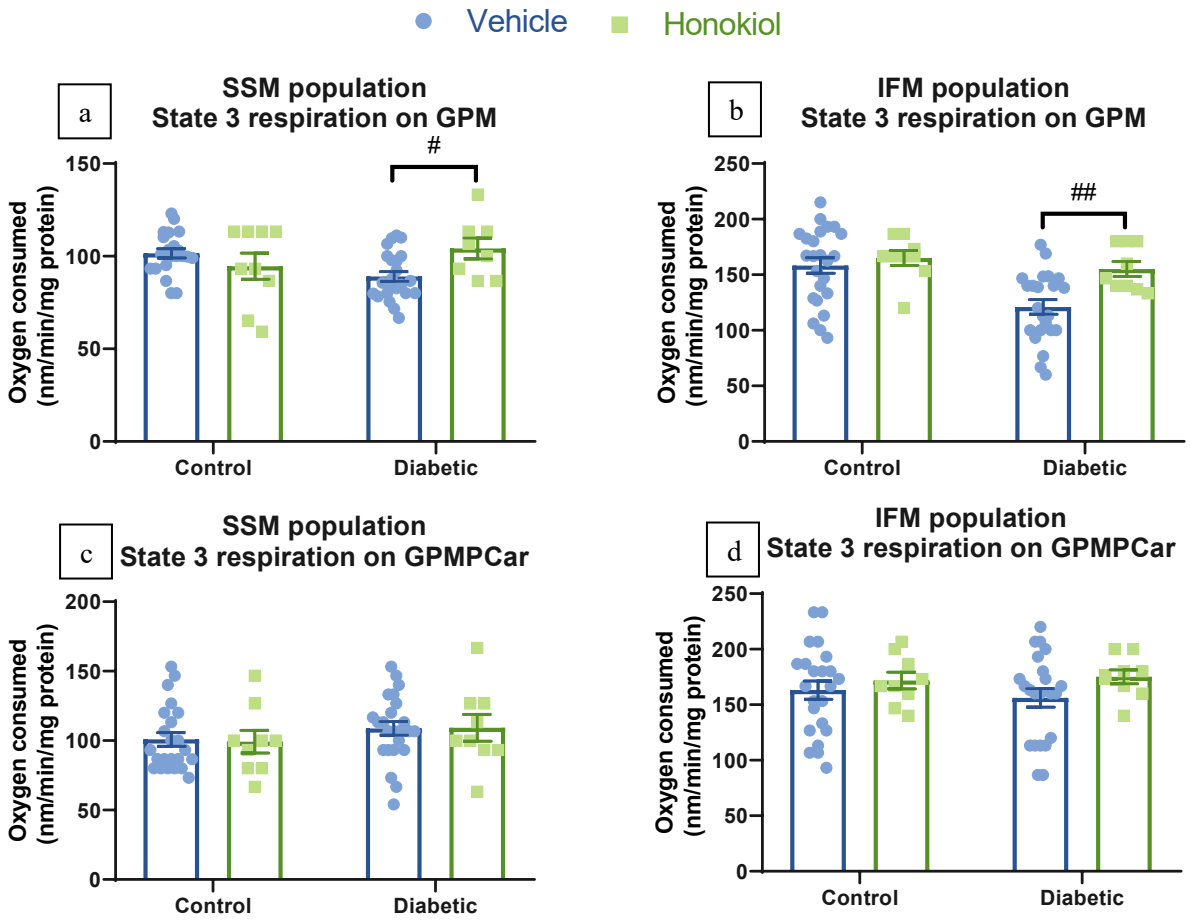

Figure 6.4 – Honokiol increased state 3 respiration in both T2D SSM (a) and IFM (b) populations, which corrected the reduced respiration associated with T2D mitochondria back to control levels when respired on glutamate, pyruvate or malate (GPM). Neither disease state, nor honokiol had a significant effect on state 3 respiration in the presence of fatty acids (GPMPCar) c,d . # denotes P<0.05, ## denotes P<0.005 for vehicle vs honokiol.

The fact that honokiol increased state 3 respiration when respired on GPM, but not when respired on GPMPCar indicated that honokiol increased flux through a pathway unique to GPM catabolism. Previous data indicated that PDK4, which regulates PDH flux, is the only enzyme differentially acetylated in the T2D heart making PDH a compelling candidate for the beneficial effects of honokiol. PDH flux was assayed *in vivo*, using ^{13}C-hyperpolarized pyruvate (figure 6.5) and demonstrated a 70% reduction in PDH flux associated with T2D. However, honokiol did not alter PDH flux in T2D.

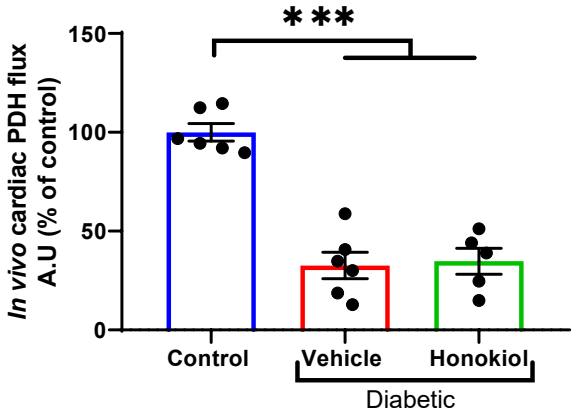

Figure 6.5 – PDH flux was measured using the bicarbonate/pyruvate ratio obtained after injection of hyperpolarized ^{13}C-pyruvate. This revealed no change in PDH flux with honokiol. There was a significant decrease associated with the diabetic state. *** denotes P<0.001 for control vs diabetic.

PDH flux was not altered *in vivo* by honokiol administration, thus the activities of other enzymes unique to GPM catabolism; malate dehydrogenase (MDH) and glutamate dehydrogenase (GDH) were assayed in the SSM population *in vitro*. PDH activity (figure 6.6a) was measured and showed a 20% depression with T2D but no change with honokiol, which confirmed the *in vivo* data shown in figure 6.5. MDH activity was unchanged by both disease state and honokiol administration (figure 6.6b), whereas GDH activity was increased by 27% in diabetic mitochondria after honokiol administration (figure 6.6c). As GDH activity was increased by honokiol administration, the activity of the downstream enzyme in the TCA cycle, α-ketoglutarate dehydrogenase (α-KGDH), was assayed, which showed a 13% upregulation in T2D mitochondria, with no change due to honokiol (figure 6.6d). To confirm the findings that GDH activity was elevated with honokiol administration, GDH activity was assayed in both SSM and IFM populations using an alternative spectrophotometric assay (figure 6.7). GDH activity was increased with honokiol in T2D mitochondria by 104% in the SSM and 43% in the IFM population. A 32% increase in GDH activity following honokiol treatment was also seen in the control IFM population.

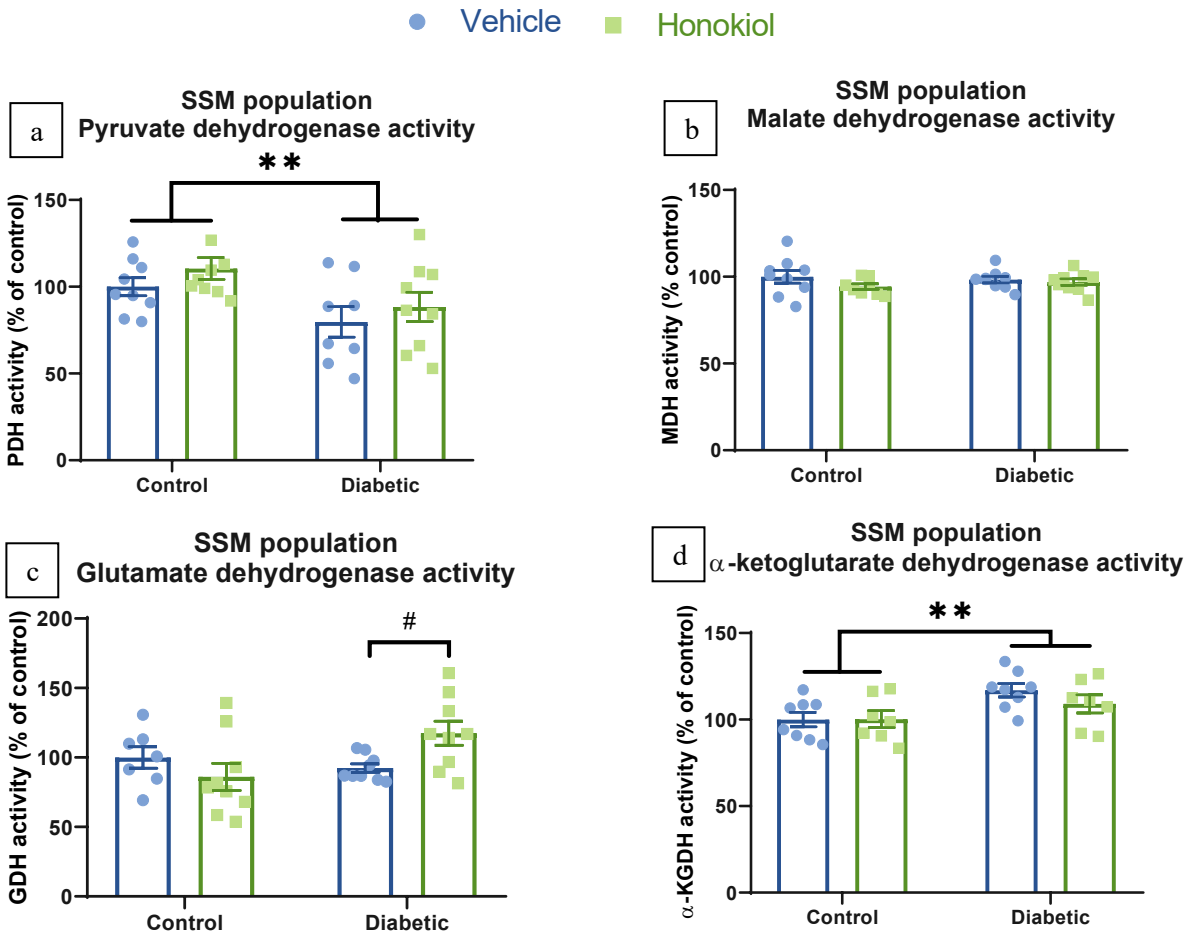

Figure 6.6 – Honokiol administration had no effect on either pyruvate (a) or malate dehydrogenase activity (b), although PDH flux was significantly reduced by T2D. Honokiol administration increased GDH flux, but only in T2D (c), but had no effect on α-KGDH flux (d), although this was elevated by T2D. ** denotes P<0.005 for control vs diabetic, # denotes P<0.05 for vehicle vs honokiol.

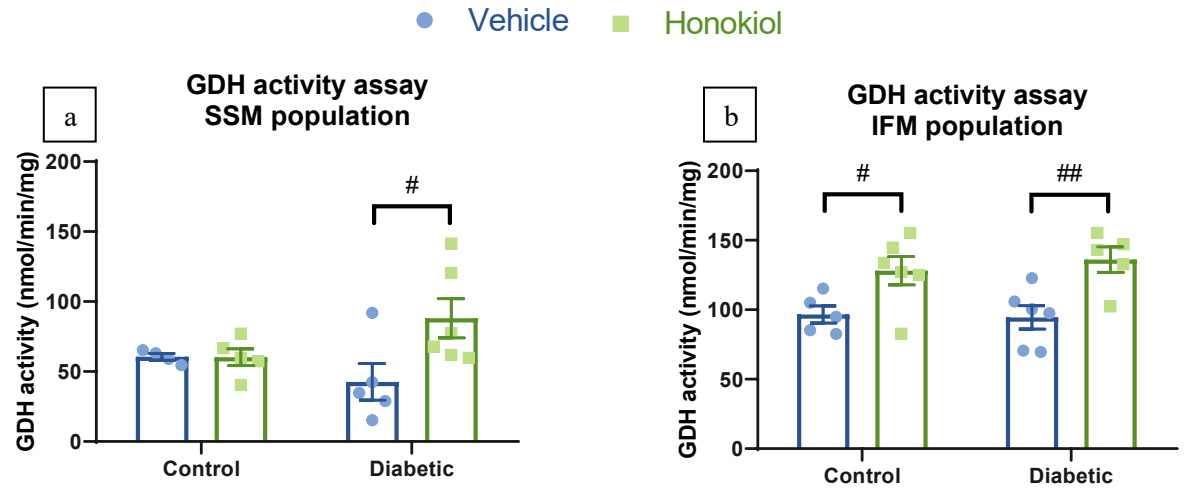

Figure 6.7 – Honokiol increased glutamate dehydrogenase activity in diabetic SSM (a) and both control and diabetic IFM (b) populations. # denotes P<0.05, ## denotes P<0.005 for vehicle vs honokiol.

These data therefore indicated that the correction of T2D mitochondrial respiration through honokiol was mediated via an increase in glutamate respiration, due to elevated flux through GDH. GDH is known to be a Sirt3 target, both transcriptionally and through deacetylation, therefore increased flux could either be due to increased protein expression, or decreased GDH acetylation. Expression of GDH was assayed through western blotting in both mitochondrial populations (figure 6.8), showing no change, either with diabetes or honokiol administration. This implicated deacetylation of GDH, through Sirt3 activation, as the driver for increased GDH flux.

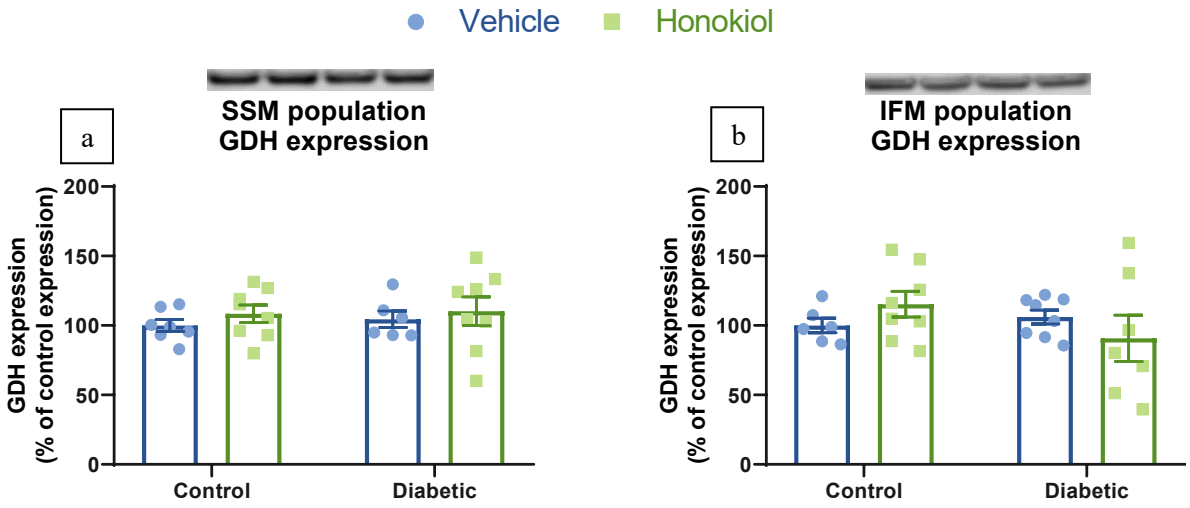

Figure 6.8 - GDH expression was assayed in both SSM (a) and IFM (b) populations through western blotting. There were no observed differences either due to disease state, or honokiol administration.

6.5.3 Honokiol corrects both the concentration of ATP and ATP turnover in the T2D heart

Previous work demonstrated that the T2D heart is energetically dysfunctional (Figures 3.5, 3.7) with reduced mitochondrial respiratory rates (Figure 3.10). As mitochondria produce the overwhelming majority of ATP for the heart, it was hypothesised that the improvements in mitochondrial respiration from honokiol in T2D may also correct energetics in the T2D heart. In order to answer this question, high energy phosphate concentrations were measured in actively contracting Langendorff perfused hearts from control and T2D rats, treated with either vehicle or honokiol. Honokiol did not change any cardiac contractile parameters, with no significant differences in either developed pressure (figure 6.9a) or heart rate (figure 6.9b) between either disease state or treatment.

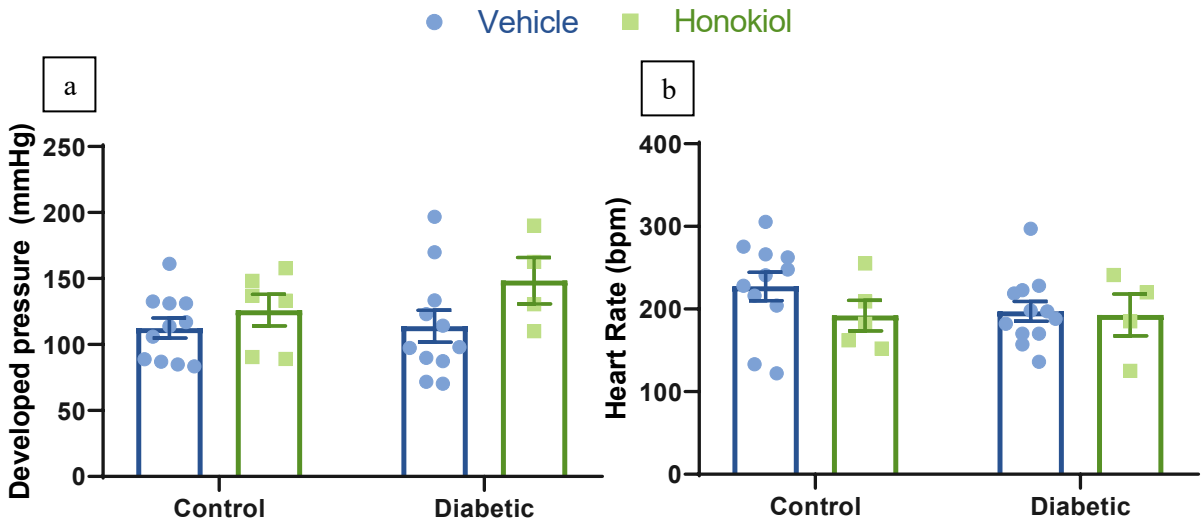

Figure 6.9 – Honokiol had no effect on developed pressure (a) or heart rate (b) in Langendorff perfused hearts.

Chapter 3 identified reduced ATP and PCr concentrations within T2D hearts, a phenomenon closely associated with increased cardiovascular mortality. ^{31}P-NMR revealed that honokiol increased the concentration of ATP by 31% and PCr by 29% in T2D hearts, whilst having no effect on myocardial energetics in control hearts (figure 6.10). This indicated that the energetic dysfunction associated with T2D may be improved through honokiol treatment.

A stronger indicator of energetic function is the turnover rate of ATP, which figure 3.7 indicated was also reduced in the T2D heart. In control hearts honokiol caused a 41% reduction in the rate constant for ATP degradation (figure 6.11a) but, due to the trend towards an increased ATP concentration within these hearts (figure 6.10a), did not alter the rate of ATP turnover (figure 6.11b). In T2D hearts honokiol increased the rate of ATP turnover by 88% (figure 6.11b). Of interest, this increase in ATP turnover rate within T2D hearts (figure 6.11b) was mediated through the 31% elevation in absolute ATP concentrations (figure 6.10a), rather than a significant increase in the rate constant for ATP degradation (figure 6.11a)

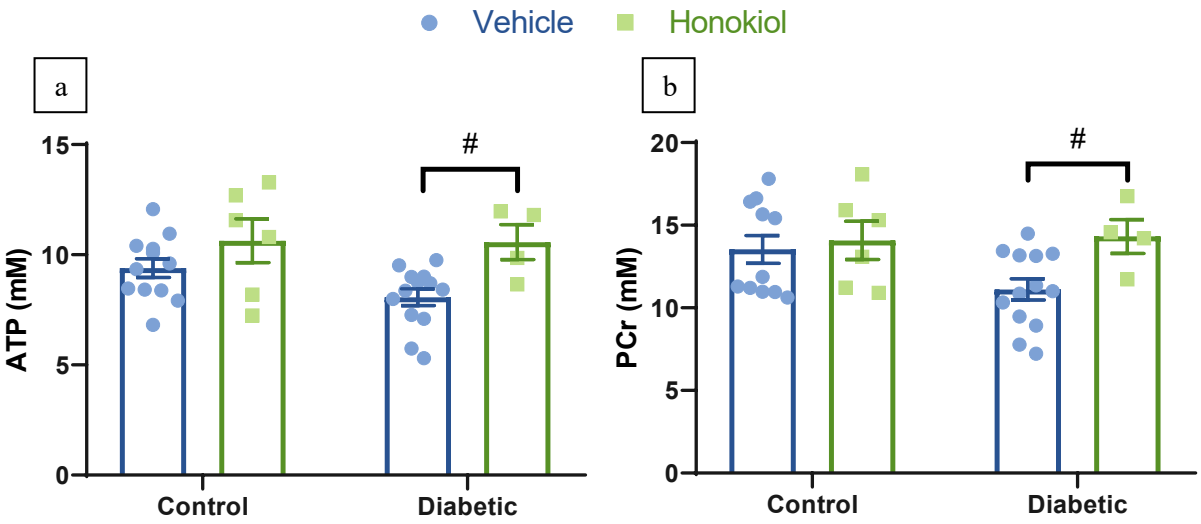

Figure 6.10 – The concentrations of ATP (a) and PCr (b) were significantly increased in the T2D heart following honokiol administration. # denotes p<0.05 for vehicle vs honokiol.

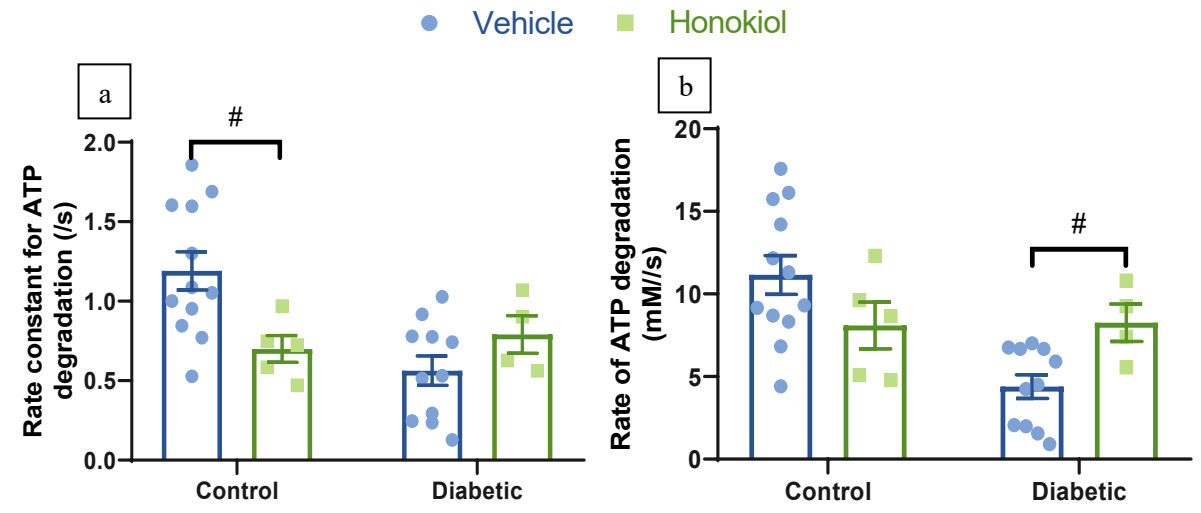

Figure 6.11 – Honokiol significantly reduced the rate constant for ATP degradation in control hearts (a), but this did not lead to a reduced rate of ATP degradation (b). The rate of ATP degradation was significantly increased by honokiol in the diabetic heart (b). # denotes P<0.05 for vehicle vs honokiol.

6.6 DISCUSSION

6.6.1 Honokiol did not alter the hyperglycaemia associated with type 2 diabetes

This study demonstrated that whilst honokiol is well tolerated by rodents (both healthy and T2D), its treatment was not associated with a reduction in hyperglycaemia. This is in contrast to some findings in the literature, which showed improved glycaemic control when mice underwent oral gavage with honokiol[285,288]. This could be due to a pharmacokinetic effect associated with honokiol regarding gavage compared with intraperitoneal injections, however, it is worth noting that the T2D mouse models used by both Sun *et al.*[288] and Atanasov *et al.*[285] display blood profiles more similar to type 1 diabetes (>25mM fasted blood glucose concentrations) with a decrease in body weight seen by Sun *et al.*[288]. It therefore appears that honokiol may improve blood parameters in a type 1 diabetes model but not a T2D diabetes model, a hypothesis supported by the lack of alteration in fasting blood glucose levels when honokiol was administered in the diet to a more mild T2D phenotype[289].

The observed decrease in fed plasma NEFAs is the first demonstration of such an effect within T2D through honokiol treatment. This is in contrast to Kim *et al.*[289] who displayed no decrease in plasma free fatty acids, although, a significant decrease in hepatic lipids was observed in this model indicating that fatty acid metabolism was altered.

6.6.2 Honokiol normalised the protein hyperacetylation associated with diabetes

Honokiol treatment normalised the hyperacetylation associated with T2D cardiac mitochondria, returning it to control levels. To our knowledge, this is the first study to show that honokiol treatment can correct global cardiac mitochondrial acetylation, a finding which agrees well with data from honokiol treated cardiomyocytes[109,110]. The observation that honokiol has no effect on control SSM acetylation and only a very modest effect on control IFM acetylation is striking, especially given the profound effect on diabetic mitochondria. This finding is supported by Huang *et al.*[110] who detected no difference in protein acetylation in control mouse hearts when honokiol was dosed for five weeks. These data therefore suggest that there is a set point for mitochondrial acetylation in the healthy heart, which can be elevated by disease states but cannot be decreased therapeutically.

6.6.3 Honokiol corrects mitochondrial and whole heart energetics in type 2 diabetes

Treatment with honokiol did not alter state 3 respiration in mitochondria isolated from control hearts. This finding is in contrast to those of Pillai *et al.*[109] and Huang *et al.*[110] who employed more chronic honokiol dosing regimens (28 and 35 days, respectively) compared to this 10 day protocol indicating that chronic PPARγ activation in these cases may have been the mechanism. In contrast, the effect of enhanced Sirt3 activity, and its associated decrease in mitochondrial acetylation, is striking in T2D cardiac mitochondria. Honokiol completely corrected state 3 respiratory rates in T2D mitochondria, reverting them to control levels, with an increase of 17% and 28% in SSM and IFM populations, respectively. It is noted that there are no current clinical therapeutic agents which have been shown to specifically increase mitochondrial respiration within T2D. Indeed, the only lifestyle intervention which has displayed improvements in respiratory function – aerobic exercise – appears to mediate its effect through enhanced mitochondrial biogenesis (at least within skeletal muscle)[291] rather than improved function. It is therefore striking that the ten-day, daily injection intervention presented in this chapter yielded improvements in mitochondrial respiration (17-28%) on a similar order to those obtained through an 84 day aerobic exercise intervention in T2D patients (33%)[291].

Our data indicates that the improvement in mitochondrial function mediated by honokiol occurred primarily through increased GDH flux. GDH is a known target of Sirt3[92] and deacetylation has been shown to increase GDH activity both at the level of the isolated enzyme[114] and in the hearts of Sirt3 KO mice[106]. This reconciles with the findings presented in this chapter, where the mitochondrial populations which were deacetylated (T2D SSM and IFM and control IFM) saw increased GDH flux, but those which were not deacetylated (control SSM) saw no change to GDH flux. It is noted that GDH activity was not decreased at baseline in the hyperacetylated phenotype associated with T2D mitochondria. Although Sirt3 is a modulator of GDH activity, GDH is also one of the only known substrates of Sirt4 mediated ADP-ribosylation, which causes a significant decrease in its activity[292]. Sirt4 activity is thought to be decreased in the T2D heart[293], indicating that the unaltered GDH activity at baseline in the T2D heart may be due to a balance between reduced Sirt3 and Sirt4 activity, although further work

should focus on characterising ADP-ribosylation and acetylation of GDH within the T2D heart. These data therefore present a case whereby honokiol increases anaplerotic flux within the T2D heart (due to increased α-ketoglutarate generation), providing substantiation that the TCA cycle may have pathologically reduced flux within T2D[294]. There was no increase in either PDH or MDH activity, despite deacetylation increasing MDH activity *in vitro*[122]. There are two possible conclusions that can be drawn from this; either the action of honokiol is not uniform in deacetylating mitochondrial proteins and MDH may have been deacetylated to a lower degree than GDH, or the sensitivity of MDH and GDH to deacetylation may be different, with MDH requiring greater levels of deacetylation to become activated to the same degree as GDH.

This increase in mitochondrial respiration due to honokiol completely corrected the dysfunctional energetics associated with the T2D heart, normalising ATP and PCr concentrations back to control concentrations within the heart and increasing ATP turnover to control levels. Two novel conclusions can therefore be drawn from this finding. Firstly, this therapeutic intervention provides the first data to support the hypothesis that early cardiac energetic dysfunction within T2D can be linked to mitochondrial dysfunction, as mediated by protein hyperacetylation. Secondly, honokiol represents the first known therapeutic intervention which increases both the absolute concentration and turnover of ATP within the T2D heart. This makes honokiol a very attractive clinical therapeutic, not only for the treatment of energetic dysfunction within T2D but also for other cardiovascular related conditions where energetic dysfunction and mitochondrial protein hyperacetylation are becoming recognised targets[295,296].

6.7 CONCLUSION

This chapter set out to investigate whether administration of the Sirt3 activator, honokiol, could deacetylate mitochondrial populations in an *in vivo* setting, and whether this could improve the otherwise dysfunctional energetics associated with the T2D heart.

The administration of honokiol for ten days was well tolerated in both control and T2D rodents and had relatively little impact on blood profiles. Honokiol had a potent effect on cardiac mitochondria, displaying complete correction of the protein hyperacetylation associated with the T2D heart. This deacetylation increased mitochondrial respiration, restoring T2D mitochondrial respiration to the level seen in control mitochondria. *In vitro* enzyme assays demonstrated that honokiol increased glutamate dehydrogenase flux, indicating that elevated glutamate-mediated anaplerosis may have been responsible for the normalisation of mitochondrial function. This recovery of mitochondrial respiratory function completely normalised cardiac energetics, as evidenced by corrected concentrations of PCr and ATP, as well as restored ATP turnover in honokiol treated diabetic hearts.

This chapter therefore provides compelling evidence for three conclusions; mitochondrial protein hyperacetylation drives reduced respiratory rates in the T2D heart, these reduced mitochondrial respiratory rates drive global energetic dysfunction within the T2D heart, and that honokiol provides an exciting novel therapeutic avenue for treatment of the T2D cardiac dysfunction.

7 GENERAL DISCUSSION

Type 1 diabetes, and its associated pathologies, were described as 'starvation in the midst of plenty' as far back as 1924[297]. More recent work within the field of cardiovascular disease has put forward a strong case for cardiac starvation, as evidenced by reduced myocardial energetics, as underpinning pathology across cardiovascular diseases[1,3–5,7–9,80]. These two settings meet within type 2 diabetic heart disease, which accounts for over 70% of mortality within type 2 diabetes (T2D)[12] and presents with reduced myocardial energetics[5], despite being substrate overloaded[258].

This thesis was an investigation into the causal factors behind the apparent energy starvation within the T2D heart. The pathology of T2D within the heart presents with many alterations to normal cardiac function and metabolism, which may have an impact on bioenergetics. Therefore, in order to define which aspects of T2D are primarily responsible for the reduced energetics, biological systems with progressively decreasing complexity were studied. With each reduction in biological system complexity, it became more apparent which factors were primarily responsible for the observed energetic dysfunction, therefore granting better understanding of the pathology. The systems discussed were grouped as follows:

1. *In vivo* heart (human)
2. *In vivo* heart (rodent)
3. *Ex vivo* heart (rodent)
4. *Ex vivo* mitochondria (rodent)
5. *In vitro* mitochondria (rodent)

7.1 LITERATURE REGARDING ENERGETIC DYSFUNCTION WITHIN THE TYPE 2 DIABETIC HEART

Over 70% of mortality within T2D patient cohorts can be attributed to cardiovascular causes[12,298], and this elevated risk remains even when other comorbidities are taken into account[299,300]. Work in the field of cardiovascular disease has presented evidence showing good correlation between increased risk of cardiovascular mortality, and reduced myocardial energetics[11]. Based on this information, groups undertook experiments to measure the energetics of the T2D heart.

Energetic dysfunction within the T2D heart can be measured *in vivo* through ^{31}P-NMR, which provides the only non-invasive methodology to assess cardiac high energy phosphates. Clinical assessments of energetics within the T2D heart report decreased PCr/ATP ratios[3,5], a marker for energetic dysfunction. This marker is employed as quantification of absolute PCr and ATP concentrations are challenging *in vivo*. Methodologies are beginning to be employed that allow absolute quantification of ATP and PCr concentrations within the heart, which agree well with measurements of the PCr/ATP ratio both within disease states[1] and the aging heart[301,302], but as of yet have not been applied to the T2D heart.

Studies on human patients present the most immediately relevant information to T2D heart disease, but they are much more costly, and do not permit *ex vivo* work compared with animal studies. Therefore groups have looked at T2D myocardial energetics within rodent populations, providing data that fits very well with that seen in T2D patients[8,10]. This represents the first movement in reducing biological system complexity to gain a better understanding of the underlying disease pathology within T2D heart disease, which can be represented as three key findings:

1. The observed increased risk of cardiovascular mortality within T2D patients.
2. Clinically measured reduced cardiac PCr/ATP ratios in T2D patients.
3. Reduced cardiac PCr/ATP ratios in T2D rodent models.

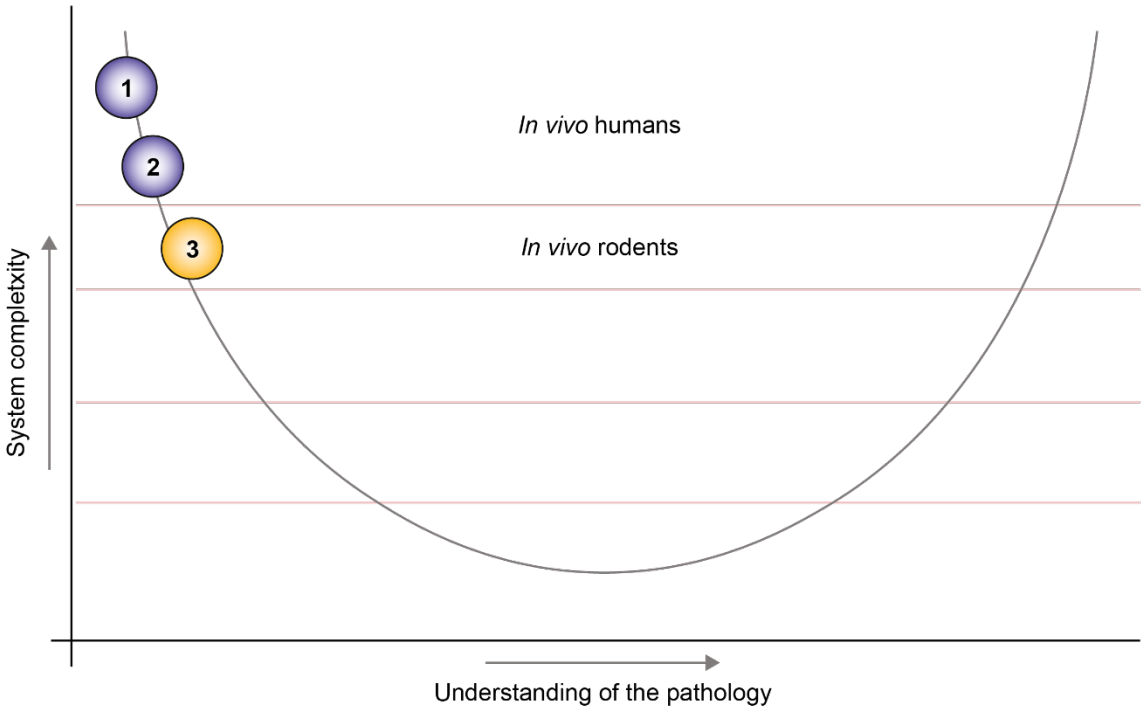

7.2 INVESTIGATION OF THE ENERGETIC LANDSCAPE OF THE TYPE 2 DIABETIC HEART

The literature surrounding T2D heart disease indicates that elevated cardiovascular mortality within T2D may be related to dysfunctional energetics and provides evidence that this translates well into rodent models of T2D. In order to investigate this further, chapter 3 utilised the *ex vivo* perfused heart, which enabled absolute quantification of PCr and ATP concentrations. The data presented in chapter 3 demonstrated that at an early stage of rodent T2D heart disease (with no functional impairments), the T2D heart had reduced concentrations of both PCr and ATP. These presented without a significant change in the PCr/ATP ratio, indicating that energetic dysfunction may occur at an earlier stage of T2D than has been measured clinically.

Although reduced ratios of PCr/ATP, and the subsequent data showing that both PCr and ATP concentrations are reduced in the T2D heart are powerful metrics for energetic dysfunction, they still only present a snapshot of the energetic state of the heart. A much more powerful measurement is the rate of ATP degradation, and synthesis within the heart, thus providing data on ATP turnover. To investigate this, saturation transfer experiments were carried out on the isolated perfused heart, which displayed a reduction in ATP turnover within the T2D heart, indicating cardiac energetic starvation.

Through the isolation of cardiac mitochondria, chapter 3 established that energetic dysfunction within the T2D heart was associated with a reduced capacity of T2D cardiac mitochondria to oxidise non-fatty acid substrates. The data in chapter 3 therefore present the first measurements of absolute PCr and ATP concentrations within the T2D heart, as well as displaying reduced ATP turnover and association with reduced rates of respiration in T2D mitochondria. These data can be summarised as the following three key findings:

4. Absolute concentrations of PCr and ATP are reduced in the T2D rodent heart.
5. ATP turnover (as measured by ATP degradation rates) is reduced in the T2D rodent heart.
6. Mitochondrial rates of respiration (and thus ATP synthesis) are reduced in T2D cardiac mitochondria.

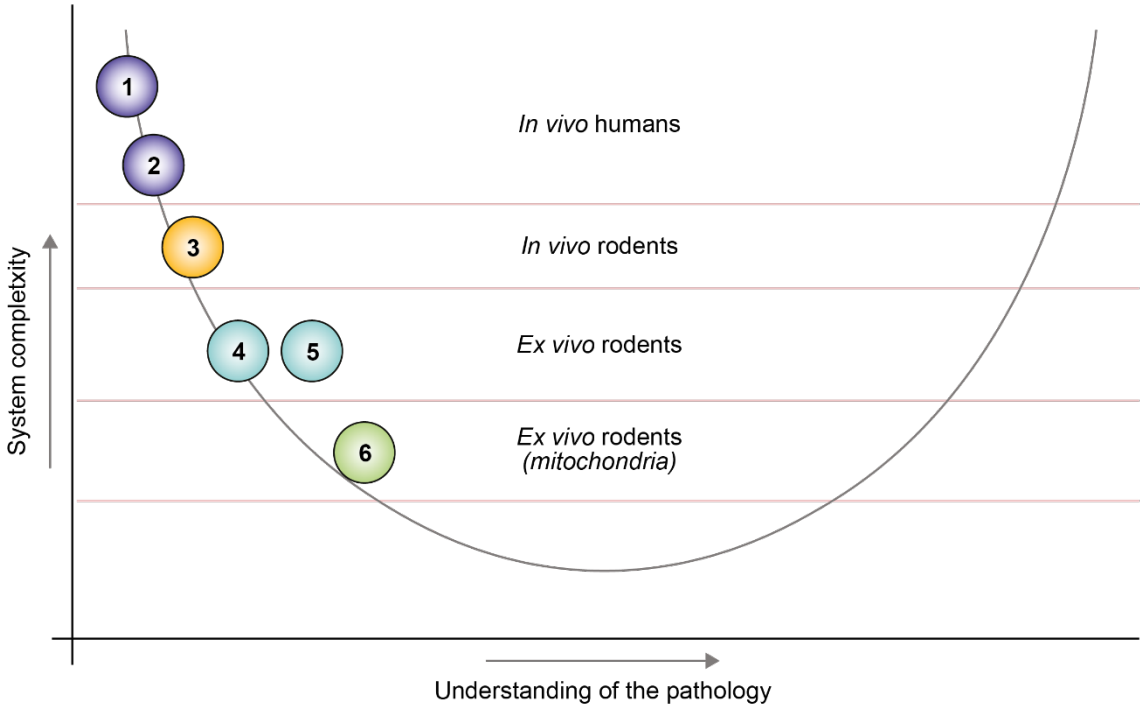

7.3 IDENTIFICATION OF ACETYLATION AS A NOVEL CAUSE OF ENERGETIC DYSFUNCTION WITHIN THE TYPE 2 DIABETIC HEART

Many theories have been put forward to explain the energetic dysfunction within T2D mitochondria, ranging from oxidative damage, to increased uncoupling, and elevated oxygen consumption. Although these factors must all play a role within T2D cardiac energetic dysfunction, none satisfactorily explain the decreased ATP synthesis rates despite the abundance of substrates in this early T2D model. In order to investigate potential explanations for this phenomena, one of the fundamental characteristics of the T2D heart; the lipid overloaded phenotype[258], was examined further.

Lipotoxicity has already been implicated in the pathology of diabetic cardiomyopathy[303], but this thesis focussed rather on the detrimental aspects of cardiac adaptation to this lipotoxic state. Maladaptation within the T2D heart has been noted previously, with the concept that the development of insulin resistance observed in the obese heart is itself an adaptive mechanism to reduce substrate uptake[304]. Indeed, the adaptation to elevated fatty acids levels within the T2D heart is a well-described phenomenon, occurring through the chronic activation of the PPARα receptor, driving a transcriptional response[305]. One of the most well studied PPARα coactivators is PGC-1α, which drives a mitochondrial biogenesis response within the heart in response to chronic PPARα activation[306]. Both chapters 3 and 4 presented data showing this mitochondrial biogenic response, first through the elevated citrate synthase activity, and then through the elevation in AAC expression at a whole heart level despite normal mitochondrial expression.

7.3.1 The T2D heart adapts to lipid overloading through post-translational protein modifications

Over the course of chapter 4, a novel adaptation within the T2D heart was demonstrated; the loss of sensitivity around the ADP/ATP carrier (AAC) with regards to long chain acyl-CoA (LCAC) inhibition. This adaptation allows the maintenance of mitochondrial respiratory rates despite the observed elevation in LCAC levels in the T2D heart. Chapter 4 showed that this altered sensitivity could not be attributed to either increased AAC expression or altered AAC isoform expression. Therefore, post-

translational modifications of the AAC were considered, which led to the uncovering of a major adaptation in the T2D heart in the form of mitochondrial protein hyperacetylation.

Chapter 5 presented data showing that mitochondria within T2D hearts are globally hyper-acetylated. This is a phenomenon more physiologically associated with chronic fasting. However, when the metabolic state of the T2D heart is considered; presenting with elevated fatty acid levels[307] and decreased NAD levels[308] it can be seen that T2D can be considered a more potent driver of acetylation than fasting (as summarised in table 7.1).

Table 7.1 – Summarising acetylation within different metabolic states

State	Fatty acids	NAD levels	Sirt3 levels	Acetylation
Fed[94,122,309]	Low	Low NAD/NADH	Unchanged	Low
Prolonged fasting [94,122,309,310]	Increased	High NAD/NADH	Increased	Moderate
Type 2 diabetes [115,178,307,308]	Increased	Reduced	Reduced	High

Hyperacetylation, and the reduction in AAC inhibition arising from LCACs, occur within two other physiological conditions which both manifest with elevated levels of intracellular fatty acids; high fat feeding[251,311] and in the muscles of endurance athletes[252].

7.3.2 Acetylation can prove maladaptive in the T2D heart

The hyperacetylation of mitochondrial proteins within the T2D heart may therefore represent an adaptive mechanism to cope with elevated levels of fatty acids, however, chronic hyperacetylation can be maladaptive in the heart preventing sensitivity to acute fatty acid elevations and decreasing respiratory rates.

The T2D heart remains in a hyper-acetylated state for longer than would be common with either chronic fasting, or during the normal fed/fasted cycle. Over time we propose this leads to chronic energy depletion within the heart, as hyperacetylation of mitochondrial proteins reduces their activities[27,29, 34–41, 42–48], explaining the decrease in high energy phosphate within the heart. Of note, this phenomenon

has also been seen in the hearts of patients fed a high fat diet, supporting the driving factor being adaptation to fats[99].

In order to better understand the effect of this mitochondrial protein hyperacetylation, *in vitro* studies were carried out on mitochondria, first to acetylate control mitochondria and then to deacetylate T2D mitochondria. Chapter 5 presented data which demonstrated that acetylation of control mitochondria reduced respiratory capacity and that deacetylation in T2D increased respiratory capacity. These findings can therefore be summarised as three key points:

7. Mitochondrial proteins are hyper-acetylated within the T2D heart.
8. The *in vitro* acetylation of control mitochondria reduces their respiratory rates.
9. The *in vitro* deacetylation of T2D mitochondria increases their maximal respiratory rates.

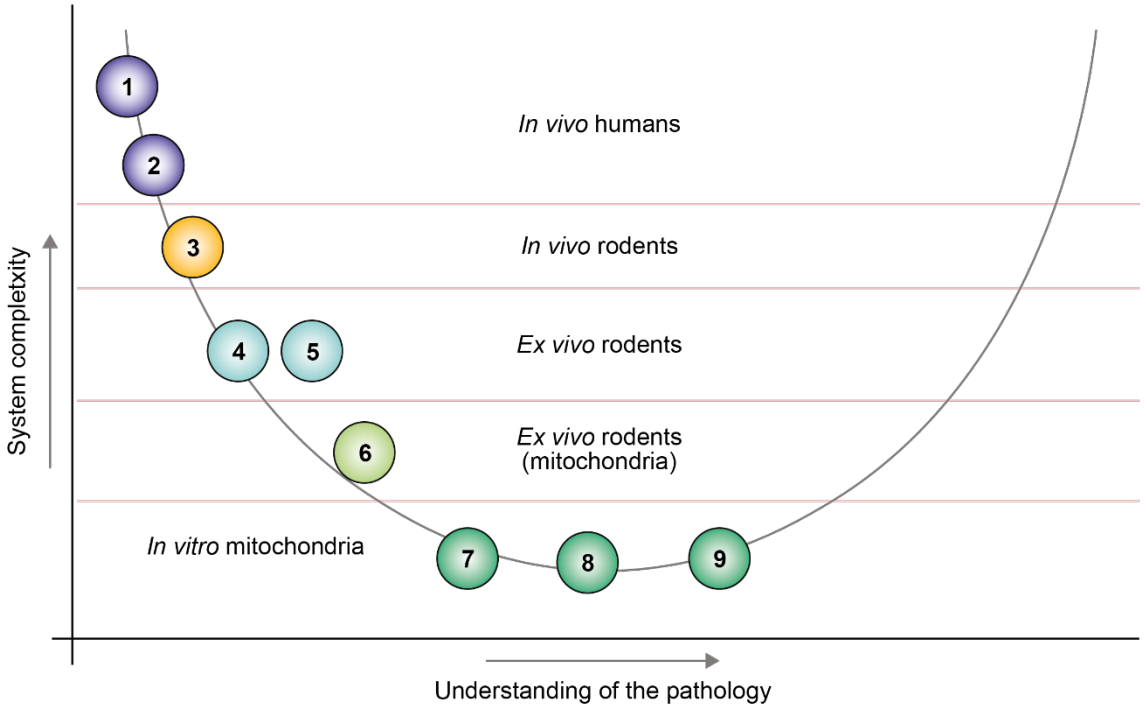

7.4 CORRECTION OF T2D MITOCHONDRIAL HYPERACETYLATION RESCUES ENERGETICS AT A MITOCHONDRIAL AND CARDIAC LEVEL

Over the course of chapters 4-6, mitochondrial protein hyperacetylation was identified as a promising candidate for the source of energetic dysfunction within the T2D heart. In order to confirm this finding, it must be shown that deacetylation of T2D mitochondria rescues the phenotype of energetic dysfunction, first at the level of isolated mitochondria, and then at a global cardiac level. The final body of work in this thesis therefore set out with the aim to correct this hyperacetylation *in vivo*.

Short term *in vivo* administration of honokiol had relatively little effect on blood parameters, indicating that mitochondrial protein acetylation, although powerful in manipulating the fed/fasted response at the cellular level, had relatively little effect at a whole organism level. This short term honokiol regimen completely corrected the hyperacetylation associated with T2D cardiac mitochondria, indicating that the mechanism for deacetylation is not lost within these mitochondria, but rather is supressed within the T2D heart.

Chapter 6 displayed data showing that deacetylation of mitochondria *in vivo* led to increased glutamate dehydrogenase activity, therefore potentially increasing flux into the TCA cycle in the T2D heart. This deacetylation of cardiac mitochondria, and subsequent elevation of glutamate dehydrogenase activity, within the T2D heart increased mitochondrial rates of respiration when respired on glutamate, pyruvate and malate, while having no effect on respiration when fatty acids were present.

Correction of mitochondrial respiratory rates through the *in vivo* administration of honokiol completely normalised ATP turnover in T2D hearts, an astonishing finding given the extent of the depression seen in the vehicle treated T2D group. This is the first study to correct the energetic dysfunction associated with the T2D heart, and so provides an exciting, and novel, potential therapeutic in the amelioration of cardiovascular related death in T2D.

These findings can therefore be summarised as four key points:

10. *In vivo* deacetylation of T2D mitochondria increases flux through glutamate dehydrogenase.
11. *In vivo* deacetylation of T2D mitochondria increases their respiratory rates.
12. *In vivo* deacetylation of T2D mitochondria increases concentrations of ATP and PCr within the T2D rodent heart.
13. *In vivo* deacetylation of T2D mitochondria increases ATP turnover within the T2D rodent heart.

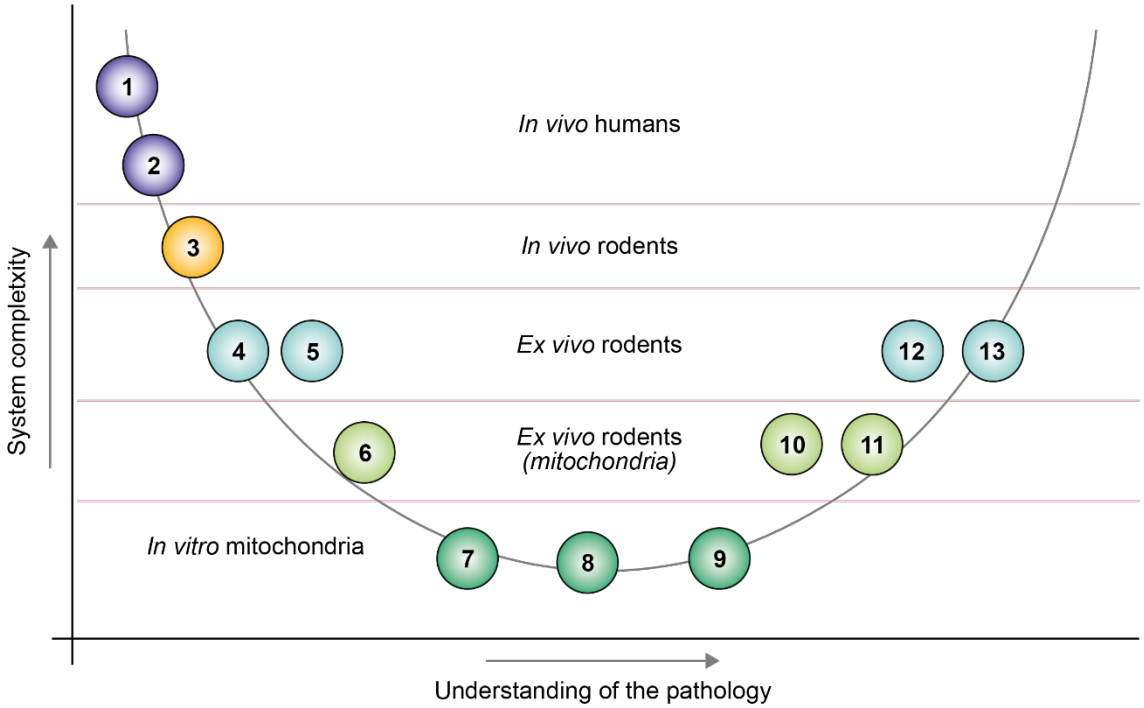

7.5 LIMITATIONS OF THE CURRENT STUDY

There are two primary limits of the current study which are both intrinsic to the nature of the experimental design. In order to identify, and correct, the pathology associated with energetic dysfunction in the T2D heart it was necessary to study rodent models of T2D (to allow wide scale *ex vivo* examination of the heart). This introduced two variables that could confound the findings of this work:

Studying, and trying to correct, a disease in rodent models can generate results which are incompatible with work in humans. However, rodents are a widely used model for cardiovascular disease[312] and it has already been shown that decreases in the PCr/ATP ratio are observed in a similar fashion in rodents as well as in humans[8,10]. Furthermore, rodents provide a good system to study the effect of diabetes on the heart, as they are relatively resistant to the development of atherosclerosis. This fits well with T2D human patients, who get cardiovascular complications without coronary heart disease[300]. Above all, it is reassuring that acetylation appears to be a fundamental motif, with acetylated peptides well-conserved between flies, worms, zebrafish and humans[313] and even at the level of *S. cerevisiae*[314]. It is therefore likely that conclusions drawn from rodent studies will be transferable to human studies.

The second concern regards the true pathology of T2D, which develops over the course of years rather than the model used in this study which develops over the course of months. It should be noted that the model of T2D used is one that has been developed with the explicit aim of mimicking cardiac metabolism within early stages of T2D, with suppressed glycolysis, elevated fatty acid oxidation and elevated oxygen usage, as seen in the other T2D models[140,315–317]. Furthermore, our T2D model does not present with cardiac hypertrophy, as seen in *ob/ob*[315], *db/db*[318] and Zucker Diabetic Fatty[319] T2D models, fitting well with T2D patient studies where cardiac hypertrophy is not seen until a late stage of T2D[320,321].

7.6 CONCLUSIONS AND FUTURE IMPLICATIONS OF THE WORK

It is hoped that the work presented in this thesis has furthered the understanding of energetic dysfunction within the type 2 diabetic heart, by first fully characterising this dysfunction within a rodent model of diabetes, and then presenting data on a novel cause of energetic dysfunction at the mitochondrial level. The culmination of this work was the identification of a potential therapeutic candidate in the treatment of T2D cardiac energetic dysfunction, which this thesis validates as effective in correcting the dysfunction associated with the T2D rodent heart. It therefore presents an intriguing, and safe, therapeutic candidate for further *in vivo* testing to hopefully improve the prognosis of a disease which claims millions of lives annually.

8 BIBLIOGRAPHY

1. Beer, M. *et al.* Absolute concentrations of high-energy phosphate metabolites in normal, hypertrophied, and failing human myocardium measured noninvasively with 31P-SLOOP magnetic resonance spectroscopy. *J. Am. Coll. Cardiol.* **40**, 1267–1274 (2002).

2. Doenst, T., Nguyen, T. D. & Abel, E. D. Cardiac metabolism in heart failure: Implications beyond atp production. *Circ. Res.* **113**, 709–724 (2013).

3. Levelt, E. *et al.* Cardiac energetics, oxygenation, and perfusion during increased workload in patients with type 2 diabetes mellitus. *Eur. Heart J.* ehv442- (2015). doi:10.1093/eurheartj/ehv442

4. Rider, O. J. *et al.* Effects of catecholamine stress on diastolic function and myocardial energetics in obesity. *Circulation* **125**, 1511–1519 (2012).

5. Scheuermann-Freestone, M. *et al.* Abnormal Cardiac and Skeletal Muscle Energy Metabolism in Patients With Type 2 Diabetes. *Circulation* **107**, 3040–3046 (2003).

6. Shen, W. *et al.* Progressive Loss of Myocardial ATP Due to a Loss of Total Purines During the Development of Heart Failure in Dogs : A Compensatory Role for the Parallel Loss of Creatine. *Circulation* **100**, 2113–2118 (1999).

7. Ingwall, J. S. & Weiss, R. G. Is the failing heart energy starved? On using chemical energy to support cardiac function. *Circ. Res.* **95**, 135–145 (2004).

8. Luptak, I. *et al.* Decreased ATP production and myocardial contractile reserve in metabolic heart disease. *J. Mol. Cell. Cardiol.* **116**, 106–114 (2018).

9. Neubauer, S. High-Energy Phosphate Metabolism in Normal, Hypertrophied and Failing Human Myocardium. *Heart Fail. Rev.* **4**, 269–280

10. Bashir, A., Coggan, A. R. & Gropler, R. J. In vivo creatine kinase reaction kinetics at rest and

stress in type II diabetic rat heart. *Physiol. Rep.* **3**, (2015).

11. Neubauer, S. *et al.* Myocardial Phosphocreatine-to-ATP Ratio Is a Predictor of Mortality in Patients With Dilated Cardiomyopathy. *Circulation* **96**, 2190–2196 (1997).

12. Laakso, M. Cardiovascular disease in type 2 diabetes: Challenge for treatment and prevention. *J. Intern. Med.* **249**, 225–235 (2001).

13. Diamant, M. *et al.* Diastolic dysfunction is associated with altered myocardial metabolism in asymptomatic normotensive patients with well-controlled type 2 diabetes mellitus. *J. Am. Coll. Cardiol.* **42**, 328–335 (2003).

14. Bing, R. J. The metabolism of the heart. *Acta Cardiol.* **10**, 1–14 (1955).

15. Bing, R. J., Siegel, A., Ungar, I. & Gilbert, M. Metabolism of the human heart. *Am. J. Med.* **16**, 504–515 (1954).

16. van der Vusse, G. J., van Bilsen, M. & Glatz, J. F. Cardiac fatty acid uptake and transport in health and disease. *Cardiovasc. Res.* **45**, 279–93 (2000).

17. Henning, S. L., Wambolt, R. B., Schönekess, B. O., Lopaschuk, G. D. & Allard, M. F. Contribution of glycogen to aerobic myocardial glucose utilization. *Circulation* **93**, 1549–55 (1996).

18. Manchester, J., Kong, X., Nerbonne, J., Lowry, O. H. & Lawrence, J. C. Glucose transport and phosphorylation in single cardiac myocytes: rate-limiting steps in glucose metabolism. *Am. J. Physiol.* **266**, E326-33 (1994).

19. Razeghi, P. *et al.* Metabolic gene expression in fetal and failing human heart. *Circulation* **104**, 2923–31 (2001).

20. Olson, A. L. & Pessin, J. E. Structure, Function, and Regulation of the Mammalian Facilitative Glucose Transporter Gene Family. *Annu. Rev. Nutr.* **16**, 235–256 (1996).

21. Brooks, G. A., Dubouchaud, H., Brown, M., Sicurello, J. P. & Eric Butz, C. Role of

mitochondrial lactate dehydrogenase and lactate oxidation in the intracellular lactate shuttle. *Proc. Natl. Acad. Sci. U. S. A.* **96**, 1129–1134 (1999).

22. Kline, E. S. *et al.* Localization of l-lactate dehydrogenase in mitochondria. *Arch. Biochem. Biophys.* **246**, 673–680 (1986).

23. Chatham, J. C., Gao, Z. P. & Forder, J. R. Impact of 1 wk of diabetes on the regulation of myocardial carbohydrate and fatty acid oxidation. *Am. J. Physiol. - Endocrinol. Metab.* **277**, E342–E351 (1999).

24. Hui, S. *et al.* Glucose feeds the TCA cycle via circulating lactate. *Nature* **551**, 115–118 (2017).

25. Schönekess, B. O. Competition between lactate and fatty acids as sources of ATP in the isolated working rat heart. *J. Mol. Cell. Cardiol.* **29**, 2725–2733 (1997).

26. BALLARD, F. B., DANFORTH, W. H., NAEGLE, S. & BING, R. J. Myocardial metabolism of fatty acids. *J. Clin. Invest.* **39**, 717–723 (1960).

27. Hauton, D., Bennett, M. J. & Evans, R. D. Utilisation of triacylglycerol and non-esterified fatty acid by the working rat heart: myocardial lipid substrate preference. *Biochim. Biophys. Acta* **1533**, 99–109 (2001).

28. Hamilton, J. A. New insights into the roles of proteins and lipids in membrane transport of fatty acids. *Prostaglandins, Leukot. Essent. Fat. Acids* **77**, 355–361 (2007).

29. Ibrahimi, A. *et al.* Expression of the CD36 homolog (FAT) in fibroblast cells: effects on fatty acid transport. *Proc. Natl. Acad. Sci. U. S. A.* **93**, 2646–51 (1996).

30. Stremmel, W., Strohmeyer, G., Borchard, F., Kochwa, S. & Berk, P. D. Isolation and partial characterization of a fatty acid binding protein in rat liver plasma membranes. *Proc. Natl. Acad. Sci. U. S. A.* **82**, 4–8 (1985).

31. Schaffer, J. E. & Lodish, H. F. Expression cloning and characterization of a novel adipocyte long chain fatty acid transport protein. *Cell* **79**, 427–36 (1994).

32. Gimeno, R. E. *et al.* Targeted Deletion of Fatty Acid Transport Protein-4 Results in Early Embryonic Lethality. *J. Biol. Chem.* **278**, 49512–49516 (2003).

33. Luiken, J. J. F. P. *et al.* Cellular fatty acid transport in heart and skeletal muscle as facilitated by proteins. *Lipids* **34**, S169–S175 (1999).

34. Luiken, J. J. F. P. *et al.* Changes in fatty acid transport and transporters are related to the severity of insulin deficiency. *Am. J. Physiol. - Endocrinol. Metab.* **283**, E612–E621 (2002).

35. Luiken, J. J. F. P. *et al.* Contraction-induced fatty acid translocase/CD36 translocation in rat cardiac myocytes is mediated through AMP-activated protein kinase signaling. *Diabetes* **52**, 1627–34 (2003).

36. Heather, L. C. *et al.* Differential Translocation of the Fatty Acid Transporter, FAT/CD36, and the Glucose Transporter, GLUT4, Coordinates Changes in Cardiac Substrate Metabolism During Ischemia and Reperfusion. *Circ. Hear. Fail.* **6**, 1058–1066 (2013).

37. Coe, N. R., Smith, A. J., Frohnert, B. I., Watkins, P. A. & Bernlohr, D. A. The fatty acid transport protein (FATP1) is a very long chain acyl-CoA synthetase. *J. Biol. Chem.* **274**, 36300–4 (1999).

38. Zierler, K. L. Fatty acids as substrates for heart and skeletal muscle. *Circ. Res.* **38**, (1976).

39. Banke, N. H. *et al.* Preferential Oxidation of Triacylglyceride-Derived Fatty Acids in Heart Is Augmented by the Nuclear Receptor PPAR. *Circ. Res.* **107**, 233–241 (2010).

40. Hammer, S. *et al.* Progressive caloric restriction induces dose-dependent changes in myocardial triglyceride content and diastolic function in healthy men. *J. Clin. Endocrinol. Metab.* **93**, 497–503 (2008).

41. Chen, Y., Liu, Y. & Dorn, G. W. Mitochondrial fusion is essential for organelle function and cardiac homeostasis. *Circ. Res.* **109**, 1327–31 (2011).

42. Duan, J. & Karmazyn, M. Relationship between oxidative phosphorylation and adenine nucleotide translocase activity of two populations of cardiac mitochondria and mechanical

recovery of ischemic hearts following reperfusion. *Can. J. Physiol. Pharmacol.* **67**, 704–9 (1989).

43. Hoppel, C. L., Moghaddas, S. & Lesnefsky, E. J. Interfibrillar cardiac mitochondrial comples III defects in the aging rat heart. *Biogerontology* **3**, 41–44 (2002).

44. Hoppel, C. L., Tandler, B., Fujioka, H. & Riva, A. Dynamic organization of mitochondria in human heart and in myocardial disease. **41**, (2009).

45. Riva, A., Tandler, B., Loffredo, F., Vazquez, E. & Hoppel, C. Structural differences in two biochemically defined populations of cardiac mitochondria. *Am. J. Physiol. Heart Circ. Physiol.* **289**, H868-72 (2005).

46. Palmer, J. W., Tandler, B. & Hoppel, C. L. Biochemical properties of subsarcolemmal and interfibrillar mitochondria isolated from rat cardiac muscle. *J. Biol. Chem.* **252**, 8731–9 (1977).

47. Palmer, J. W., Tandler, B. & Hoppel, C. L. Biochemical differences between subsarcolemmal and interfibrillar mitochondria from rat cardiac muscle: Effects of procedural manipulations. *Arch. Biochem. Biophys.* **236**, 691–702 (1985).

48. Duan, J. & Karmazyn, M. Relationship between oxidative phosphorylation and adenine nucleotide translocase activity of two populations of cardiac mitochondria and mechanical recovery of ischemic hearts following reperfusion. *Can. J. Physiol. Pharmacol.* **67**, 704–709 (1989).

49. Dabkowski, E. R. *et al.* Diabetic cardiomyopathy-associated dysfunction in spatially distinct mitochondrial subpopulations. *Am. J. Physiol. Heart Circ. Physiol.* **296**, H359-69 (2009).

50. Kudo, N., Barr, A. J., Barr, R. L., Desai, S. & Lopaschuk, G. D. High Rates of Fatty Acid Oxidation during Reperfusion of Ischemic Hearts Are Associated with a Decrease in Malonyl-CoA Levels Due to an Increase in 5'-AMP-activated Protein Kinase Inhibition of Acetyl-CoA Carboxylase. *J. Biol. Chem.* **270**, 17513–17520 (1995).

51. Lopaschuk, G. D., Witters, L. A., Itoi, T., Barr, R. & Barr, A. Acetyl-CoA carboxylase

involvement in the rapid maturation of fatty acid oxidation in the newborn rabbit heart. *J. Biol. Chem.* **269**, 25871–8 (1994).

52. Thampy, K. G. Formation of malonyl coenzyme A in rat heart. Identification and purification of an isozyme of A carboxylase from rat heart. *J. Biol. Chem.* **264**, 17631–4 (1989).

53. Dyck, J. R., Barr, A. J., Barr, R. L., Kolattukudy, P. E. & Lopaschuk, G. D. Characterization of cardiac malonyl-CoA decarboxylase and its putative role in regulating fatty acid oxidation. *Am. J. Physiol.* **275**, H2122-9 (1998).

54. Hopkins, T. A., Dyck, J. R. B. & Lopaschuk, G. D. AMP-activated protein kinase regulation of fatty acid oxidation in the ischaemic heart. *Biochem. Soc. Trans.* **31**, 207–12 (2003).

55. Saha, A. K. *et al.* Activation of malonyl-CoA decarboxylase in rat skeletal muscle by contraction and the AMP-activated protein kinase activator 5-aminoimidazole-4-carboxamide-1-beta -D-ribofuranoside. *J. Biol. Chem.* **275**, 24279–83 (2000).

56. Aoyama, T. *et al.* Purification of human very-long-chain acyl-coenzyme A dehydrogenase and characterization of its deficiency in seven patients. *J. Clin. Invest.* **95**, 2465–2473 (1995).

57. Aoyama, T., Ueno, I., Kamijo, T. & Hashimoto, T. *Rat very-long-chain acyl-CoA dehydrogenase, a novel mitochondrial acyl- CoA dehydrogenase gene product, is a rate-limiting enzyme in long-chain fatty acid ??-oxidation system. cDNA and deduced amino acid sequence and distinct specificities of the cDNA-exp*. *Journal of Biological Chemistry* **269**, (1994).

58. Izai, K., Uchida, Y., Orii, T., Yamamoto, S. & Hashimoto, T. *Novel fatty acid β-oxidation enzymes in rat liver mitochondria: I. Purification and properties of very-long-chain acyl-coenzyme A dehydrogenase*. *Journal of Biological Chemistry* **267**, (1992).

59. Krebs, H. A. & Johnson, W. A. The Role of Citric Acid in Intermediate Metabolism in Animal Tissues. *Enzymologia* **4**, 148_156 (1937).

60. Comte, B. *et al.* A 13 C mass isotopomer study of anaplerotic pyruvate carboxylation in perfused rat hearts. *J. Biol. Chem.* **272**, 26125–26131 (1997).

61. Kerbey, A. L. *et al.* Regulation of pyruvate dehydrogenase in rat heart. Mechanism of regulation of proportions of dephosphorylated and phosphorylated enzyme by oxidation of fatty acids and ketone bodies and of effects of diabetes: role of coenzyme A, acetyl-coenzyme A and reduced and oxidized nicotinamide-adenine dinucleotide. *Biochem. J.* **154**, 327–48 (1976).

62. Linn, T. C., Pettit, F. H., Hucho, F. & Reed, L. J. Alpha-keto acid dehydrogenase complexes. XI. Comparative studies of regulatory properties of the pyruvate dehydrogenase complexes from kidney, heart, and liver mitochondria. *Proc. Natl. Acad. Sci. U. S. A.* **64**, 227–34 (1969).

63. Seifert, E. L. *et al.* Natural and induced mitochondrial phosphate carrier loss: Differential dependence of mitochondrial metabolism and dynamics and cell survival on the extent of depletion. *J. Biol. Chem.* **291**, 26126–26137 (2016).

64. Borutaité, V., Mildažiene, V., Katiliuté, Z., Kholodenko, B. & Toleikis, A. The function of ATP/ADP translocator in the regulation of mitochondrial respiration during development of heart ischemic injury. *BBA - Bioenerg.* **1142**, 175–180 (1993).

65. Kholodenko, B. *et al.* The role of adenine nucleotide translocators in regulation of oxidative phosphorylation in heart mitochondria. *FEBS Lett.* **223**, 247–250 (1987).

66. Levy, S. E., Chen, Y. S., Graham, B. H. & Wallace, D. C. Expression and sequence analysis of the mouse adenine nucleotide translocase 1 and 2 genes. *Gene* **254**, 57–66 (2000).

67. Stepien, G., Torroni, A., Chung, A. B., Hodge, J. A. & Wallaces, D. C. *Differential expression of adenine nucleotide translocator isoforms in mammalian tissues and during muscle cell differentiation*. *Journal of Biological Chemistry* **267**, (1992).

68. Rodić, N. *et al.* DNA Methylation Is Required for Silencing of Ant4 , an Adenine Nucleotide Translocase Selectively Expressed in Mouse Embryonic Stem Cells and Germ Cells . *Stem Cells* **23**, 1314–1323 (2005).

69. Stepien, G., Torroni, A., Chung, A. B., Hodge, J. A. & Wallace, D. C. Differential expression of adenine nucleotide translocator isoforms in mammalian tissues and during muscle cell

differentiation. *J. Biol. Chem.* **267**, 14592–7 (1992).

70. Traba, J., Satrústegui, J. & Del Arco, A. Adenine nucleotide transporters in organelles: Novel genes and functions. *Cell. Mol. Life Sci.* **68**, 1183–1206 (2011).

71. De Marcos Lousa, C., Trézéguet, V., Dianoux, A. C., Brandolin, G. & Lauquin, G. J. M. The human mitochondrial ADP/ATP carriers: Kinetic properties and biogenesis of wild-type and mutant proteins in the yeast S. cerevisiae. *Biochemistry* **41**, 14412–14420 (2002).

72. Narula, N. *et al.* Adenine nucleotide translocase 1 deficiency results in dilated cardiomyopathy with defects in myocardial mechanics, histopathological alterations, and activation of apoptosis. *JACC Cardiovasc. Imaging* **4**, 1–10 (2011).

73. Kokoszka, J. E. *et al.* Deficiency in the mouse mitochondrial adenine nucleotide translocator isoform 2 gene is associated with cardiac noncompaction. *Biochim. Biophys. Acta - Bioenerg.* **1857**, 1203–1212 (2016).

74. Portman, M. A. Adenine nucleotide translocator in heart. *Mol. Genet. Metab.* **71**, 445–450 (2000).

75. Dörner, A. & Schultheiss, H. P. Adenine Nucleotide Translocase in the Focus of Cardiovascular Diseases. *Trends Cardiovasc. Med.* **17**, 284–290 (2007).

76. Schultheiss, H. P. & Bolte, H. D. Immunological analysis of auto-antibodies against the adenine nucleotide translocator in dilated cardiomyopathy. *J. Mol. Cell. Cardiol.* **17**, 603–617 (1985).

77. Dörner, A. *et al.* An isoform shift in the cardiac adenine nucleotide translocase expression alters the kinetic properties of the carrier in dilated cardiomyopathy. *Eur. J. Heart Fail.* **8**, 81–89 (2006).

78. Rosca, M. G. *et al.* Altered expression of the adenine nucleotide translocase isoforms and decreased ATP synthase activity in skeletal muscle mitochondria in heart failure. *J. Mol. Cell. Cardiol.* **46**, 927–35 (2009).

79. Liao, R., Nascimben, L., Friedrich, J., Gwathmey, J. K. & Ingwall, J. S. Decreased energy reserve in an animal model of dilated cardiomyopathy: Relationship to contractile performance. *Circ. Res.* **78**, 893–902 (1996).

80. Shen, W., Vatner, D. E., Vatner, S. F. & Ingwall, J. S. Progressive loss of creatine maintains a near normal ΔG∼ATP in transgenic mouse hearts with cardiomyopathy caused by overexpressing Gsα. *J. Mol. Cell. Cardiol.* **48**, 591–599 (2010).

81. Laser, A. *et al.* Long-term beta-blocker treatment prevents chronic creatine kinase and lactate dehydrogenase system changes in rat hearts after myocardial infarction. *J. Am. Coll. Cardiol.* **27**, 487–493 (1996).

82. Pfeffer, M. A. *et al.* Effect of Captopril on Mortality and Morbidity in Patients with Left Ventricular Dysfunction after Myocardial Infarction. *N. Engl. J. Med.* **327**, 669–677 (1992).

83. Group*, T. C. T. S. Effects of Enalapril on Mortality in Severe Congestive Heart Failure. *N. Engl. J. Med.* **316**, 1429–1435 (1987).

84. Swedberg, K., Hjalmarson, A., Waagstein, F. & Wallentin, I. Beneficial effects of long-term beta-blockade in congestive cardiomyopathy. *Br. Heart J.* **44**, 117–133 (1980).

85. Horn, M. *et al.* Preservation of left ventricular mechanical function and energy metabolism in rats after myocardial infarction by the angiotensin-converting enzyme inhibitor quinapril. *J. Cardiovasc. Pharmacol.* **27**, 201–210 (1996).

86. Anderson, K. A. & Hirschey, M. D. Mitochondrial protein acetylation regulates metabolism. *Essays Biochem.* **52**, 23–35 (2012).

87. Carrico, C., Meyer, J. G., He, W., Gibson, B. W. & Verdin, E. The Mitochondrial Acylome Emerges: Proteomics, Regulation by Sirtuins, and Metabolic and Disease Implications. *Cell Metab.* **27**, 497–512 (2018).

88. Scott, I., Wang, L., Wu, K., Thapa, D. & Sack, M. N. GCN5L1/BLOS1 Links Acetylation, Organelle Remodeling, and Metabolism. *Trends Cell Biol.* **28**, 346–355 (2018).

89. Casey, J. R., Grinstein, S. & Orlowski, J. Sensors and regulators of intracellular pH. *Nat. Rev. Mol. Cell Biol.* **11**, 50–61 (2010).

90. Wagner, G. R. & Payne, R. M. Widespread and enzyme-independent Nε-acetylation and Nε-succinylation of proteins in the chemical conditions of the mitochondrial matrix. *J. Biol. Chem.* **288**, 29036–29045 (2013).

91. Michishita, E., Park, J. Y., Burneskis, J. M., Barrett, J. C. & Horikawa, I. Evolutionarily conserved and nonconserved cellular localizations and functions of human SIRT proteins. *Mol. Biol. Cell* **16**, 4623–4635 (2005).

92. Lombard, D. B. *et al.* Mammalian Sir2 Homolog SIRT3 Regulates Global Mitochondrial Lysine Acetylation. *Mol. Cell. Biol.* **27**, 8807–8814 (2007).

93. Du, J. *et al.* Sirt5 is a NAD-dependent protein lysine demalonylase and desuccinylase. *Science (80-.).* **334**, 806–809 (2011).

94. Schwer, B. *et al. Calorie restriction alters mitochondrial protein acetylation*. *Aging Cell* **8**, 604–606 (NIH Public Access, 2009).

95. Jing, E. *et al.* Sirt3 regulates metabolic flexibility of skeletal muscle through reversible enzymatic deacetylation. *Diabetes* **62**, 3404–3417 (2013).

96. Kendrick, A. A. *et al.* Fatty liver is associated with reduced SIRT3 activity and mitochondrial protein hyperacetylation. *Biochem. J.* **433**, 505–514 (2011).

97. Picklo, M. J. Ethanol intoxication increases hepatic N-lysyl protein acetylation. *Biochem. Biophys. Res. Commun.* **376**, 615–619 (2008).

98. Holloway, C. J. *et al.* A short-term, high fat diet impairs cardiac high energy phosphate metabolism, without change in cardiac function. *J. Cardiovasc. Magn. Reson.* **11**, O72 (2009).

99. Holloway, C. J. *et al.* A high-fat diet impairs cardiac high-energy phosphate metabolism and cognitive function in healthy human subjects. *Am. J. Clin. Nutr.* **93**, 748–755 (2011).

100. Hoeks, J. *et al.* Prolonged fasting identifies skeletal muscle mitochondrial dysfunction as consequence rather than cause of human insulin resistance. *Diabetes* **59**, 2117–2125 (2010).

101. Vadvalkar, S. S. *et al.* Metabolic inflexibility and protein lysine acetylation in heart mitochondria of a chronic model of Type 1 diabetes. *Biochem. J.* **449**, 253–261 (2013).

102. Metzler, B. *et al.* Decreased high-energy phosphate ratios in the myocardium of men with diabetes mellitus type I. *J. Cardiovasc. Magn. Reson.* **4**, 493–502 (2002).

103. Cheung, K. G. *et al.* Sirtuin-3 (SIRT3) protein attenuates doxorubicin-induced oxidative stress and improves mitochondrial respiration in H9c2 cardiomyocytes. *J. Biol. Chem.* **290**, 10981–10993 (2015).

104. Eidenschink, A. B., Schröter, G., Müller-Weihrich, S. & Stern, H. Myocardial high-energy phosphate metabolism is altered after treatment with anthracycline in childhood. *Cardiol. Young* **10**, 610–7 (2000).

105. Ahn, B. H. *et al.* A role for the mitochondrial deacetylase Sirt3 in regulating energy homeostasis. *Proc. Natl. Acad. Sci. U. S. A.* **105**, 14447–14452 (2008).

106. Koentges, C. *et al.* SIRT3 deficiency impairs mitochondrial and contractile function in the heart. *Basic Res. Cardiol.* **110**, 1–20 (2015).

107. Hirschey, M. D. *et al.* SIRT3 regulates mitochondrial fatty-acid oxidation by reversible enzyme deacetylation. *Nature* **464**, 121–125 (2010).

108. Scott, I., Webster, B. R., Li, J. H. & Sack, M. N. Identification of a molecular component of the mitochondrial acetyltransferase programme: A novel role for GCN5L1. *Biochem. J.* **443**, 655–661 (2012).

109. Pillai, V. B. *et al.* Honokiol blocks and reverses cardiac hypertrophy in mice by activating mitochondrial Sirt3. *Nat. Commun.* **6**, 6656 (2015).

110. Huang, L. *et al.* Honokiol protects against doxorubicin cardiotoxicity via improving

mitochondrial function in mouse hearts. *Sci. Rep.* **7**, 11989 (2017).

111. Liang, L., Li, Q., Huang, L., Li, D. & Li, X. Sirt3 binds to and deacetylates mitochondrial pyruvate carrier 1 to enhance its activity. *Biochem. Biophys. Res. Commun.* **468**, 807–812 (2015).

112. Hallows, W. C., Lee, S. & Denu, J. M. Sirtuins deacetylate and activate mammalian acetyl-CoA synthetases. *Proc. Natl. Acad. Sci. U. S. A.* **103**, 10230–10235 (2006).

113. Fernandes, J. *et al.* Lysine Acetylation Activates Mitochondrial Aconitase in the Heart. *Biochemistry* **54**, 4008–4018 (2015).

114. Schlicker, C. *et al.* Substrates and Regulation Mechanisms for the Human Mitochondrial Sirtuins Sirt3 and Sirt5. *J. Mol. Biol.* **382**, 790–801 (2008).

115. Hirschey, M. D. *et al.* SIRT3 deficiency and mitochondrial protein hyperacetylation accelerate the development of the metabolic syndrome. *Mol. Cell* **44**, 177–190 (2011).

116. Alrob, O. A. *et al.* Obesity-induced lysine acetylation increases cardiac fatty acid oxidation and impairs insulin signalling. *Cardiovasc. Res.* **103**, 485–97 (2014).

117. Bharathi, S. S. *et al.* Sirtuin 3 (SIRT3) protein regulates long-chain acyl-CoA dehydrogenase by deacetylating conserved lysines near the active site. *J. Biol. Chem.* **288**, 33837–33847 (2013).

118. Cimen, H. *et al.* Regulation of succinate dehydrogenase activity by SIRT3 in mammalian mitochondria. *Biochemistry* **49**, 304–311 (2010).

119. Finley, L. W. S. *et al.* Succinate dehydrogenase is a direct target of sirtuin 3 deacetylase activity. *PLoS One* **6**, e23295 (2011).

120. Rahman, M. *et al.* Drosophila sirt2/mammalian SIRT3 deacetylates ATP synthase β and regulates complex V activity. *J. Cell Biol.* **206**, 289–305 (2014).

121. Mielke, C. *et al.* Adenine Nucleotide Translocase Is Acetylated *in Vivo* in Human Muscle: Modeling Predicts a Decreased ADP Affinity and Altered Control of Oxidative Phosphorylation.

Biochemistry **53**, 3817–3829 (2014).

122. Hebert, A. S. *et al.* Calorie Restriction and SIRT3 Trigger Global Reprogramming of the Mitochondrial Protein Acetylome. *Mol. Cell* **49**, 186–199 (2013).

123. He, X., Zeng, H. & Chen, J. X. Ablation of SIRT3 causes coronary microvascular dysfunction and impairs cardiac recovery post myocardial ischemia. *Int. J. Cardiol.* **215**, 349–357 (2016).

124. Klishadi, M. S. *et al.* Losartan protects the heart against ischemia reperfusion injury: Sirtuin3 involvement. *J. Pharm. Pharm. Sci.* **18**, 112–123 (2015).

125. Sundaresan, N. R. *et al.* Sirt3 blocks the cardiac hypertrophic response by augmenting Foxo3a-dependent antioxidant defense mechanisms in mice. *J. Clin. Invest.* **119**, 2758–2771 (2009).

126. Hafner, A. V. *et al.* Regulation of the mPTP by SIRT3-mediated deacetylation of CypD at lysine 166 suppresses age-related cardiac hypertrophy. *Aging (Albany. NY).* **2**, 914–923 (2010).

127. Pillai, V. B. *et al.* Sirt3 protects mitochondrial DNA damage and blocks the development of doxorubicin-induced cardiomyopathy in mice. *Am. J. Physiol. - Hear. Circ. Physiol.* **310**, H962–H972 (2016).

128. Yu, W. *et al.* Sirt3 deficiency exacerbates diabetic cardiac dysfunction: Role of Foxo3A-Parkin-mediated mitophagy. *Biochim. Biophys. Acta - Mol. Basis Dis.* **1863**, 1973–1983 (2017).

129. Robertson, R. P. Antagonist: diabetes and insulin resistance--philosophy, science, and the multiplier hypothesis. *J. Lab. Clin. Med.* **125**, 560–4; discussion 565 (1995).

130. Kahn, C. R. Insulin Action, Diabetogenes, and the Cause of Type II Diabetes. *Diabetes* **43**, 1066–1085 (1994).

131. An, D. & Rodrigues, B. Role of changes in cardiac metabolism in development of diabetic cardiomyopathy. *AJP Hear. Circ. Physiol.* **291**, H1489–H1506 (2006).

132. McGill, J. B. *et al.* Potentiation of abnormalities in myocardial metabolism with the development of diabetes in women with obesity and insulin resistance. *J. Nucl. Cardiol.* **18**, 421–429 (2011).

133. Herrero, P. *et al.* Increased Myocardial Fatty Acid Metabolism in Patients With Type 1 Diabetes Mellitus. *J. Am. Coll. Cardiol.* **47**, 598–604 (2006).

134. Mather, K. J. *et al.* Assessment of myocardial metabolic flexibility and work efficiency in human type 2 diabetes using 16-[^{18} F]fluoro-4-thiapalmitate, a novel PET fatty acid tracer. *Am. J. Physiol. - Endocrinol. Metab.* **310**, E452–E460 (2016).

135. Rijzewijk, L. J. *et al.* Altered myocardial substrate metabolism and decreased diastolic function in nonischemic human diabetic cardiomyopathy: studies with cardiac positron emission tomography and magnetic resonance imaging. *J. Am. Coll. Cardiol.* **54**, 1524–32 (2009).

136. Peterson, L. R. *et al.* Effect of Obesity and Insulin Resistance on Myocardial Substrate Metabolism and Efficiency in Young Women. *Circulation* **109**, 2191–2196 (2004).

137. Lopaschuk, G. D. & Tsang, H. Metabolism of palmitate in isolated working hearts from spontaneously diabetic 'BB' Wistar rats. *Circ. Res.* **61**, 853–8 (1987).

138. Aasum, E., Hafstad, A. D., Severson, D. L. & Larsen, T. S. Age-dependent changes in metabolism, contractile function, and ischemic sensitivity in hearts from db/db mice. *Diabetes* **52**, 434–41 (2003).

139. Belke, D. D., Larsen, T. S., Gibbs, E. M. & Severson, D. L. Altered metabolism causes cardiac dysfunction in perfused hearts from diabetic (db/db) mice. *Am. J. Physiol. Endocrinol. Metab.* **279**, E1104-13 (2000).

140. Buchanan, J. *et al.* Reduced cardiac efficiency and altered substrate metabolism precedes the onset of hyperglycemia and contractile dysfunction in two mouse models of insulin resistance and obesity. *Endocrinology* **146**, 5341–9 (2005).

141. Wang, P., Lloyd, S. G., Zeng, H., Bonen, A. & Chatham, J. C. Impact of altered substrate utilization on cardiac function in isolated hearts from Zucker diabetic fatty rats. *AJP Hear. Circ. Physiol.* **288**, H2102–H2110 (2005).

142. van den Brom, C. E. *et al.* Altered myocardial substrate metabolism is associated with

myocardial dysfunction in early diabetic cardiomyopathy in rats: studies using positron emission tomography. *Cardiovasc. Diabetol.* **8**, 39 (2009).

143. Mansor, L. S. *et al.* Increased oxidative metabolism following hypoxia in the type 2 diabetic heart, despite normal hypoxia signalling and metabolic adaptation. *J. Physiol.* **594**, 307–20 (2016).

144. Rijzewijk, L. J. *et al.* Myocardial Steatosis Is an Independent Predictor of Diastolic Dysfunction in Type 2 Diabetes Mellitus. *J. Am. Coll. Cardiol.* **52**, 1793–1799 (2008).

145. Levelt, E. *et al.* Ectopic and Visceral Fat Deposition in Lean and Obese Patients With Type 2 Diabetes. *J. Am. Coll. Cardiol.* **68**, 53–63 (2016).

146. Goldberg, I. J., Trent, C. M. & Schulze, P. C. Lipid metabolism and toxicity in the heart. *Cell Metab.* **15**, 805–812 (2012).

147. Finck, B. N. *et al.* The cardiac phenotype induced by PPARalpha overexpression mimics that caused by diabetes mellitus. *J. Clin. Invest.* **109**, 121–30 (2002).

148. Drosatos, K. & Schulze, P. C. Cardiac Lipotoxicity: Molecular Pathways and Therapeutic Implications. *Curr. Heart Fail. Rep.* **10**, 109–121 (2013).

149. Zlobine, I., Gopal, K. & Ussher, J. R. Lipotoxicity in obesity and diabetes-related cardiac dysfunction. *Biochim. Biophys. Acta - Mol. Cell Biol. Lipids* **1861**, 1555–1568 (2016).

150. Hafstad, A. D., Khalid, A. M., How, O.-J., Larsen, T. S. & Aasum, E. Glucose and insulin improve cardiac efficiency and postischemic functional recovery in perfused hearts from type 2 diabetic (db/db) mice. *AJP Endocrinol. Metab.* **292**, E1288–E1294 (2007).

151. Boardman, N., Hafstad, A. D., Larsen, T. S., Severson, D. L. & Aasum, E. Increased O2 cost of basal metabolism and excitation-contraction coupling in hearts from type 2 diabetic mice. *AJP Hear. Circ. Physiol.* **296**, H1373–H1379 (2009).

152. Murray, A. J., Panagia, M., Hauton, D., Gibbons, G. F. & Clarke, K. Plasma free fatty acids and

peroxisome proliferator-activated receptor alpha in the control of myocardial uncoupling protein levels. *Diabetes* **54**, 3496–502 (2005).

153. O'Donnell, J. M. *et al.* Accelerated triacylglycerol turnover kinetics in hearts of diabetic rats include evidence for compartmented lipid storage. *Am. J. Physiol. - Endocrinol. Metab.* **290**, (2006).

154. Edwards, L. M., Ashrafian, H. & Korzeniewski, B. In silico studies on the sensitivity of myocardial PCr/ATP to changes in mitochondrial enzyme activity and oxygen concentration. *Mol. Biosyst.* **7**, 3335–3342 (2011).

155. Kuo, T. H., Moore, K. H., Giacomelli, F. & Wiener, J. Defective oxidative metabolism of heart mitochondria from genetically diabetic mice. *Diabetes* **32**, 781–7 (1983).

156. Kuo, T. H., Giacomelli, F. & Wiener, J. Oxidative metabolism of Polytron versus Nagarse mitochondria in hearts of genetically diabetic mice. *BBA - Bioenerg.* **806**, 9–15 (1985).

157. Boudina, S. *et al.* Reduced mitochondrial oxidative capacity and increased mitochondrial uncoupling impair myocardial energetics in obesity. *Circulation* **112**, 2686–95 (2005).

158. Ye, G. *et al.* Catalase Protects Cardiomyocyte Function in Models of Type 1 and Type 2 Diabetes. *Diabetes* **53**, 1336–1343 (2004).

159. Savu, O. *et al.* Increase in Total Antioxidant Capacity of Plasma despite High Levels of Oxidative Stress in Uncomplicated Type 2 Diabetes Mellitus. *J. Int. Med. Res.* **40**, 709–716 (2012).

160. Furukawa, S. *et al.* Increased oxidative stress in obesity and its impact on metabolic syndrome. *J. Clin. Invest.* **114**, 1752–1761 (2004).

161. Shen, X., Zheng, S., Metreveli, N. S. & Epstein, P. N. Protection of cardiac mitochondria by overexpression of MnSOD reduces diabetic cardiomyopathy. *Diabetes* **55**, 798–805 (2006).

162. Anderson, E. J. *et al.* Substrate-specific derangements in mitochondrial metabolism and redox

balance in the atrium of the type 2 diabetic human heart. *J. Am. Coll. Cardiol.* **54**, 1891–8 (2009).

163. Katunga, L. A. *et al.* Obesity in a model of gpx4 haploinsufficiency uncovers a causal role for lipid-derived aldehydes in human metabolic disease and cardiomyopathy. *Mol. Metab.* **4**, 493–506 (2015).

164. Sesso, H. D. *et al.* Vitamins E and C in the prevention of cardiovascular disease in men: The physicians' health study II randomized controlled trial. *JAMA - J. Am. Med. Assoc.* **300**, 2123–2133 (2008).

165. Ye, Y., Li, J. & Yuan, Z. Effect of Antioxidant Vitamin Supplementation on Cardiovascular Outcomes: A Meta-Analysis of Randomized Controlled Trials. *PLoS One* **8**, e56803 (2013).

166. Stepaniak, U. *et al.* Antioxidant vitamin intake and mortality in three Central and Eastern European urban populations: the HAPIEE study. *Eur. J. Nutr.* **55**, 547–560 (2016).

167. Bugger, H. *et al.* Tissue-specific remodeling of the mitochondrial proteome in type 1 diabetic akita mice. *Diabetes* **58**, 1986–1997 (2009).

168. Shen, X. *et al.* Cardiac mitochondrial damage and biogenesis in a chronic model of type 1 diabetes. *Am. J. Physiol. - Endocrinol. Metab.* **287**, E896–E905 (2004).

169. Turko, I. V. & Murad, F. Quantitative protein profiling in heart mitochondria from diabetic rats. *J. Biol. Chem.* **278**, 35844–35849 (2003).

170. Hamblin, M. *et al.* Alterations in the diabetic myocardial proteome coupled with increased myocardial oxidative stress underlies diabetic cardiomyopathy. *J. Mol. Cell. Cardiol.* **42**, 884–895 (2007).

171. Turko, I. V. *et al.* Protein tyrosine nitration in the mitochondria from diabetic mouse heart: Implications to dysfunctional mitochondria in diabetes. *J. Biol. Chem.* **278**, 33972–33977 (2003).

172. Hu, Y. *et al.* Increased enzymatic O-GlcNAcylation of mitochondrial proteins impairs

mitochondrial function in cardiac myocytes exposed to high glucose. *J. Biol. Chem.* **284**, 547–555 (2009).

173. Dabkowski, E. R. *et al.* Mitochondrial dysfunction in the type 2 diabetic heart is associated with alterations in spatially distinct mitochondrial proteomes. *Am. J. Physiol. Heart Circ. Physiol.* **299**, H529-40 (2010).

174. Boudina, S. *et al.* Mitochondrial Energetics in the Heart in Obesity-Related Diabetes: Direct Evidence for Increased Uncoupled Respiration and Activation of Uncoupling Proteins. *Diabetes* **56**, 2457–2466 (2007).

175. Wang, Y. *et al.* Myocardial overexpression of adenine nucleotide translocase 1 ameliorates diabetic cardiomyopathy in mice. *Exp. Physiol.* **94**, 220–7 (2009).

176. Walther, T. *et al.* Accelerated mitochondrial adenosine diphosphate/adenosine triphosphate transport improves hypertension-induced heart disease. *Circulation* **115**, 333–44 (2007).

177. Gollmer, J., Zirlik, A. & Bugger, H. Established and Emerging Mechanisms of Diabetic Cardiomyopathy. *J. Lipid Atheroscler.* **8**, 26 (2019).

178. Jing, E. *et al.* Sirtuin-3 (Sirt3) regulates skeletal muscle metabolism and insulin signaling via altered mitochondrial oxidation and reactive oxygen species production. *Proc. Natl. Acad. Sci. U. S. A.* **108**, 14608–14613 (2011).

179. Mansor, L. S. *et al.* Cardiac metabolism in a new rat model of type 2 diabetes using high-fat diet with low dose streptozotocin. *Cardiovasc. Diabetol.* **12**, 136 (2013).

180. Spencer, R. G., Balschi, J. A., Leigh, J. S. & Ingwall, J. S. *ATP synthesis and degradation rates in the perfused rat heart. 31P-nuclear magnetic resonance double saturation transfer measurements*. *Biophysical Journal* **54**, (1988).

181. Aigner, C. S., Clason, C., Rund, A. & Stollberger, R. Efficient high-resolution RF pulse design applied to simultaneous multi-slice excitation. *J. Magn. Reson.* **263**, 33–44 (2016).

182. Vanhamme, van den Boogaart A & Van Huffel S. Improved method for accurate and efficient quantification of MRS data with use of prior knowledge. *J. Magn. Reson.* **129**, 35–43 (1997).

183. Stefan, D. *et al.* Quantitation of magnetic resonance spectroscopy signals: the jMRUI software package. *Meas. Sci. Technol.* **20**, 104035 (2009).

184. Naressi, A. *et al.* Java-based graphical user interface for the MRUI quantitation package. *Magma Magn. Reson. Mater. Physics, Biol. Med.* **12**, 141–152 (2001).

185. Heather, L. C. *et al.* Critical role of complex III in the early metabolic changes following myocardial infarction. *Cardiovasc. Res.* **85**, 127–136 (2010).

186. Åkerman, K. E. O. & Wikström, M. K. F. Safranine as a probe of the mitochondrial membrane potential. *FEBS Lett.* **68**, 191–197 (1976).

187. Vercesi, A. E., Bernardes, C. F., Hoffmann, M. E., Gadelha, F. R. & Docampo, R. Digitonin permeabilization does not affect mitochondrial function and allows the determination of the mitochondrial membrane potential of Trypanosoma cruzi in situ. *J. Biol. Chem.* **266**, 14431–14434 (1991).

188. Darley-Usmae, V., Rickwood, D. & Wilson, M. Mitochondria: A Practical Approach. *Biochem. Soc. Trans.* **16**, 1096–1096 (1988).

189. Wallach, J. *Enzymatic analysis. A practical guide*. *Biochemical Education* **23**, (Humana Press, 1995).

190. Minkler, P. E., Kerner, J., Ingalls, S. T. & Hoppel, C. L. Novel isolation procedure for short-, medium-, and long-chain acyl-coenzyme A esters from tissue. *Anal. Biochem.* **376**, 275–276 (2008).

191. Rider, O. J. *et al.* Effects of weight loss on myocardial energetics and diastolic function in obesity. *Int. J. Cardiovasc. Imaging* **29**, 1043–1050 (2013).

192. Cassidy, S. *et al.* High intensity intermittent exercise improves cardiac structure and function

and reduces liver fat in patients with type 2 diabetes: a randomised controlled trial. *Diabetologia* **59**, 56–66 (2016).

193. Van Der Meer, R. W. *et al.* Pioglitazone improves cardiac function and alters myocardial substrate metabolism without affecting cardiac triglyceride accumulation and high-energy phosphate metabolism in patients with well-controlled type 2 diabetes mellitus. *Circulation* **119**, 2069–2077 (2009).

194. Neubauer, S. The Failing Heart — An Engine Out of Fuel. *N. Engl. J. Med.* **356**, 1140–1151 (2007).

195. Forsén, S. & Huffman, R. A. Study of moderately rapid chemical exchange reactions by means of nuclear magnetic double resonance. *J. Chem. Phys.* **39**, 2892–2901 (1963).

196. Hoffman, R. A. & Forsén, S. High resolution nuclear magnetic double and multiple resonance. *Prog. Nucl. Magn. Reson. Spectrosc.* **1**, 15–204 (1966).

197. Boudina, S. *et al.* Reduced mitochondrial oxidative capacity and increased mitochondrial uncoupling impair myocardial energetics in obesity. *Circulation* **112**, 2686–95 (2005).

198. Vinnakota, K. C. & Bassingthwaighte, J. B. Myocardial density and composition: A basis for calculating intracellular metabolite concentrations. *Am. J. Physiol. - Hear. Circ. Physiol.* **286**, H1742–H1749 (2004).

199. Clarke, K., Anderson, R. E., Nédélec, J. -F, Foster, D. O. & Ally, A. Intracellular and extracellular spaces and the direct quantification of molar intracellular concentrations of phosphorus metabolites in the isolated rat heart using 31P NMR spectroscopy and phosphonate markers. *Magn. Reson. Med.* **32**, 181–188 (1994).

200. Cross, H. R., Clarke, K., Opie, L. H. & Radda, G. K. Is lactate-induced myocardial ischaemic injury mediated by decreased pH or increased intracellular lactate? *J. Mol. Cell. Cardiol.* **27**, 1369–1381 (1995).

201. Le Page, L. M. *et al.* Increasing Pyruvate Dehydrogenase Flux as a Treatment for Diabetic

Cardiomyopathy: A Combined 13C Hyperpolarized Magnetic Resonance and Echocardiography Study. *Diabetes* **64**, 2735–43 (2015).

202. Boudina, S. *et al.* Contribution of impaired myocardial insulin signaling to mitochondrial dysfunction and oxidative stress in the heart. *Circulation* **119**, 1272–1283 (2009).

203. Montaigne, D. *et al.* Myocardial contractile dysfunction is associated with impaired mitochondrial function and dynamics in type 2 diabetic but not in obese patients. *Circulation* **130**, 554–64 (2014).

204. Duncan, J. G., Fong, J. L., Medeiros, D. M., Finck, B. N. & Kelly, D. P. Insulin-Resistant Heart Exhibits a Mitochondrial Biogenic Response Driven by the Peroxisome Proliferator-Activated Receptor- /PGC-1 Gene Regulatory Pathway. *Circulation* **115**, 909–917 (2007).

205. Finck, B. N. *et al.* A potential link between muscle peroxisome proliferator- activated receptor-α signaling and obesity-related diabetes. *Cell Metab.* **1**, 133–144 (2005).

206. Stanley, W. C., Lopaschuk, G. D. & McCormack, J. G. Regulation of energy substrate metabolism in the diabetic heart. *Cardiovasc. Res.* **34**, 25–33 (1997).

207. Marciniak, C., Marechal, X., Montaigne, D., Neviere, R. & Lancel, S. Cardiac contractile function and mitochondrial respiration in diabetes-related mouse models. *Cardiovasc. Diabetol.* **13**, 118 (2014).

208. Saraste, M. & Walker, J. E. Internal sequence repeats and the path of polypeptide in mitochondrial ADP/ATP translocase. *FEBS Lett.* **144**, 250–254 (1982).

209. Kunji, E. R. S. & Harding, M. Projection structure of the atractyloside-inhibited mitochondrial ADP/ATP carrier of Saccharomyces cerevisiae. *J. Biol. Chem.* **278**, 36985–36988 (2003).

210. Pebay-Peyroula, E. *et al.* Structure of mitochondrial ADP/ATP carrier in complex with carboxyatractyloside. *Nature* **426**, 39–44 (2003).

211. Robinson, A. J. & Kunji, E. R. S. *Mitochondrial carriers in the cytoplasmic state have a common*

substrate binding site. *Proceedings of the National Academy of Sciences* **103**, 2617–2622 (National Academy of Sciences, 2006).

212. Kunji, E. R. S. & Robinson, A. J. The conserved substrate binding site of mitochondrial carriers. *Biochim. Biophys. Acta - Bioenerg.* **1757**, 1237–1248 (2006).

213. King, M. S., Kerr, M., Crichton, P. G., Springett, R. & Kunji, E. R. S. Formation of a cytoplasmic salt bridge network in the matrix state is a fundamental step in the transport mechanism of the mitochondrial ADP/ATP carrier. *Biochim. Biophys. Acta - Bioenerg.* **1857**, 14–22 (2016).

214. Kunji, E. R. S. *et al.* The transport mechanism of the mitochondrial ADP/ATP carrier. *Biochim. Biophys. Acta - Mol. Cell Res.* **1863**, 2379–2393 (2016).

215. Klingenberg, M., Grebe, K. & Heldt, H. W. On the inhibition of the adenine nucleotide translocation by bongkrekic acid. *Biochem. Biophys. Res. Commun.* **39**, 344–351 (1970).

216. Vignais, P. V., Duee, E. D., Vignais, P. M. & Huet, J. Effects of atractyligenin and its structural analogues on oxidative phosphorylation and on the translocation of adenine nucleotides in mitochondria. *Biochim. Biophys. Acta* **118**, 465–483 (1966).

217. Pande, S. V. & Blanchaer, M. C. Reversible inhibition of mitochondrial adenosine diphosphate phosphorylation by long chain acyl coenzyme A esters. *J. Biol. Chem.* **246**, 402–411 (1971).

218. Lerner, E., Shug, A. L., Elson, C. & Shrago, E. Reversible inhibition of adenine nucleotide translocation by long chain fatty acyl coenzyme A esters in liver mitochondria of diabetic and hibernating animals. *J. Biol. Chem.* **247**, 1513–1519 (1972).

219. Belzacq, A.-S. *et al.* Bcl-2 and Bax Modulate Adenine Nucleotide Translocase Activity. *Cancer Res.* **63**, 541–546 (2003).

220. Riccio, P., Aquila, H. & Klingenberg, M. Purification of the carboxy-atractylate binding protein from mitochondria. *FEBS Lett.* **56**, 133–8 (1975).

221. Aquila, H., Eiermann, W., Babel, W. & Klingenberg, M. Isolation of the ADP/ATP translocator

from beef heart mitochondria as the bongkrekate-protein complex. *Eur. J. Biochem.* **85**, 549–60 (1978).

222. Lauquin, G. J. M., Villiers, C., Michejda, J. W., Hryniewiecka, L. V. & Vignais, P. V. Adenine nucleotide transport in sonic submitochondrial particles. Kinetic properties and binding of specific inhibitors. *Biochim. Biophys. Acta - Bioenerg.* **460**, 331–345 (1977).

223. Woldegiorgis, G. & Shrago, E. The recognition of two specific binding sites of the adenine nucleotide translocase by palmitoyl CoA in bovine heart mitochondria and submitochondrial particles. *Biochem. Biophys. Res. Commun.* **89**, 837–844 (1979).

224. Morel, F., Lauquin, G., Lunardi, J., Duszynski, J. & Vignais, P. V. An appraisal of the functional significance of the inhibitory effect of long chain acyl-CoAs on mitochondrial transports. *FEBS Lett.* **39**, 133–8 (1974).

225. Idell-Wenger, J. A., Grotyohann, L. W. & Neely, J. R. Coenzyme A and carnitine distribution in normal and ischemic hearts. *J. Biol. Chem.* **253**, 4310–8 (1978).

226. Kobayashi, A. & Fujisawa, S. Effect of L-carnitine on mitochondrial acyl CoA esters in the ischemic dog heart. *J. Mol. Cell. Cardiol.* **26**, 499–508 (1994).

227. Faergeman, N. J. & Knudsen, J. Role of long-chain fatty acyl-CoA esters in the regulation of metabolism and in cell signalling. *Biochem. J.* **323 (Pt 1**, 1–12 (1997).

228. Vasiljevich Panov, A., Konstantinov, V. M. & Lyakhovich, V. V. The possible role of palmitoyl-CoA in the regulation of the adenine nucleotides transport in mitochondria under different metabolic states. *J. Bioenerg.* **7**, 75–85 (1975).

229. Ciapaite, J. *et al.* Modular Kinetic Analysis of the Adenine Nucleotide Translocator-Mediated Effects of Palmitoyl-CoA on the Oxidative Phosphorylation in Isolated Rat Liver Mitochondria. *Diabetes* **54**, 944–951 (2005).

230. Chevrollier, A. *et al.* ANT2 isoform required for cancer cell glycolysis. *J. Bioenerg. Biomembr.* **37**, 307–316 (2005).

231. Chevrollier, A., Loiseau, D., Reynier, P. & Stepien, G. Adenine nucleotide translocase 2 is a key mitochondrial protein in cancer metabolism. *Biochimica et Biophysica Acta - Bioenergetics* **1807**, 562–567 (2011).

232. Whitmer, J. T., Idell-Wenger, J. A., Rovetto, M. J. & Neely, J. R. Control of fatty acid metabolism in ischemic and hypoxic hearts. *J. Biol. Chem.* **253**, 4305–4309 (1978).

233. St-Pierre, J., Brand, M. D. & Boutilier, R. G. Mitochondria as ATP consumers: Cellular treason in anoxia. *Proc. Natl. Acad. Sci. U. S. A.* **97**, 8670–8674 (2000).

234. Grover, G. J. *et al.* Excessive ATP hydrolysis in ischemic myocardium by mitochondrial F 1 F 0 -ATPase: Effect of selective pharmacological inhibition of mitochondrial ATPase hydrolase activity. *Am. J. Physiol. - Hear. Circ. Physiol.* **287**, H1747–H1755 (2004).

235. Campanella, M., Parker, N., Tan, C. H., Hall, A. M. & Duchen, M. R. IF1: setting the pace of the F1Fo-ATP synthase. *Trends Biochem. Sci.* **34**, 343–350 (2009).

236. Atwal, K. S. *et al.* Small Molecule Mitochondrial F 1F 0 ATPase Hydrolase Inhibitors as Cardioprotective Agents. Identification of 4-(N-Arylimidazole)-Substituted Benzopyran Derivatives as Selective Hydrolase Inhibitors. *J. Med. Chem.* **47**, 1081–1084 (2004).

237. Halestrap, A. P. What is the mitochondrial permeability transition pore? *J. Mol. Cell. Cardiol.* **46**, 821–831 (2009).

238. Zamzami, N. & Kroemer, G. *The mitochondrion in apoptosis: How Pandora's box opens*. *Nature Reviews Molecular Cell Biology* **2**, (2001).

239. Kokoszka, J. E. *et al.* The ADP/ATP translocator is not essential for the mitochondrial permeability transition pore. *Nature* **427**, 461–465 (2004).

240. Halestrap, A. P., Clarke, S. J. & Javadov, S. A. Mitochondrial permeability transition pore opening during myocardial reperfusion - A target for cardioprotection. *Cardiovasc. Res.* **61**, 372–385 (2004).

241. ZOCCARATO, F., RUGOLO, M., SILIPRANDI, D. & SILIPRANDI, N. Correlated Effluxes of Adenine Nucleotides, Mg2+ and Ca2+ Induced in Rat-Liver Mitochondria by External Ca2+ and Phosphate. *Eur. J. Biochem.* **114**, 195–199 (1981).

242. Javadov, S. A. *et al.* Ischaemic Preconditioning Inhibits Opening of Mitochondrial Permeability Transition Pores in the Reperfused Rat Heart. *J. Physiol.* **549**, 513–524 (2003).

243. Petronilli, V., Cola, C. & Bernardi, P. Modulation of the mitochondrial cyclosporin A-sensitive permeability transition pore. II. The minimal requirements for pore induction underscore a key role for transmembrane electrical potential, matrix pH, and matrix Ca2+. *J. Biol. Chem.* **268**, 1011–6 (1993).

244. Figueira, T. R., Melo, D. R., Vercesi, A. E. & Castilho, R. F. Safranine as a fluorescent probe for the evaluation of mitochondrial membrane potential in isolated organelles and permeabilized cells. in *Methods in Molecular Biology* **810**, 103–117 (Humana Press, 2012).

245. Bajaj, M. *et al.* Effect of a sustained reduction in plasma free fatty acid concentration on intramuscular long-chain fatty acyl-CoAs and insulin action in type 2 diabetic patients. *Diabetes* **54**, 3148–3153 (2005).

246. LaNoue, K. F., Watts, J. A. & Koch, C. D. Adenine nucleotide transport during cardiac ischemia. *Am J Physiol Hear. Circ Physiol* **241**, H663-671 (1981).

247. Klingenberg, M., Scherer, B., Stengel-Rutkowski, L., Buchholz, M. & Grebe, K. Experimental Demonstration of the Reorienting (Mobile) Carrier Mechanism Exemplified By the Mitochondrial Adenine Nucleotide Translocator. in *Mechanisms in Bioenergetics* 257–284 (1973). doi:10.1016/b978-0-12-068960-6.50024-1

248. Feng, J. *et al.* Phosphoproteome analysis of isoflurane-protected heart mitochondria: Phosphorylation of adenine nucleotide translocator-1 on Tyr194 regulates mitochondrial function. *Cardiovasc. Res.* **80**, 20–29 (2008).

249. Queiroga, C. S. F. *et al.* Glutathionylation of Adenine Nucleotide Translocase Induced by

Carbon Monoxide Prevents Mitochondrial Membrane Permeabilization and Apoptosis. *J. Biol. Chem.* **285**, 17077–17088 (2010).

250. Yan, L. J. & Sohal, R. S. Mitochondrial adenine nucleotide translocase is modified oxidatively during aging. *Proc. Natl. Acad. Sci. U. S. A.* **95**, 12896–12901 (1998).

251. Smith, B. K. *et al.* Submaximal ADP-stimulated respiration is impaired in ZDF rats and recovered by resveratrol. *J. Physiol.* **591**, 6089–101 (2013).

252. Ludzki, A. *et al. Rapid repression of adp transport by palmitoyl-COA is attenuated by exercise training in humans: A potential mechanism to decrease oxidative stress and improve skeletal muscle insulin signaling*. *Diabetes* **64**, (2015).

253. Shrago, E. The effect of long chain fatty acyl CoA esters on the adenine nucleotide translocase and myocardial metabolism. *Life Sci.* **22**, 1–5 (1978).

254. Shrago, E., Woldegiorgis, G., Ruoho, A. E. & DiRusso, C. C. Fatty acyl CoA esters as regulators of cell metabolism. *Prostaglandins, Leukot. Essent. Fat. Acids* **52**, 163–166 (1995).

255. Ciapaite, J. *et al.* Modular Kinetic Analysis of the Adenine Nucleotide Translocator-Mediated Effects of Palmitoyl-CoA on the Oxidative Phosphorylation in Isolated Rat Liver Mitochondria. *Diabetes* **54**, 944–951 (2005).

256. Shug, A. L., Shrago, E., Bittar, N., Folts, J. D. & Koke, J. R. Acyl-CoA inhibition of adenine nucleotide translocation in ischemic myocardium. *Am. J. Physiol.* **228**, 689–92 (1975).

257. Bittar, N., Shug, A. L., Koke, J. R., Folts, J. D. & Shrago, E. S. Inhibited adenine nucleotide translocation in mitochondria isolated from ishcemic myocardium. *Recent Adv. Stud. Cardiac Struct. Metab.* **7**, 137–43 (1975).

258. Kerr, M., Dodd, M. S. & Heather, L. C. The 'Goldilocks zone' of fatty acid metabolism; to ensure that the relationship with cardiac function is just right. *Clin. Sci.* **131**, 2079–2094 (2017).

259. Buechler, J. A., Vedvick, T. A. & Taylor, S. S. Differential labeling of the catalytic subunit of

cAMP-dependent protein kinase with acetic anhydride: Substrate-induced conformational changes. *Biochemistry* **28**, 3018–3024 (1989).

260. Gertz, M. *et al.* A Molecular Mechanism for Direct Sirtuin Activation by Resveratrol. *PLoS One* **7**, e49761 (2012).

261. Howitz, K. T. *et al.* Small molecule activators of sirtuins extend Saccharomyces cerevisiae lifespan. *Nature* **425**, 191–196 (2003).

262. Chen, T. *et al.* Activation of SIRT3 by resveratrol ameliorates cardiac fibrosis and improves cardiac function via the TGF-β/smad3 pathway. *Am. J. Physiol. - Hear. Circ. Physiol.* **308**, H424–H434 (2015).

263. Yu, L. *et al.* Melatonin ameliorates myocardial ischemia/reperfusion injury in type 1 diabetic rats by preserving mitochondrial function: Role of AMPK-PGC-1α-SIRT3 signaling. *Sci. Rep.* **7**, 41337 (2017).

264. Zhang, M. *et al.* Melatonin protects against diabetic cardiomyopathy through Mst1/Sirt3 signaling. *J. Pineal Res.* **63**, e12418 (2017).

265. Diaz-Morales, N. *et al.* Does Metformin Protect Diabetic Patients from Oxidative Stress and Leukocyte-Endothelium Interactions? *Antioxidants Redox Signal.* **27**, 1439–1445 (2017).

266. Zhou, G. *et al.* Role of AMP-activated protein kinase in mechanism of metformin action. *J. Clin. Invest.* **108**, 1167–1174 (2001).

267. Wang, Z. *et al.* Cyclic AMP mimics the anti-ageing effects of calorie restriction by up-regulating sirtuin. *Sci. Rep.* **5**, 12012 (2015).

268. Chen, Y. *et al.* AMPK attenuates ventricular remodeling and dysfunction following aortic banding in mice via the Sirt3/Oxidative stress pathway. *Eur. J. Pharmacol.* **814**, 335–342 (2017).

269. Liu, T. F. *et al.* Sequential actions of SIRT1-RELB-SIRT3 coordinate nuclear-mitochondrial

communication during immunometabolic adaptation to acute inflammation and sepsis. *J. Biol. Chem.* **290**, 396–408 (2015).

270. Kong, X. *et al.* Sirtuin 3, a new target of PGC-1α, plays an important role in the suppression of ROS and mitochondrial biogenesis. *PLoS One* **5**, e11707 (2010).

271. Sun, W. *et al.* MicroRNA-210 Modulates the Cellular Energy Metabolism Shift during H 2 O 2 -Induced Oxidative Stress by Repressing ISCU in H9c2 Cardiomyocytes. *Cell. Physiol. Biochem.* **43**, 383–394 (2017).

272. Chen, X. & Rosbash, M. MicroRNA-92a is a circadian modulator of neuronal excitability in Drosophila. *Nat. Commun.* **8**, 14707 (2017).

273. Syed, M., Skonberg, C. & Hansen, S. H. Effect of some organic solvents on oxidative phosphorylation in rat liver mitochondria: Choice of organic solvents. *Toxicol. Vitr.* **27**, 2135–2141 (2013).

274. Mansor, L. S. *et al.* Inhibition of sarcolemmal FAT/CD36 by sulfo-N-succinimidyl oleate rapidly corrects metabolism and restores function in the diabetic heart following hypoxia/reoxygenation. *Cardiovasc. Res.* **113**, 737–748 (2017).

275. Ferreira, R. *et al.* Subsarcolemmal and intermyofibrillar mitochondria proteome differences disclose functional specializations in skeletal muscle. *Proteomics* **10**, 3142–3154 (2010).

276. Hollander, J. M., Thapa, D. & Shepherd, D. L. Physiological and structural differences in spatially distinct subpopulations of cardiac mitochondria: Influence of cardiac pathologies. *Am. J. Physiol. - Hear. Circ. Physiol.* **307**, H1 (2014).

277. Skulachev, V. P. Mitochondrial filaments and clusters as intracellular power-transmitting cables. *Trends Biochem. Sci.* **26**, 23–29 (2001).

278. Alrob, O. A. *et al.* Obesity-induced lysine acetylation increases cardiac fatty acid oxidation and impairs insulin signalling. *Cardiovasc. Res.* **103**, 485–497 (2014).

279. Dong, J. X. *et al.* Mitochondrial dysfunction induced by honokiol. *J. Membr. Biol.* **246**, 375–381 (2013).

280. Mielke, C. *et al.* Adenine nucleotide translocase is acetylated in vivo in human muscle: Modeling predicts a decreased ADP affinity and altered control of oxidative phosphorylation. *Biochemistry* **53**, 3817–29 (2014).

281. Tsai, T. H., Chou, C. J., Cheng, F. C. & Chen, C. F. Pharmacokinetics of honokiol after intravenous administration in rats assessed using high-performance liquid chromatography. *J. Chromatogr. B. Biomed. Appl.* **655**, 41–5 (1994).

282. Chen, F. *et al.* Honokiol: A potent chemotherapy candidate for human colorectal carcinoma. *World J. Gastroenterol.* **10**, 3459–3463 (2004).

283. Wang, Y. *et al.* Honokiol protects rat hearts against myocardial ischemia reperfusion injury by reducing oxidative stress and infammation. *Exp. Ther. Med.* **5**, 315–319 (2013).

284. Zhang, B. *et al.* Honokiol Ameliorates Myocardial Ischemia/Reperfusion Injury in Type 1 Diabetic Rats by Reducing Oxidative Stress and Apoptosis through Activating the SIRT1-Nrf2 Signaling Pathway. *Oxid. Med. Cell. Longev.* **2018**, 3159801 (2018).

285. Atanasov, A. G. *et al.* Honokiol: A non-adipogenic PPARγ agonist from nature. *Biochim. Biophys. Acta - Gen. Subj.* **1830**, 4813–4819 (2013).

286. Choi, S. S. *et al.* Honokiol enhances adipocyte differentiation by potentiating insulin signaling in 3T3-L1 preadipocytes. *J. Nat. Med.* **65**, 424–430 (2011).

287. Petersen, K. F. *et al.* Mechanism of troglitazone action in type 2 diabetes. *Diabetes* **49**, 827–831 (2000).

288. Sun, J. *et al.* Hypoglycemic effect and mechanism of honokiol on type 2 diabetic mice. *Drug Des. Devel. Ther.* **9**, 6327–6342 (2015).

289. Kim, Y. J. & Jung, U. J. Honokiol improves insulin resistance, hepatic steatosis, and

inflammation in type 2 diabetic db/db mice. *Int. J. Mol. Sci.* **20**, 2303 (2019).

290. Dodd, M. S. *et al.* In vivo alterations in cardiac metabolism and function in the spontaneously hypertensive rat heart. *Cardiovasc. Res.* **95**, 69–76 (2012).

291. Phielix, E., Meex, R., Moonen-Kornips, E., Hesselink, M. K. C. & Schrauwen, P. Exercise training increases mitochondrial content and ex vivo mitochondrial function similarly in patients with type 2 diabetes and in control individuals. *Diabetologia* **53**, 1714–1721 (2010).

292. Haigis, M. C. *et al.* SIRT4 Inhibits Glutamate Dehydrogenase and Opposes the Effects of Calorie Restriction in Pancreatic β Cells. *Cell* **126**, 941–954 (2006).

293. Hoelscher, M. E. *et al.* P2095SIRT4 regulates fatty acid utilisation and cardiac function in the normal and diabetic heart. *Eur. Heart J.* **38**, (2017).

294. Schrauwen, P. & Hesselink, M. K. C. Reduced tricarboxylic acid cycle flux in type 2 diabetes mellitus? *Diabetologia* **51**, 1694–1697 (2008).

295. Stram, A. R. *et al.* Progressive mitochondrial protein lysine acetylation and heart failure in a model of Friedreich's Ataxia cardiomyopathy. *PLoS One* **12**, e0178354 (2017).

296. Li, P., Ge, J. & Li, H. Lysine acetyltransferases and lysine deacetylases as targets for cardiovascular disease. *Nat. Rev. Cardiol.* 1–20 (2019). doi:10.1038/s41569-019-0235-9

297. Hoskins, R. C. *The Functions of the Endocrine Organs. Scientific Monthly, New York* **18**, (1924).

298. Garcia, M. J., McNamara, P. M., Gordon, T. & Kannell, W. B. Morbidity and mortality in diabetics in the Framingham population. Sixteen year follow up study. *Diabetes* **23**, 105–111 (1974).

299. Stamler, J., Vaccaro, O., Neaton, J. D. & Wentworth, D. Diabetes, other risk factors, and 12-yr cardiovascular mortality for men screened in the multiple risk factor intervention trial. *Diabetes Care* **16**, 434–444 (1993).

300. Rubler, S. *et al.* New type of cardiomyopathy associated with diabetic glomerulosclerosis. *Am.*

J. Cardiol. **30**, 595–602 (1972).

301. Köstler, H. *et al.* Age and gender dependence of human cardiac phosphorus metabolites determined by SLOOP31P MR spectroscopy. *Magn. Reson. Med.* **56**, 907–911 (2006).

302. Esterhammer, R. *et al.* Cardiac high-energy phosphate metabolism alters with age as studied in 196 healthy males with the help of 31-phosphorus 2-dimensional chemical shift imaging. *PLoS One* **9**, e97368 (2014).

303. Wende, A. R. & Abel, E. D. Lipotoxicity in the heart. *Biochim. Biophys. Acta - Mol. Cell Biol. Lipids* **1801**, 311–319 (2010).

304. Harmancey, R., Wilson, C. R. & Taegtmeyer, H. Adaptation and maladaptation of the heart in obesity. *Hypertension* **52**, 181–187 (2008).

305. SHARMA, S. *et al.* Intramyocardial lipid accumulation in the failing human heart resembles the lipotoxic rat heart. *FASEB J.* **18**, 1692–1700 (2004).

306. Duncan, J. G., Fong, J. L., Medeiros, D. M., Finck, B. N. & Kelly, D. P. Insulin-resistant heart exhibits a mitochondrial biogenic response driven by the peroxisome proliferator-activated receptor-alpha/PGC-1alpha gene regulatory pathway. *Circulation* **115**, 909–17 (2007).

307. Goldberg, I. J. Diabetic Dyslipidemia: Causes and Consequences. *J. Clin. Endocrinol. Metab.* **86**, 965–971 (2001).

308. Yoshino, J., Mills, K. F., Yoon, M. J. & Imai, S. I. Nicotinamide mononucleotide, a key NAD + intermediate, treats the pathophysiology of diet- and age-induced diabetes in mice. *Cell Metab.* **14**, 528–536 (2011).

309. Joesting, J. J. *et al.* Fasting induces IL-1 resistance and free-fatty acid-mediated up-regulation of IL-1R2 and IL-1RA. *Front. Immunol.* **5**, 315 (2014).

310. Hirschey, M. D. *et al.* SIRT3 regulates mitochondrial fatty-acid oxidation by reversible enzyme deacetylation. *Nature* **464**, 121–125 (2010).

311. Beaudoin, M. S. *et al.* Impairments in mitochondrial palmitoyl-CoA respiratory kinetics that precede development of diabetic cardiomyopathy are prevented by resveratrol in ZDF rats. *J. Physiol.* **592**, 2519–2533 (2014).

312. Bugger, H. *et al.* Rodent models of diabetic cardiomyopathy. *Dis. Model. Mech.* **2**, 454–66

313. Weinert, B. T. *et al.* Proteome-wide mapping of the Drosophila acetylome demonstrates a high degree of conservation of lysine acetylation. *Sci. Signal.* **4**, ra48–ra48 (2011).

314. Henriksen, P. *et al.* Proteome-wide analysis of lysine acetylation suggests its broad regulatory scope in saccharomyces cerevisiae. *Mol. Cell. Proteomics* **11**, 1510–1522 (2012).

315. Mazumder, P. K. *et al.* Impaired cardiac efficiency and increased fatty acid oxidation in insulin-resistant ob/ob mouse hearts. *Diabetes* **53**, 2366–74 (2004).

316. How, O. J. O.-J. O.-J. *et al.* Increased Myocardial Oxygen Consumption Reduces Cardiac Efficiency in Diabetic Mice. *Diabetes* **55**, 466–473 (2006).

317. How, O. J. O.-J. O.-J. *et al.* Influence of substrate supply on cardiac efficiency, as measured by pressure-volume analysis in ex vivo mouse hearts. *Am. J. Physiol. Heart Circ. Physiol.* **288**, H2979–H2985 (2005).

318. Aasum, E., Hafstad, A. D., Severson, D. L. & Larsen, T. S. Age-Dependent Changes in Metabolism, Contractile Function, and Ischemic Sensitivity in Hearts From db/db Mice. *Diabetes* **52**, 434–441 (2003).

319. Fredersdorf, S. *et al.* Myocardial hypertrophy and enhanced left ventricular contractility in Zucker diabetic fatty rats. *Cardiovasc. Pathol.* **13**, 11–19 (2004).

320. Srivastava, P. M. *et al.* Prevalence and predictors of cardiac hypertrophy and dysfunction in patients with Type 2 diabetes. *Clin. Sci.* **114**, 313–320 (2008).

321. Somaratne, J. B. *et al.* Screening for left ventricular hypertrophy in patients with type 2 diabetes mellitus in the community. *Cardiovasc. Diabetol.* **10**, 29 (2011).

322. Mizuno, Y. *et al.* The diabetic heart utilizes ketone bodies as an energy source. *Metabolism.* **77**, 65–72 (2017).